Characterization of the Usher Syndrome Gene CDH23: Implications for Mechanosensation in the Vertebrate Inner Ear

Inauguraldissertation

Zur
Erlangung der Würde eines Doktors der Philosophie
vorgelegt der
Philosophisch-Naturwissenschaftlichen Fakultät
der Universität Basel

von

Jan-Erik Siemens

aus Schleswig, Deutschland

Basel, 2004

Genehmigt von der Philosophisch-Naturwissenschaftlichen Fakultaet auf Antrag von Prof. Dr. Denis Monard, Prof. Dr. Esther Stoeckli und Prof. Dr. Ulrich Mueller

Basel, den 6.4.2004

Prof. Dr. Marcel Tanner

“We now return to the problem of the high sensitivity of the ear. From a purely physical point of view, it is startling that a displacement whose magnitude is the diameter of an atom can produce enough voltage to trigger a nerve ending. I have no solution to this problem. But since we have seen how, step by step, the anatomical structures in the ear localize the vibration forces in smaller and smaller compartments, it does not seem impossible that the final mechanical transformer is of molecular dimensions.”

Georg von Bekesy, 1962

Table of Contents

SUMMARY 1

1. INTRODUCTION 4
    1.1.The Vertebrate Ear: Anatomy and Sensory Transduction 4
    1.2. Development of the Sensory Organ of the Inner Ear 15
    1.3. Hair Bundle Morphogenesis 19
    1.4. Deafness and Deaf-Blindness 22
    1.5. Cadherin Molecules and their Implication in Deafness 31

2. THE AIM OF THE THESIS 39

3. PAPER I: The Usher Syndrome Proteins Cadherin 23 and Harmonin form a Complex by means of PDZ-Domain Interactions 42
    3.1. Abstract 42
    3.2. Introduction 43
    3.3 Materials and Methods 45
    3.4. Results 52
    3.5. Discussion 62
    Acknowledgements 64

4. PAPER II: Cadherin 23 is a Component of the Tip Link in Hair Cell Stereocilia 66
    4.1. Abstract 66
    4.2. Introduction 67
    4.3. Results 67
    4.4 Discussion 75
    4.5. Materials and Methods 76
    Acknowledgements 84
    4.6. Supplementary Figures 85

5. ADDITIONAL RESULTS 89

- 5.1. Mislocalization of Truncated CDH23 Protein in *v2j* Mutant Mice 89
- 5.2. Ultrastructural Localization of CDH23 in Retinal Photoreceptors of the Mouse 91
- 5.3. Expression of CDH23 in Tissues other than Ear and Eye 93
- 5.4. Introduction of Specific Mutations in the *Cdh23* Gene of the Mouse 98

6. FINAL DISCUSSION 104

- 6.1. The Tip Link of Hair Cell Stereocilia 105
- 6.2. Tip Link – Gate Keeper? 111
- 6.3. CDH23 in Photoreceptors of the Vertebrate Retina 125
- 6.4. Usher Syndrome Type I 131

7. FUTURE PROSPECTS 137

8. REFERENCES 145

ACKNOWLEDGEMENTS 170

CURRICULUM VITAE 173

Summary

Deafness is the most common form of sensory impairment afflicting the human population. Approximately one in eight hundred children is born with serious hearing impairment and more than half of these cases are likely due to single gene defects. In addition to hearing loss, mutations in some genes cause Usher Syndrome, not only affecting the auditory apparatus but also causing visual impairment eventually leading to blindness. Several genetic loci have been linked to Usher Syndrome Type I, the most severe form of the disease, and so far five of the relevant genes have been identified. Understanding their molecular role in the context of ear and retina physiology will be invaluable to the design of effective therapies against this devastating disease.

Some forms of Usher Syndrome as well as other hearing disorders are caused by defects in the inner ear that contains the end organs for the perception of sound waves, the cochlea, and for the detection of gravity and acceleration, the vestibule. Both end organs contain mechanosensory hair cells that are named after actin rich stereocilia projecting from their apical surface. The stereocilia contain mechanically gated ion channels that open or close upon deflection of the stereocilia. This in turn triggers ion influx into the hair cells, causing changes in cell polarization and alterations in the rate of neurotransmitter release from the hair cells onto innervating neurons. The mechanically gated transduction channel implicated in this event has remained elusive.

Mechanical gating of the transduction channel is believed to be triggered by thin filaments, the tip links, connecting adjacent stereocilia into a bundle. It has been suggested that these connector molecules are being stretched during hair cell stimulation, thereby actively pulling open the transduction channel. Although these filaments are clearly detectable on the ultrastructural level, their molecular nature has remained elusive.

One molecule that might participate in mechanoelectrical transduction is the transmembrane protein cadherin 23 (CDH23). Mutations in its gene can cause Usher Syndrome, non-syndromic forms deafness and age-related hearing loss in human patients. Mice and zebrafish that carry mutations in the orthologous genes show splayed stereocilia bundle morphology, arguing for a function of the protein product in the cell compartment harboring the transduction channel. Furthermore, CDH23 is large enough to be the tip link, the extracellular filament proposed to gate the mechanotransduction channel.

Here we show that antibodies against CDH23 label the entire stereocilia bundle during hair cell morphogenesis. In mature hair cells CDH23 labelling is confined to the tip links. Further, CDH23 has biochemical properties similar to those of the tip link. In cell-aggregation experiments CDH23 displays Ca^{2+}-dependent, homophilic adhesion potential, an attribute typically observed for members of the cadherin superfamily, which may explain how adjacent stereocilia are linked together. Moreover, CDH23 forms a complex with myosin 1c (MYO1C), the only known component of the mechanotransduction apparatus, suggesting that CDH23 and MYO1C cooperate to regulate the activity of mechanically gated ion channels in hair cells.

Computer assisted alignments with sequences encoding the cytosolic domain of CDH23 reveal two putative PDZ-binding motifs. Others and we can show that CDH23 interacts with the product of a second Usher Syndrome gene, harmonin. Two PDZ domains within harmonin interact with two complementary binding surfaces in the CDH23 cytoplasmic domain. One of the binding surfaces is disrupted by sequences encoded by an alternatively spliced CDH23 exon that is expressed in hair cells, but not in any other tissue analyzed so far. In the ear, harmonin is expressed in the stereocilia of developing hair cells. Since mice with a targeted deletion of the harmonin gene have been reported to phenocopy the splayed stereocilia bundle morphology observed in CDH23 deficient mice, the complex of the two Usher Syndrome proteins is predicted to be important for the stereocilia bundle. Whether the harmonin–CDH23 complex might be involved in mechanotransduction is unclear, since harmonin´s presence in mature stereocilia has not been reported yet.

We concluded that CDH23 may serve a dual function in auditory hair cells: together with harmonin the molecule is important to shape the hair bundle during hair bundle morphogenesis and in mature stereocilia the molecule is part of the tip link complex.

Introduction

1. Introduction

1.1 The Vertebrate Ear: Anatomy and Sensory Transduction

Auditory sensation begins with the collection of sound energy by the external ear. Sound is carried as a pressure oscillation of air through the middle ear into the inner ear, where the oscillating force is finally conveyed upon mechanically gated ion channels of the primary mechanosensors, the hair cells. Sensory transduction –the process of converting the physical stimulus to a neuronal signal- begins when the force opens and closes these channels, cycle by cycle, to allow a pulsatile flow of ionic current to enter the hair cells.

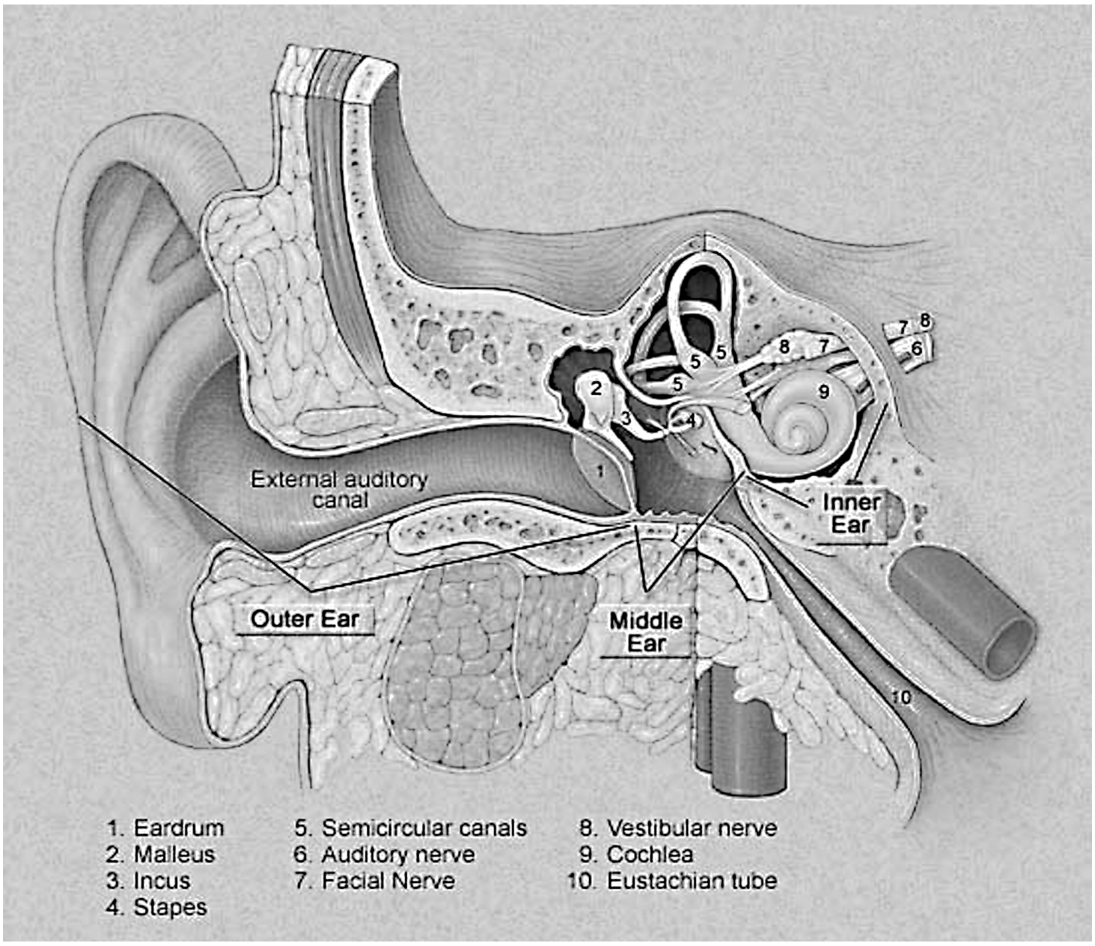
External auditory canal
Outer Ear
Middle Ear
Inner Ear
1
2
3
4
5
5
5
6
7
7
8
8
9
10
1. Eardrum
2. Malleus
3. Incus
4. Stapes
5. Semicircular canals
6. Auditory nerve
7. Facial Nerve
8. Vestibular nerve
9. Cochlea
10. Eustachian tube

Figure 1.1. The Vertebrate Ear
The diagram displays the spatial relationship between outer, middle and inner ear (Modified from: http://www.tchain.com/otoneurology/disorders/bppv/otoliths.html.).

1.1a. External and Middle Ear (Fig. 1.1)

The external ear collects sound and funnels it into the external auditory canal, where it causes vibration of the eardrum, the tympanic membrane. The tympanic membrane drives vibration of three middle ear bones, the ossicles: the malleus, which is attached to the tympanic membrane, the incus and the stapes. The footplate of the stapes is connected to the oval window, a flexible membrane separating the air filled middle ear from the fluid phase within the cochlea. The function of the ossicles is to transform energy: they convert the high amplitude, low-force vibration of air to a low-amplitude, high force vibration in the fluid of the cochlea. If the middle ear were absent, sounds would reach the fluid at the oval window directly. In that event, most of the sound energy would be reflected because fluid has a higher acoustic impedance than air and as result the sound pressure required for hearing would be elevated. In addition to the system of levers formed by the ossicles, which increases the pressure on the round window, the area of the tympanic membrane is greater than the area of the oval window giving rise to another pressure enhancement in the fluid phase.

1.1b. The Inner Ear

The inner ear contains end organs of two sensory systems: the Vestibule and the Cochlea. Although both organs have a different organization and different function, both of them utilize hair cells as their primary sensory cells.

The vestibular organs (the saccule, utricle and three semicircular canals) sense tilt and acceleration of the head and subserve the sense of balance. The hair cells of the balance system are organized in discrete patches that are interconnected by fluid-filled cannels (Fig. 1.2).

The cochlea senses the vibration of sound and therefore is the organ for the perception of acoustic stimuli. Due to the similarity of hair cells within the hearing and balance organ, this chapter will mainly focus on one of the two, namely the hearing organ. The sensory cells are situated in the so-called Organ of Corti within the cochlea. The cochlea is a snail-shaped organ that spirals through three turns in humans. Each cochlea turn has three fluid-filled spaces (Fig. 1.3) with differing ionic composition: while the perylymph in scala tympani and scala vestibuli (ST and SV) is much like normal extracellular fluid, the endolymph in scala media (SM) has a high K^+, low Na^+ and low Ca^{2+} ion composition similar to intracellular fluid and a standing voltage of about +80 mV (Table 1.1). The basilar membrane, a flexible structure like a very long drumhead, separates scala tympani from scala media. The compression phase of each oscillation cycle is relayed from the oval window through scala vestibuli and scala tympani and pushes down on the basilar membrane.

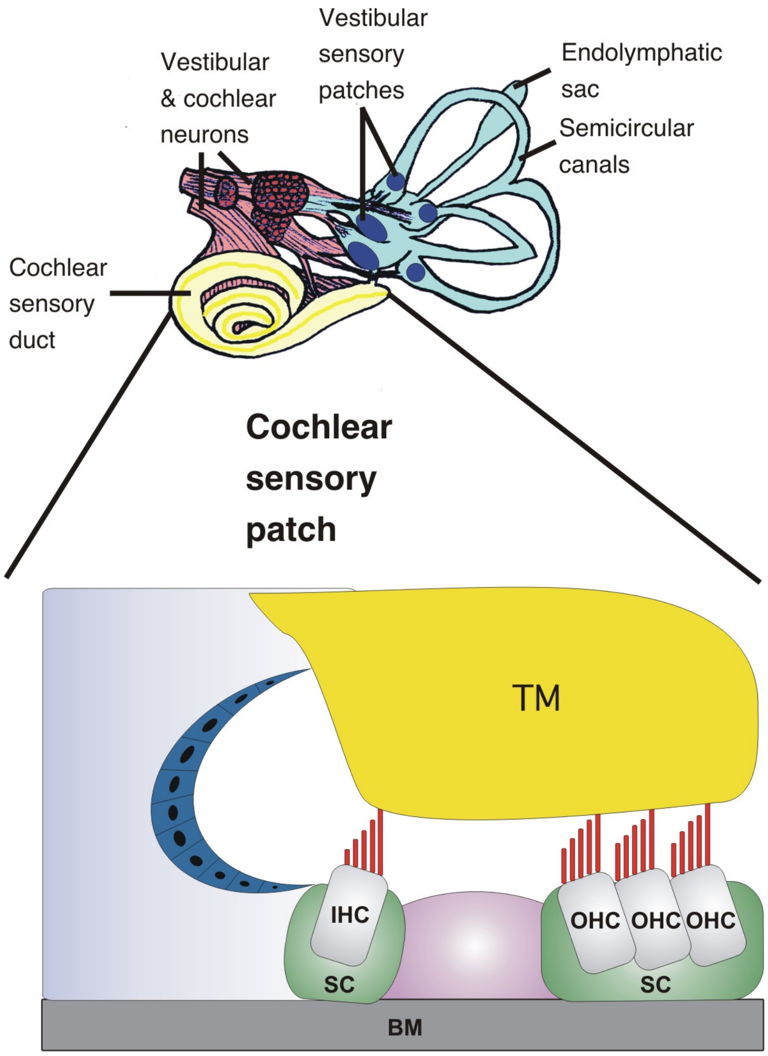
Vestibular & cochlear neurons
Vestibular sensory patches
Endolymphatic sac
Semicircular canals
Cochlear sensory duct
Cochlear sensory patch
TM
IHC
OHC
OHC
OHC
SC
SC
BM

Figure 1.2. The Inner Ear and Organ of Corti
The upper panel displays an overview diagram of the mammalian inner ear encompassing the cochlea and the vestibule. Magnified in the lower panel is an artistic representation of the organ of Corti with its one row of inner hair cells (IHC) and three rows of outer hair cells (OHC) running along the cochlea duct. The stereocilia (red) project from the apical hair cell surface. Only the largest stereocilia are in contact with the overlaying Tectorial Membrane (TM). Support cells (SC) are located in between hair cells and Basilar Membrane (BM). (Modified from: *Trends Cell Biol.* 2001; 11; 334-342)

Component	*Perilymph*	*Endolymph*
Na^+	144	1.3
K^+	5	157
Ca^{2+}	0.8	0.025
Cl^-	120	132
HCO_3^-	20	31

Table 1.1. Ion Composition of cochlear perilymph and endolymph
Concentrations of the respective ions are given in millimolar (mM); all values are averages of data obtained in guinea pigs and rodents, assembled from various references. No major differences are assumed to exist among mammalian species.

The basilar membrane increases in stiffness from the apical to the basal end of the cochlea, which allows discrimination of sound frequencies along the cochlea duct reflected by a tonotopic gradient: any given frequency of sound causes a wave in the basilar membrane that has its maximum amplitude at a unique point along the basilar membrane. For high sound frequencies this point is close to the base, for low frequencies more distal (Fig 3 right panel) (Dallos, 1996; Slepecky, 1996).

1.1c. The Hair Cells in the Cochlea

Riding on the basilar membrane is the organ of Corti, which harbors the principal receptor cells, the hair cells. Hair cells are named after actin rich protrusions, the stereocilia, emanating from their apical surfaces (Fig. 2 and 4). The hair cells run in one row of inner and three rows of outer hair cells (IHC and OHC) throughout the length of the cochlea duct. The organ of Corti also contains supporting cells and cells secreting the tectorial membrane, a specialized filamentous extracellular matrix, that overlies the organ of Corti and attaches to the tops of the largest stereocilia at the hair cells' apical surface. Sound-evoked vibration of the basilar membrane causes a shearing movement between the tectorial membrane and the organ of Corti. Since the tectorial membrane is attached primarily to the tips of stereocilia, an upwards movement of the organ of Corti –due to the pushing force relayed from the basilar membrane- produces shear that deflects stereocilia against the tectorial membrane leading to ion channel opening and subsequent downstream neuronal responses (Fig. 4 and 5) (Corey, 2003; Hudspeth, 1997; Sukharev and Corey, 2004). While both IHC and OHC are mechanosensitive, only the signal emanating from IHC is relayed to brain nuclei, since they receive 95% of the afferent innervation (Rubel and Fritzsch, 2002). OHC receive efferent innervation but are not involved in passing on the acoustic information to neurons. Rather, they are involved in signal amplification as described below.

1.1d. The Hair Bundle

30-300 stereocilia, depending on species and kind of hair cell, project from each hair cell's apical surface. Stereocilia are usually ~0.2 µm in diameter and between 6 and 7 µm long in the mammalian cochlea, although in the vestibular system bundles of up to 50 µm in length can be found (Flock et al., 1977). This hair bundle is arranged in a highly polarized staircase-like pattern: in all vertebrate hair cells, heights of stereocilia increase uniformly from one row to the next. However the overall height, width and shape of the bundle vary among organs and species (Corey, 2003). Outer hair cells of the mammalian cochlea have a V- or W- shaped bundle as described below. Next to the largest stereocilia is a tubulin-based cilium, the kinocilium, which has a more sinuous shape. The axonemal patterns are heterogenous among kinocilia, most prominent in mature kinocilia is the 9+0 (doublet) form of microtubules but a modified 8+1 (doublet) form and the classical 9+2 (single) form exist as well (Sobkowicz et al., 1995). There is no evidence for a motile axonemal structure within kinocilia. Other than the stereocilia, the kinocilium serves mainly a developmental function and is not needed for mechanosensation (Hudspeth and Jacobs, 1979). The kinocilium is not maintained in hair cells of some species after the hair bundle is properly established.

Rigidity within the stereocilia is provided by hexagonally packed unipolar actin filaments that run from the distal tip of the stereocilia to the apical surface of the hair cell (Fig. 4) (Tilney et al., 1992). These actin filaments are highly crosslinked by bridging molecules such as fimbrin and espin and a third unknown molecule may attach actin fibers to the plasma membrane along the stereocilia shaft (Drenckhahn et al., 1991; Zheng et al., 2000c; Zine et al., 1995). Extensive actin cross-linking results in the stereocilia being stiff (Flock et al., 1977). Some of the actin filaments, the rootlet filaments, are firmly anchored within an actin-spectrin meshwork at the apical surface of the hair cell, a region known as cuticular plate. These rootlet fibers are bound by tropomyosin, which has been suggested to prevent their depolymerization (Slepecky and Chamberlain, 1985; Slepecky and Ulfendahl, 1992).

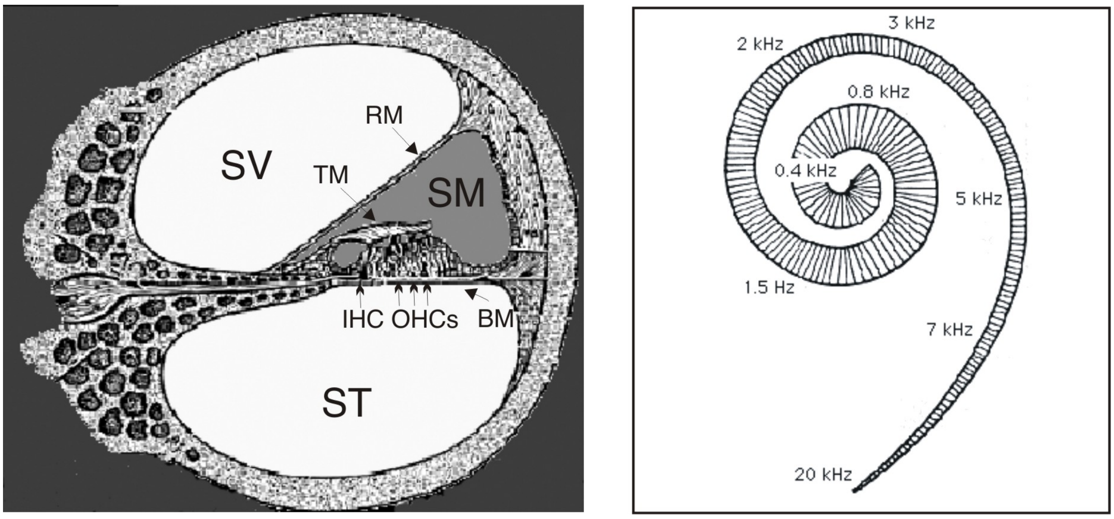

Figure 1.3. The Cochlea Duct
The left panel shows a schematic representation of a cross section through the Cochlea Duct. The 3 different fluid compartments are visible: The Scala Vestibuli (SV) and Scala Tympani (ST) filled with Perilymph and the Scala Media (SM) filled with Endolymph. The Reissner´s Membrane (RM) and the Basilar Membrane (BM) separate the Scala Media from the two Perilymph compartments. The one row of inner hair cells (IHC) and the three rows of outer hair cells (OHC) are covered by the Tectorial Membrane (TM) and are situated on the Basilar Membrane. The right panel shows the frequency susceptibility of the hair cells along the Cochlear Duct. (Modified from: www.mediathek.ac.at/marchetti/a4ohr/a43E.htm)

The apical compartment of the hair cell also contains the zonula adherens (adherens junction), a ring of mixed polarity actin fibers running in a circumferential belt parallel to the plasma membrane. This coherent adherens junction might provide tension across the apical hair cell surface to stabilize the cuticular plate with its emanating stereocilia (Hirokawa and Tilney, 1982). Between the circumferential belt and the cuticular plate is the pericuticular necklace, a microtubule- and vesicle-rich region. One role of this membranous region is to provide and store transmembrane proteins packed into vesicles, which are targeted for the stereocilia. Vesicles fuse with the plasma membrane of the pericuticular necklace and transmembrane proteins get transported within the membrane to the stereocilia. Vesicles appear to be excluded from stereocilia.

The intricate actin cytoskeleton is optimized for the conversion of mechanical stimuli into regulated stereocilia movements.

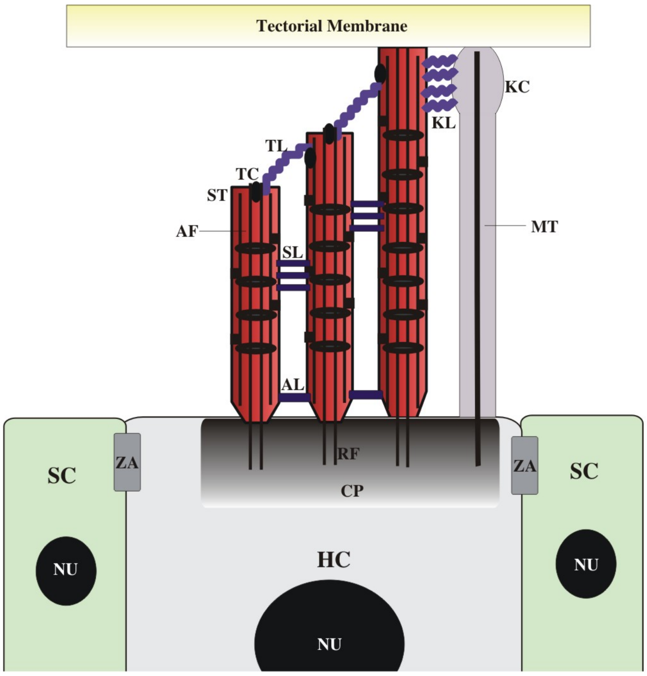

Figure 1.4. The Hair Cell
The diagram displays a cross-section of the apical part of a hair cell (HC) and two neighboring support cells (SC). The stereocilia (ST) contain actin filaments (AF) connected to the plasma membrane (black squares) and cross-linked by bundling proteins (black discs). The stereocilia are arranged in a staircase pattern and the largest ones reach into the tectorial membrane. A Kinocilium (KC) organizes the stereocilia bundle and degenerates in some species afterwards. Along the lateral borders of stereocilia and kinocilium are bridging molecules forming tip link (TL), side or shaft link (SL), ankle link (AL) and kinocilary link (KL). The distal parts of the stereocilia are believed to harbor the mechanically gated ion channel (TC). The basal domain of the stereocilium is anchored via actin rootlet filaments (RF) in the cuticular plate (CP). (ZA: zonula adherens; NU: nucleus).

1.1e. Stereocilia Linker Molecules

The stereocilia are interconnected by a number of extracellular linkages (Fig. 1.4): close to the cell surface are the ankle links (AL), at the medial part are the side links - or shaft links- (SL) and at the top are the tip links (TL). The kinocilium is linked to the largest stereocilia by kinocilary links (KL) (Corwin and Warchol, 1991; Hackney and Furness, 1995; Tsuprun and Santi, 1998). Apart from one candidate protein for the side link molecule, a receptor-like inositol lipid phosphatase (Goodyear et al., 2003), none of the linker molecules have been cloned or characterized in any detail. Nevertheless antibodies have been generated that recognize some of these connectors or proteins in their vicinity, but the identities of the corresponding epitopes are still not known. (Goodyear and Richardson, 1999; Goodyear and Richardson, 2003). Due to the linker molecules, the stereocilia bundle behaves like a single unit during deflection (fig. 1.5)(Corwin and Warchol, 1991).

1.1f. Auditory Transduction

Additionally, the tip link is believed to serve another purpose. A multitude of evidence has accumulated suggesting that the tip link is involved in gating of the putative mechanosensory transduction channel situated at hair cell stereocilia tips. The tip link runs as fine extracellular filament along the axis from short to tall stereocilia. Hair cells respond physiologically to deflections of the bundle along this axis, the axis of mechanical sensitivity, but not to deflections toward the sides (Fig. 1.5) (Shotwell et al., 1981). Disrupting the tip links proteolytically or chemically, for example by digestion with the protease elastase or by chelating Ca^{2+} ions, abolishes the physiological response. The responsiveness returns when tip links regenerate in 5-10 hours (Assad et al., 1991; Duncan et al., 1998; Meyer et al., 1998; Osborne and Comis, 1990; Zhao et al., 1996). By electron microscopic measurements, tip links generally are 150-300 nm long, 8-11 nm thick, and appear as a helix of two filaments, which at either end contain a visible intracellular osmiophilic density (Kachar et al., 2000; Tsuprun and Santi, 2000). Deflection of a hair bundle opens transduction channels within microseconds that are located near the tips of the stereocilia. The speed of the response suggests that the stimulus is conveyed directly to the –still unknown- ion channel, without the need of any second messenger (Corey and Hudspeth, 1983b). Due to the staircase geometry of the bundle, such deflections would either stretch or relax the tip links, depending on the direction of the movement (Fig 1.5). A particularly attractive model for transduction is that tip links form a macromolecular complex with transduction channels in the stereocilia membrane. On the cytoplasmic side, this complex would be anchored in turn to the actin cytoskeleton so that stretch causes tension on the channel protein and promotes a conformational change to open the channel pore allowing the influx of K^+ ions and Ca^{2+} ions (Corey, 2003; Sukharev and Corey, 2004).

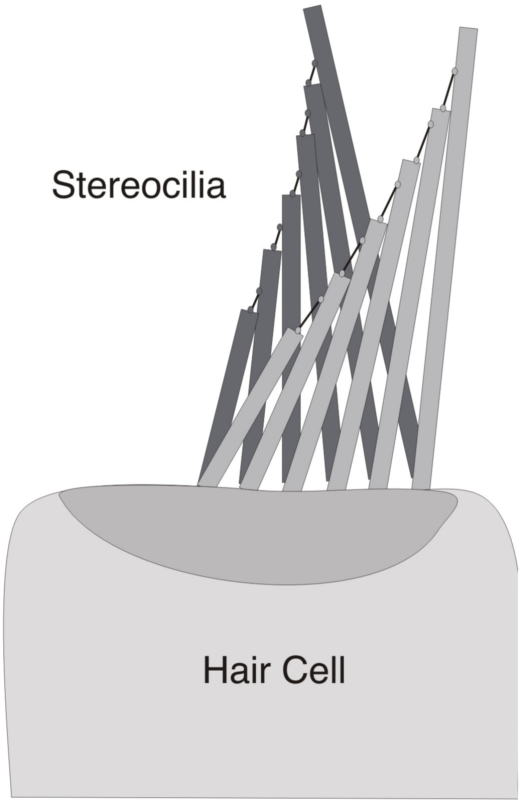

Figure 1.5. Stereocilia Deflection Model.
The tip links are stretched in case of positive deflection (to the right) and relaxed for negative deflection (to the left).

1.1g. Adaptation

As small static deflections could open or close all the transduction channels, rendering a hair cell insensitive to small vibratory stimuli that come thereafter, hair cells also have several mechanisms to regulate or bias the open probability of transduction channels. One such mechanism involves mobilization of myosin molecules such as myosin 1c (MYOIC). It is thought that these motor proteins, connected to the cytoplasmic end of each transduction complex, are continuously trying to climb along the actin filament of the stereocilium (Fig. 1.6). At some tension the motor slips as fast as it climbs and the stall force is just sufficient to keep channels open 10-15% of the time. A deflection that increases tension and opens channels also causes the motor to slip along the actin filaments, allowing channels to close again. A deflection that relaxes tension and closes channels allows the motor to climb along the actin core to restore tension again. Firm evidence that MYOIC is involved in the adaptation process comes from an elegant study utilizing transgenic mice with a subtle mutation in *Myo1C*, rendering the altered protein susceptible to chemical inhibition. In the mutant mice the transducer currents, induced by mechanical hair bundle deflection, decreased much more slowly than in wild-type controls suggesting altered adaptation properties upon MYO1C inhibition. (Garcia et al., 1998; Gillespie and Corey, 1997; Holt et al., 2002; Steyger et al., 1998).

Another report suggests that MYOVIIA is involved in gating of the transduction channel as well. Mutations in the gene encoding MYOVIIA alter gating properties in such a way, that hair bundles need to be deflected beyond their physiological range in order for the transduction channel to open (Kros et al., 2002).

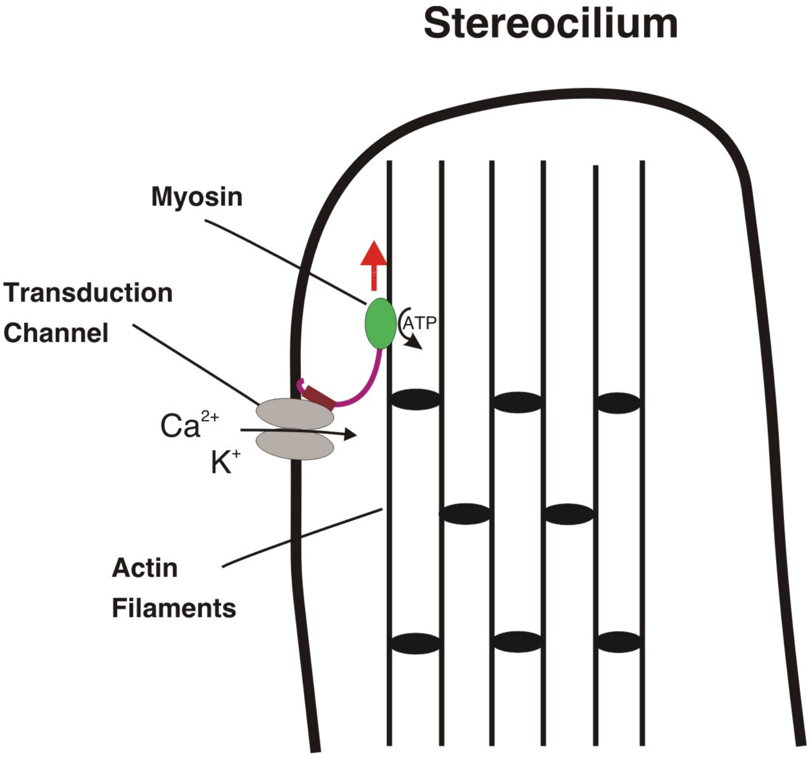

Figure 1.6. Adaptation by Myosin Motors.
The schematic diagram depicts the tip of a stereocilium. Transduction channels are believed to be connected directly or indirectly to MYO1C or MYOVIIA which apply tension to the channel protein by climbing along actin fibers. Tension conveyed upon the ion channel supposedly regulates its gating. The tip link, believed to apply tension force onto the ion channel in the opposite direction, is omitted for clarity. Note that myosin motors only travel toward the growing end (plus end) of actin filaments and therefore climb toward the tip of stereocilia.

Ca^{2+} ion influx is believed to be involved in a fast adaptation process of a hair cell to a stimulus. Ca^{2+} ions, entering the cell through the non-selective cationic transduction channel, modulate the open probability of the transducer channel by binding to its cytosolic portion directly or via calmodulin, which is localized at the stereocilia apex (Furness et al., 2002; Holt and Corey, 2000).

1.1h. Amplification

Both the inner hair cells (IHC) and outer hair cells (OHC) of the organ of Corti transduce mechanical stimuli into electrical signals by modulating a cationic current in response to stereocilia displacement. This current is mainly composed of K^+ ions, which are in abundance in the cochlear endolymph, the extracellular fluid that the stereocilia are bathing in (see 1.1b) (Bosher and Warren, 1978). This current induces a receptor potential across the basolateral membrane of the cell, which promotes the release of neurotransmitter. Evidence has accumulated that an interaction between OHCs and IHCs promotes the highly selective and highly sensitive response to high frequency acoustic stimulation. However, a potential mechanism for such a signal amplification remained obscure until Brownell observed twitching of outer hair cells in response to electrical stimulation (Brownell et al., 1985). This phenomenon, known as hair cell electromotility, allows reverse transduction and is believed –although controversial- to be the basis of the cochlear amplifier. This amplification process envisions an acoustically evoked feedback mechanism between the OHCs and the Basilar Membrane: The acoustically triggered electrical response of the OHCs are assumed to effect rapid mechanical length changes by these cells which boost the mechanical input to the IHCs, the receptor cells that receive up to 95% of the afferent innervation (see 1.1c) (Rubel and Fritzsch, 2002). There is some evidence that three genes of the *SLC26A* family, which are implicated in non-syndromic deafness, may be responsible for these outer hair cell movements. The *SLC26A5* gene encodes the anion transporter prestin, which is highly and selectively expressed at the lateral membrane of the OHCs and the *Prestin* knockout mouse is defective in cochlear amplification and hair cell motility, however, prestin ablation also leads to hair cell death in mutant mice (Liberman et al., 2002; Liu et al., 2003; Zheng et al., 2000a). How prestin may convey electromotility to the OHCs is still under investigation.

1.2 Development of the Sensory Organ of the Inner Ear

During development, the sensory organs of the inner ear are all derived from the otic placode, an epithelia sheet of the head ectoderm, that forms right after closure of the neural tube (Fig. 1.7) (Bryant et al., 2002; Müller and Evans, 2001). The otic placode transforms into a hollow, pear-shaped structure, the otocyst, from which neuroblasts delaminate. These neuroblasts give rise to neurons that send projections back to the sensory epithelia and innervate the hair cells. Although these neurons become critically dependent on trophic support from the hair cells (Fritzsch et al., 2004; Pirvola and Ylikoski, 2003; Rubel and Fritzsch, 2002), there is little evidence that they influence the development of hair and supporting cells.

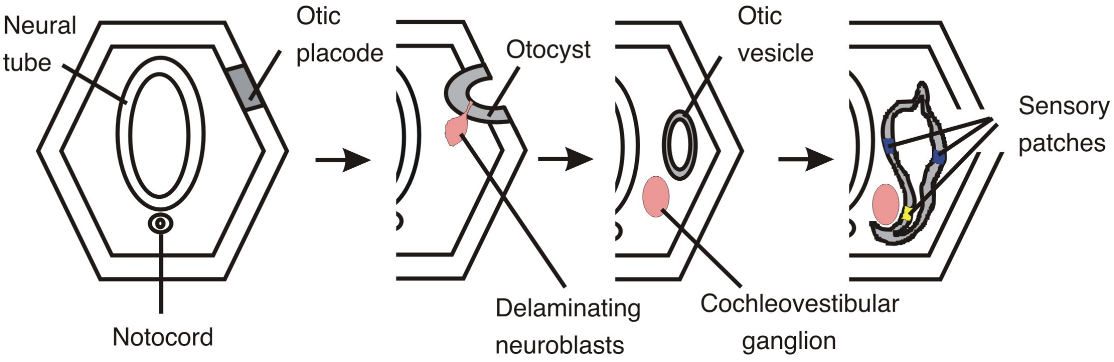

Figure 1.7. Development of the Vertebrate Inner Ear.
The inner ear develops from the otic placode at the lateral side of the head. The placode invaginates and forms the otocyst from which neuroblasts delaminate to form the cochleovestibular ganglion. The otic vesicle gives rise to all the inner ear structures including the sensory epithelia containing the hair cells. The hair cells are innervated by the neurons of the cochleovestibular ganglion. (Adopted from: *Trends Cell Biol.* 2001; 11; 334-342).

1.2a. Genes Involved in Early Development of the Otocyst

Hair cells, support cells and spiral ganglion cells innervating the hair cells are all derived from a single patch of cells in the ventromedial wall of the otocyst. Later on the support cells separate the hair cells from each other, giving rise to a regular mosaic pattern (Torres and Giraldez, 1998). In the chick embryo this prosensory area of the otocyst can be defined by the expression pattern of developmental genes *Serrate1* (in mammals *Jagged1*), *Lunatic Fringe* and *Ben* (Goodyear et al., 2001; Wu and Oh, 1996). Serrate 1 is a transmembrane ligand for Notch, a membrane receptor which is involved in many different aspects of development (Bray, 1998). Lunatic fringe modulates interaction between Notch and its ligands. Ben is a cell-cell adhesion receptor of the Ig superfamily (Moloney et al., 2000; Pourquie et al., 1992). Notch is widely expressed in the otocyst and Serrate 1 may serve to maintain high levels of Notch activation within the pro-sensory patch, endowing this region with the capacity to form sensory organs, and preventing the premature differentiation of hair cells. Additionally, Notch signaling is thought to select delaminating neurons in the otocyst (Fig. 1.8), since neuroblasts express *Delta1*, another Notch ligand (Adam et al., 1998; Eddison et al., 2000). The role of *Lunatic Fringe* is unclear since *Lfng*$^{(-/-)}$ mice do not have any ear abnormalities (Zhang et al., 2000). As a cell-cell adhesion molecule, Ben may serve to stop the cells of the pro-sensory patch from mixing with cells in other regions of the otocyst. Although these molecules have potential roles in defining the pro-sensory region, it is at present unclear what signals determine its formation, or from where these signals emanate.

A boundary model has been proposed to account for how the different sensory organs of the inner ear are specified (Fekete and Wu, 2002). This model postulates that the different sensory organs form at or in proximity to different compartments, the regions of which are defined by the expression of a small set of genes. Candidate genes such as the transcription factors *Pax2, Dlx5, Otx1* and *Hmx3* are expressed in such broad domains in the otocyst and data from knockout mice are consistent with the boundary model (Brigande et al., 2000; Cantos et al., 2000).

1.2b. Math1 and Brn3.1 in Hair Cell Development

A key transcription factor for the development of hair cells is *Math1*, the mouse ortholog of the *Drosophila* proneural gene *atonal*. *Math1* encodes a basic helix-loop-helix transcription factor (bHLH) that is expressed in the otocyst and becomes restricted to hair cells. Hair cells are absent from the inner ears of *Math1*$^{(-/-)}$ mice by birth and the ectopic expression of *Math1* in the non-sensory cells of the greater epithelial ridge, a region adjacent to the organ of Corti, results in the production of extra hair cells (Bermingham et al., 1999; Zheng and Gao, 2000). These results indicate that *Math1* is both necessary and sufficient for hair cell differentiation in the context of the tissues analyzed. Albeit the close similarity of atonal’s function in insect mechanosensory development, *Math1* is not acting as a true proneural gene:

While *Drosophila atonal* mutants lack all the cells necessary to build the fly's auditory organ (Jarman et al., 1993), *Math1* mouse mutants only display hair cell loss.

The gene for POU domain transcription factor *Brn3.1* (also referred to as *Brn3c*) is specifically expressed by hair cells within the mouse inner ear. In *Brn3.1*$^{(-/-)}$ mice, hair cells are generated and express some early hair cell marker molecules such as MYOVIIA and calretinin but they fail to develop sensory hair bundles and hair cells are lost from the inner ear by Postnatal day 14 (P14) (Erkman et al., 1996; Keithley et al., 1999; Xiang et al., 1998). Unlike ectopic expression of *Math1*, ectopic expression of *Brn3.1* does not lead to the production of extra hair cells, indicating *Brn3.1* is only required for the later aspects of hair cell differentiation. It is hypothesized that *Brn3.1* may be downstream of *Math1* (Bryant et al., 2002).

1.2c. Notch Signaling in the Sensory Epithelium of the Inner Ear

In hearing organs of both mammals and birds, hair and supporting cells at any one place are born simultaneously, suggesting they may share a common lineage. Retroviral tracing studies in the chick auditory organ have provided firm experimental evidence for this suggestion. Furthermore it has been shown that the potential to become either a hair cell or a supporting cell is retained by a progenitor cell until it has passed through its final mitotic division, as two-cell clones were found that contained either two supporting cells, two hair cells or both cell types (Fekete et al., 1998; Lang and Fekete, 2001).

The decision to become either a hair cell or a supporting cell most probably involves lateral inhibition mediated by the Notch signaling pathway (Fig. 1.8). The *Notch* ligands *Delta1* and *Serrate2* (*Jagged2* in mammals) are expressed in newly born hair cells and may inhibit neighboring, *Notch*-expressing support cells of adopting the same fate (Lanford et al., 1999; Morrison et al., 1999). Functional studies uphold this view since interference with *Notch, Delta1* or *Jagged2* leads to the production of supernumerary hair cells (Eddison et al., 2000; Lanford et al., 1999; Riley et al., 1999; Zine et al., 2000).

Mammalian orthologs of the *Drosophila hairy* and *enhancer of split* genes *Hes1* and *Hes5*, transcription factors that act downstream of *Notch*, are expressed by support cells, most likely triggered by *Delta1* and *Jagged2* activation (Bryant et al., 2002). Interestingly additional inner hair cells are observed in *Hes1*$^{(-/-)}$ mutant mice, and additional outer hair cells are observed in *Hes5*$^{(-/-)}$ mice (Zine et al., 2001). The findings are consistent with the role of these two *Hes* genes as negative regulators of hair cell differentiation. *Hes1* may directly antagonize the activity of *Math1*, as cotransfection of cochlea cultures with *Hes1* and *Math1* blocks the effect of ectopic *Math1* expression, reducing the production of supernumerary hair cells (Zheng et al., 2000b).

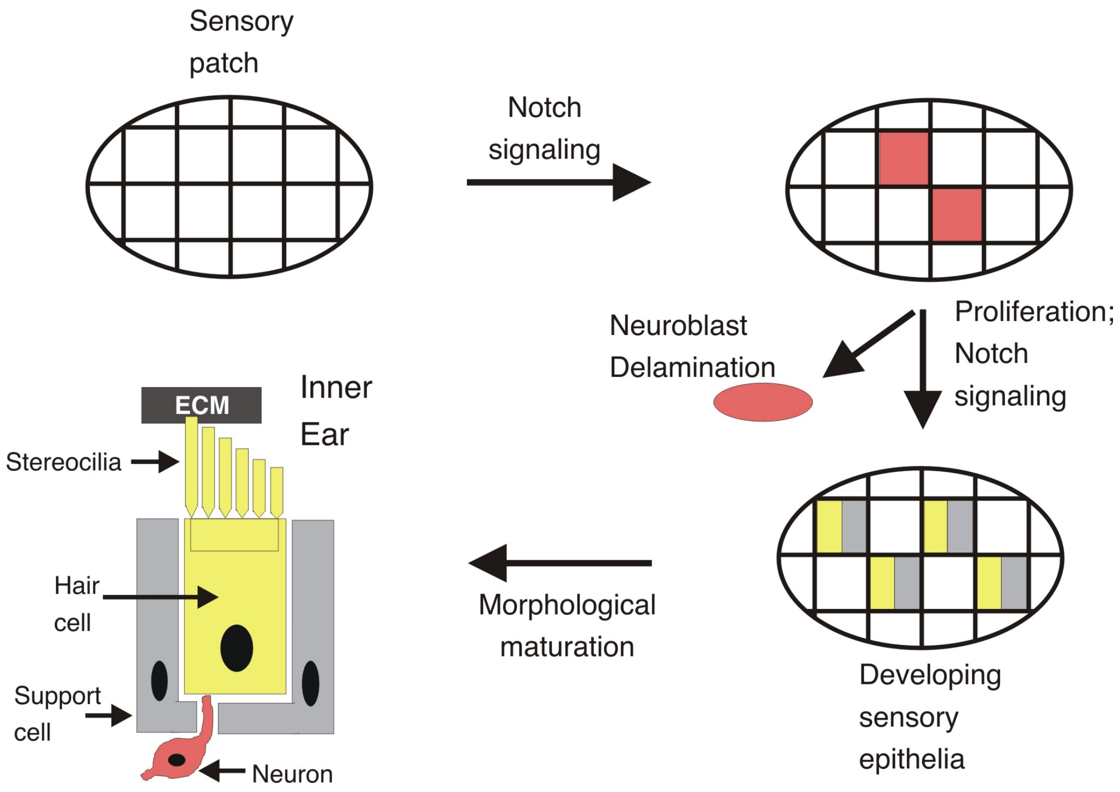
Sensory patch
Notch signaling
Neuroblast Delamination
Proliferation; Notch signaling
Inner Ear
ECM
Stereocilia
Hair cell
Support cell
Neuron
Morphological maturation
Developing sensory epithelia

Figure 1.8. Notch Signaling in Vertebrate Inner Ear Development.
Neuroblasts (red) are initially selected by Notch signaling from sensory patches and delaminate. Subsequently, the fate of hair cells (yellow) and support cells (grey) is again determined by Notch signaling and both cell types develop within the sensory epithelia. (Adopted from: *Trends Cell Biol.* 2001; 11; 334-342).

1.3 Hair Bundle Morphogenesis

Among the factors that specify the appearance of a hair bundle the following are of high importance for hair cell function: the length of the kinocilium; the shape of its tip; the length, diameter, and taper of the individual stereocilia; the number and arrangement of the stereocilia in the hair bundle and the bundle's polarity with respect to those of its neighbors. The values of these parameters vary greatly among vertebrate species, among the different auditory and vestibular organs in a species, and even among hair cells in the same organ. However, the values are precisely controlled, and a hair bundle at a particular place in a particular organ will have the same shape and polarity from individual to individual. The pattern of variation parallels that of other hair-cell properties, such as the types, numbers, and kinetics of ion channels. This systematic fine-tuning of mechanical and electrical characteristics enables hair cells to extract amplitude, frequency, and phase from a wide range of stimuli and to rapidly and faithfully convey this information to the brain.

1.3a. Formation of the Stereocilia Staircase Pattern

The elaborate structure of the hair bundle is formed by elongation of the stereocilia's actin filaments in a precisely choreographed series of steps. Our understanding of this process is based mainly on the work of Lewis Tilney and colleagues, who have thoroughly examined the ultrastructure of the embryonic chicken cochlea, with special emphasis on stereocilia morphogenesis and the respective actin cytoskeleton (Tilney and DeRosier, 1986; Tilney et al., 1983; Tilney and Saunders, 1983; Tilney et al., 1988; Tilney et al., 1986). Very little is known however, about the molecular mechanisms that establish and maintain a hair bundle's shape. It seems reasonable to assume that hair-bundle morphogenesis is driven, at least in part, by localized actin polymerization and that it requires input from outside the hair cell.

When the stereocilia first emerge from the apical surface of a hair cell, they are actin-filled projections of uniform height and surround a central true cilium, or kinocilium (Fig. 1.9). At this stage some microtubules can be observed to run parallel to the apical hair cell surface. After the stereocilia have emerged, the kinocilium moves to one side of the hair bundle. Subsequently, as the first sign of planar cell polarization, all the kinocilia move to the same side of each cell (Denman-Johnson and Forge, 1999).

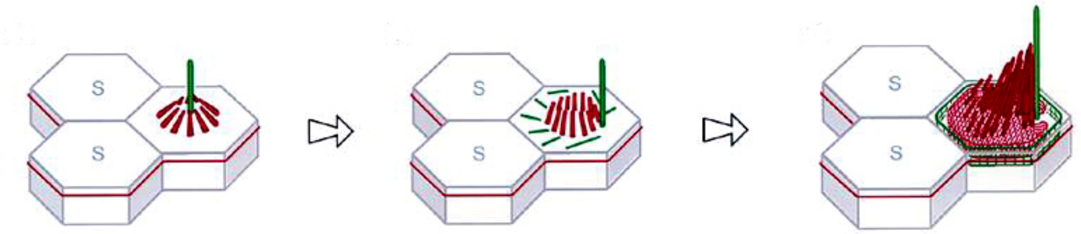

Fig 1.9. Maturation of the hair bundle.
This cartoon displays the process of hair bundle morphogenesis and maturation. Initially the kinocilium (containing microtubules shown in green) grows out from the center of a hair cell and small microvillar-like stereocilia (containing actin fibers shown in red) arrange around it. Subsequently the kinocilium moves to one side of the cell and triggers the staircase-like pattern of the stereocilia. In the elongation phase the stereocilia adopt their final height. In mammalian cochlea Hair cells, the kinocilium degenerates afterwards (S: support cell). (Taken from: *Curr Opin Cell Biol.* 1997; 9; 860-866)

The stereocilia then begin an asymmetric growth phase; stereocilia on the side closest to the kinocilium begin elongation sooner and cease elongation later than those more distant from the kinocilium. As a result, stereocilia become organized into a staircase, with the tallest stereocilia adjacent to the kinocilium. As the stereocilia grow in height, they also extend actin filaments basally into the cell body. These rootlet fibers become anchored in the cuticular plate (see also Fig. 1.4). At the end of this process the sensory hair cells display an asymmetric distribution of stereocilia on their apical surface a phenomenon referred to as planar cell polarization (PCP) (Fig. 1.10).

1.3b. Genes Involved in Planar Cell Polarization (PCP)

In the mammalian cochlea, stereocilia bundles located on the apical surface of mechanosensory hair cells within the sensory epithelium are unidirectionally orientated. Development of this planar polarity is necessary for normal hearing as stereociliary bundles are only sensitive to deflections in a single plane. The signals and molecules involved in PCP are only beginning to be discovered but fortunately seem to be conserved between mammals and flies, in which planar cell polarization has been extensively studied. Wing hairs and sensory bristles of *Drosophila* are most directly relevant to the vertebrate theme. Both these types of structure develop as oriented protrusions from the apical surface, containing both microtubules and actin filaments. In this respect they show some resemblance to the hair bundles of vertebrate hair cells, even though the actin filaments and microtubules are contained in a single protrusion and not separated into stereocilia and kinocilium (Eaton, 1997; Lewis and Davies, 2002). From the PCP signaling genes known to be involved in the establishment of PCP in fly wings, eyes and bristles the following vertebrate orthologs have been found to be expressed in inner ear sensory patches: 1) *Frizzled*, encoding a seven-pass transmembrane receptor belonging to the family of receptors for wingless/wnt (Stark et al., 2000). 2) *Wnt*, encoding a ligand for the frizzled receptor (Hollyday et al., 1995; Jasoni et al., 1999). 3) *Celsr 1-3*, encoding cadherin-like seven-pass transmembrane receptors orthologs to the *Drosophila flamingo* gene (Shima et al., 2002).

Functional implication for involvement of these genes in PCP comes from mouse models and *in vitro* studies. Mutation of *Celsr1* has been shown to disrupt PCP of mouse inner ear hair cells (Curtin et al., 2003)

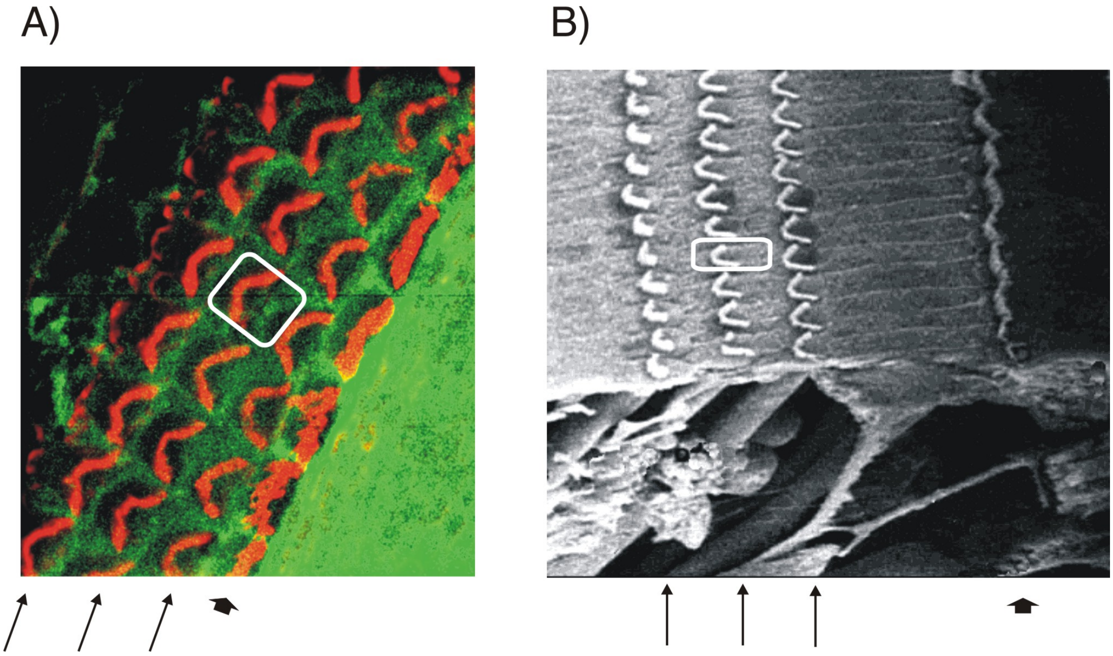

Fig 1.10. Planar Cell Polarity of the Organ of Corti.
Panel A shows a fluoromicrograph displaying the apical surface of the organ of Corti. The stereocilia –labelled for actin in red- project form the apical surface (green) towards the observer. Panel B is an electronmicrograph with a similar view on top of the hair cell surfaces. White boxes in A and B depict the surface area of one hair cell. Note the highly regular pattern of the V-shaped hair bundles, which all point into the same direction. Arrows depict the position of the three rows of outer hair cells and the arrow head the position of the one row of inner hair cells. (Right panel adopted from: http://www.neurophys.wisc.edu/~ychen/auditory/anatomy/a01img.html).

Further, mutations in *Vangl2* and *Scrib1* the mouse orthologs of the fly PCP genes *strabismus* and *scribble*, respectively also cause the stereocilia bundle to be missoriented as a result of defects in movement and/or anchoring of the kinocilium within each hair cell (Montcouquiol et al., 2003). A similar phenotype is observed in mice and zebrafish with mutations in *myosin VIIa* (*MyoVIIa)* (Ernest et al., 2000; Gibson et al., 1995), the ortholog to the *Drosophila* PCP gene *Crinkled* and in mice defective for the novel cadherin gene *Protocadherin 15* (*Pcdh15*) (Alagramam et al., 2001a), which is related to the *Drosophila* PCP gene *dachsous*. Both, *MyoVIIa* and *Pcdh15* deficient mice are deaf and have grossly disorganized stereocilia bundle and abnormally placed kinocilia. Although these findings are indicative for a function in PCP, the splayed stereocilia in mice with mutations in either of the two genes may also argue for a function in hair bundle integrity.

In vitro organ cultures of mouse cochlea sensory hair cell patches display abnormal hair bundle orientation when inhibitors of Wnt signaling are applied during stereocilia maturation (Dabdoub et al., 2003).

Together these findings argue for a conservation of the establishment of planar cell polarity in the fly and vertebrate inner ear. How these molecules act in concert to establish planar polarity is largely unknown; the extent to which these proteins cooperate to organize polarity in hair cells is also unclear. It is interesting that several of the mentioned genes (at least in *Drosophila)* give rise to proteins that are concentrated at cell-cell junctions, where the distal end of one cell contacts the proximal end of the neighboring cell, which is the direction of the planar polarity axis.

1.4 Deafness and Deaf-Blindness

A large proportion of the human population suffers from varying degrees of hearing loss. About one in eight hundred children is born with serious hearing impairment and many more people suffer from progressive hearing loss during aging. In fact, a staggering 60% of humans over 70 years of age are afflicted with significant hearing loss. Single gene defects are responsible for about 50% of the hearing defects in newborns, and genetic predisposition is an important determinant in some forms of age related hearing loss (Gorlin, 1995; Siemens et al., 2001; Steel and Kros, 2001). Hearing impairment can be inherited both as a dominant and recessive trait. A large number of genetic loci have been identified that are associated with non-syndromic forms of hearing loss, i.e. hearing impairment is the only discernable defect (sometimes also associated with balance defects) in the people affected.

Hearing loss also frequently accompanies syndromic diseases that in addition afflict other tissues and organs. Over 400 syndromes with deafness as one of the symptoms have been described in the literature (Ahmed et al., 2003a; Keats and Corey, 1999; Petit, 2001). They include a vast ensemble of hereditary diseases in which hearing loss is associated with miscellaneous disorders of the musculoskeletal, cardiovascular, urogenital, nervous, endocrine, digestive, or integumentary systems. About 40 of these syndromes include an ocular disorder.

1.4a. Usher Syndrome

Among those with eye defects is Usher syndrome (USH), defined by a bilateral sensorineural deafness that originates in the cochlea and a loss of vision due to retinitis pigmentosa. This syndrome is the most frequent cause of deafness accompanied by blindness. It accounts for more than 50% of individuals who are both deaf and blind. Its prevalence is between 1/16,000 and 1/50,000, based on studies of Scandinavian (Grondahl, 1987; Hallgren, 1959; Nuutila, 1970; Rosenberg et al., 1997), Columbian (Tamayo et al., 1991), British (Hope et al., 1997), and American (Boughman et al., 1983) populations. Usher syndrome involves at least 12 genetic loci and due to the clinical heterogeneity of the syndrome, a classification into three subtypes, Usher Type I (USH1), type II (USH2) and type III (USH3), was proposed in 1977 by Davenport and Omenn (Davenport and Omenn, 1977). During the 1990s, each of these clinical forms was shown to be genetically heterogeneous. Genetic loci identified for Usher type I are *MYO7A* (USH1B, encoding MYOVIIA) (Gibson et al., 1995; Weil et al., 1995), *CDH23* (USH1D, encoding CDH23) (Bolz et al., 2001; Bork et al., 2001), *PCDH15* (USH1F encoding protocadherin 15) (Alagramam et al., 2001a; Alagramam et al., 2001b), *USH1C* (encoding the PDZ domain protein harmonin) (Bitner-Glindzicz et al., 2000; Verpy et al., 2000), and *USH1G* (encoding the ankyrin domain protein sans) (Kikkawa et al., 2003; Weil et al., 2003). Transcripts from all these genes are found in many tissues/cell types other than the inner ear and retina. The genes transcribed from the Usher type I loci A (USH1A) and E (USH1E) remain to be identified.

The study of USH may offer a unique opportunity to decipher the molecular basis of some of the developmental and functional similarities existing between the retinal and the cochlear sensory cells, i.e., the photoreceptor cells and the hair cells. Indeed, at least in some genetic forms of the disease, these cells have been shown to be the primary targets of the gene defect. What are the main structural features common to the photoreceptor cell and the auditory hair cell? First, both are ciliated cells: Photoreceptors possess a connecting cilium linking the internal segment to the external segment (Fig. 1.11); embryonic auditory hair cells have an apical cilium, the kinocilium, which disappears soon after birth in mammals. Second, both cell types possess microvillar structures. In vertebrates, photoreceptors contain lamellar structures, forming discs where the phototransduction occurs; in invertebrates, discs are replaced by rhabdomeres, which are tightly packed genuine microvilli. Nevertheless, vertebrate photoreceptors contain microvillar-like protrusions, the so-called calycal processes, adjacent to the connecting cilium. The apical part of auditory hair cells carries up to 300 specialized microvilli, the stereocilia, where the mechanotransduction takes place. Third, the synapses of both photoreceptors and auditory sensory cells have special characteristics: They are called ribbon synapses in reference to their plate-like presynaptic bodies to which synaptic vesicles are tethered. From a functional point of view, these synapses are characterized by a massive, rapid, and sustained discharge of neurotransmitters. Finally, the molecular analysis of Usher syndrome may also lead to the discovery of novel biological processes shared by cochlear and retinal sensory cells.

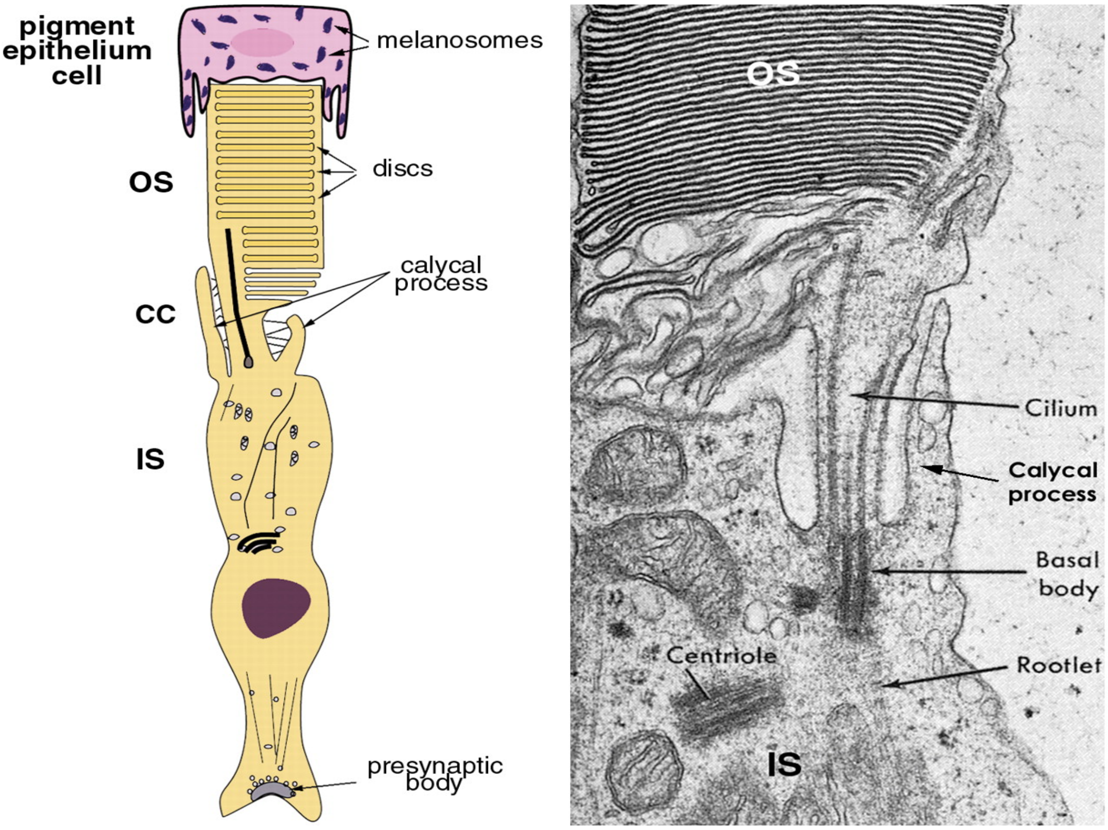

Figure 11. Structure of a Vertebrate Photoreceptor.
The left panel is a schematic representation of a pigment epithelium cell and underlying photoreceptor cell. The right panel is an electronmicrograph of a photoreceptor cell. The photoreceptor cell is composed of an outer segment (OS), containing the photosensitive rhodopsin molecules in membranous discs, a connecting cilium (CC, Cilium) and an inner segment (IS) that contains the various cell organelles. (Adopted from *Annu Rev Genomics Hum Genet.* 2001; 2; 271-297).

1.4b. Positional Cloning of Deafness Genes

In recent years, we have witnessed tremendous progress in the positional cloning of genes which cause hearing loss when mutated. This genomic approach has shown that genes encoding a wide variety of molecules with divergent functions are implicated in deafness. Table 1.2 lists this still growing number of genes implicated in deafness (newly discovered gene mutations can be seen at: http://www.uia.ac.be/dnalab/hhh/). The characterization of these genes provides a starting point for understanding auditory function and will help to unravel disease mechanisms at the molecular and cellular level. Many but not all forms of deafness are caused by defects in the inner ear and the sensory epithelium. Particularly these mutations may give hints about development, maintenance and transduction mechanism of the hair cells.

Molecule	Gene	Mouse mutant	Human disease
Extracellular matrix molecules			
Otogelin	OTOG	twister + targeted mutation	
Usherin	*USH2A*		Usher A
Coch	*COCH*		DFNA9
□-tectorin	*TECTA*	targeted mutation	DFNA8,DFNA1
Collagen 11A2	*COL11A2*		DFNA13, Stickler
Collagen 11A1	*COL11A1*		Stickler syndrome
Collagen 2A1	*COL2A1*		Stickler syndrome
Collagen 4A5	*COL4A5*		Alport syndrome
Collagen 4A3	*COL4A3*	targeted mutation	Alport syndrome
Collagen 4A4	*COL4A4*		Alport syndrome
Cell-surface receptors			
Otocadherin	*CDH23*	*waltzer*	Usher 1D, DFNB12
protocadherin 15	*PCDH15*	*ames waltzer*	Usher 1F
Integrin α8	*ITGA8*	targeted mutation	
Cytoplasmic proteins			
Myosin IIIa	*MyoIIIa*		DFNB30
MYOVIIA	*MYO7A*	*shaker 1*	Usher 1B,DFNA11/B2
Myosin XV	*MYO15*	*shaker 2*	DFNB3
Myosin VI	*MYO6*	*snells waltzer*	DFNA22
Myosin IX	*MYH9*		DFNA17
Diaphanous	*DIAPH1*		DFNA1
Espin	*ESPN*	jerker	
Channel components			
connexin 26	*GJB2*	targeted mutation	DFNB1, DFNA3
connexin 31	*GJB3*	targeted mutation	DFNA2 and recessive form
connexin 30	*GJB6*		DFNA3
connexin 32	*GJB1*	targeted mutation	Charcot-Marie-Tooth
KCNQ4	*KCNQ4*		DFNA2
KvLQT1	*KCNQ1*	targeted mutation	Jervell and L-Nielsen syndrom
Isk	*KCNE1*	targeted mutation	Jervell and L-Nielsen syndrome
Transcription factors			
POU3F4	*POU3F4*	targeted mutation	X-linked DFN3
POU4F3	*POU4F3*	targeted mutation	DFNA15
EYA1	*EYA1*	targeted mutation	Branchio-oto-renal syndrome
PAX3	*PAX3*	*splotch*	Waardenburg syndrome
MITF	*MITF*	micropthalmia	Waardenburg syndrome
SOX10	*SOX10*	*dominant megacolon*	Waardenburg syndrome
EYA4	*EYA4*		DFNA10
Ion transporters and pumps			
Pendrin	*PDS*	targeted mutation	DFNB4 and Pendreds syndrome
ATP6B1	*ATP6B1*		renal tubular acidosis and deafness

Others			
Harmonin	*USH1C*		Usher 1C
Sans	*USH1G*		Usher 1G
Whirlin	*DFNB3*1		DFNB31
DDP	*TIMM8A*		DFN1
norrin	*norrin*	targeted mutation	Norrie disease
treacle	*TCOF1*		Treacher Collins syndrome
FGFR3	*FGFR3*	targeted mutation	craniosynoctosis with deafnes
EDN3	*EDN3*	*spotting lethal*	Waardenburg type 4 syndrome
EDNRB	*EDNRB*	*piebald*	Waardenburg type 4 syndrome
claudin14	*CLDN14*		DFNB29
TMPRSS3	*TMPRSS3*		DFNB10, DFNB8
DFNA5	*DFNA5*		DFNA5
otoferlin	*OTOF*		DFNB9
DSPP	*DSPP*		DFNA39
stereocilin	*STRC*		DFNB16
USH3	*USH3*		Usher 3

Table 1.2. Mutations causing Deafness. (DFNA: autosomal dominant loci; DFNB: autosomal recessive loci)

1.4c. Mutations affecting the Cytoskeleton and Hearing

Deafness-causing mutations have been identified in a number of genes that probably affect the actin cytoskeleton of hair cells. These studies also have shed further light on the function of these molecules. In the mouse mutant *jerker*, hair cell stereocilia develop, but rapidly lose stiffness, shorten, and degenerate. The mutated gene encodes espin, one of the two known actin cross-linking molecules of stereocilia (see also 1.1d). Abnormalities coincided with onset of auditory function which involves influx of Ca^{2+} ions into hair cells (Zheng et al., 2000c). The F-actin bundling activity of espin is not blocked by Ca^{2+} ions, in contrast to fimbrin (Bartles et al., 1998; Chen et al., 1999). Espin may therefore maintain actin filament integrity during mechanical stimulation.

Small GTPases of the RHO family regulate cytoskeletal remodeling in many cell types. Their function in hair cells is currently unknown, but a downstream effector of RHOA, diaphanous-1 (DIA1) has recently been implicated in deafness. Mutations in DIA1 lead to DFNA1, a progressive form of autosomal dominant hearing-loss. DFNA1 patients express an aberrant form of DIA1 (Lynch et al., 1997), a cytosolic molecule of the formin-homology (FH) family, proteins that are involved in regulating assembly of the cytoskeleton (Wallar and Alberts, 2003; Wasserman, 1998). In fibroblasts, DIA1 cooperates with the RHO-activated kinase ROCK and

VAsodilator-Stimulated Phosphoprotein (VASP) in the formation of F-actin containing stress fibers (Grosse et al., 2003; Nakano et al., 1999). One could envision a similar role for a DIA1 complex in hair cells, where they may cooperate downstream of RHOA to control the assembly of the hair cell cytoskeleton. However, DFNA1 patients suffer from late onset hearing loss, suggesting that DIA1 may function to maintain the hair cell cytoskeleton rather than to be important in its initial assembly. Alternatively, the hair cell cytoskeleton may not be properly assembled, leading to structural instability and cumulative defects during aging.

Several hearing and balance disorders coincide with mutations in different myosin genes. Myosins are actin based molecular motors that contain a conserved motor-domain and a non-conserved tail domain. Myosin molecules have been implicated in the regulation of many cellular processes including actin organization, regulation of tension on the actin cytoskeleton, and transport of organelles (Mermall et al., 1998). Mutations in the genes encoding the unconventional myosins MYOIIIA, MYOVI, MYOVIIA, MYOIX, and MYOXV have been linked to deafness and vestibular dysfunction (Müller and Evans, 2001; Steel and Kros, 2001).

It is likely that individual myosin motors fulfill specialized functions within hair cells for several reasons. First, the subcellular distribution of the myosin motors differs. For example, MYOVI is enriched in the cuticular plate and MYOVIIA is more widespread as it is present in the cell body and along the stereocilia (Hasson et al., 1997). Second, the phenotype of mice carrying mutations in individual myosin motors differs. Stereocilia in *MyoVI* mutant mice are fused, those in *MyoVIIA* mutant mice are splayed, while stereocilia in *MyoXV* mutant mice are short (Friedman et al., 1999; Steel and Kros, 2001). MYOXV localizes to stereocilia tips in several animal species and MYOXVA-GFP is targeted to stereocilia tips in transfected organ cultures. Therefore it has been suggested that MYOXV is essential for the graded elongation of stereocilia during hair cell maturation (Belyantseva et al., 2003). While further work is necessary, several studies suggest that some of these myosins may generate tension force between the actin cytoskeleton relative to attachment points at the cell surface (Müller and Evans, 2001). Accordingly, the connection between the hair cell cytoskeleton and the cell surface is defective in the absence of MYOVI (Self et al., 1999). Furthermore, MYOVIIA binds through its tail domain to a transmembrane protein termed vezatin, and it is localized in several epithelia to adherens junctions that contain cadherins (Kussel-Andermann et al., 2000).

MYOVIIA has also been suggested to be involved in adaptation of the transduction channel (Kros et al., 2002) as described in section 1.1g above. The MYOVIIA protein localizes to several compartments within the hair cell, including stereocilia. Further, MYOVIIA is a common component of cilia and microvilli, suggesting multiple functions for this protein (Wolfrum et al., 1998).

As described in section 1.4c below, splayed stereocilia are also observed in mice that carry mutations in genes affecting cell adhesion receptors that belong to the cadherin superfamily. Therefore these adhesion receptors may be in a common molecular pathway with Vezatin and or MYOVIIA

1.4d. Mutations in Extracellular Matrix Molecules and Deafness

Mutations in several different genes that encode ECM molecules lead in mice and humans to hearing loss and vestibular dysfunction (Table 2). The analysis of the disease phenotype in humans and mouse model systems has provided first insights into the specific functions of individual ECM components in the inner ear. Several mutations in ECM components affect the integrity and function of the mammalian tectorial membrane that contains collagenous and non-collagenous ECM components. Collagen 11α2 as well as the non-collagenous ECM components α̃ and β-tectorin, and otogelin are affected. Mutations in genes that encode collagen 11α2, α-tectorin and otogelin lead to structural defects in the tectorial membrane and to hearing impairment (Legan et al., 2000; Simmler et al., 2000b; Simmler et al., 2000a). So far no mutation in otogelin has been linked to disease in humans, but this gene is mutated in the *twister* mouse, and a targeted mutation in the otogelin gene has also been generated (Table 2). The mutant mice show impairment in both vestibular and auditory function. In the vestibule, otogelin is required for anchoring of the otoconial membranes (the equivalent of the tectorial membrane) to the sensory epithelium. In the cochlea, otogelin appears to be involved in organizing the fibrillar network of the tectorial membrane and it likely has a role in determining the resistance of this membrane to sound stimulation.

The analysis of mutations in the human *α-tectorin* gene highlights an important point. Both autosomal dominant (DFNA8, DFNA12) and recessive (DFNB21) forms of hearing loss (Table 2) are associated with mutations in *α-tectorin*. Thus, depending on the particular mutation within a gene, the disease phenotype can be inherited in different ways. Presumably, recessive mutations lead to a loss of function phenotype while dominant mutations lead to the generation of an abnormal protein that interferes with the function of the wild-type protein expressed from the unmutated allele. The analysis of mice that carry a targeted mutation in the *α-tectorin* gene have provided first insights into the mechanism of disease. Abnormal otoconial and tectorial membranes form, and the latter detach from the hair cell surface. In the tectorial membrane, all non-collagenous proteins are absent indicating that α-tectorin also has an effect on membrane integrity. The data suggest an important function for α-tectorin in organizing the structure of the tectorial membrane and determining its biophysical properties that are important for sound amplification (Legan et al., 2000).

Mutations that affect the basement membrane collagen IV lead to Alport syndrome (Kashtan, 2000). The afflicted patients suffer not only from varying degrees of hearing loss, but also from renal disease. The mechanism of disease progression in the ear is at present not clear, but studies in the kidney have provided evidence that collagen IV plays a pivotal role in the structural organization and stability of basement membranes. While a mouse model is available that recapitulates the kidney dysfunction of Alports patients, the mice do not faithfully recapitulate the inner ear defects seen in humans (Cosgrove et al., 1998). Thus, further studies will be necessary to understand collagen IV function in the ear.

1.4f. Integrins and Deafness

As outlined above, extracellular matrix molecules have been implicated in hair cell development in mice and men. Integrins are prominent receptors for ECM components (Hemler, 1999). Strikingly, mutation of an integrin gene causes vestibular dysfunction in the mouse. By gene targeting it has been shown that mice lacking the integrin $\alpha\square\beta_1$ show severe defects in the integrity of hair cell stereocilia in a subpopulation of hair cells in the vestibule. Loss of this integrin causes balance disturbances which are in line with the detected stereocilial abnormalities. Intriguingly, the $\alpha\square\beta_1$ protein, its ligand fibronectin and the integrin activated cytoplasmic focal adhesion kinase FAK colocalize to the apical hair cell surface during stereocilia formation. The localization of FAK and fibronectin is disrupted in the absence of the integrin $\alpha\square\beta_1$, suggesting that this integrin is required to assemble a transmembrane complex that regulates formation or stability of the cytoskeleton of hair cell stereocilia (Littlewood Evans and Muller, 2000). This interpretation is in agreement with findings in other cell types such as fibroblasts, where integrins regulate actin cytoskeletal dynamics by activating FAK (Giancotti and Ruoslahti, 1999). Interestingly, Integrins are linked to the RHO/DIA pathway (Palazzo et al., 2004), molecules which appear likewise to be important in hair cell function, since mutations in DIA1 cause deafness, as described in section 1.14c above. A different important downstream player of integrins is Integrin-Linked Kinase (ILK), a component mediating the connection of integrins to the actin cytoskeleton (Brakebusch and Fassler, 2003). Whether ILK plays a role in the establishment of the intricate actin cytoskeleton of the hair cell has not been established.

Further studies will be necessary to determine whether additional members of the extended integrin family also affect hair cell function. Furthermore, it will be important to establish whether mutations in integrins are also found in human patients suffering from deafness or vestibular dysfunction.

1.5. Cadherin Molecules and their Implication in Deafness

1.5a. The Superfamily of Cadherins

In the early 1980s Jacob and Coworker first described E-cadherin (uvomorulin), a cell surface glycoprotein involved in cell compaction (Hyafil et al., 1981; Peyrieras et al., 1983). Subsequently, a Ca^{2+} ion-dependent transmembrane cell-cell adhesion molecule with prominent expression in neural tissue, N-cadherin, was cloned and analyzed (Nose et al., 1987). This protein shares common amino acid sequences throughout its entire coding region with chicken L-CAM/E-cadherin and mouse uvomorulin/E-cadherin as well as the more recently cloned placental P-cadherin. These proteins are now all known to be part of the classical cadherin family, members of which confer Ca^{2+} ion-dependent intercellular adhesion via homophilic interaction.

Since then the discovery of novel cadherins has exploded, and it is now clear that the classical cadherins are only a fraction of the cadherin-related molecules and that these constitute a cadherin superfamily that has a multitude of diverse members (Fig 1.12) (Angst et al., 2001; Yagi and Takeichi, 2000b). Cadherins are characterized by a unique domain, called cadherin motif or Extracellular Cadherin domain (EC domain), containing the negatively charged DXD, DRE, and DXNDNAPXF sequence motifs, which are involved in Ca2+ binding (Takeichi, 1990). Although the presence of the EC domains is the hallmark or molecular signature of this protein family, their extracellular portions show a plethora of divergent structural elements. They can have 5 to 34 EC domain repeats of ~110 amino acid residues per EC domain. The vast majority of cadherins have a transmembrane domain but some are anchored to the plasma membrane via a glycosylphosphatidyinositol (GPI) moiety. Particularly, the cytoplasmic domain significantly diverges among the superfamily members, suggesting specific interactions with their respective cytosolic binding partners. Their spatial and temporal expression is complex and highly specific to the particular cell that synthesizes them, even within a single tissue. So far cadherins have been shown to be involved in many biological processes including cell adhesion, morphogenesis, cytoskeletal organization and cell sorting/migration, as well as in pathological conditions such as cancer and deafness.

Classical Cadherins

Classical cadherins are homophilic adhesion molecules, and for their homophilic interactions, the first N-terminal EC domain is of crucial importance. The intracellular domains are conserved among the members of each subfamily, and in the case of classic cadherins, they interact with catenin p120ctn and β-catenin at different portions of the cytoplasmic domain. The latter binds to α-catenin, and this molecular complex further associates with vinculin and other cytoskeletal proteins, resulting in the organization of adherens junction, or zonula adherens in polarized epithelial cells (Angst et al., 2001).

Seven-pass Transmembrane Cadherins

Recently, an unusual class of cadherins with a seven-pass transmembrane domain, which have similarity to a group of peptide hormone-binding, G-protein-coupled receptors have been identified in both vertebrates and invertebrates. One of these cadherins, *Drosophila flamingo* or *starry night*, is located at cell-cell boundaries in a polarized fashion. As mentioned in section 1.3b above, it functions together with *frizzled* in the acquisition of planar cell polarity (PCP) of wing hair cells. The extracellular portion of the molecule consists of nine EC domains but also contains EGF-like and laminin motifs. The cytoplasmic region lacks catenin-binding sites, and no putative cytoplasmic binding partners have been identified. This cadherin mediates homophilic interaction. Mutant flies lacking *flamingo* exhibit disorganized PCP, and the polarized distribution of Flamingo is influenced by alternating patterns of Frizzled expression. Such actions of Flamingo are likely mediated by a cytoplasmic signaling cascade distinct from that for classic cadherins (Yagi and Takeichi, 2000a). The functions of the three mammalian orthologs of *flamingo* (*CELSR1-3*) are only beginning to be understood as a mutation in *CELSR1* also affects PCP in the vertebrate inner ear (see .1.3b)

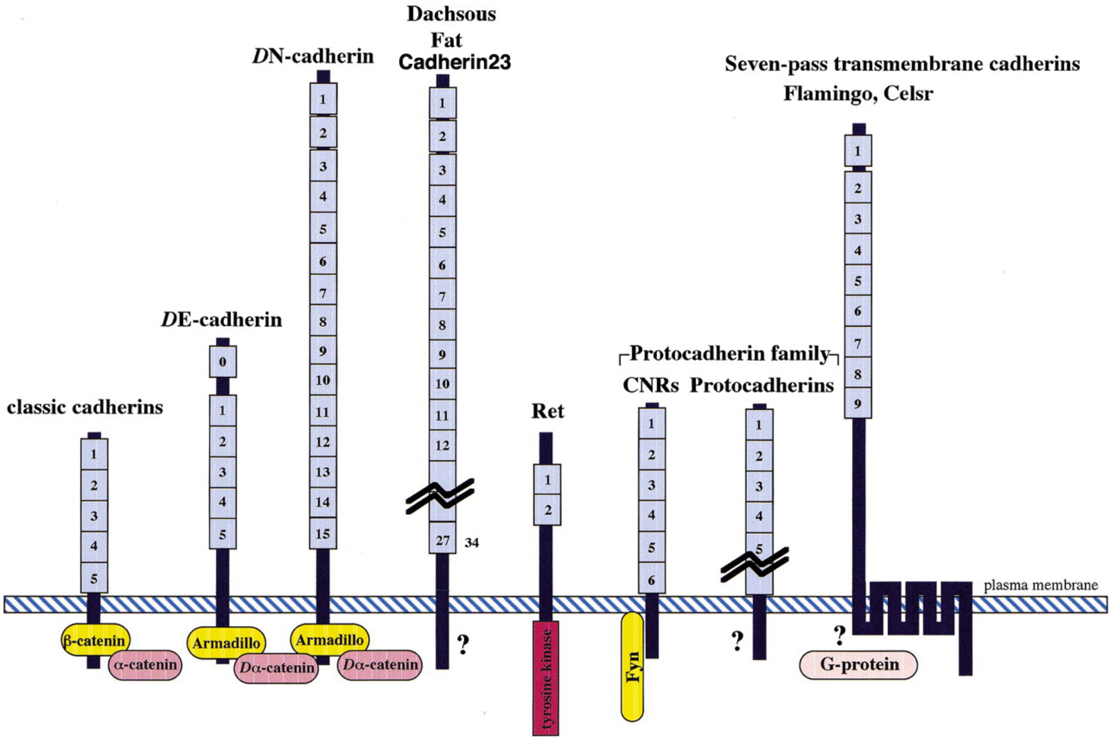
Dachsous
Fat
Cadherin23
*D*N-cadherin
Seven-pass transmembrane cadherins
Flamingo, Celsr
*D*E-cadherin
Protocadherin family
CNRs
Protocadherins
classic cadherins
Ret
27
34
plasma membrane
β-catenin
α-catenin
Armadillo
*D*α-catenin
Armadillo
*D*α-catenin
?
tyrosine kinase
Fyn
?
?
G-protein

Fig 1.12. The Superfamily of Cadherins
Schematically depicted are representative cadherin proteins of the Superfamily of cadherins. The grey, numbered boxes denote the number of EC domains in the extracellular portions of the proteins. The oval-shaped yellow and pink boxes represent cytosolic binding partners β-catenin (or the *Drosophila* ortholog *amadillo*), α-catenin or the Tyrosine kinase Fyn (D: *Drosophila*). (Taken from: *Genes Dev.* 2000; 14; 1169-1180).

Protocadherins

The protocadherin family is large and heterogenous. Members have up to 11 extracellular EC domains, a single transmembrane region and divergent and distinct cytoplasmic portions. Similar to classical cadherins, at least for one members of this cadherin family Ca^{2+}-dependent homophilic interaction has been demonstrated (Obata et al., 1995).

Protocadherins have been found not only in vertebrates but also in a variety of lower multicellular organisms which indicates that protocadherins may be the ancestral cadherins from which other families have evolved (from the Greek word `protos` - the first) (Frank and Kemler, 2002; Sano et al., 1993).

In mammals, multiple protocadherins are highly expressed in the nervous system; in fact, cadherins and in particular protocadherins are far more numerous in the brain than in any other tissue. Conservative estimates put the number of cadherins expressed in the brain at >80, and three clusters comprising a total of 52 novel protocadherins have been discovered on chromosome 5q31. The protocadherins within each of these three clusters or subfamilies share a common cytoplasmic tail, but differ in their extracellular domains, which gives each subfamily a multitude of possible extracellular interactions (Wu and Maniatis, 1999). Throughout brain development, protocadherins show distinct spatiotemporal expression patterns linked to other positional cues, which relate to the development of the brain in discrete segmental and functional subdivisions and provide a scaffold of adhesive clues (Arndt and Redies, 1998). Additionally Shapiro and Colman have proposed that cadherins are the cell surface lock-and-key molecules of synaptic adhesion (Shapiro and Colman, 1999). Their structural properties fit the structure as well as the spacing requirements of CNS synapses, and their known adhesion function and clustering in the synaptic junctions at electron-dense membrane-thickenings strongly point to them as the molecules responsible for adhesion between the pre- and postsynaptic neurons.. Additional evidence for the importance of protocadherin genes for neurons comes from the observation that interneurons are critically dependent on the protocadherin gamma cluster and degenerate in the absence of this cadherin cluster (Wang et al., 2002) Interestingly, the protocadherins contain a conserved N-terminal RGD motif, which suggests that they may also act as membrane-associated ligands for integrins.

Another group of protocadherin-type molecules, designated as CNR (Cadherin-related Neuronal Receptor), has been identified in the CNS through the yeast two-hybrid system approach using Fyn tyrosine kinase as bait (Kohmura et al., 1998). Fyn is crucial for normal brain organization and function. Mice lacking Fyn exhibit behavioral abnormalities, and also display electrophysiological deficits in induction of LTP in the excitatory synapses and the GABAergic synaptic response, as well as morphological abnormalities during the migration of neurons and formation of dendrites (Yagi, 1999). In neurons, Fyn is enriched in nerve growth cone membranes and the postsynaptic density fraction (Bixby and Jhabvala, 1993; Grant et al., 1992). The function of CNR cadherins could be coupled with these activities of Fyn. CNRs have a unique cytoplasmic region with a Fyn binding site, and carry six EC domains with an RGD motif in EC repeat 1 of their ectodomain. This first EC domain of CNR1 has been shown to interact with the large protein Reelin, produced by specialized neurons, the Cajal-Retzius cells in the marginal zone of the cortex (Senzaki et al., 1999). The interaction of Reelin with CNR1 has been proposed to trigger a signaling cascade which is of great importance for the development of the cerebral cortex in mammals, since Reelin deficiency in the *reeler* mouse leads to inverted layering in the cerebral cortex (D'Arcangelo et al., 1999)

The Fat Family of Cadherins

Fat and dachsous encompass another subfamily, both containing large tandem arrays of EC domains. Recessive lethal mutations in the *ft* (*fat*) gene cause hyperplastic, tumor-like overgrowth of larval imaginal discs in a cell-autonomous fashion, defects in differentiation and morphogenesis, and death during the pupal stage of *Drosophila*. These findings point to *fat* as a tumor suppressor gene at least in *Drosophila* (Buratovich and Bryant, 1997; Mahoney et al., 1991). In contrast, the ablation of the mouse *Fat* gene does not cause abnormalities in proliferation. Instead, the *Fat* knockout mice show defects in renal differentiation, forebrain and eye development (Ciani et al., 2003). The *Drosophila* dachsous molecule is a cadherin of 27 EC domains and highly homologous to the fat molecule which has 34 EC domains. Mutations in the *dachsous* gene lead to defects in the morphogenesis of the thorax, legs, and wings during *Drosophila* development of imaginal discs (Clark et al., 1995).

Both fat and dachsous molecules have cytoplasmic domains predicted to bind β-catenin.

Given the size of their extracellular domains, it seems unreasonable to assume these molecules engage in cell-cell adhesion in the same way as classical cadherins do with only 5 EC domains; Fat or Fat-like cadherins appear far too large to fit into the intercellular space between closely apposed adhering cells. Rather, the large extracellular domain of these proteins could maintain an extracellular gap between adjacent plasma membranes wider than normally found in adhesion junctions. This repulsion or spacer function has been suggested to explain the renal phenotype in the mouse *Fat* knockout where renal glomerular slit junctions are lost and the epithelial cell processes fuse (Ciani et al., 2003). Slit junctions are modified adhesion junctions, with a wide intercellular space allowing renal filtration. Mouse *Fat* is expressed at these sites and appears to be the spacer maintaining the wide gap between neighboring cells (Inoue et al., 2001).

1.5b Cadherins and Deafness

Two novel members of the cadherin superfamily, CDH23 (CDH23) and, protocadherin 15 (PCDH15), have been implicated in deafness in mice and man (Alagramam et al., 2001a; Alagramam et al., 2001b; Astuto et al., 2002; Ben-Yosef et al., 2003; Bolz et al., 2001; Bork et al., 2001; Di Palma et al., 2001b; Noben-Trauth et al., 2003; Wilson et al., 2001). As mentioned earlier, mutations in these genes can lead to Usher syndrome: Mutations in the gene encoding for Protocadherin 15 (pcdh15) lead to Usher Syndrome 1F and the gene encoding CDH23 also known as Otocadherin is mutated in patients suffering from Usher Syndrome 1D. Point mutations in other parts of *CDH23* lead to non-syndromic as well as age-related hearing loss in human patients (Davis et al., 2003; Davis et al., 2001; Holme and Steel, 2004; Noben-Trauth et al., 2003). PCDH15 has 11 EC domains and CDH23 contains 27 extracellular repeats, the same number as the *Drosophila* Dachsous molecule. With its large extracellular domain CDH23 has closest homology to the FAT proteins, but lacks their catenin binding-sites in the cytosolic tail.

Different to classical cadherins, which link adjacent cells together, one of the novel cadherins could crosslink adjacent stereocilia within one hair cell, thereby helping to organize and maintain hair bundle integrity. While connectors between hair cell stereocilia have been detected by ultrastructural studies, the molecular identity of these cross linkers is largely unknown. Particularly CDH23 is a particularly attractive candidate due to its large extracellular domain, which may enable the protein to bridge the gap between adjacent stereocilia.

The Aim of the Thesis

2. The Aim of the Thesis

The differentiation and maturation of hair cells in the vertebrate inner ear requires a series of steps including the elaboration of the unique hair bundle, which is located directly at the interface between the physical stimulus and the downstream signaling events of the cell. As pointed out in section 1.1e of chapter 1, this bundle, consisting of individual stereocilia is shaped and stabilized by linker molecules which crosslink adjacent stereocilia. Moreover the uppermost linker molecule, the tip link, is hypothesized to constitute part of the intricate transduction apparatus and may thus be involved in transduction channel gating. Although these linker molecules are clearly detectable at the ultrastructural level and some of their biochemical properties are known, non of the relevant genes have been identified to date.

In order to identify any components of this intricate linker system we considered deafness genes as candidates, reasoning that the loss of one class of linker molecules would lead to impaired auditory function. Stereocilia linker molecules have been suggested to be comprised of extracellular matrix (ECM) molecules and mutations of several genes encoding ECM components give rise to deafness. However, electron microscopic studies revealed that the linker molecules appear to consist of two components, peripheral ECM material (mostly glycoconjugates, commonly referred to as glycocalix) and a filamentous core component likely to be a transmembrane protein. We therefore hypothesized that a linker molecule is comprised of a cytosolic and an extracellular domain. We further envisioned that the plasma membranes of opposing stereocilia may be similar to plasma membranes of neighboring cells in any given tissue, which are interconnected by adhesion receptors. The observation that tip- and ankle links are sensitive to Ca^{2+} chelation indicated that a Ca^{2+}-dependent adhesion mechanism may indeed play a role between stereocilia. Different to cell-cell contacts of a few nanometers, the gap between adjacent stereocilia is 150 – 300 nm, a distance that could be spanned by molecules with unusually large extracellular domains only.

Two putative adhesion receptors have been implicated in several forms of deafness: CDH23 and PCDH15. Although their localization has previously not been established, evidence for their implication in hair bundle integrity came from the observation that mice with natural occurring mutations in either gene, the *walzer*

(*Cdh23*) and *ames walzer* (*Pcdh15)* mice, display splayed stereocilia bundle morphology (Alagramam et al., 2001a; Di Palma et al., 2001b). CDH23 was chosen as the more attractive candidate due to its larger extracellular domain. Assuming a structure of the extracellular domain similar to classical cadherins, the PCDH15 domain would be too short to span the gap.

To understand the function of CDH23 in the context of the inner ear, emphasis was placed on the characterization of three different aspects of this protein: localization of the protein in the inner ear at the ultrastructural level, biochemical properties of the cytosolic portion of CDH23 -which lacks any known structural motifs- and biochemical properties of its extracellular domain containing 27 EC domains.

Due to the very fact that mutations in the *CDH23* gene cause Usher Syndrome or increase the risk of a predisposition to Age-related or Noise-induced Hearing loss, this study may not only elucidate the role of CDH23 in these pathological manifestations but also point in new therapeutic directions. Since Usher Syndrome is accompanied by retinal degeneration, this study may also encourage further analysis of common themes between the auditory and visual system.

Paper I

The Usher Syndrome Proteins Cadherin 23 and Harmonin form a Complex by means of PDZ-Domain Interactions

Jan Siemens, Piotr Kazmierczak, Anna Reynolds, Melanie Sticker, Amanda Littlewood-Evans, and Ulrich Müller

Proceedings of the National Academy of Sciences, Vol. 99, 14946-51, Nov. 2002

3.1. Abstract

Usher syndrome type 1 (USH1) patients suffer from sensorineuronal deafness, vestibular dysfunction, and visual impairment. Several genetic loci have been linked to USH1, and four of the relevant genes have been identified. They encode the unconventional myosin VIIa (MYOVIIA), the PDZ-domain protein harmonin, and the putative adhesion receptors cadherin 23 (CDH23) and protocadherin 15 (PCDH15). We show here that CDH23 and harmonin form a protein complex. Two PDZ domains in harmonin interact with two complementary binding surfaces in the CDH23 cytoplasmic domain. One of the binding surfaces is disrupted by sequences encoded by an alternatively spliced CDH23 exon that is expressed in the ear, but not the retina. In the ear, CDH23 and harmonin are expressed in the stereocilia of hair cells, and in the retina within the photoreceptor cell layer. Since CDH23-deficient mice have splayed stereocilia, our data suggest that CDH23 and harmonin are part of a transmembrane complex that connects stereocilia into a bundle. Defects in the formation of this complex are predicted to disrupt stereocilia bundles and cause deafness in USH1 patients.

3.2. Introduction

About 1 in 800 children is born with hearing impairment and large parts of the aging population are afflicted by age-related hearing loss. Single gene defects are responsible for ~ 50% of the hearing defects in newborns, and genetic predisposition is an important determinant in some forms of age-related hearing loss. Approximately 50 deafness genes have been identified, but the mechanisms by which these genes exert their functions are largely unclear (Hone and Smith, 2001; Müller and Evans, 2001; Steel and Kros, 2001).

Many forms of deafness involve defects in hair cells, the mechanosensors for sound waves in the cochlea of the inner ear. Each hair cell has an apical bundle of 30-300 stereocilia that contain mechanotransduction channels. The channels change their open probability during stereocilia deflection. Importantly, individual stereocilia of a hair cell do not act alone. They are connected through linkage systems such as tip links, side links, ankle links, and top connectors into a bundle that moves as a whole during sound stimulation (Fig. 1a) (Müller and Evans, 2001; Steel and Kros, 2001). Antibodies that recognize extracellular linkages in stereocilia have been raised (Goodyear and Richardson, 1999; Richardson et al., 1990), but the molecules that form the linkages are not known. The tip link may serve as a gating spring that regulates opening and closing of the transduction channel (Corey and Hudspeth, 1983a; Pickles et al., 1984). Side and ankle links may mediate adhesion between stereocilia to connect them and to coordinate their movement (Gillespie and Walker, 2001; Hudspeth, 1992).

By positional cloning and through the analysis of genetically modified mice several deafness genes have been identified that affect the integrity of the stereocilia bundle. Promising candidate molecules to connect stereocilia are CDH23 and PCDH15, members of the cadherin superfamily of cell adhesion molecules (Yagi and Takeichi, 2000a). Mutations in the *CDH23* and *PCDH15* gene cause USH1D and USH1F, respectively, as well as other forms of deafness (Ahmed et al., 2001; Alagramam et al., 2001b; Bolz et al., 2001; Bork et al., 2001). Stereocilia are splayed in *Cdh23*- and *Pcdh15*-deficient *waltzer* and *Ames waltzer* mice, suggesting that both molecules have specialized adhesive functions important to maintain the integrity of the stereocilia bundle (Alagramam et al., 2001b; Alagramam et al., 2000; Di Palma et al., 2001a; Raphael et al., 2001). PCDH15 is expressed in hair cells (Alagramam et al., 2001b), but the expression pattern of CDH23 has not been reported. Likewise, downstream effectors of these cadherins are not known. The PCDH15 cytoplasmic domain contains proline-rich regions that may mediate protein-protein interactions (Alagramam et al., 2001b). No protein interaction surfaces or catalytic domains have been described in the CDH23 cytoplasmic domain. Candidate molecules to mediate PCDH15 and CDH23 functions are myosin VIIa, and the PDZ domain protein harmonin. Both proteins are expressed in hair cells, and mutations in their genes lead to USH1B and USH1C, respectively (Bitner-Glindzicz et al., 2000; Verpy et al., 2000; Weil et al., 1995). Furthermore, myosin VIIa deficient *shaker-1* mice have splayed stereocilia (Self et al., 1998). Myosin VIIa is expressed at adherence junctions in several tissues, where it binds via vezatin and catenins to classical cadherins. In hair cells, myosin VIIa and vezatin colocalize at ankle links (Kussel-Andermann et al., 2000). Since classical cadherins and catenins are not expressed in stereocilia, other receptors such as CDH23 and PCDH15 may recruit the vezatin/MYOVIIA complex in hair cells.

As a first step towards understanding the function of CDH23, we have determined its expression pattern in the inner ear and retina and searched for proteins that interact with its cytoplasmic domain. We show that CDH23 is expressed in hair cell stereocilia and the photoreceptor layer in the retina, and that it binds to harmonin. Interestingly, complex formation between CDH23 and harmonin is regulated by an alternatively spliced exon in the CDH23 gene that is specifically expressed in the ear. Since stereocilia are splayed in *Cdh23*-deficient mice (Di Palma et al., 2001a), our data suggest that CDH23 and harmonin cooperate to assemble a transmembrane complex that connects stereocilia.

3.3. Material and Methods

If not stated differently, all chemicals were purchased from Sigma.

Antibodies

Rabbit antisera were raised against Glutathione-S-Transferase (GST) fused to the cytodomain of CDH23, expressed in and purified from *E. coli* (Sambrook and Russell, 2001). Inner ear RNA was reverse transcribed (RT) and the CDH23 cytoplasmic domain amplified by polymerase chain reaction (PCR)(5'-GGGGGATCCAACT GGTACTACAGGACCA-3'; 5'-CGCGAATTCTCACAGC TCCGTGATTTCCAG AG-3'). The fragments were cloned into the BamHI/EcoRI site of the pGEX-2TK vector (Amersham Pharmacia Biotech). The fusion protein was expressed and purified from *E.coli* as described below in the chapter "GST pull-down experiments". The protein was eluted from the Glutathione sepharose 4B GST affinity column (Amersham Pharmacia Biotech) by incubation with 50 mM Tris buffer pH 8 containing 15 mM Glutathione, 150 mM NaCl. The eluate was dialyzed against multiple changes of 50 mM Tris pH 7.5 containing 150 mM NaCl. Immunization was carried out at Eurogentech, Belgium. The antisera were purified against a fusion protein between the CDH23 cytodomain and the maltose binding protein expressed from pMAL-c2 (New England Biolabs). The CDH23 cytodomain was therefore cloned into the BamHI site of the pMAL-c2 vector. The MAL-CDH23 fusion protein was produced in the same way as the GST-CDH23 fusion protein with the difference that the fusion protein was eluted from an amylose resin (New England Biolabs) in 20 mM Tris pH 7.4 containing 150 mM NaCl and 10 mM Maltose. The MAL-CDH23 fusion protein was dialyzed against Coupling buffer (0.1 M Sodium Hydrogencarbonate pH 8; 0.5 M NaCl) and then coupled to HCl-activated Cyan bromide sepharose 4B beads (Amersham Pharmacia Biotech) for two hours at room temperature on a rotating wheel. After several washes with Coupling buffer, the affinity column was blocked by incubation with 0.1 M Tris pH 8 over night at 4°C. Subsequently, the column was washed 3x by alternating between solutions of 0.1 M Sodium Acetate pH 4 containing 0.5 M NaCl and 0.1 M Tris pH 8 containing 0.5 M NaCl. The sepharose-coupled MAL-CDH23 protein was packed into columns and washed with PBS 0.1% Tween-20. The affinity resin was then washed with 10 bed volumes 0.2 M Glycine pH 2.5 and again flushed with PBS 0.1% Tween-20 until neutral pH was reached. For antisera purification, a saturated Ammonium sulfate solution was slowly added to 10 ml of serum until 50% saturation was reached. The solution was stirred for 10′ in the cold room and then centrifuged down for 30′ at 10000 rpm in a SS34 rotor. The supernatant was discarded and the pellet resuspended in 10 ml PBS. The solution was dialyzed against multiple changes of PBS to eliminate Ammonium sulfate from the antibody solution. 3 to 5 ml of this Immunoglobulin-enriched serum fraction was applied to the affinity column and washed with PBS containing 0.1% Tween-20 until the flow-through did not contain protein anymore, as determined by the OD_{280}. The antibodies were eluted from the columns by applying 0.2M Glycine pH 2.5 and 0.8 ml aliquots were collected and immediately neutralized by the addition of 200 µl 1M Tris pH 8. The OD_{280} of all aliquots were determined and the aliquots with highest protein content pooled and dialyzed against multiple changes of PBS.

Harmonin antisera were raised against a mixture of two peptides (NH_2-MDRKVAREFRHKVDFC-COOH, and NH_2-CRSRKLKEVRLDRLHP-COOH). Immunization was carried out at Eurogentech (Parc Industriel, Belgium). Antisera were purified against the peptides used as an immunogen. Coupling of the peptides to activated Cyan bromide sepharose was essentially the same as described above (Harlow and Lane, 1999).

All antibodies were tested for their specificity by Western blot with protein extracts from cells overexpressing CDH23 fusion proteins or Harmonin as described below. For Immunohistochemistry the CDH23 cytodomain antibody was utilized at a final dilution of 1:400 to 1:1000.

Immunohistochemistry

Immunohistochemistry was carried out on 8 µm to 12 µm thick cryosections of OCT embedded mouse inner ears or mouse heads. Tissues had been fixed in PBS containing 4% PFA at 4°C over night prior to OCT embedding and cryosectioning. Sections collected on glass slides were left to dry, then rehydrated in PBS for 10′ at room temperature, blocked for 20′ in PBS containing 100 mM Glycine and then blocked in PBS 8% NGS, 0.3% BSA, 0.2% Triton for 30′ to 1 hour. 1st Antibody was diluted in PBS 4%NGS, 0.15% BSA, 0.1% Triton and sections incubated over night at 4°C in a humidified chamber. Subsequently, sections were washed 3x in PBS for

10′ at room temperature. Alexa 594- or Biotin labelled goat anti-rabbit 2nd Antibodies (Molecular Probes, Vector Labs) were diluted together with Alexa 488-Phalloidin (1:100; Molecular Probes), in PBS 4% NGS, 0.15% BSA, 0.1% Triton and sections incubated for 1 to 2 hours at room temperature in a humidified chamber. After 3x washing steps in PBS (10′ each), sections were mounted with Vectashield (Vector Labs). In case of labelling with a biotinylated 2nd antibody for light microscopy, a further incubation step with the ABC complex solution (ABC reagent, Vector Labs) was carried out according to the supplier's protocol. Fluorescent images were collected on a Deltavision microscope and processed by deconvolution.

Expression Analysis of CDH23 Splice Variants.

RNA from mouse tissues was prepared using Trizol (Life Technology) and total RNA prepared as described by the manufacturer's protocol. RT-PCR was carried out with the following primers (1: 5'-GACAACATCGCCAAGCTG-3'; 2: 5'-ATGAACCATGTG GATTCCATC-3'; 3: 5'-GCAAGCTGTTGAGATCAGTGG-3'). The PCR Protocol used started with an annealing temperature of 61°C dropping down to 55°C in increments of 1°C in every successive cycle with annealing-, elongation- and denaturation times of 45′′ and an elongation temperature of 72°C and a denaturation temperature of 95°C. Once the annealing temperature of 55°C was reached, 30 more PCR cycles, employing the above mentioned temperature and time constrains, were run.

PCR products were separated on 1% Agarose gels and visualized by Ethidiumbromide staining of DNA fragments.

Yeast Two-Hybrid Assays

CDH23 constructs were expressed as fusions with the Gal4 DNA binding domain from pGBKT7 (Clontech). Harmonin constructs were expressed from pGBKT7, or as fusions to the Gal4 activation domain using pGADT7 (Clontech). DNA fragments were amplified by PCR and cloned into NdeI/BamHI sites (CDH23) or SmaI/BamHI sites (Harmonin). For the Yeast two-hybrid assay a Yeast colony from the AH109 strain was inoculated in 4 ml of YPAD medium (6g Yeast extract (Difco), 12 g Peptone (Difco), 12 g Glucose, 60 mg Adenine Hemisulphat, 600 ml water) and incubated over night at 30°C rotating horizontally at 300 rpm. Yeast cells were seeded out in a density of 5×10^6/ml in 50 ml of pre-warmed fresh YPAD medium and incubated at 30°C on a shaker for another 4 hours. The Yeast cells were collected by centrifugation at 30000 x g for 5′, the medium was discarded and the cell pellet taken up in 25 ml of sterile water followed by centrifugation. The cell pellet was washed once with water containing 0.1 M LiAc, and taken up 1 ml water containing 0.1 M LiAc. 50 µl of this cell suspension were employed per yeast transformation by removing the supernatant and adding 240 µl Polyethylene Glycol (50% w/v), 36 µl 1 M LiAc, 25 µl boiled Salmon Sperm DNA (2 mg/ml), 0.1 µg to 10 µg Plasmid DNA and water to a final volume of 360 µl. This transformation mixture was mixed extensively, incubated at 30°C for 30′ followed by a 30′ heat shock at 42° C. Subsequently, the yeast cells were pelleted in a micro-centrifuge, the transformation solution removed and the yeast cells taken up in 0.5 ml of sterile water. 50 µl to 100 µl of this cell suspension were streaked out on agar plates containing synthetic drop out medium (4 g Yeast Nitrogen Base (w/o amino acids, Difco), 12 g Glucose, 10 g Bacto Agar (Difco), 600 ml water and 0.5 g of the following amino acid mixture: 2 g Arginine HCl; 2 g Isoleucine; 2 g Lysine HCl; 2 g Methionine; 3 g Phenylalanine; 6 g Homoserine; 2 g Tyrosine; 1.2 g Uracil and 9 g Valine. For the transformation control 2 g Leucine and 3 g Tryptophan were added as well) either lacking Adenine and Histidine for control of the transformation efficiency or lacking Adenine, Histidine, Leucine and Tryptophan to measure protein interactions under selective pressure (Gietz and Woods, 2002).

GST Pull-Down Experiments

Harmonin and PDZ domains were expressed via the T7 promotor from pGADT7 by *in vitro* transcription/translation using the TNT Coupled Reticulocyte Lysate System (Promega) in the presence of radiolabelled S-35-methionin (Amersham Pharmacia Biotech). The cytosolic domain of CDH23 splice variants as well as truncated versions of it were cloned into EcoRI/BamHI restriction sites of the pGEX-2TK vector (Amersham Pharmacia Biotech) to give respective fusions with sequences encoding Glutathione-S-Transferase (GST). The GST fusion proteins were produced in the bacterial *E.coli* strain DH5α in 100 ml over night culture (37°C, 220 rpm). After 12 hours incubation the cultures were diluted 1:10 in fresh medium and induced for target protein expression by the addition of Isopropyl-β-D-Thiogalactopyranosid (IPTG) to a final concentration of 1 mM. After incubation for another 3 to 4 hours at 37°C (in case of constructs encoding the CDH23 splice variant with exon 68, induction temperature was decreased to 30°C, due to inclusion bodies formed in bacteria at higher temperatures) the bacteria were lysed in 10-20 ml NETN-buffer (50 mM Tris-buffer of pH 7.5 containing 150 mM NaCl, 1 mM EDTA, 0.5% NP40, 50 mM NaF, 1 mM Phenyl methyl sulfonyl fluoride (PMSF), Protease Inhibitor Cocktail (Roche) and 1 mM DTT) by sonication 3x 20´´ at 4°C. Subsequently, the cell debris was centrifuged down for 10′ at 12000x g and soluble proteins in the supernatant bound to glutathione sepharose beads (Amersham Pharmacia Biotech) for 1 hour at 4°C. After 3x washing in NETN-buffer, the *in vitro* transcribed/translated radioactively labelled Harmonin proteins were incubated with the GST-fusion proteins bound to Glutathione Sepharose in NETN-buffer. After 2 hours of incubation at 4ºC the reactions were washed 4x with NETN-buffer and the bound Harmonin proteins were eluted by boiling the samples in Laemmli sample buffer (Sambrook and Russell, 2001), subjected to SDS-PAGE electrophoresis (described below) and detected by radiography**.** For quantification, Harmonin bands were cut out from SDS-PAGE gels and radioactivity measured by scintillation counting. Input amounts of GST-CDH23 were determined by densitometrical scanning of Coomassie stained SDS-PAGE gels. The amount of radioactivity was normalized against the amount of GST-CDH23 fusion protein.

Cell Transfections, Immuno-precipitations and Western blotting

The cDNA encoding a Harmonin splice variant (amino acid 1 to 548) was cloned into the C1-GFP vector (Clontech). Harmonin was amplified by PCR (5’-TAAC CCGGGGATGGACCGGAAGGTGGCCC-3’; 5’-CGCGGATCCTT AAAAGAAGGTTAGCTCGTCATC-3’). The CDH23 cytoplasmic domains were amplified by PCR (5’-GGGAATTCAAGCTTAACTGGTACTACAGGAC-3’; 5’-GGGCCGCTCGAGTCACAGCTCCGTGATTTCCAG-3’) and inserted into pCMVIL2R (Akiyama et al., 1994). For cell transfections, 3x10^5 HEK 293 cells or 1x10^5 COS cells were seeded out per 6-well dish. 24 hours later cells were transfected with 0.5µg of each DNA plasmid employing the method of Chen and Okayama (Chen and Okayama, 1987) or using Fugene (Roche) according to the suppliers protocol. 48

h after transfection, protein extracts were prepared in Lysis buffer (50 mM HEPES, pH 7.5; 150 mM NaCl; 1.5 mM $MgCl_2$; 1 mM EDTA; 10 % (vol/vol) glycerol; 1% Triton X-100; 100 mM NaF; 1 mM Phenylmethylsulfonyl fluoride; 10 μg/ml Aprotinin) and used for Western blots (Muller et al., 1995). In brief, extracts were subjected to electrophoresis on 10% SDS-polyacrylamide gels (SDS-PAGE). Proteins were transferred onto Polyvinylidine difluoride (PVDF) membrane (Immobilon^{TM} P, Millipore) with a wet blotter. Prior to blotting the membrane was briefly soaked in methanol followed by water. For blotting the membrane and SDS-gel were assembled between 2 layers of 3 MM paper and sponges. This sandwich was immersed into transfer buffer (14.5 g Tris, 67 g Glycine and 1.2 l of methanol filled up to a total volume of 6 l with water) in the blotting chamber. Proteins were transferred at an electric current of 1 mA/cm^2 for 1 to 2 hours. Subsequently the membrane was blocked in 10% horse serum (Gibco-BRL) in TBST (50 mM Tris-HCl pH 7.4, 150 mM NaCl, 0.05% Tween-20) for 1 hour at room temperature and incubated with primary rabbit polyclonal antibodies directed against CDH23-cyto (1:2000); Harmonin (1:200); GFP (1:2000, immunogen: GST-GFP; antisera prepared by Dr. U. Müller); IL2-Recptor α (1:200, Santa Cruz) in TBST containing 10% horse serum at 4°C over night on a rocking platform. After washing 3x 10´ in TBST the membrane was incubated with the secondary antibody (anti-rabbit coupled to peroxidase, 1:15000, Amersham Pharmacia Biotech) for 1 hour in TBST containing 10% horse serum. Subsequently, the membrane was washed in TBST, incubated with chemiluminescence detection solution (ECL-Western Blotting Detection System, Amersham Pharmacia Biotech) and exposed to autoradiography film (Biomax^{TM}, Kodak) for various time spans (1′ to 30′). For re-probing the membrane, the blot was incubated in a solution containing 100 mM β-mercaptoethanol, 2% SDS, and 62.7 mM Tris pH 6.8 for 30′ at 60°C. Before the membrane was subjected to blocking and reprobing with a different antibody, the membrane was extensively washed in water.

For immunoprecipitation from transfected cells, protein extracts were prepared in lysis buffer, as described above. For immunoprecipitation from tissue, the brain of a P6 C57Bl/6 mouse was homogenized in RIPA buffer (50mM Tris pH 7.5, 150mM NaCl, 1% Triton X-100, 0.5% DOC, 0.1% SDS, 1 mM phenylmethylsulfonyl fluoride; 10 μg/ml aprotinin), with a Dounce Tissue Homogenizer and diluted 1:1 with 50mM Tris, 150mM NaCl pH 7.5. The cell– and tissue debris was removed from the protein extract by centrifugation (5′, 14000 rpm in an Eppendorf table top centrifuge at 4°C) two times and the supernatant further precleared by incubation with 50 µl slurry Protein A sepharose for 30′ at 4°C on a rotating wheel. The supernatant was transferred to a fresh tube and supplemented with 30 µl slurry Protein A sepharose as well as either 3 µg of anti-Harmonin antibody, 3 µg of mouse anti-Il-2 Receptor α antibody (Upstate Biotechnologies) or 3 µg rabbit anti-GFP antibody. After incubation at 4°C on a rotating wheel for 4 hours to over night, the sample was washed 3x in ice-cold HNTG (50 mM Hepes pH 7.4, 150 mM NaCl, 0.1% Triton, 10% Glycerol) and subjected to Western blot analysis as described above.

3.4. Results

3.4a. The CDH23 Cytoplasmic Domain: PDZ-binding Domains and Alternative Splicing.

To identify downstream effectors of CDH23, we analyzed the sequence of its cytoplasmic domain. We identified two putative binding sites for PDZ-domains (referred to as PDZ-binding interfaces, PBIs). PBIs are frequently found at the C terminus of cell surface receptors and have been categorized based on their sequence and binding specificity as class-I, -II, -III, and -IV PBIs (Harris and Lim, 2001; Sheng and Sala, 2001; Vaccaro and Dente, 2002). A putative class-I PBI is present at the C terminus of CDH23 (Fig. 3.1b). Less frequently, proteins contain internal PBIs, but no consensus sequence had emerged (Harris et al., 2001; Hillier et al., 1999). The CDH23 cytoplasmic domain contains a stretch with significant homology to a protein domain in the adaptor protein Ril, which functions as an internal PBI (Cuppen et al., 1998) (Fig. 3.1b). This is the first example of such sequence conservation and suggests that amino acids 91-184 of CDH23 are part of a PBI. Two CDH23 mRNAs that differ by an insert of 105 bp have been described. The 105 bp are encoded by an alternatively spliced exon (exon 68) (Bork et al., 2001; Di Palma et al., 2001c), and insert 35 amino acids into the putative internal PBI of CDH23 (Fig. 3.1b). mRNA containing exon 68 is expressed preferentially in inner ear sensory epithelia. Other tissues such as heart, kidney, spleen, brain, and retina contain CDH23 mRNA lacking exon 68 (Fig. 3.1c, and data not shown). This suggests that exon 68 encoded sequences regulate CDH23 function in the inner ear.

3.4b. Harmonin: PDZ Domains and Interactions with CDH23 in Yeast.

To identify proteins that bind to the CDH23 cytoplasmic domain, we searched for PDZ domains in known deafness genes. Three putative PDZ domains are present in harmonin (Bitner-Glindzicz et al., 2000; Verpy et al., 2000), and we identified a putative class-I PBI at its C terminus (Fig. 3.1d). We refer to the PDZ domains, from the N- to the C-terminus, as PDZ1, PDZ2, and PDZ3. PDZ domains harbor characteristic amino acid sequences, such as the R/K-XXX-GLGF motif that forms part of the protein interaction surface. Differences in surrounding amino acids provide interaction-specificity for target proteins (Sheng and Sala, 2001; Songyang et al., 1997). PDZ1 and PDZ2 of harmonin contain variations of the R/K-XXX-GLGF motif, with only the GLG sequence being conserved. PDZ3 does not contain the GLG motif, but a distant variant with homology to a PDZ domain in p55 (Fig. 3.1d), (Marfatia et al., 1997). This suggests that each PDZ domain of harmonin engages in interactions with different PBIs.

Candidate target PBIs include the two PBIs of CDH23, and the C terminal PBI of harmonin. We tested whether harmonin interacts with itself and with CDH23 by yeast two-hybrid analysis (Fig. 3.2). Harmonin interacted with harmonin, but interactions were disrupted when the C terminal PBI was deleted in both harmonin molecules used to measure interactions (harm□7). Harmonin fragments containing PDZ1, but not PDZ2 and PDZ3, interacted with full length harmonin, suggesting that PDZ1 interacted with the C terminal PBI in harmonin (Fig. 3.2c,d). The CDH23(-68) and CDH23(+68) cytoplasmic domains also interacted with harmonin, but not with enigma, a protein that contains a PDZ domain homologous to PDZ1 and PDZ2 of harmonin (Guy et al., 1999) (Fig. 3.2e,f; and data not shown).

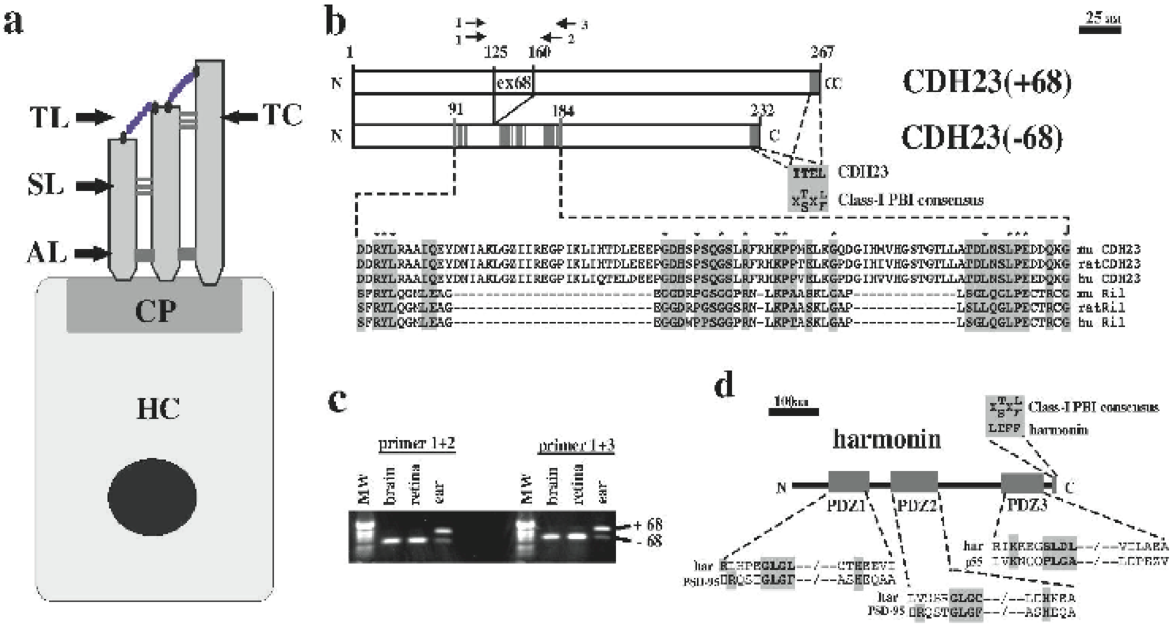
a
TL
SL
AL
TC
CP
HC
b
1
2
3
1
125
160
267
N
ex68
CC
CDH23(+68)
91
184
232
N
C
CDH23(-68)
ITEL CDH23
$x^T_S x^L_F$ Class-I PBI consensus
25 aa
DDRYLRAAIQEYDNIAKLGZIIREGPIKLIKTDLEEEPGDHSPSQGSLRFRHKPPMELKGQDGIHMVHGSTGTLLATDLNSLPEDDQKG mu CDH23
DDRYLRAAIQEYDNIAKLGZIIREGPIKLIKTDLEEEPGDHSPSQGSLRFRHKPPTELKGPDGIHIVHGSTGTLLATDLNSLPEDDQKG ratCDH23
DDRYLRAAIQEYDNIAKLGZIIREGPIKLIQTELDEEPGDHSPSQGSLRFRHKPPVELKGPDGIHVVHGSTGTLLATDLNSLPEEDQKG hu CDH23
SFRYLQGMLEAG-------------------------EGGDRPGSGGPRN-LKPAASKLGAP-------------LSGLQGLPECTRCG mu Ril
SFRYLQGMLEAG-------------------------EGGDRPGSGGSRN-LKPAASKLGAP-------------LSLLQGLPECTRCG ratRil
SFRYLQGMLEAG-------------------------EGGDWPPSGGPRN-LKPTASKLGAP-------------LSGLQGLPECTRCG hu Ril
c
primer 1+2
primer 1+3
MW
brain
retina
ear
MW
brain
retina
ear
+ 68
- 68
d
100 aa
$x^T_S x^L_F$ Class-I PBI consensus
LIFF harmonin
harmonin
N
C
PDZ1
PDZ2
PDZ3
har
PSD-95
har
PSD-95
har
p55

Fig. 3.1. Hair Cell Diagram, Protein-Protein Interaction Domains in CDH23 and Harmonin, and Alternative Splicing of CDH23. (a) A diagram of a hair cell (HC) is shown. The stereocilia are anchored at the cuticular plate (CP) to the hair cell body. They are connected to each other through extracellular linkages such as the tip link (TL), top connectors (TC), side links (SL), and ankle links (AL). (b) The cytoplasmic domain of CDH23 contains two putative PBIs. The C terminus of CDH23 fits the consensus sequence for class-I PBIs (Sheng and Sala, 2001). An internal domain in the CDH23(-68) cytoplasmic domain shows homology to a PBI in Ril (Cuppen et al., 1998). In the CDH23(+68) isoform, 35 amino acids that are encoded by the alternatively spliced exon 68 are inserted into the Ril homology region. Grey boxes outline amino acids that are identical/conserved between CDH23 and Ril. Identical amino acids are indicated by an asterisk (*). (c) RT-PCR was carried out with RNA from adult mice using two sets of CDH23 specific primers (see panel b). The identity of the fragments was confirmed by DNA-sequencing. The CDH23 isoform containing exon 68 was expressed in the inner ear but not in the brain or retina. MW, molecular weight marker. (d) Harmonin contains three PDZ domains (Bitner-Glindzicz et al., 2000; Verpy et al., 2000), and a class-I PBI. PDZ1 and PDZ2 have similarity to PDZ domains in PSD-95 (Kim et al., 1995; Kornau et al., 1995). PDZ3 shows similarity to a PDZ domain in p55 (Marfatia et al., 1997).

Truncations that deleted the putative C terminal PBI of CDH23 (CDH23ΔC(+68) and CDH23ΔC1(-68)) interacted with harmonin, while deletion of both putative PBIs (CDH23ΔC2(-68)) abolished interaction (Fig. 3.2e,f). We next identified domains in harmonin that mediate interactions with CDH23. Harmonin fragments containing PDZ1 or PDZ2 interacted with CDH23(-68) and CDH23(+68). Interactions with PDZ2 were disrupted when the C terminal PBI of CDH23 was deleted. Interactions with PDZ1 were abolished by deletion of both PBIs. PDZ3 did not interact with CDH23 (Fig. 3.2e,f).

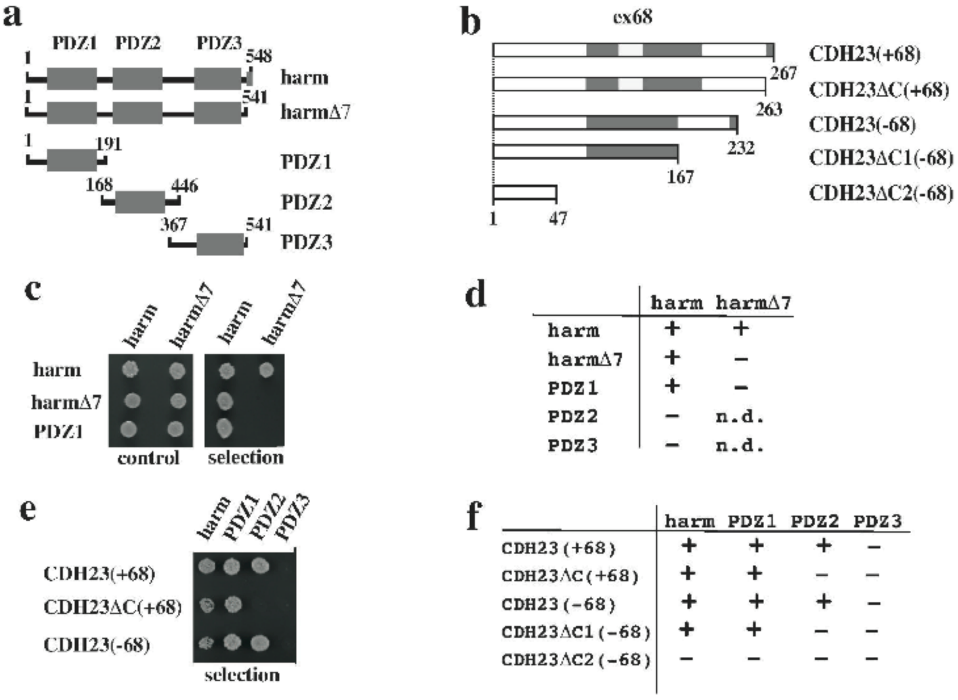
a
PDZ1
PDZ2
PDZ3
1
548
harm
1
541
harmΔ7
1
191
PDZ1
168
446
PDZ2
367
541
PDZ3
b
ex68
CDH23(+68)
267
CDH23ΔC(+68)
263
CDH23(-68)
232
CDH23ΔC1(-68)
167
CDH23ΔC2(-68)
1
47
c
harm
harmΔ7
harm
harmΔ7
harm
harmΔ7
PDZ1
control
selection
d
harm harmΔ7
harm + +
harmΔ7 + −
PDZ1 + −
PDZ2 − n.d.
PDZ3 − n.d.
e
harm
PDZ1
PDZ2
PDZ3
CDH23(+68)
CDH23ΔC(+68)
CDH23(-68)
selection
f
harm PDZ1 PDZ2 PDZ3
CDH23(+68) + + + −
CDH23ΔC(+68) + + − −
CDH23(-68) + + + −
CDH23ΔC1(-68) + + − −
CDH23ΔC2(-68) − − − −

Fig. 3.2. In yeast, Harmonin Interacts with Harmonin and with CDH23.
(a, b) Diagram of the harmonin and CDH23 fragments used in the two-hybrid assays. (c) Representative example of a yeast growth assay to measure harmonin-harmonin interactions. The left panel shows growth in non-selective medium (control), the right panel shows growth in selective medium lacking histidine (selection). (d) Summary of the results establishing harmonin-harmonin interactions. (e) Representative example of a yeast growth assay to determine CDH23-harmonin interactions. (f) Summary of the results establishing CDH23-harmonin interaction. +, growth; -, no growth under selective pressure; n.d., not determined.

We conclude that PDZ1 of harmonin can bind to the C terminal PBI of harmonin, and to the internal PBI of CDH23. PDZ2 of harmonin can bind to the C terminal PBI of CDH23. Surprisingly, interactions of PDZ1 with the internal PBI of CDH23 are not affected by exon 68 encoded sequences. Since different expression levels of the fusion proteins in yeast could mask differences in interaction strength, we analyzed the effect of exon 68 in biochemical assays.

3.4c. Regulation of CDH23-Harmonin Interactions by Alternative Splicing.

To analyze CDH23-harmonin interactions biochemically, we carried out GST-pull down and co-immunoprecipitation experiments. For pull-down experiments, harmonin and fragments containing individual PDZ domains were radiolabeled by *in vitro* transcription/translation (Fig. 3.3a), and analyzed for complex formation with GST-CDH23 fusion proteins (Fig. 3.3b). To allow for a quantitative comparison of complex formation, similar amounts of the GST-CDH23(-68) and GST-CDH23(+68) proteins were used (Fig. 3.3c, lower panel). Harmonin interacted with GST-CDH23(-68) and GST-CDH23(+68), but ~10 fold greater amounts of harmonin were recovered with GST-CDH23(-68) (Fig. 3.3c,d). This suggests that amino acids encoded by exon 68 affect the interaction of harmonin with CDH23.

To define the mechanism by which alternative splicing affects CDH23-harmonin complex formation, we analyzed fragments containing individual PDZ domains of harmonin for interaction with CDH23. In agreement with the two-hybrid results, PDZ2 containing fragments interacted with CDH23(-68) and CDH23(+68), but not with a truncated CDH23(+68) lacking the C terminal PBI (CDH23ΔC(+68); Fig. 3.3e). Deletion of the C terminal PBI did not affect binding of PDZ1 to CDH23 (data not shown). We next mixed PDZ1 and PDZ2 fragments that were generated independently by *in vitro* transcription/translation. This allowed us to directly compare the amount of PDZ1 and PDZ2 recovered with GST-CDH23(-68) and GST-CDH23(+68). PDZ2 interacted equally well with both CDH23 isoforms, while PDZ1 interacted preferentially with the CDH23(-68) isoform (Fig. 3.3f). PDZ3 did not bind to either CDH23 isoform (data not shown).

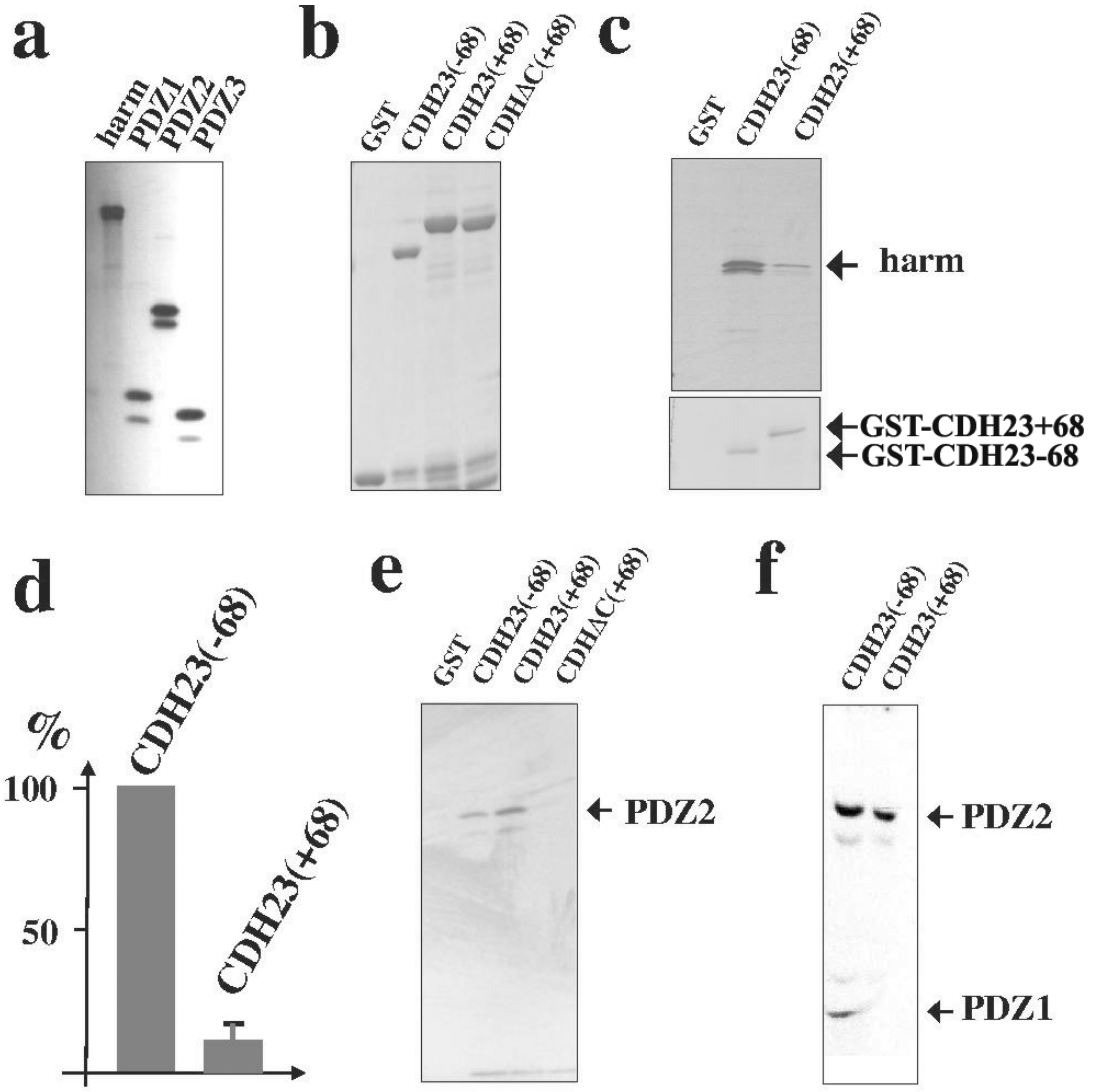

Fig. 3.3. Exon 68 Encoded Amino Acids Affect CDH23-Harmonin Interactions in GST Pull-Down Experiments.
(a) Harmonin and its PDZ domains were expressed by *in vitro* transcription/translation in the presence of ^{35}S-Met, resolved by SDS-PAGE and visualized by autoradiography. (b) Purified GST-CDH23 fusion proteins were resolved on SDS-PAGE gels and visualized by Coomassie staining. (c) Representative GST pull-down experiment. The input amount of GST-fusion proteins is shown in the lower panel. (d) The amount of harmonin that formed a complex with GST-CDH23 isoforms was quantified by scintillation counting and normalized against the input amount of GST-CDH23. The amount of harmonin interacting with GST-CDH23(-68) was set at 100%. Three experiments were carried out and the mean ± standard deviation was determined. (e, f) Individual PDZ domains were used in GST pull-down experiments. The input proteins are shown in panel a. (e) PDZ2 was used for the GST pull-down experiments. (f) PDZ1 and PDZ2 were independently generated by *in vitro* translation and mixed.

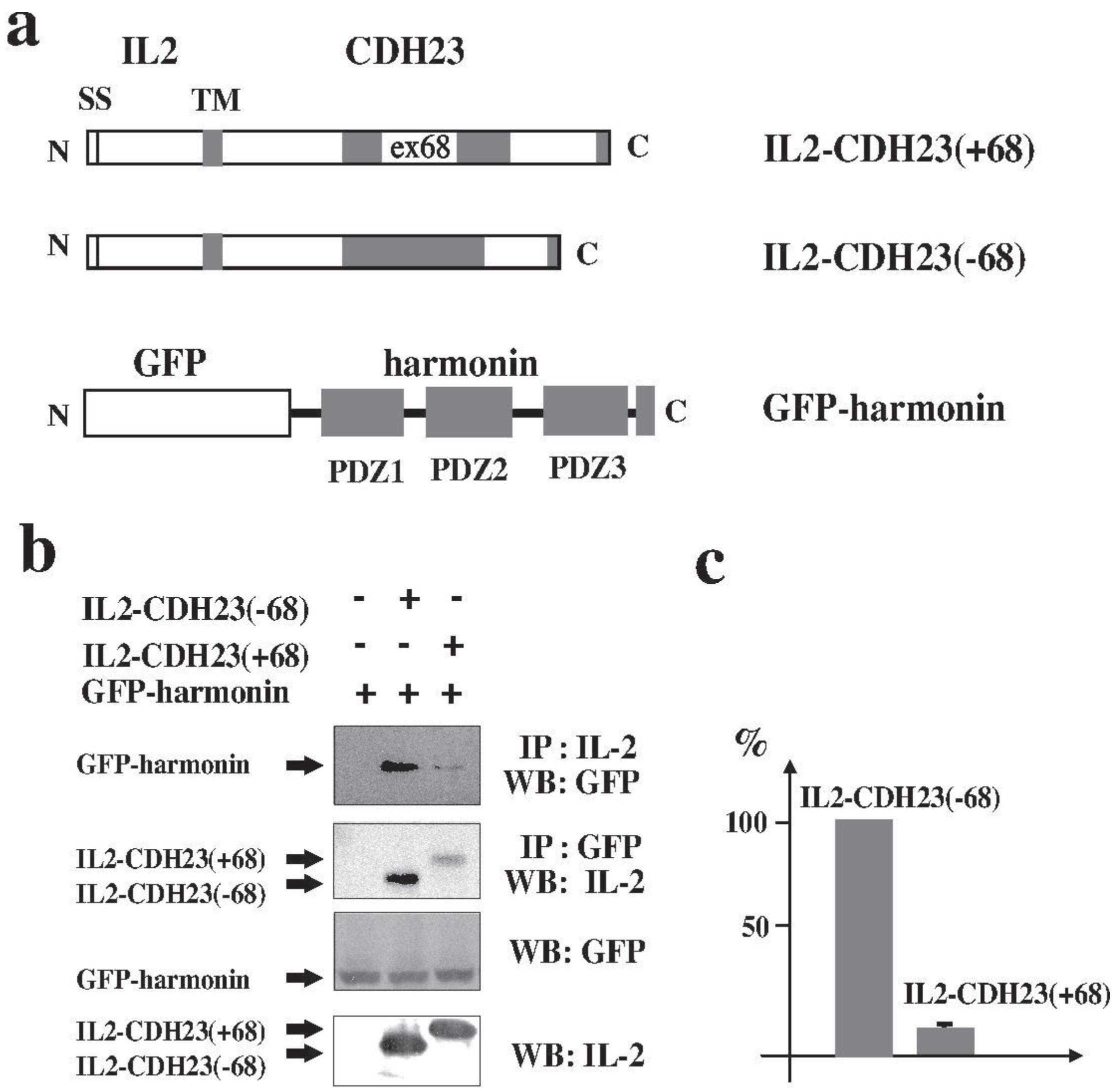
a
IL2
CDH23
SS
TM
N
ex68
C
IL2-CDH23(+68)
N
C
IL2-CDH23(-68)
GFP
harmonin
N
C
GFP-harmonin
PDZ1
PDZ2
PDZ3
b
IL2-CDH23(-68) - + -
IL2-CDH23(+68) - - +
GFP-harmonin + + +
GFP-harmonin
IP : IL-2
WB: GFP
IL2-CDH23(+68)
IL2-CDH23(-68)
IP : GFP
WB: IL-2
GFP-harmonin
WB: GFP
IL2-CDH23(+68)
IL2-CDH23(-68)
WB: IL-2
c
%
100
50
IL2-CDH23(-68)
IL2-CDH23(+68)

Fig. 3.4. Coimmunoprecipitation Experiments from Transfected Cells. (a) Diagram of the fusion proteins (SS, signal sequence; TM, transmembrane domain). (b) Extracts from cells transfected to express the constructs shown in panel (a) were used for immunoprecipitation (IP) experiments with antibodies specific for IL-2 or GFP. Proteins were separated by SDS-PAGE and visualized by Western blotting (WB) with GFP or IL-2 antibodies. As a control, proteins were separated by SDS-PAGE without immunoprecipitation, and visualized by Western blotting. (c) The amount of harmonin that co-precipitated with IL-2 antibodies was densitometrically quantified. Three independent experiments were carried out and harmonin levels recovered with CDH23(-68) were set at 100%. The mean ± standard deviation is indicated.

We conclude that binding of CDH23 to harmonin is mediated by binding of the internal- and C-terminal PBIs in CDH23 to PDZ1 and PDZ2 of harmonin, respectively. Sequences encoded by exon 68 perturb interactions between the internal PBI of CDH23 with PDZ1, but do not affect interactions of the C-terminal PBI of CDH23 with PDZ2 of harmonin.

We next analyzed whether CDH23 and harmonin interact in the physiologically more relevant cellular context, and whether complex formation under these conditions is affected by alternative splicing. To mimic the membrane localization of CDH23, we generated a chimera containing the signal sequence, extracellular domain, and transmembrane domain of the interleukin 2 receptor (IL-2) fused to the CDH23 cytoplasmic domain. We also generated a fusion between the green fluorescence protein (GFP) and harmonin (Fig. 3.4a). The constructs were expressed in COS and 293 cells, and complex formation was analyzed in co-immunoprecipitation experiments using antibodies to IL-2 and GFP (Fig. 3.4b,c). Both proteins could be co-immunoprecipitated as a complex. Substantially less harmonin co-precipitated with the CDH23(+68) as compared to the CDH23(-68) isoform (Fig. 3.4b,c), demonstrating that complex formation under physiological conditions is modulated by sequences encoded by exon 68.

Fig. 3.5. (next page) CDH23-Harmonin Complex Formation *in vivo*, and CDH23 Expression in Hair Cells and the Retina. (a) Whole cell extracts (WCL) from P6 mouse brains were resolved on SDS-PAGE gels, either directly (lane 1, 2), or after immunoprecipitation with harmonin-specific antiserum (lane 4), or after a mock immunoprecipitation without antiserum (lane 3). Proteins were detected by Western blot with harmonin (lane 1) or CDH23 specific antiserum (lane 2-4). (b-i) Analysis of CDH23 expression in the apical part of the cochlea at P0. (b) The section shows the position of the inner and outer hair cells (IHC, OHC). (c) No signal was detected with preimmune serum. (d) CDH23 is expressed in hair cell stereocilia. (e-g) Immunofluorescence analysis: (e) F-actin, labeled with FITC-phalloidin, is present in the cuticular plate and stereocilia (arrows); (f) CDH23 is expressed in stereocilia only; (g) double exposure. (h) Immunofluorescence analysis of a P6 whole mount cochlea stained with CDH23 specific antiserum, followed by rhodamine-conjugated secondary antibody. CDH23 was expressed in stereocilia of inner and outer hair cells. The arrows point to the one row of inner hair cells. (i) Whole mounts were labeled with FITC-phalloidin to reveal F-actin. The double exposure shows localization of CDH23 and F-actin. (j, k) Sections of P0 retinas were stained with preimmune serum, or with CDH23 specific serum. CDH23 expression was strongest in the photoreceptor layer (arrows). The size bar corresponds to 15 µm (b-d), 5 µm (e-g), 30 µm (h,i), 20 µm (j,k).

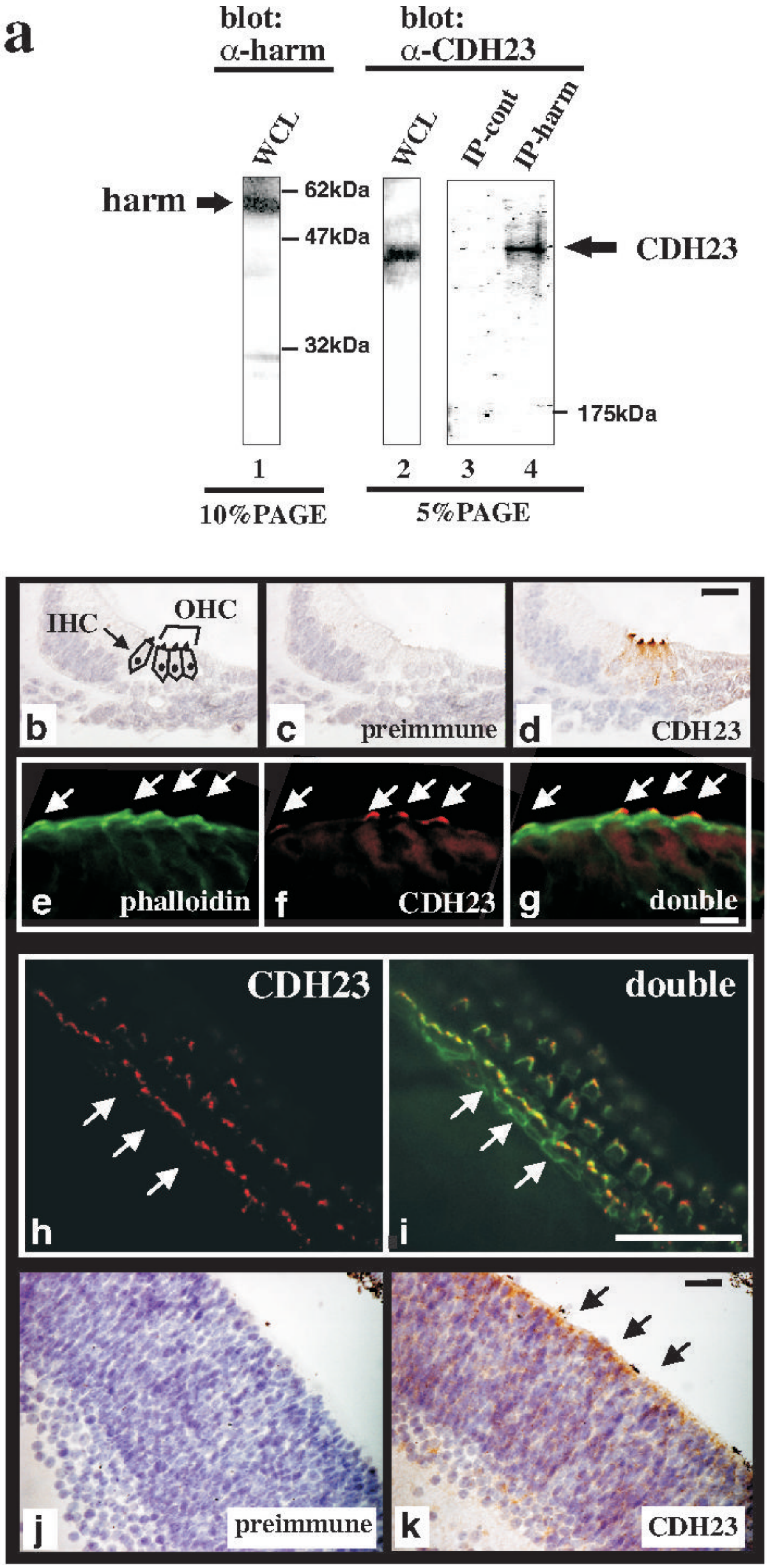
a
blot:
α-harm
blot:
α-CDH23
WCL
WCL
IP-cont
IP-harm
harm
62kDa
47kDa
32kDa
CDH23
175kDa
1
2
3
4
10%PAGE
5%PAGE
IHC
OHC
b
c
preimmune
d
CDH23
e
phalloidin
f
CDH23
g
double
CDH23
double
h
i
j
preimmune
k
CDH23

3.4d. CDH23-Harmonin Interaction *in vivo*, and CDH23 Expression in Hair Cells and the Retina.

To analyze whether CDH23 and harmonin form a protein complex *in vivo*, we performed co-immunoprecipitation experiments with antisera raised against CDH23 and harmonin, utilizing protein extracts from mouse tissue. The affinity purified antisera recognized their respective antigen with high specificity in Western blots and immunoprecipitations carried out with extracts from mouse tissues, or from cells transfected to express CDH23 or harmonin (Fig. 3.5a, lane 1 and 2; data not shown). To analyze complex formation, extracts were prepared from P6 mouse brains, and immunoprecipitations were carried out with the harmonin-specific antiserum. CDH23 was specifically detectable in the harmonin immunoprecipitates, but not in control precipitates (Fig. 3.5a, lane 3 and 4), demonstrating that CDH23 and harmonin form a complex *in vivo*.

Previous studies have shown that stereocilia are splayed in CDH23-deficient *waltzer* mice (Di Palma et al., 2001a), and that harmonin is expressed in hair cells and their stereocilia (Verpy et al., 2000). Expression of CDH23 in the inner ear has not been reported. We therefore stained cochlear sections and whole-mounts with a CDH23-specific antiserum (Fig. 3.5b-i). CDH23 was specifically expressed in the stereocilia of hair cells (Fig. 3.5d,f,h), where it is expected to exert its function as a complex with harmonin.

Since harmonin is widely expressed in hair cells (Verpy et al., 2000), it may interact with additional proteins in other locations in hair cells.

Because Usher 1 patients suffer from visual impairment, we also stained retinas with CDH23 antibodies (Fig. 3.5j,k). A low signal was detectable throughout the retina, but the signal was particularly strong in the photoreceptor layer, suggesting that CDH23 regulates photoreceptors development or function.

3.5. Discussion

Our data provide evidence that the two Usher syndrome proteins CDH23 and harmonin act in a common molecular pathway. The two proteins bind to each other, are co-expressed in hair cell stereocilia, and mutations in the genes encoding CDH23 and harmonin cause similar symptoms in USH1 patients (Bitner-Glindzicz et al., 2000; Bolz et al., 2001; Bork et al., 2001; Verpy et al., 2000). The observation that stereocilia are splayed in CDH23-deficient *waltzer mice* (Di Palma et al., 2001a) suggests that CDH23 and harmonin are components of the tip-, ankle-, side-links, or top connectors that link stereocilia into a bundle. Top connectors have not been observed in rodents, and the tip- and ankle-links, but not side links are sensitive to treatment with Ca^{2+} chelators (Assad et al., 1991; Goodyear and Richardson, 1999; Zhao et al., 1996). Since Ca^{2+} chelators abolish cadherin function, it is likely that CDH23 is a component of the tip- or ankle-link, or both. Future three-dimensional reconstructions using quantitative immunoelectron microscopy should help to clarify this issue.

Previously no sequence motifs have been described in the CDH23 cytoplasmic domain that may mediate protein:protein interactions. We now describe two PBIs in the CDH23 cytoplasmic domain: an internal domain with homology to a PBI in the adaptor protein Ril (Cuppen et al., 1998), and a PBI at the C terminus fitting the consensus for class I PBIs (Sheng and Sala, 2001). The Ril homology region in CDH23 mediates interactions with the PDZ1 of harmonin, while its C terminal PBI interacts with PDZ2. Interestingly, PDZ1 of harmonin also interacts with the C terminus of harmonin itself. Since the structure of PDZ domains is optimized to interact with free carboxylate groups (Harris and Lim, 2001; Sheng and Sala, 2001), we expected that the C terminus of CDH23 and harmonin would interact with PDZ1 of harmonin. We were surprised to identify an internal PBI within the CDH23 cytoplasmic domain. Internal PBIs have been found only in a few proteins including Ril and the neuronal nitric oxide synthase (Cuppen et al., 1998; Hillier et al., 1999). The internal PBI of neuronal nitric oxide synthase adopts a conformation with an exposed hairpin turn that mimics the overall structure of C terminal PBIs (Hillier et al., 1999), suggesting that the internal PBI in CDH23 has a similar structure. Interestingly, the homology between Ril and CDH23 is the first example of sequence conservation between internal PBIs, raising the possibility that additional similar PBIs remain to be discovered.

Formation of the CDH23-harmonin complex is regulated by sequences encoded in the alternatively spliced exon 68 that is expressed in inner ear, but not the retina. Our data suggest that PDZ1 and PDZ2 of harmonin bind to CDH23(-68) isoforms in the retina. In the ear, interactions of PDZ1 with CDH23 are perturbed by the insertion of 35 amino acids encoded by exon 68. PDZ1 is therefore free to engage with other proteins, for example with the C terminal PBI in harmonin. This suggests that the overall composition and function of the CDH23-harmonin complex differs in ear and retina. For example, CDH23(+68) may be clustered more efficiently than CDH23(-68) by harmonin-harmonin interactions (Fig. 3.6). PDZ1, as well as other protein interaction motifs in harmonin such as PDZ3 may recruit additional proteins. This is consistent with the function of other PDZ domain proteins that serve as assembly platforms for signaling complexes, for example at epithelial cell junctions (Nagafuchi, 2001). Interestingly, alternatively spliced isoforms have been described not only for CDH23 but also for harmonin (Verpy et al., 2000), suggesting that different CDH23-harmonin containing protein complexes are assembled in different cell types. Understanding the differences in complex composition may shed light on the molecular pathogenesis leading to sensorineuronal deafness and retinitis pigmentosa in USH1 patients.

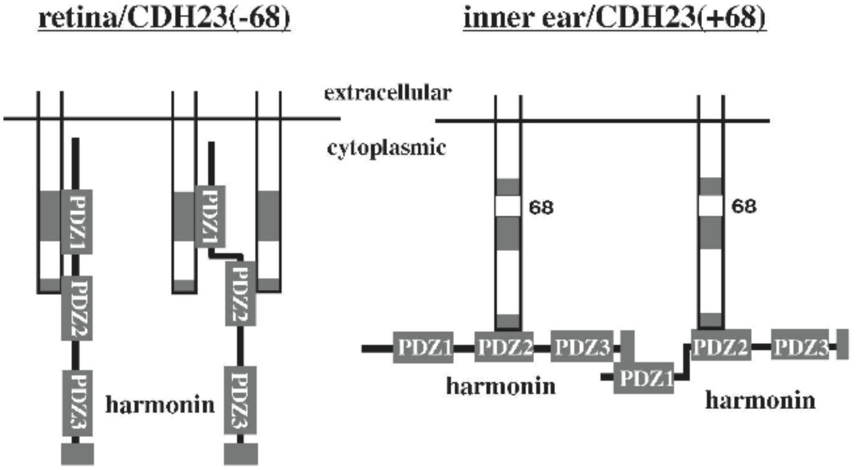
retina/CDH23(-68)
inner ear/CDH23(+68)
extracellular
cytoplasmic
PDZ1
PDZ2
PDZ3
harmonin
68
PDZ1
PDZ2
PDZ3
harmonin
PDZ1
PDZ2
PDZ3
harmonin

Fig. 3.6. Model for CDH23-Harmonin Complex Formation and its Regulation by Alternative Splicing. Based on our data, we propose the following model. PDZ1 and PDZ2 of harmonin interact with the internal and C terminal PBI of CDH23(-68), respectively. This could lead to binding of harmonin to one CDH23 molecule, or it could crosslink two receptors (left panel). Insertion of the sequence encoded by exon 68 perturbs interactions between PDZ1 of harmonin and the internal PBI of CDH23(+68). This poises the complex for alternative interactions (right panel). Notably, the PDZ1 domain of harmonin may be available to interact with other proteins when harmonin is bound to CDH23(+68), but not to CDH23(-68). Binding partners for PDZ1 include harmonin, leading to the formation of harmonin-harmonin oligomers. Since CDH23(+68) is expressed in the ear but not the retina, splicing may control the architecture and composition of CDH23-harmonin complexes in a tissue specific manner.

Acknowledgements

We thank M. Senften and A. Kralli for advice and comments on the manuscript. The Novartis Research Foundation supported the work. J.S. is supported by the Boehringer Ingelheim Fonds; A.J.R. by a C.J. Martin Fellowship (ID: 148939) from the NHMRC of Australia.

Paper II

Cadherin 23 is a Component of the Tip Link in Hair Cell Stereocilia

Jan Siemens, Concepcion Lillo, Rachel A. Dumont, Anna Reynolds, David S. Williams, Peter G. Gillespie, and Ulrich Müller

Nature, Vol. 428, 950-955, April 2004

4.1. Abstract

Mechanoelectrical transduction, the conversion of mechanical force into electrochemical signals, underlies a range of sensory phenomena, including touch, hearing and balance. Hair cells of the vertebrate inner ear are specialized mechanosensors that transduce mechanical forces arising from sound waves and head movement to provide our senses of hearing and balance (Gillespie and Walker, 2001; Müller and Evans, 2001). The mechanotransduction channel of hair cells and the molecules that regulate channel activity have, however, remained elusive. One molecule that might participate in mechanoelectrical transduction is cadherin 23 (CDH23); mutations in its gene cause deafness and age-related hearing loss (Bolz et al., 2001; Bork et al., 2001; Di Palma et al., 2001b; Noben-Trauth et al., 2003). Furthermore, CDH23 is large enough to be the tip link, the extracellular filament proposed to gate the mechanotransduction channel (Pickles et al., 1984). Here we show that antibodies against CDH23 label the tip link, and that CDH23 has biochemical properties similar to those of the tip link. Morover, CDH23 forms a complex with myosin-1c (MYO1C), the only known component of the mechanotransduction apparatus (Holt et al., 2002), suggesting that CDH23 and MYO1C cooperate to regulate the activity of mechanically gated ion channels in hair cells.

4.2. Introduction

The mechanically sensitive organelle of the hair cell, the hair bundle, contains dozens of actin-rich stereocilia and a single microtubule-based kinocilium (Fig. 4.1a). Mechanotransduction channels are located towards stereociliary tips and open or close upon deflection of the stereocilia (Gillespie and Walker, 2001; Müller and Evans, 2001). Excitatory stimuli stretch a gating spring, an elastic element that gates the mechanotransduction channels (Corey and Hudspeth, 1983b). Of the extracellular filaments that interconnect stereocilia or stereocilia and the kinocilium, only the 150-200 nm tip link is correctly positioned to control opening of mechanotransduction channels (Assad et al., 1991; Pickles et al., 1984). The molecular composition of the tip link is not known, but it has similarities with links between kinocilia and stereocilia; both structures are recognized by an antibody against an unknown protein termed the tip link antigen (Goodyear and Richardson, 2003). The tip link also shares features with members of the cadherin superfamily. Not only does the tip link mediate adhesive interactions between adjacent plasma membranes, but Ca^{2+} chelating agents disrupt the tip link (Assad et al., 1991) and cadherin adhesive function (Takeichi, 1990). Because single cadherin domains span ~4 nm (Boggon et al., 2002), homophilically interacting CDH23 molecules, with 27 cadherin domains each, could span >200 nm.

4.3. Results

Two alternatively spliced CDH23 isoforms differing with respect to the inclusion of exon 68, encoding part of the intracellular CDH23 domain, have been described (Fig. 4.1b) (Bork et al., 2001; Di Palma et al., 2001b; Siemens et al., 2002). Using RT-PCR, we detected mRNAs encoding CDH23(+68) and CDH23(-68) in inner ears of adult mice; CDH23(+68) was particularly prominent, and was not detected in other tissues (Fig. 4.1c, and data not shown). To localize the CDH23 isoforms, we used an antibody (CDH23*cyto) that recognizes the cytoplasmic domain of both isoforms and another antibody (CDH23*68) that is specific for CDH23(+68) (Supplementary Fig.

S1). At P0 and P5, when cochlear hair cells are immature and contain a kinocilium, CDH23*cyto detected CDH23 in the developing hair bundle and in Reissner's membrane (Fig. 4.1e,g,h). By contrast, CDH23*68 detected the CDH23(+68) isoform only in the hair bundle (Fig. 4.1f). At P42, when hair cells are mature and have lost their kinocilium, CDH23 was still expressed in cochlear hair cells, but only near stereociliary tips (Fig. 4.1i). In vestibular hair cells, which reach maturity around birth, CDH23 was already confined at P5 to stereociliary tips (Fig. 4.1k). No CDH23 immunoreactivity was observed in *Cdh23*-deficient waltzer mice (Fig. 4.1j).

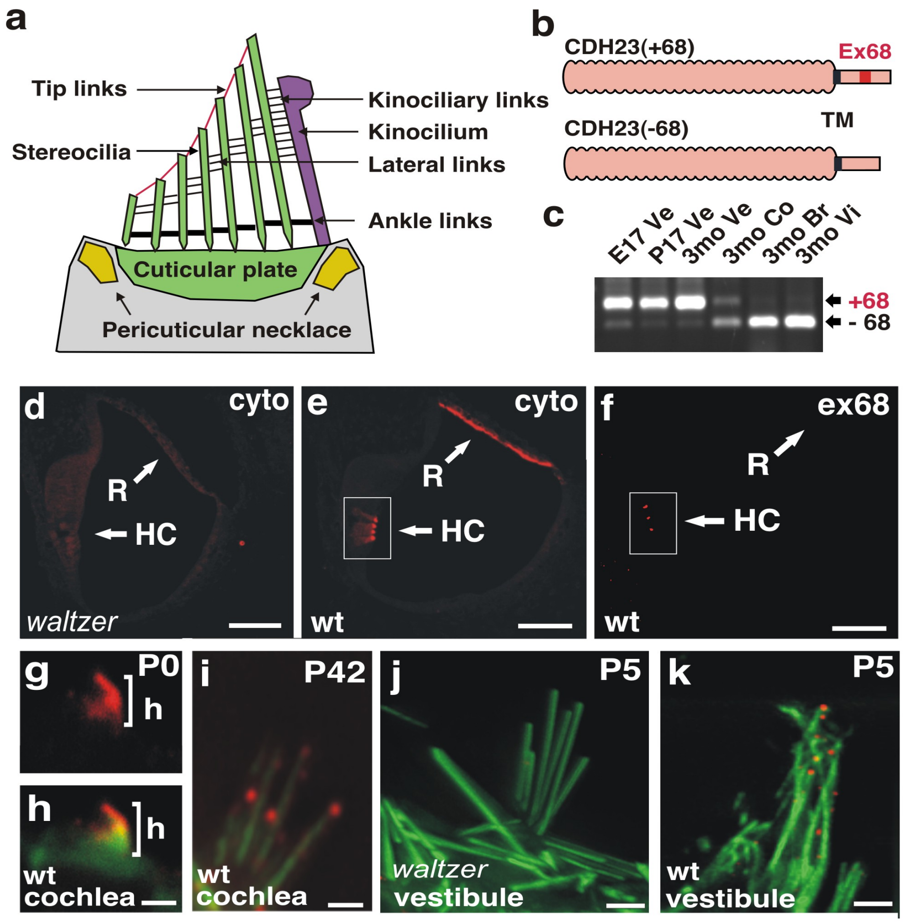
a
Tip links
Stereocilia
Kinociliary links
Kinocilium
Lateral links
Ankle links
Cuticular plate
Pericuticular necklace
b
CDH23(+68)
Ex68
CDH23(-68)
TM
c
E17 Ve
P17 Ve
3mo Ve
3mo Co
3mo Br
3mo Vi
+68
- 68
d
cyto
R
HC
waltzer
e
cyto
R
HC
wt
f
ex68
R
HC
wt
g
P0
h
h
h
wt
cochlea
i
P42
wt
cochlea
j
P5
waltzer
vestibule
k
P5
wt
vestibule

Figure 4.1. CDH23 expression in mouse inner ears. a, Hair bundle diagram. Stereocilia are connected through tip , lateral , and ankle links, and to the kinocilium through kinocilia links. **b**, Diagram of CDH23 protein. Exon 68 is present only in CDH23(+68) (TM, transmembrane domain). **c**, Analysis of CDH23 expression in the vestibule (VE), cochlea (Co), brain (Br), and vibrissae (Vi) by RT-PCR. **d-f**, Section of a P5 cochlea. **d, e,** CDH23*cyto (red) stained hair cells (HC) and Reissners membrane (R) in wild type, but not in *Cdh23*-deficient *waltzer* mice. **f,** CDH23*68 stained hair bundles only. **g, h,** CDH23 (red) in immature P0 cochlear hair cells was distributed throughout the hair bundle (green, phalloidin) **i-k,** CDH23 (red) in mature hair cells was confined to stereociliary tips (green, phalloidin), but was absent in *waltzer* mice Scale bars: d-f, 40 μm; g-k, 1.25 μm.

The CDH23*cyto antiserum crossreacted with bullfrog CDH23 (Supplementary Fig. S2), enabling the analysis of CDH23 expression in bullfrog hair cells, which are larger than mouse hair cells and offer more precise resolution of hair bundle antigens. In contrast to mouse cochlear hair cells, bullfrog hair cells do not lose their kinocilium, allowing the analysis of CDH23 distribution at links between stereocilia and the kinocilium. Optical sections with a perpendicular orientation to the stereocilia bundle revealed that CDH23 was concentrated in stereocilia near their tips (Fig. 4.2a,b). In confocal sections of isolated hair cells, CDH23 was concentrated where the tallest stereocilia contact the terminal bulb of the kinocilium (Fig. 4.2c). In addition, we detected punctate staining for CDH23 at stereociliary tips (Fig. 4.2d).

To determine definitively whether CDH23 is a component of the tip links, we employed immunoelectron microscopy. CDH23*cyto but not a control antibody labeled both ends of tip links in mouse and bullfrog hair cells (Fig. 4.2e-j). 80% of all gold particles colocalize with the tip link. 57% of all gold particles (n=192) were found at stereociliary tips, where the lower end of the tip link is expected to inserted into stereocilia. The position of the side plaque marking the upper end of each tip link can be inferred from the postion of the shorter adjacent stereocilium, and is several hundred nm higher (see Methods); 23% of the gold particles were detected in this position. Only 10% of the gold particles were distributed randomly along stereocilia, and 10% were located outside stereocilia. We observed immunogold labeling intracellularly at tip link insertion points, and extracellularly close to the plasma membrane. The length of the two-antibody sandwich (~20-30 nm) and membrane rupture at tip links (Furness et al., 2002; Pickles et al., 1991) could account for the apparent extracellular localization of gold particles. We observed similar extracellular immunogold localization when detecting the membrane phospholipid PIP_2 in hair bundles (data not shown). In bullfrog, CDH23*cyto also strongly labeled the links between the kinocilium and adjacent stereocilia (Supplementary Fig. S3; gold particles not included in quantification).

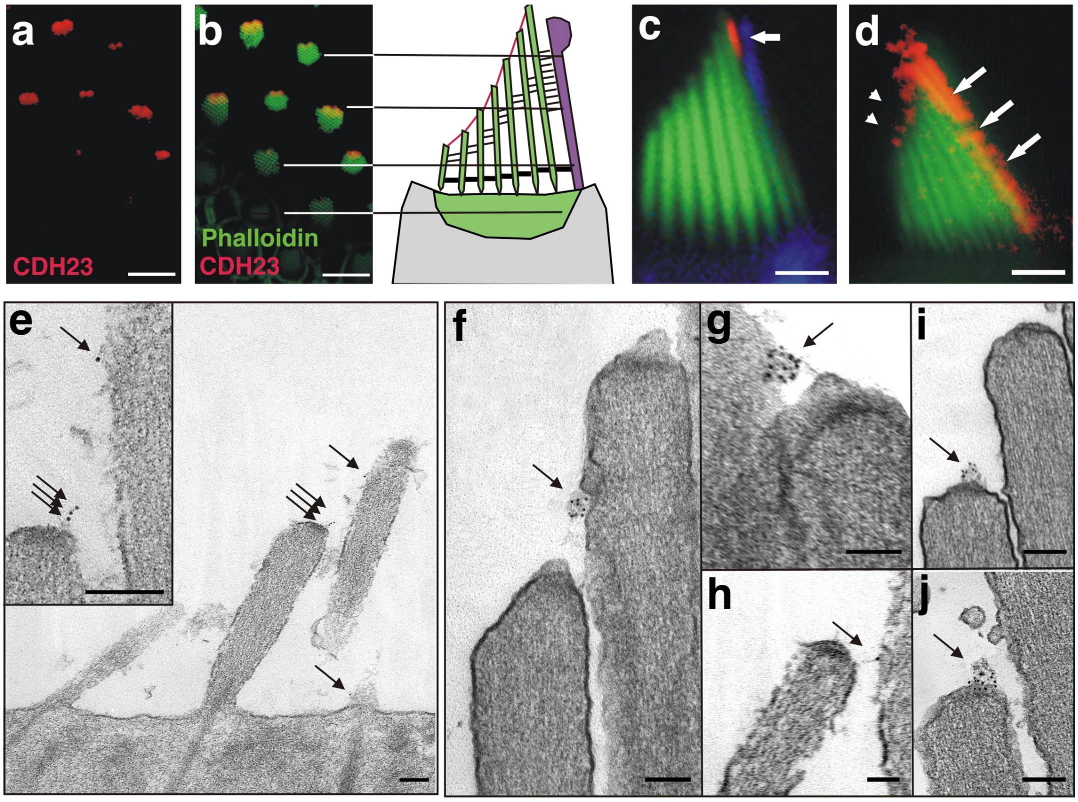

Figure 4.2. CDH23 expression in hair cells. a, b, Whole mount bullfrog saccules were stained with CDH23*cyto antibody (red) and with phalloidin (green). Optical sections cut through hair bundles at levels approximately as indicated. CDH23 was localized towards stereociliary tips. **c, d,** Isolated bullfrog hair cells were stained with CDH23*cyto (red), phalloidin (green) (c and d), and anti tubulin (blue) (c only). In (c) the intensity-gain was decreased during imaging to highlight CDH23 localization at the stereocilium-kinocilium interface (arrow). CDH23 was also localized at stereociliary tips (d-arrowheads). **e-j,** Immunogold electron microscopy; In mouse **(e)** and bullfrog **(f-j)** hair cells, CDH23 colocalized with the tip link. Arrows, localization of all gold particles in images. Scale bars: a,b, 11 µm; c,d 5 µm; e-h, 100 nm.

The tip link is disrupted upon exposure of hair cells to Ca^{2+} chelators and La^{3+} (Assad et al., 1991; Kachar et al., 2000). Treatment of hair cells with EGTA (Fig. 4.3a-d) or BAPTA (data not shown) abolished bundle staining of CDH23 in ~3/4 of the hair cells. Instead, intense staining was observed in most hair cells in the pericuticular necklace (Fig. 4.3b), a vesicle-rich compartment at the apical surface of hair cells (Hasson et al., 1997). This pool of CDH23 could arise from new synthesis, redistribution from the soma, or redistribution from stereocilia. In bundles that retained immunoreactivity, labeling in stereocilia adjacent to the kinocilium was usually distributed more longitudinally than in controls (data not shown), supporting the latter hypothesis. Tip links reappear 12-24 hours after removal of Ca^{2+} chelators (Zhao et al., 1996); consistent with this observation, we detected robust CDH23 immunoreactivity 24 hours after removal of EGTA or BAPTA (Fig. 4.3d). Finally, treatment with La^{3+} not only disrupted the tip link, but also caused immediate loss of CDH23 immunoreactivity from stereocilia; in contrast to results with Ca^{2+} chelators, no elevated pericuticular necklace labeling was observed (Fig. 4.3e,f).

The tip link is sensitive to proteolytic digestion by elastase, but not by subtilisin, which cleaves ankle links (Goodyear and Richardson, 1999; Osborne and Comis, 1990). We expressed the full length CDH23 mRNA in HEK293 cells, treated them with elastase and subtilisin, and detected CDH23 by Western blotting. CDH23 was degraded by elastase, but not by subtilisin (Fig. 4.3g).

Observation of CDH23 at upper and lower tip-link anchors suggests that it may connect stereocilia by a homophilic binding mechanism. To test CDH23 adhesive function, we established L929 cell lines that express full length CDH23 (L-CDH23 cells) or, as a control, E-cadherin (L-ECDH cells) (Supplementary Fig. S4). In cell aggregation assays, L-ECDH cells and L-CDH23 cells, but not parental L929 cells, formed aggregates. Cell aggregation between L-CDH23 cells was inhibited by EGTA (Fig. 4.3h,i). Because aggregation of L-CDH23 cells could be mediated by homophilic interactions between CDH23 molecules or by heterophilic interactions between CDH23 and another cell surface receptor, we labeled cell lines with the lipophilic fluorescence dyes DiI and DiO, and analyzed aggregate formation by immunofluorescence microscopy. DiI labeled L-CDH23 cells formed mixed aggregates with DiO labeled L-CDH23 cells, but not with parental L929 cells or with L-ECDH cells (Fig. 4.3j). L-CDH23 and L-ECDH cells segregated into separate aggregates (Fig. 4.3j), while parental L929 cells remained as single cells (data not shown). These findings demonstrate that CDH23 mediates Ca^{2+} dependent, homophilic cell adhesion.

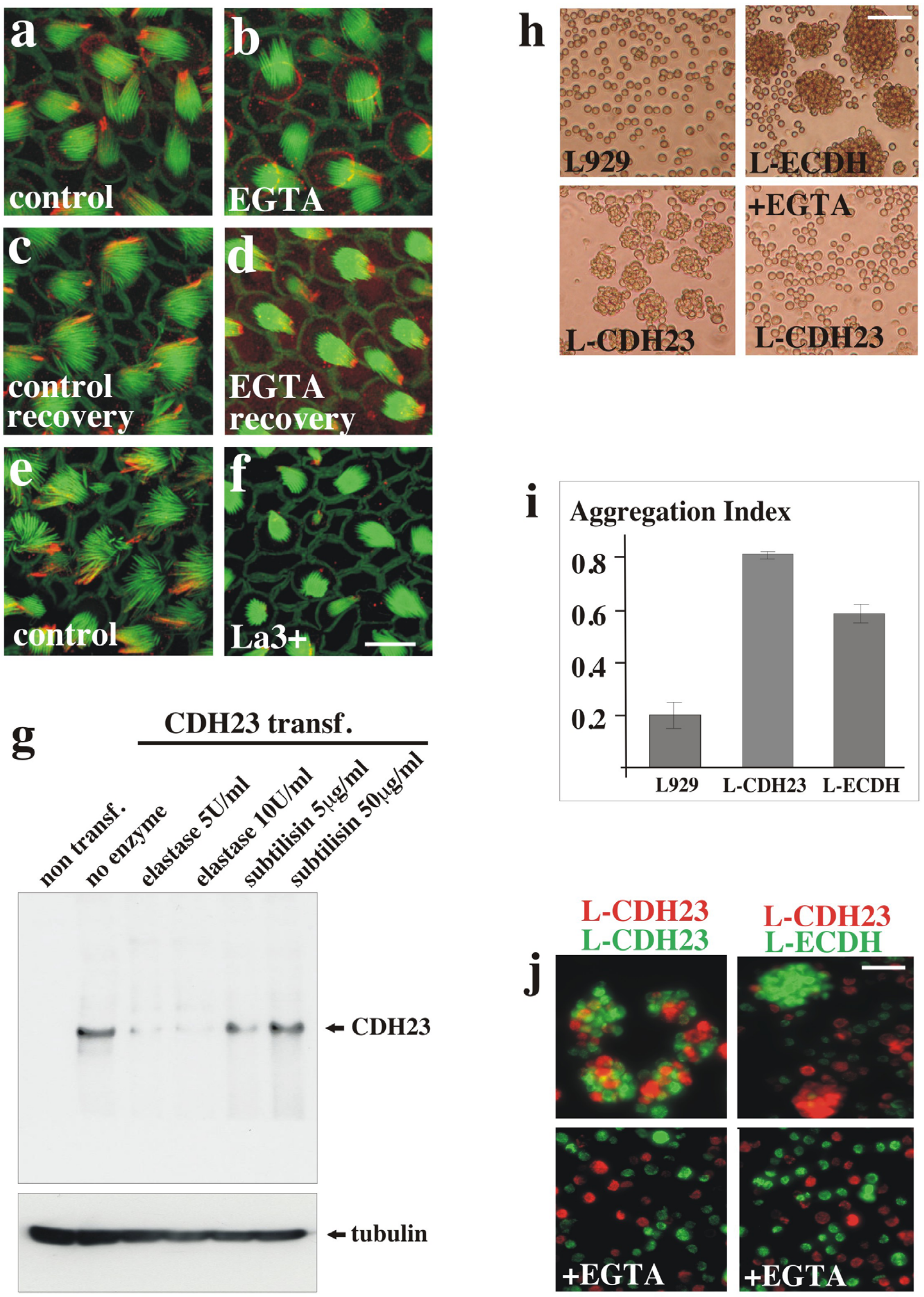
a
control
b
EGTA
c
control recovery
d
EGTA recovery
e
control
f
La3+
h
L929
L-ECDH
L-CDH23
+EGTA
L-CDH23
i
Aggregation Index
0.8
0.6
0.4
0.2
L929
L-CDH23
L-ECDH
g
CDH23 transf.
non transf.
no enzyme
elastase 5U/ml
elastase 10U/ml
subtilisin 5µg/ml
subtilisin 50µg/ml
CDH23
tubulin
j
L-CDH23
L-CDH23
L-CDH23
L-ECDH
+EGTA
+EGTA

Figure 4.3. Biochemical Properties of CDH23. **a-d,** Bullfrog saccules were treated with EGTA and stained with CDH23*cyto antibody (red) and with phalloidin (green). After EGTA treatment, CDH23 disappeared from stereocilia and appeared at the apical hair cell surface; upon EGTA removal, CDH23 reappeared in the bundle after 24 hrs (recovery). **e, f,** La^{3+} treatment caused loss of CDH23 immunostaining. **g,** Recombinant CDH23 protein expressed in HEK293 cells was sensitive to digestion by elastase but not subtilisin. Control tubulin protein was insensitive to both proteases. **h-j,** Cell aggregation assays. **h,** L-CDH23 and L-ECDH cells formed aggregates. L-CDH23 aggregates were disrupted by EGTA. **i,** The aggregation index was determined(Nagafuchi and Takeichi, 1988) (N0-Nt/N0; N0=number of particle with EGTA, NT=number of particles without EGTA), and the mean and standard deviation determined. **j,** DiI labeled L-CDH23 cells (red) formed mixed aggregates with DiO labeled L-CDH23 cells (green), but not with L-ECDH cells. Aggregation was blocked by EGTA. Scale bar: Size bars: a-f, 8 µm; h,j, 60 µm.

MYO1C is localized at tips of stereocilia (Walker et al., 1993) and acts as an adaptation motor for the mechanotransduction channel (Holt et al., 2002). To test whether MYO1C and CDH23 can interact directly or indirectly, we coexpressed in HEK293 cells MYO1C and a fusion protein containing the cytoplasmic domain of CDH23 and the transmembrane and extracellular domains of the IL2 receptor (Fig. 4.4a) (Siemens et al., 2002). As a control, we expressed a construct lacking the CDH23 cytoplasmic domain (IL2R-□Cyto). All constructs were expressed efficiently (Fig. 4.4b; middle and lower panels). MYO1C coprecipitated with IL2R-CDH23(-68) and IL2R-CDH23(+68), but not with IL2R-□Cyto (Fig. 4.4b, upper panel). Likewise IL2R-CDH23(+68), but not IL2R-□Cyto coprecipitated with MYO1C (Fig. 4.4c). Using immunofluorescence microscopy of transfected HEK293 cells (Fig. 4.4d) or COS cells (Supplementary Fig. S5), we found both molecules colocalized at the cell periphery. Colocalization was dependent on the CHD23 cytoplasmic domain.

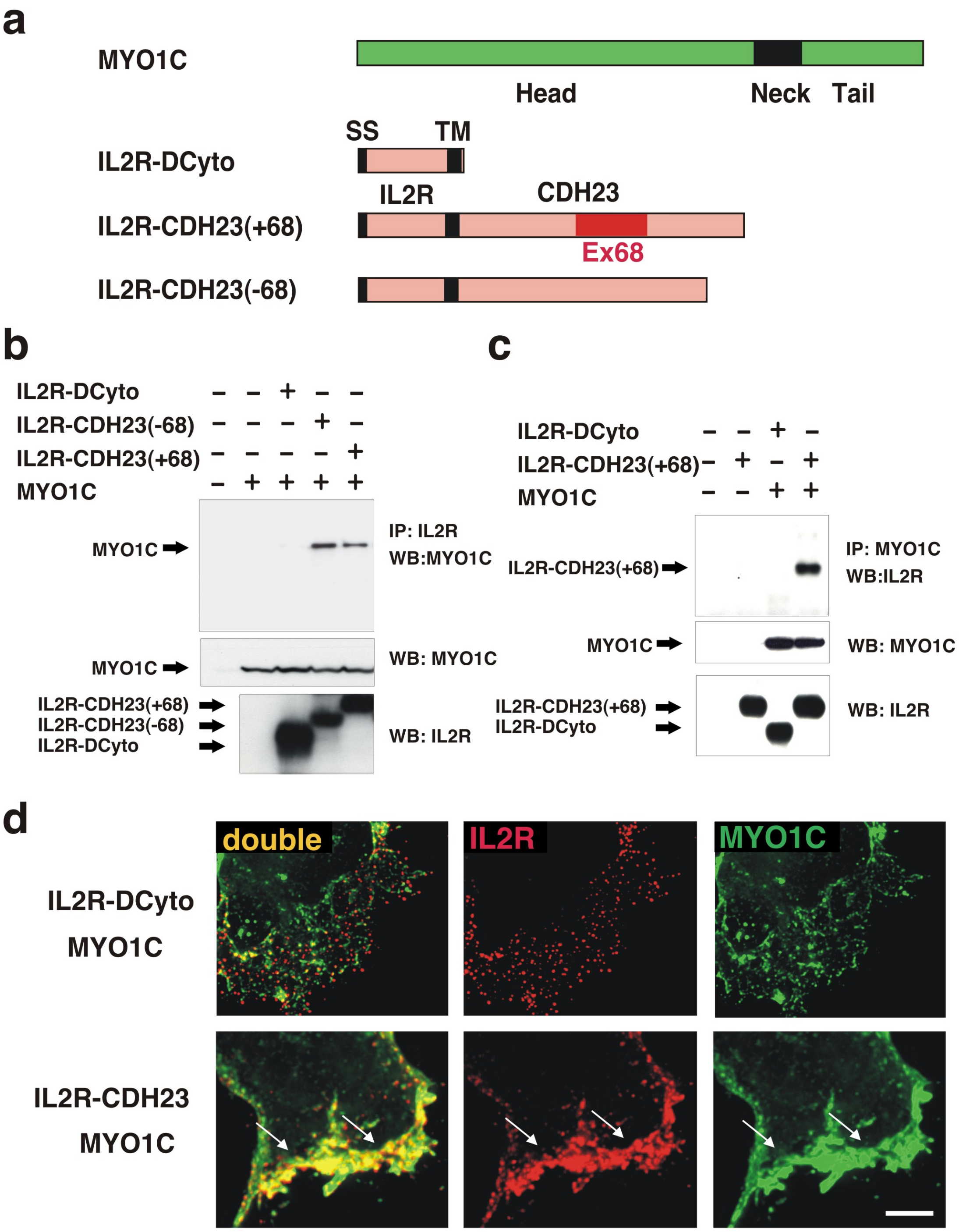
a
MYO1C
Head
Neck
Tail
SS
TM
IL2R-DCyto
IL2R
CDH23
IL2R-CDH23(+68)
Ex68
IL2R-CDH23(-68)
b
IL2R-DCyto – – + – –
IL2R-CDH23(-68) – – – + –
IL2R-CDH23(+68) – – – – +
MYO1C – + + + +
MYO1C
IP: IL2R
WB:MYO1C
MYO1C
WB: MYO1C
IL2R-CDH23(+68)
IL2R-CDH23(-68)
IL2R-DCyto
WB: IL2R
c
IL2R-DCyto – – + –
IL2R-CDH23(+68) – + – +
MYO1C – – + +
IL2R-CDH23(+68)
IP: MYO1C
WB:IL2R
MYO1C
WB: MYO1C
IL2R-CDH23(+68)
IL2R-DCyto
WB: IL2R
d
double
IL2R
MYO1C
IL2R-DCyto
MYO1C
IL2R-CDH23
MYO1C

Figure 4.4. Interaction of IL2R-CDH23 with MYO1C. a, Diagram of MYO1C and of fusion proteins containing the extracellular and transmembrane (TM) domain of the IL2 receptor (IL2R) and the cytoplasmic domain of CDH23. **b,** Extracts from 293HEK cells transfected to express the constructs indicated on top of the panel were immunoprecipitated (IP) with IL2R or MYO1C antibodies. Proteins were visualized by western blotting (WB). As expression control, extracts were analyzed without immunoprecipitation. **b,** MYO1C coprecipitated with IL2R-CDH23(-68) and IL2R-CDH23(+68), but not with IL2R-DCyto. **c,** IL2R-CDH23(+68) but not IL2R-DCyto coimmunoprecipitated with MYO1C. **d,** Transfected cells were stained with IL2R (red) and MYO1C (green) antibodies. MYO1C colocalized with IL2R-CDH23(+68), but not with IL2R-DCyto. Scale bars: 3.5 μm.

4.4. Discussion

We provide here six lines of evidence that support the conclusion that CDH23 is a tip link component in adult hair cells. First, CDH23 localizes at tip links. Second, CDH23 localizes to kinociliary links, which are immunologically related to tip links (Goodyear and Richardson, 2003). Third, reagents that are known to disrupt tip link integrity, such as La^{3+} and EGTA (Assad et al., 1991; Kachar et al., 2000) perturb CDH23 subcellular distribution in hair cells. Fourth, elastase disrupts the tip link (Osborne and Comis, 1990) and cleaves CDH23 protein, while both tip links and CDH23 resist subtilisin proteolysis, which is known to cleave the ankle link (Goodyear and Richardson, 1999). Fifth, CDH23 mediates homophilic interactions, and Ca^{2+} chelators that disrupt the tip link also disrupt CDH23 adhesive function. Sixth, CDH23 coimmunoprecipitates with MYO1C, the motor for slow adaptation of the mechanotransduction channel that is localized near stereocilia tips (Holt et al., 2002). In agreement with our findings, tip links (but no other linkages that connect stereocilia) are absent in zebrafish that carry a mutation in the CDH23 gene (Söllner et al., accompanying manuscript). Our findings suggest an explanation why CDH23 expression was not previously detected in mouse hair cells after P30 (Boeda et al., 2002); the kinocilium is not maintained in adult mouse hair cells, and low expression at stereocilia tips may have prevented detection.

Our data are consistent with a model where CDH23 connects stereociliary tips by a homophilic binding mechanism. Because the tip link forks into two strands at its upper end and is larger in diameter than a cadherin dimer (Kachar et al., 2000), the tip link itself likely is constructed of more than one CDH23 homophilic dimer. It may contain additional molecules such as the tip link antigen (Goodyear and Richardson, 2003), which could engage in heterophilic interactions with CDH23. Because adaptation requires >50 MYO1C molecules per tip link (Hudspeth and Gillespie, 1994) and the transduction channel must be in series between the tip link and motor complex, MYO1C and CDH23 probably interact in hair cells and in tissue culture cells through one or more intermediate molecules. Although CDH23 has previously been shown to play a role in the assembly and maintenance of hair bundles during development (Di Palma et al., 2001b), a function that is potentially mediated by interactions between CDH23 and the multi-PDZ domain protein harmonin (Boeda et al., 2002; Noben-Trauth et al., 2003; Siemens et al., 2002), its primary role in adult hair cells is to form kinociliary links, which couple the stereocilia to the kinocilium, and tip links, which transmit force to mechanically gated ion channels and are essential for mechanotransduction. A dual function for CDH23 in developing and adult hair cells could explain the phenotypic variability that is caused by mutations in the *Cdh23* gene. Mutations that affect assembly and maintenance of hair bundles likely inactivate *Cdh23* function (Di Palma et al., 2001b). In contrast, age-related hearing loss is caused by polymorphisms in an exon that encodes part of the extracellular domain (Noben-Trauth et al., 2003). This mutation may reduce CDH23 adhesive function and affect transduction channel gating.

4.5. Materials and Methods

Generation of Antibodies

The CDH23*cyto antibody has been described (Siemens et al., 2002). CDH23*68 was raised in rabbits against a GST fusion protein containing amino acids 3133-3291 of CDH23, encompassing exon 68 (amino acid numbers refer to accession number NM_023370 of the NCBI database). The CDH23 fragment was generated with the primer pair
5'-CGCGGATCCCTGGACCCCTTCTGCCGGAACC-3' (forward) and
5'-ATTGAATTCTCATGTGCCCGTGCTGCCATGAAC-3' (reverse)
and cloned into the BamHI/EcoRI sites of the pGEX2TK vector (Amersham Pharmacia Biotech) to give the desired fusion protein. The antiserum was affinity purified against a peptide with the amino acid sequence encoded by exon 68 of CDH23 (amino acids 3212 to 3246) generated with a peptide synthesizer at the FMI core facility and coupled to CNBr-Sepharose column (Amersham Pharmacia Biotech).

The rabbit polyclonal antiserum against the first 4 EC-domains (amino acids 40 to 471) of mouse CDH23, CDH23*ecto, was generated with a baculo virus system in insect cells (BD Biosciences) according to the manufacturer's protocol. Primers used to amplify the antigen were:

5’-ATCCCGGGCTGCTCATCAGTGAAGACACGC-3’ (forward)
5’-TCAACCGGCGTAGTCGGGCACGTCGTAGGGGTAACCATGATGATGA
TGATGATGCTCATACAGGCTGACATTGTAGAG-3’ (reverse).

The PCR amplification attached sequences encoding (Histidin)$_6$- and HA-epitope tags to the 3’ end of the CDH23 DNA fragment which was cloned into the XmnI/EcoRI site of the pAcGP67A vector (BD Bioscience). The CDH23 epitope-tagged protein produced in insect cells was enriched via a His-tag column and purified further from Acrylamide gels before it was utilized for rabbit immunization. Purification of antigens, coupling of antigens to generate affinity matrices, as well as affinity purification of antibodies was carried out as described in chapter 3.3.

Immunohistochemistry

Inner ears of 6 to 8 week old C57BL/6 mice were dissected in fixative containing 3.7% formaldehyde, 0.025% glutaraldehyde in 0.1 M phosphate buffer pH 7.4. The isolated inner ears were cleaned of extraneous tissue and perfused with a syringe (needle size 0.45 mm x 10 mm; Mirolance^{TM}, Becton Dickinson) through the oval window by slowly applying 0.3 ml to 0.5 ml of fixative. Dripping of fixative from the other side of the ear was indicative that the solution had reached the organ of Corti. Subsequently, the cochlea was cut off the rest of the inner ear and its bony shell was carefully removed. The cochlear duct of adult C57BL/6 mice spirals 2.5 times around the modiolus, a bony structure within the center of the cochlea harboring the spiral ganglion cells. The modiolus and most parts of the peripheral processes emanating from the spiral ganglion cells were removed, the cochlea duct opened and divided into half-turns. The spiral ligament, forming the lateral wall of the cochlear duct, was carefully removed. Half-turns of the organ of Corti extending from the lip of the osseous spiral lamina, were transferred to 24-well plates (Corning) and incubated in fixative for 1 h at RT. In order not to damage the fragile organ of Corti by pulling the samples through the meniscus of a liquid solution, the samples were transferred with the help of a pasteur pipet. To verify that hair cells/hair bundles were still intact after the dissection procedure, samples were analyzed under the microscope at 20x magnification: light flickering at the hair cell apical surface revealed the presence of hair bundles.

Dissection of utricular hair cell patches from inner ears of 6 day old C57BL/6 mice was performed in PBS. Prior to fixation in the above mentioned fixative, the otolithic membrane on top of the hair bundles was removed carefully with fine forceps. The tissues were embedded in OCT and 8 to 16 µm sections were cut on a cryo-microtome, and further processed as described in chapter 3.3.

For the dissection of saccular whole mounts from bullfrog (*Rana catesbeina*), sacculi were isolated in low Ca^{2+} saline (10 mM Hepes pH 7.4; 3 mM D-glucose; 2 mM $MgCl_2$; 2 mM KCl; 110 mM NaCl; 0.1 mM $CaCl_2$), and cleaned of extraneous tissue. Otolithic membranes overlying saccular epithelia were removed with fine forceps after incubation of the tissue in 50 to 75 µg/ml of subtilisin (type XXIV or XXVIII protease) in low Ca^{2+} saline, and, where indicated, treated for 15′ - 20′ with 5 mM La^{3+}, EGTA or BAPTA in low Ca^{2+} saline. For recovery experiments, sacculi were incubated for 24 h at 18˚C in 80% MEM (GibcoBRL) containing 25 mM HEPES pH7.4. Subsequently, the frog sacculi were fixed for 20′ in ice-cold 3-4% formaldehyde in PBS. Sacculi were simultaneously blocked and permeabilized for 1 hour in 3% donkey serum, 0.2% saponin, and 1% BSA prepared in PBS. Subsequently the sacculi were incubated overnight at 4˚C in blocking solution containing CDH23*cyto antibody (1:400) and mouse anti-β tubulin antibody (1:1000, Sigma). Then the sacculi were washed 3 times with PBS and incubated with Donkey anti-rabbit-Alexa 568 antibody (1:300), Donkey anti-mouse-Alexa 350 antibody (1:300) and Alexa 488-Phalloidin (1:100; all reagents from Molecular Probes) for 1 h at room temperature. After a final wash, the sacculi were mounted in Vectashield (Vector labs).

Immunogold Electron Microscopy

Mouse tissues and bullfrog sacculi were dissected and fixed as described above. Subsequently, the samples were washed with 150 mM NaCl and 10 mM Tris-HCl, pH 7.4 (TBS), blocked in TBS containing 10% horse serum and 0.05% Tween 20 (TBS/HS), and incubated with CDH23*cyto antibody in TBS/HS over night at 4ºC. After extensive washing in TBS/HS, samples were incubated with 5 nm gold anti-rabbit antibody (Amersham Pharmacia Biotech) 1:10 diluted in TBS/HS containing 1 mM sodium azide at 4ºC for 48-72 hours with subtle shaking. After 4x washes in TBS/HS for 20′ each and 1x wash in TBS the specimen were postfixed for 1 h with 2.5% glutaraldehyde in 0.1M sodium cacodylate buffer pH 7.4. Samples were fixed for 1 hour in a solution of 1% osmium tetroxide and 1% potassium ferricyanide in destilled water and subsequently washed several times with water. Dehydration was performed at 4°C in an ascending series of ethanol solutions (50%; 70%; 80%; 90%; and 100% for 10′ each with subtle shaking) and washed 3x 10′ in propylene oxide before infiltration with Epon 812 resin (20 ml Epon 812; 16 ml dodecenylsuccinic anhydride (DDSA); 8ml methylnadicanhydride (MNA); 0.66 ml 2,4,6-tri(diethylaminomethyl)phenol (DMP-30); all chemicals purchased from Electron Microscopy Sciences) by incubation of the specimen at room temperature and shaking in an ascending series of Epon resin mixed in propylene oxide (25% Epon for 1 hour; 50% Epon over night; 75% Epon for 1 hour; 100% Epon for 2 hours). Subsequently, the specimen were embedded in Epon and 50-75 nm sections were cut on a Leica microtome, placed on copper grids, stained for 1 h with 2% uranyl acetate in 50% ethanol, for 45´ with lead citrate, and imaged on a Philips EM 208 microscope. The procedure produces good gold labeling, but tip links are less apparent (Garcia et al., 1998). The position of the side plaque marking the upper end of each tip link can be inferred from the position of the shorter adjacent stereocilium. The side plaque should be higher on the adjacent stereocilium by d•sinθ (d = tip link length (150-200 nm); θ = the angle it forms relative to the tip of the short stereocilium (~60°)). The plaque can move up by 50-100 nm if tip links break (Shepherd and Corey, 1992), and the membrane at the shorter stereocilium can be tented upwards by 25 nm or more (Assad et al., 1991). We therefore looked for gold particles associated with stereociliary tips, and with the side plaque 100-300 nm higher than the tip of the shorter adjacent stereocilium. Gold particles were also counted elsewhere along stereocilia, and elsewhere on the sections outside hair cells or at the apical hair cell surface.

CDH23 and Myosin Ic cDNA clones

Mouse CDH23 was cloned by RT-PCR from mouse vestibular RNA. A 5’- and 3’-fragment was amplified with the primers:
5’-ACCATGAGGTACTCCCTGGTCACA-3’;
5’-GCCAGGAATGTCCACACTCTGG-3’;
5-’GAATGACATCAATGACAATGTGCC-3’;
5’-AAAGCTTTCACAGCTCCGTGATTTCCAGAGG-3’.
During amplification, a HindIII site was introduced after the CDH23 stop codon. The fragments were cloned into pCRbluntII (Invitrogen). EcoRI/AatII and AatII/HindIII

sites were used to clone the fragments into pcDNA3.1 (Invitrogen). Mouse MYO1C cDNA was amplified from the EST-clone 5344331 obtained from the IMAGE consortium with the primers:

5’-ATAAGCTTACCATGGAGAGCGCCTTGACTG-3’;

5’-ATGAGATCCTCACCGAGAATTCAGCCGTGG-3’

and cloned into the HindIII/BamHI site of pcDNA3.1. The IL2-□Cyto, IL2-CDH23(+68), and IL2-CDH23(-68) constructs have been described (Siemens et al., 2002).

L929 Cell Lines

L929 cells were propagated in alpha formulated MEM medium (MEMα) containing 10% Horse Serum, 2mM Glutamine, 0.15% Sodium Bicarbonate (GibcoBRL) in a humidified Incubator at 37°C and in an atmosphere containing 5% CO_2. The cells were transfected at 60% to 80% confluency in 10 cm dishes with 0.5 µg pSV2neo DNA plasmid (ATCC) and 5 µg DNA expression vectors for E-cadherin or CDH23 using Fugene 6 transfection reagent (Roche), according to the supplier’s protocol. 48 hours after transfection, the cells were split 1:10, 1:20 and 1:100 and subjected to G418 selection (500 µg/ml) in propagation medium. Old selection medium containing dying cells was removed every 3 days and replaced by fresh medium supplemented with G418. After 12 to 14 days, selected clones were recovered and analyzed by Western blotting employing the CDH23*cyto antibody.

One CDH23 expressing clone was enriched by Fluorescent activated cell sorting (FACS) employing the CDH23*ecto antibody, in order to obtain cells with highest CDH23 expression at the cell surface. The cells were labelled at room temperature with CDH23*ecto antibody diluted 1:50 in culture medium for 15′ with agitation. The cells were centrifuged at 300x g and washed once with medium and subsequently incubated for 15′ at room temperature with Phycoerythrin- (PE-) coupled goat anti-rabbit antibody (Molecular Probes) diluted 1:200 in PBS containing 0.5% BSA (PBSB). After washing the cells once in PBSB, the cells were taken up in 5 ml of PBSB and subjected to fluorescent cell sorting on a FACSVantage DiVa I instrument (BD Biosience), collecting cells with the strongest PE signal. The CDH23 enriched cell clone was subsequently expanded in medium containing G418 and CDH23 expression verified by Western blotting.

Cell Aggregation Assay

For cell aggregation assays, L929 cell lines below confluency were washed twice with Hanks Balanced Salt Solution (HBSS; Gibco Life Technologies) and then trypsinized in HBSS 0.05% Trypsin, 0.02% EDTA (Gibco Life Technologies) for 10' at 37ºC. After the addition of Soy Bean Trypsin inhibitor (Sigma) to a final concentration of 0.05% the cells were triturated until a single-cell-suspension was obtained. The cells were washed once with MEMα medium containing 10% horse serum and taken up in the same medium supplemented with 50 µg/ml DNase I (Roche) and 25 mM Hepes solution pH 7.4. 1 x 10^5 cells in 0.5 ml supplemented medium were seeded into low attachment 24-well plates (Corning; NY) and rotated at 100 rpm at 37ºC for 18 to 20 hours. In control samples the medium was additionally supplemented with 3 mM EGTA to chelate free Ca^{2+}. The cells were fixed by the addition of 200 µl of 25% glutaraldehyde. Formation of aggregates was quantified by determining particle number with a Coulter Counter (Nagafuchi and Takeichi, 1988) and plotting the aggregation index N_0-N_T / N_0 for each individual cell line, were N_0 is the number of particles in the presence of EGTA and N_T the number of particles in the absence of EGTA. The Standard Deviation was determined from 6 independent experiments (N=6).

For the mixed aggregation experiments cadherin transfected L929 cell lines were labeled over night in monolayers with either 1:2500 of DiI (1,1'-dioctadecyl-3,3,3',3'-tetramethylindocarbocyanine perchlorate; Molecular Probes) in saturated ethanol solution or 1:250 of DiO (3,3'-dioctdecyloxacarbocyanine perchlorate; Molecular Probes) in saturated ethanol solution. The cells were washed extensively with HBSS to prevent cross contamination of the dyes. The aggregation assay was carried out as described above with cells from two different cell lines labeled with the two distinct lipophilic dyes and cell aggregates analyzed on an inverted fluorescent microscope in the 24 well plates.

Protease Treatment

3 x 10^5 HEK293 cells were seeded per well in a 6-well dish and 20 hours later transfected with 0.1 µg pcDNA-CDH23 delivered via Fugene 6 reagent (Roche) following the manufacturer's protocol. 36 h later the cells were washed 2 times with HBSS containing 10 mM Hepes (HHBSS) and then treated with 5 - 20 units Elastase

or 5 to 50 μg/ml subtilisin in HHBSS for 10′ at room temperature on a shaker. The reaction was stopped by putting the cells on ice and washing the cells with HHBSS containing 2 mM PMSF and a Protease inhibitor cocktail (Roche). The cells were lysed in 50 mM Hepes, pH 7.4; 150 mM NaCl; 1.5 mM $MgCl_2$; 1 mM $CaCl_2$; 10% (vol/vol) glycerol; 1% Triton plus Protease inhibitors, and subjected to Western blot analysis.

Immunoprecipitation

3x10^5 HEK293 cells per 6-well dish were seeded out in DMEM culture medium containing 10% FCS. 20-24 hours later cells were transfected as described by Chen and Okayama (Chen and Okayama, 1987): The transfection mixture contained the following ingredients:

Il2-CDH23 fusion expression plasmid:	0.7 μg
MyoIc expression plasmid:	1 μg
Salmon sperm DNA:	2.3 μg
1M $CaCl_2$:	25 μl
H_20:	added to a volume of 100 μl

The solution was mixed and 100 μl of 50 mM N-N-Bis(2-hydroxyethyl)-2-aminoethansulfonic acid (2x BBS, pH 6.96) was added, the solution mixed again and incubated at room temperature for 15′ to 20′. Subsequently the solution was added to a 6-well dish of HEK293 cells, swirled to mix and incubated for 4 hours at 37°C and 3% CO_2. The cells were washed with medium once and then incubated in fresh medium for another 18 to 24 hours. The cells were harvested by washing them off the plate and collected by centrifugation for 2’ at 5000 rpm in a table-top centrifuge. The cells were washed once with PBS, centrifuged again and lysed on ice in 400 μl RIPA buffer (50 mM Tris, pH 7.4, 150 mM NaCl, 1% NP40, 0.5% deoxycholate, 0.1% SDS, 1 mM phenylmethylsulfonyl fluoride and 10 μg/ml aprotinin). The cell debris was removed by centrifugation for 5’ with 14000x g at 4°C and the supernatant transferred to a new tube. For direct Western blot analysis of protein expression 10 μl whole cell lysate was subjected to SDS-PAGE. For Immunoprecipitation 2.5 μg mouse anti-Il-2-Receptor α antibody (UBI) or 3 μg mouse anti-MYOIC, MT2, (Walker et al., 1993) were added to 350 μl of whole cell lysate, supplemented with 25 μl slurry Protein A sepharose or Protein G sepharose respectively. The immunoprecipitation was incubated at 4°C on a rotating wheel over night and then washed 3x with RIPA buffer. After the final wash, 25 µl of Laemmli sample buffer was added and the samples incubated at 95°C for 5′. SDS-gel electrophoresis and Western blotting with rabbit ant-IL-2-Receptor α (1:200, Santa Cruz) or mouse anti-MYOIC (MT2, 1:800) was performed as described. (Siemens et al., 2002).

Immunocytochemistry

2x 10^5 HEK293 cells were seeded out on coverslips in 6-well dishes and transfected as described above. 36 hours post transfection, the cells were washed once in PBS and then fixed in PBS containing 2% PFA for 10′ at room temperature. The cells were washed twice with PBS and residual PFA quenched with PBS containing 100 mM Glycine for 15′ at room temperature. Cells were blocked for 1 hour at room temperature in PBS containing 5% FCS, 0.5% BSA and 0.1% Triton-X100 and subsequently incubated in blocking solution with mouse anti-MYOIC (MT2, 1:400) and goat anti-IL-2-Recptor α (1:100; R and D Systems) over night at 4°C. Cells were washed with PBS and incubated in blocking solution containing Alexa 488-conjugated anti-mouse antibodies (1:400; Molecular Probes) and Cy3-conjugated anti-goat antibodies (1:500, Jackson ImmunoResearch) for 1 hour at room temperature. After three final washing steps with PBS, the cells were mounted with Vectashield containing DAPI (Vector Labs). Images were collected on a Deltavision microscope and processed by deconvolution.

Genotyping of *Waltzer* Mice

DNA was prepared from tips of mouse tails by digestion with a buffer containing 0.5% SDS, 0.1 M NaCl, 0.05 M Tris pH 8.0, 3 mM EDTA and 0.1 mg/ml Proteinase K over night at 60°C. 0.15 volume of 8 M potassium acetate and 1 volume of chloroform were added to the digested sample, vortexed and frozen at -80°C. Samples were thawed and centrifuged at 14000 rpm for 10′ in a micro-centrifuge. The supernatant was transferred to a fresh tube and 2 volumes of absolute ethanol were added, mixed and centrifuged again at 14000 rpm for 5′. The pellet was washed once with 70% ethanol, air-dried and taken up in 100 µl of water. 1 µl of the DNA sample was used for PCR amplification with 0.2 µM of each of the two primers:

Taqf: 5’-CCTCTTCAAGATAGATGCTATCTCG-3’

Taqr: 5’-GGCTCAATAAATACACGC-3’

Additionally the PCR reaction mix contained 0.2 mM dNTPs, 5 µl 10x PCR buffer (Roche) and 1 U TaqDNA Polymerase (Roche). PCR conditions were as follows: 2′ 94°C, followed by 30 cycles (1′ 94°C; 1′ 58°C, 1′ 72°C). The PCR product was subsequently cleaned with the Qiagen PCR purification kit (Quiagen) according to the supplier’s protocol and eluted in 30 µl of water. The PCR product was digested with TaqI restriction endonuclease by the addition of 3.5 µl 10x TaqI buffer (New England Biolabs), 0.34 µl 100x bovine serum albumin (New England Biolabs) and 1.5 µl of 25 U/µl TaqI (New England Biolabs). The sample was incubated at 65°C for 2 hours and DNA fragments separated on a 2% agarose gel. The wild type DNA fragment contained 100 base pairs and the *waltzer* point mutation gave rise to DNA fragments of 80 base pairs and of 20 base pairs.

Acknowledgements

We thank R. Kemler (MPI Freiburg) for E-cadherin clones; M. Senften (Scripps) for L929 cells expressing E-cadherin; T. Hasson (UCSD), B. Ranscht and H.C. VanSteenhouse (Burnham Institute) for technical advice; A. Kralli, L. Stowers, and A. Patapoutian (Scripps) for critical reading of the manuscript. J.S. was supported by a fellowship from the Boehringer Ingelheim Fonds; A.R. by a C.J. Martin Fellowship from the National Health and Medical Research Council (Australia). The work was supported by RO1 grants from the NIH (U.M, P.G.G. and D.S.W.).

4.6. Supplementary Figures

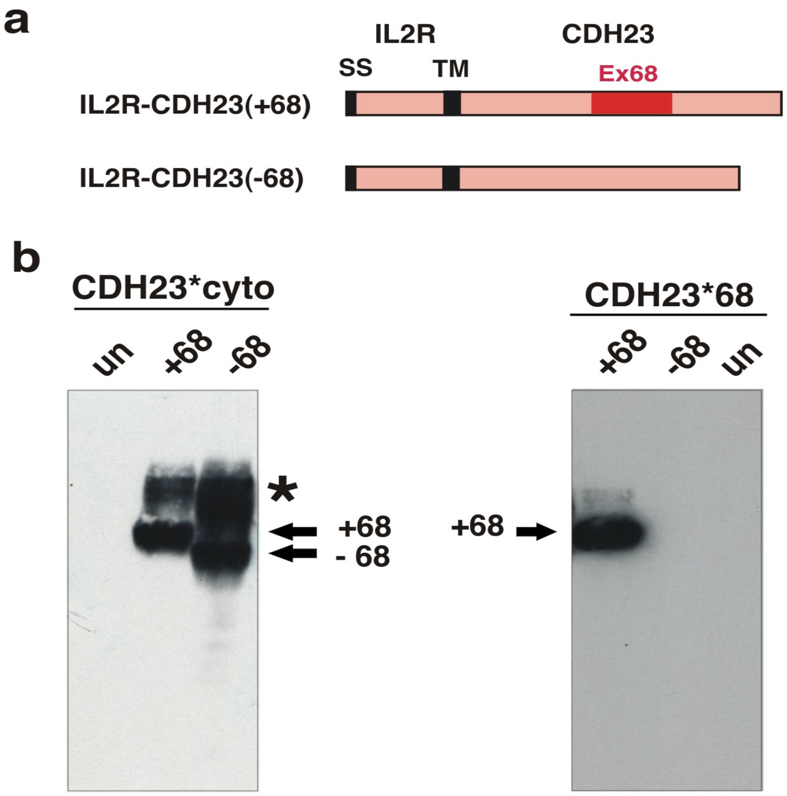
a
IL2R
CDH23
SS
TM
Ex68
IL2R-CDH23(+68)
IL2R-CDH23(-68)
b
CDH23*cyto
un
+68
-68
*
+68
- 68
CDH23*68
+68
-68
un
+68

Supplement Fig. S1: Characterization of CDH23 specific antibodies. **a,** Fusion proteins between the extracellular and transmembrane domain of the IL2 receptor and the CDH23 cytoplasmic domains containing/lacking exon 68 encoded amino acids were expressed in HEK293 cells. **b,** Protein extracts were prepared and analyzed by Western blotting with antibodies directed against the CDH23 cytoplasmic domain (CDH23*cyto) or against the exon 68 containing isoform (CDH23*68). CDH23*cyto recognized all CDH23 isoforms, while CDH23*68 specifically recognized exon 68 containing isoforms. (The asterisk denotes a background band that is occasionally observed in extracts from transfected cells).

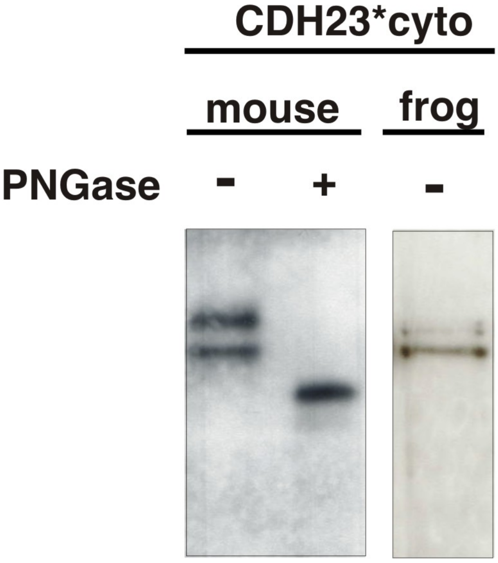

Supplement Fig. S2: **Crossreaction of CDH23*cyto with bullfrog CDH23.** Protein extracts from mouse or bullfrog brains were analyzed by Western blotting with antibody CDH23*cyto. The antibody recognized two bands in mouse tissue, representing two distinct N-glycosylated isoforms of CDH23, as revealed by treatment of samples with PNGase. In bullfrog extracts, two bands of similar size were observed.

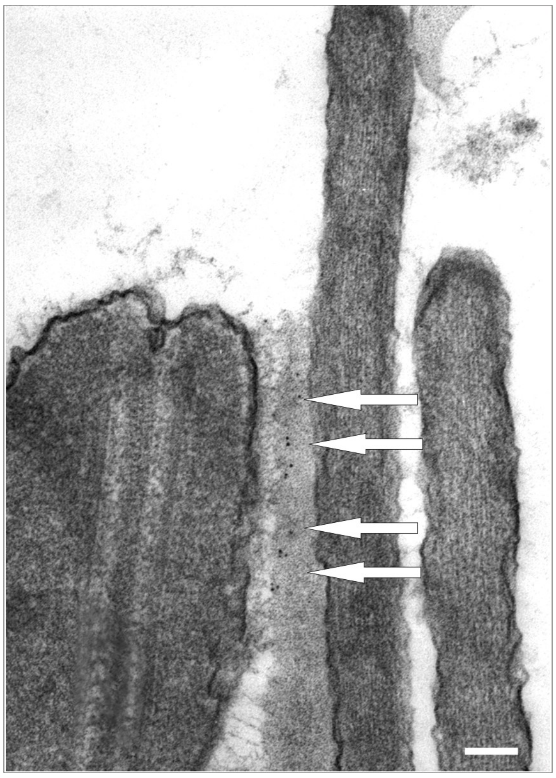

Supplement Fig. S3: Electron micrograph of the kinocilium and adjacent stereocilia of a bullfrog hair cell. The kinociliary links connect the kinocilium at the left to the light grey stereocilium in the background. Arrows point to gold particles that indicate the localization of CDH23 immunoreactivity. Scale bar: 100 nm.

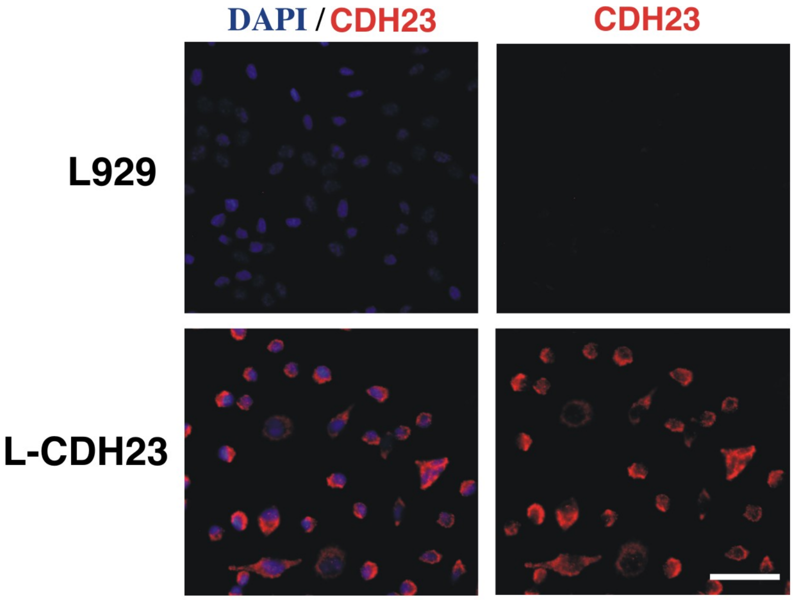
DAPI / CDH23
CDH23
L929
L-CDH23

Supplement Fig. S4: CDH23 expressing cell lines. Parental L929 cells and a sublines stably transfected with a CDH23 expression vector were stained with DAPI (blue) and CDH23*cyto antibodies (left panels, double-staining; right panels, CDH23*cyto staining). L-CDH23 but not L929 cells expressed CDH23. Scale bar: 40 µm.

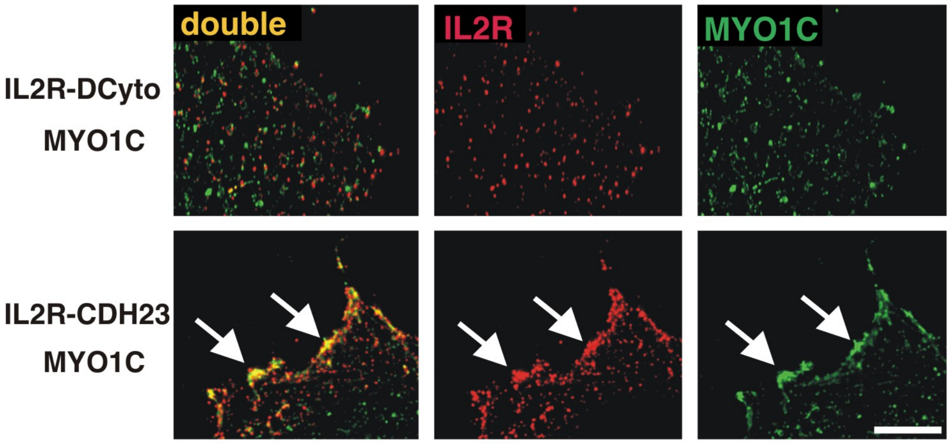
double
IL2R
MYO1C
IL2R-DCyto
MYO1C
IL2R-CDH23
MYO1C

Supplement Fig. S5: Colocalization of IL2R-CDH23 with MYO1C also in COS cells. Transfected cells were stained with IL2R (red) and MYO1C (green) antibodies. MYO1C colocalized with IL2R-CDH23(+68), but not with IL2R-DCyto. Scale bars: 3.5 µm

Additional Results

5. Additional Results

5.1. Mislocalization of Truncated CDH23 Protein in *v2j* Mutant Mice

We have shown that CDH23 is expressed in stereocilia of inner ear hair cells in wild-type mice, frogs and chicken (paper 1 and 2 and data not shown). Within the inner ear, we detected by immunostaining with an antibody directed against the C-terminal cytosolic portion of CDH23 (CDH23-cyto) that a second cell type also expressed the protein. These cells are part of Reissner´s Membrane, a structure consisting of two cell layers that separates the K^+-rich endolymphatic fluid from the perilymph. The apical hair cell surface, including the stereocilia, is immersed in the endolymph, the ionic composition of which is important for auditory transduction (Wangemann, 2002). The Reissner´s Membrane harbors mesenchymal cells on the perilymphatic side and epithelial cells facing the endolymphatic duct. We detected CDH23 protein on the apical surface of the epithelial cells, which contain microvilli and is believed to produce a tight seal separating the two different ionic compartments. As expected the CDH23-cyto antibody failed to recognize an epitope in either hair cell or Reissner´s Membrane cells of *v2j* mice with a mutation in the *Cdh23* gene.

The *v2j* mutation is a G-A transition in intron 32 of the *Cdh23* gene, which disrupts a wild-type donor splice site. Concomitantly, splicing of *Cdh23* transcripts is aberrant in mutant mice leading to a putative truncation of CDH23 protein in EC-domain 13 of its extracellular domain. Since the putative truncated product has a proper signal sequence but lacks the transmembrane domain and cytosolic tail, it is conceivable that the aberrant protein is secreted into the extracellular space.

We generated an antibody directed against the first four N-terminal EC-domains of CDH23 (amino acid residues 40-471; CDH23-ecto) and performed immunohistochemical stainings on histological sections of wild-type and *v2j* mutant mice. In inner ear sections of wild-type mice the labelling pattern mirrored exactly the pattern observed with the CDH23-cyto antibody, and showed staining of hair cells and the Reissner´s Membrane. In contrast, on sections of mutant mice we still detected a signal from the CDH23-ecto antibody in the vicinity of the hair cell stereocilia and Reissner´ss Membrane. Closer examination of the staining at the Reissner´s Membrane revealed, that the protein recognized by this antibody is not localized at the apical cell surface of the epithelial cells facing the endolymphatic lumen anymore, but is rather distributed around these cells (Fig. 5.1.). From the staining it is not clear if the epitope recognized by CDH23-ect antibody is secreted or rather contained in the cells.

These results suggest that indeed a truncated CDH23 product is generated in *v2j* mutant mice but due to the loss of its plasma membrane anchor and lack of its cytosolic tail the peptide is mislocalized and therefore most likely not functional.

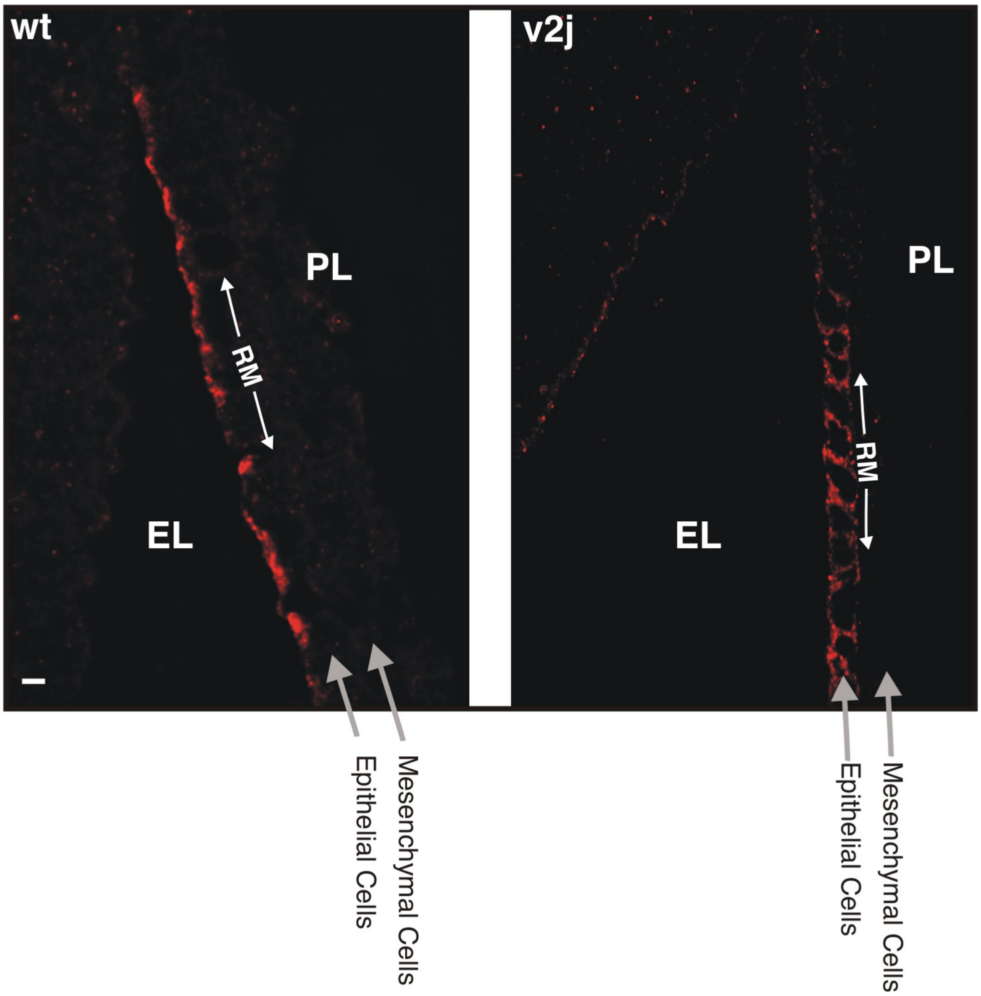

Figure 5.1. Mislocalization of Truncated CDH23 Protein in the Reissner´s Membrane of *v2j* Mutant Mice.
Histological sections of inner ears obtained from newborn wild-type (WT) or *v2j* homozygous mutant mice were stained with an antibody recognizing the N-terminal, extracellular first 4 EC-domains of CDH23, CDH23-ecto (red). In wild-type mice only the apical surface of the epithelial cells was labelled, while in the mutant mice the whole epithelial cell surface appeared to light up. RM: Reissner´s Membrane, EL: Endolymph, PL: Perilymph, size bar: 10 µm.

The function of CDH23 within the Reissner´ss Membrane of wild-type mice is not known. Likewise it is not established if absence of functional CDH23 protein from the Reissner´s Membrane contributes to the phenotype observed in *v2j* mutant mice and/or causes leakiness of the ionic barrier resulting in altered endocochlear potential.

5.2. Ultrastructural Localization of CDH23 in Retinal Photoreceptors of the Mouse

Mutations of *CDH23* can lead to Usher Syndrome in human patients not only affecting the auditory system but also vision. We detected CDH23 expression in the retinal photoreceptor layer of newly born, wild-type mice by light microscopy. In order to localize CDH23 protein more precisely, we carried out Immuno-Electronmicroscopy in a similar fashion as for hair cells, described in Paper 2. We reproducibly localized the protein at the membrane of the connecting cilium and some labelling was also detectable within the membranous disc stacks of the outer segment (Fig. 5.2.).

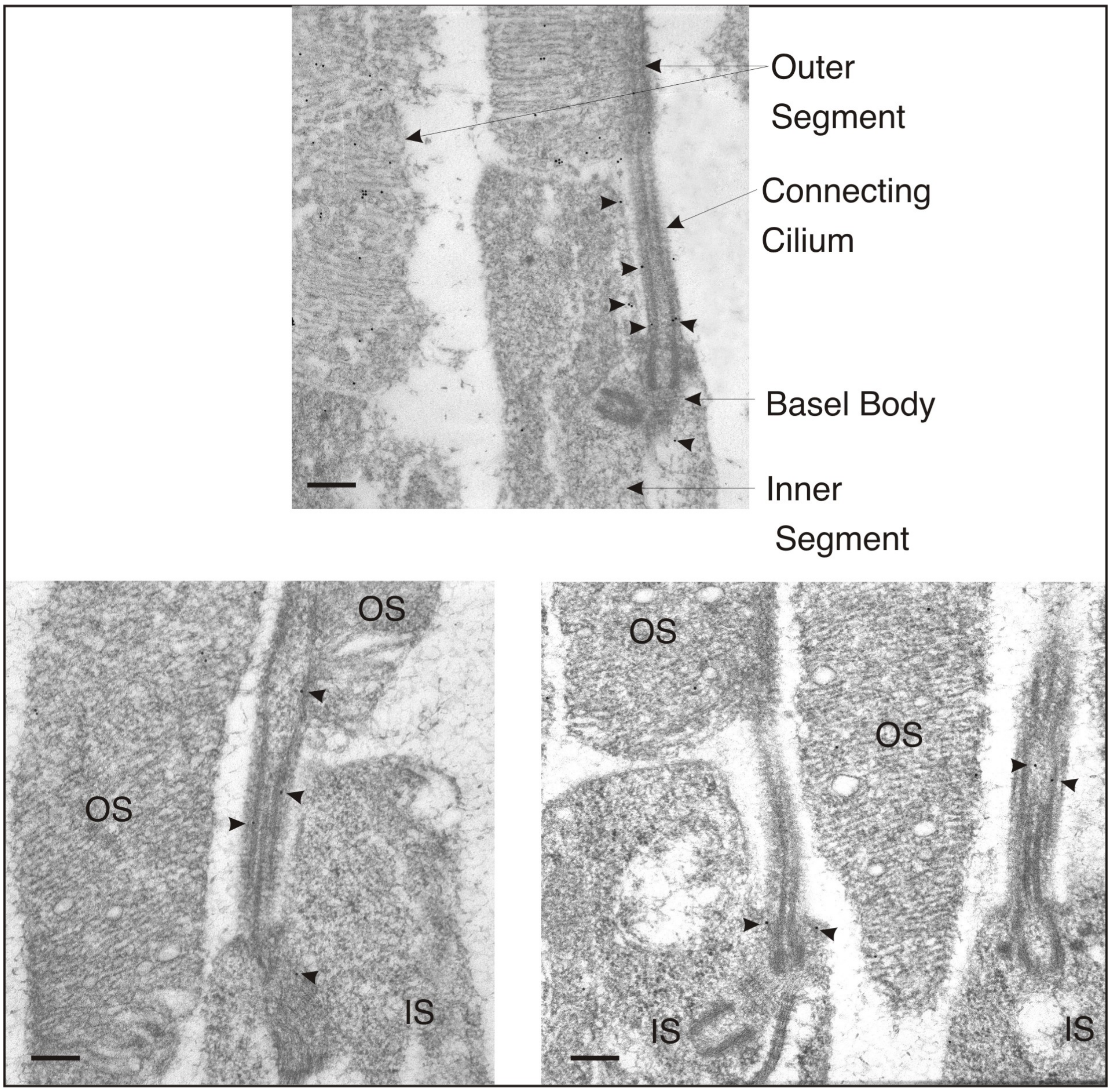
Outer
Segment
Connecting
Cilium
Basel Body
Inner
Segment
OS
OS
IS
OS
OS
IS
IS

Figure 5.2. Ultrastructural Localization of CDH23 in Mouse Photoreceptors. Displayed are three electron micrographs of retina samples from adult mice that have been immuno-gold labelled with anti-CDH23 antibody (CDH23-cyto). In the upper picture prominent features of the photoreceptor cells have been indicated by arrows, in the lower two pictures outer segments (OS) and inner segments (IS) have been denoted for better orientation. Labelling for CDH23 at or near the connecting cilium is pointed out by arrowheads. Note that some labelling (although not in all micrographs) is visible in the outer segment as well (scale bars: 200 nm).

5.3. Expression of CDH23 in Tissues other than Ear and Eye

We detected CDH23 expression in primary sensory cells of the auditory and visual systems of mice. Likewise, the proteins MYOVIIA and harmonin which can form a complex with CDH23, have been detected in the same cells by us and others. To investigate whether CDH23, harmonin and MYOVIIA may play a role in other sensory systems we carried out immunohistochemistry with antibodies directed against the respective proteins on histological sections of the mouse olfactory epithelium and whisker pads. The stainings were conducted on tissues of adult wild-type mice as described in Materials and Methods of paper 1.

5.3a. Olfactory Epithelium

The olfactory epithelium is composed of three cell types, the Receptor cells which are bipolar sensory neurons, the supporting cells (also referred to as Sustentacular cells) and the Basal cells (Fig. 5.3.). The Receptor cell contains a specialized dendrite from which olfactory cilia project into the lumen of the nasal cavity. These cilia harbor the „olfactosom“, the machinery which detects chemical stimuli (odorants) and relays the signal into the cell interior. From the apical surface of the supporting cells microvilli protrude into the mucus film of the lumen.

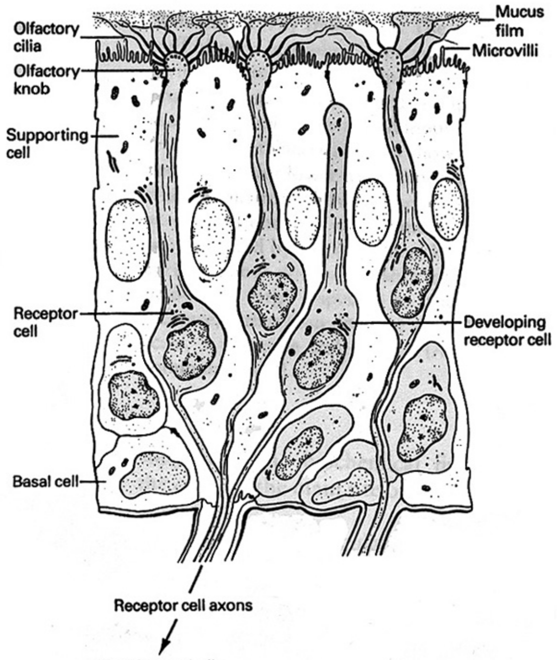

Figure 5.3. Schematic Representation of the Olfactory Epithelium.
Depicted in this cartoon are the most prominent structures of the olfactory epithelium, including the Receptor cell dendrites with the olfactory cilia and the supporting cells projecting microvilli from their apical surface into the nasal cavity. (Adopted from: http://www.du.edu/~kinnamon/3640/smell/smell.html).

Residing at the basolateral membrane of the olfactory epithelium are the Basal cells, which constitute the precursors of both the olfactory Receptor cells and the Supporting cells. Due to mechanical and chemical abrasion the olfactory neurons have to be substituted constantly.

By fluorescent analysis of histological sections we detected CDH23 expression at the apical surface of the olfactory epithelium in the region where supporting cell microvilli and sensory cilia are found (Fig. 5.4). Harmonin and MYOVIIA staining overlapped with CDH23 labelling at the apical surface of the olfactory epithelium. MYOVIIA has been shown to localize to both sensory cilia and microvilli by ultrastructural analysis. MYOVIIA and harmonin appeared to be broader expressed compared to the CDH23 labelling, the CDH23 signal rather seemed to orginate from discrete spots at the apical surface and occasionally from elongated structures arising from the cell nuclear layer (Fig. 5.4 panel 5) visualized here by Dapi counter staining. Therefore CDH23 may primarily reside in the ciliated sensory dendrites while harmonin and MYOVIIA are expressed in both the microvilli and sensory cilia. Future studies with markers specifically labelling sensory dendrites and ultrastructural localization of CDH23 in the olfactory epithelium will have to clarify the interpretation of this immunohistochemical analysis.

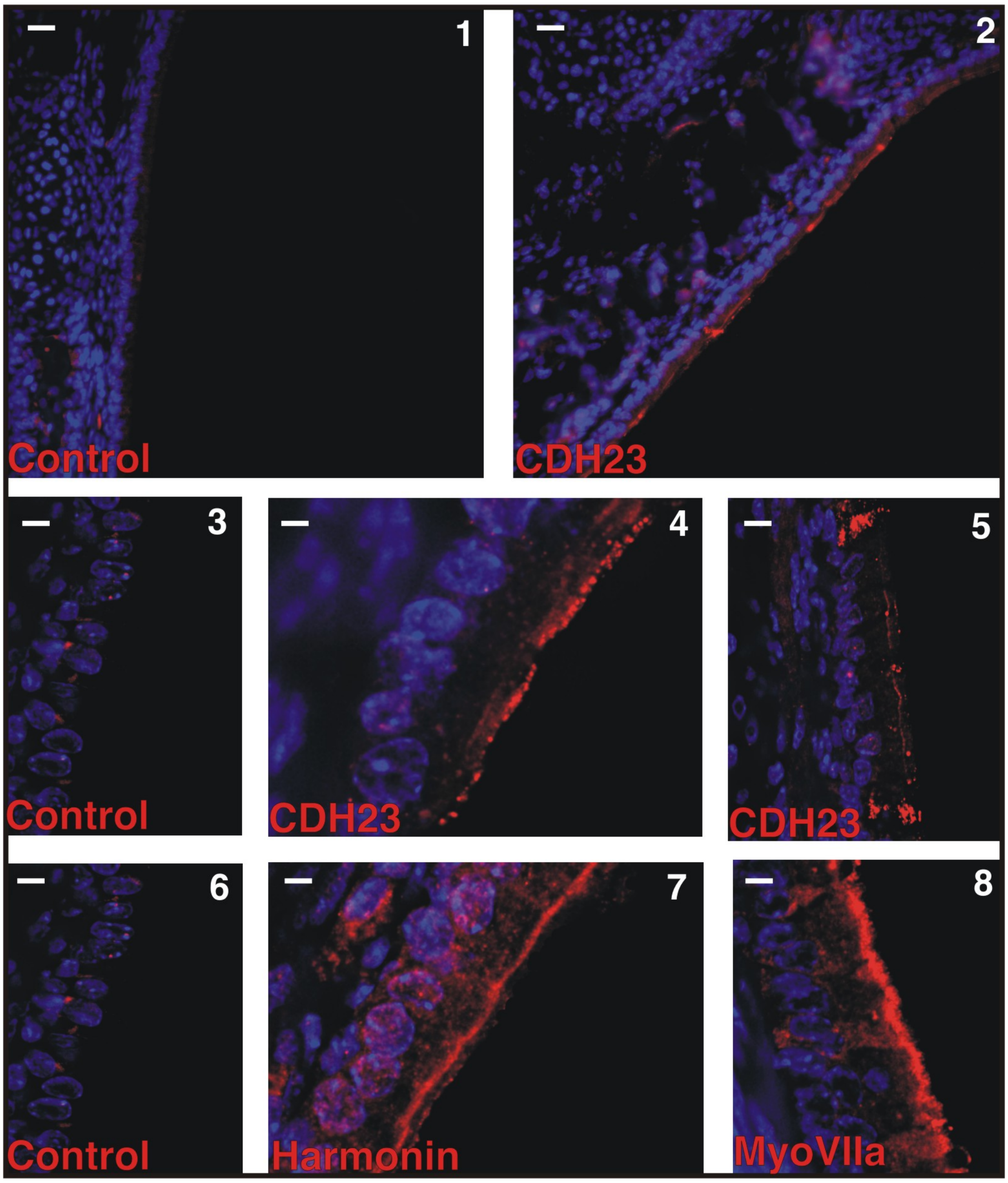
1
Control
2
CDH23
3
Control
4
CDH23
5
CDH23
6
Control
7
Harmonin
8
MyoVIIa

Figure 5.4. Localization of CDH23, Harmonin and MYOVIIA in Adult Mouse Olfactory Epithelium.
Cross-section through the nasal cavity. In all pictures the lumen of the nasal cavity is to the right and the olfactory epithelium is on the left side. Cell nuclei are visualized by Dapi staining in blue. The respective proteins are labelled in red; CDH23 staining is shown in pictures 2, 4, and 5; harmonin staining is shown in picture 7 and MYOVIIA in 8. Scale bars are: 60 µm in 1 and 2; 10 µm in 3, 5 and 6; 5 µm in 4, 7 and 8.

5.3b. Whisker Follicle

The skin of every species contains a variety of different sensors for the perception of mechanical, thermal and chemical stimuli. Specialized mechanical receptors are the whiskers in rodents and other animals. Whisker follicles have an overall structure that is highly similar to hair follicles but differs in size. The follicle is composed of an outer root sheath (ORS) that is contiguous with the epidermis, an inner root sheath (IRS) and the hair shaft itself (Fig. 5.5.). The actively dividing undifferentiated matrix cells give rise to IRS and hair shaft. The matrix surrounds a pocket of specialized mesenchymal cells, called the dermal papilla (DP). The DP is essential to follicle formation, it is the follicle organizer. The characteristics of the appendage generated (whisker or body hair in mouse; feather or scale in the chicken) are determined by the epithelial cells that make up the follicle. The lower segment of each hair follicle cycles through periods of active growth (anagen), destruction (catagen) and quiescence (telogen). During anagen, matrix cells proliferate rapidly. As they move upward, they leave the cell cycle and differentiate according to a strict plan, giving rise to concentric rings of the differentiated cell types of the IRS and hair shaft. During catagen, the lower follicle undergoes concerted apoptotic death. The DP moves upward until it rests beneath the bulge, where it remains during telogen. Induction of a new anagen occurs when the DP recruits bulge cells to regenerate the follicle by proliferating.

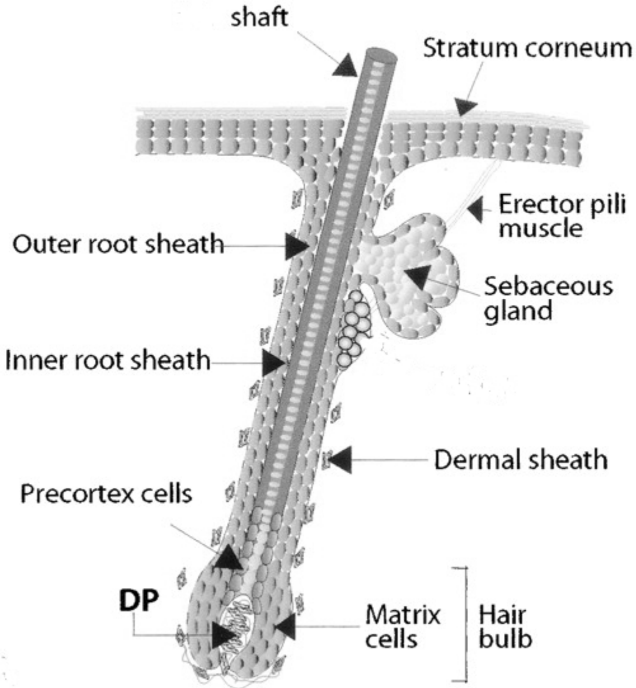

Figure 5.5. Schematic Drawing of a Whisker Follicle.
From inside out there are the hair shaft, precortical cells, inner root sheath cells and outer root sheath cells within the follicle. At the bottom of the follicle are matrix cells that surround the dermal papilla (DP). (Adopted from: *Genes Dev.* 2003; 17; 1189-1200).

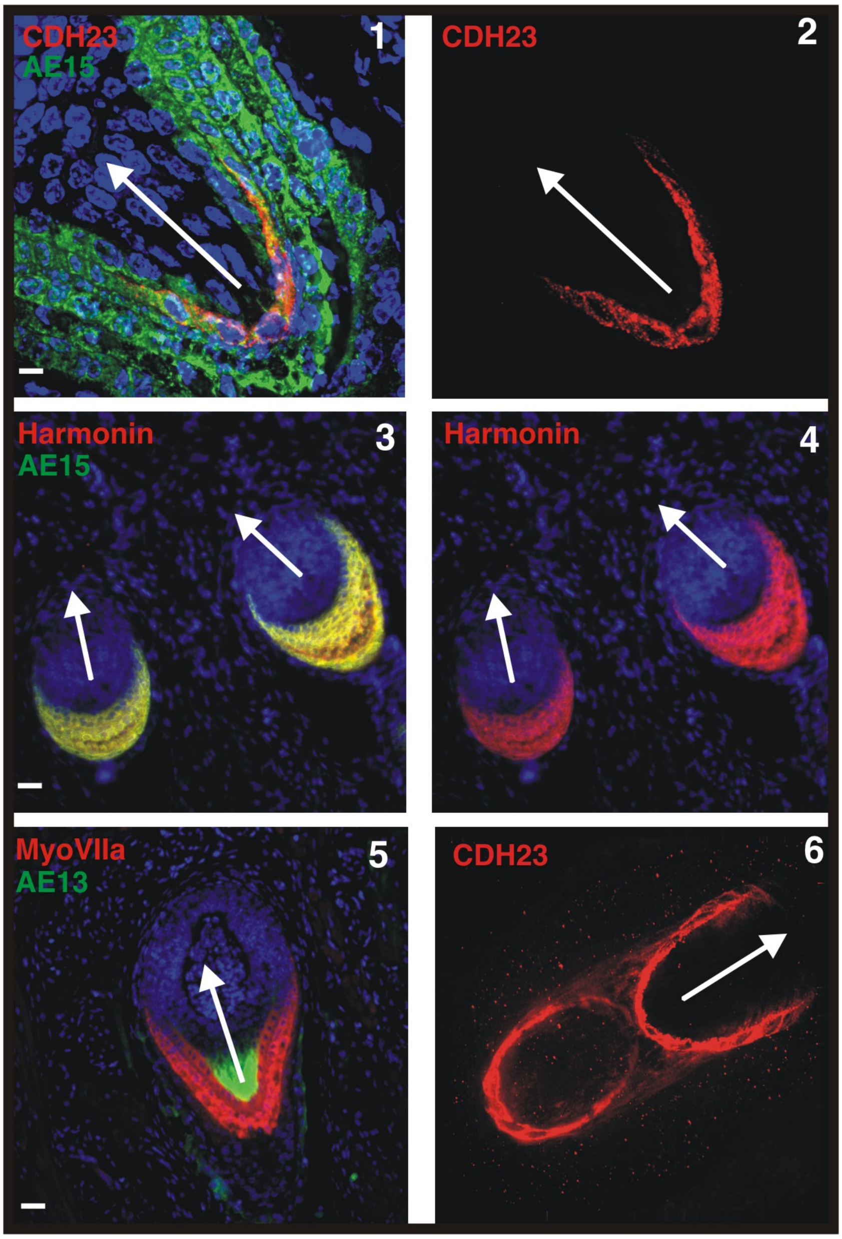
CDH23
AE15
1
CDH23
2
Harmonin
AE15
3
Harmonin
4
MyoVIIa
AE13
5
CDH23
6

Figure 5.6. CDH23, Harmonin and MYOVIIA Coexpression in the Cuticle of Hair Follicles.
Histological sections of adult mouse whisker pads were fluorescently labelled with antibodies against the indicated protein in red. The IRS or the hair shaft is visualized by the respective marker antibodies AE15 or AE13 in green. Dapi staining in blue shows cell nuclei. The white arrow indicates the position of the hair shaft with the arrow head pointing towards the skin surface. Scale bars are 10 µm in panel 1 and 30 µm in panels 3 and 5.

We investigated CDH23, harmonin and MYOVIIA expression in adult mouse whisker pads and pelage skin. For immunohistochemical analysis we counterstained histological sections with marker antibodies for the IRS (antibody AE15) (O'Guin et al., 1992) or hair shaft (antibody AE13) (Dhouailly et al., 1989; Lynch et al., 1986). The mouse monoclonal antibodies AE15 and AE13 were employed at a dilution of 1:30 each on histological sections as described above. We detected high expression of CDH23 in the cuticle, the inner most cell layer of the IRS directly contacting the hair shaft (Fig. 5.6). In three dimensional reconstruction of fluorescent whisker follicle images it appeared that CDH23 was expressed in discrete cuticle cells comprising two rings around the hair shaft (Fig. 5.6 panel 6). harmonin and MYOVIIA were both strongly expressed in the entire IRS as visualized by counterstains for the IRS or hair shaft.

In summary, while harmonin and MYOVIIA are more widely expressed through out the IRS, all three proteins (CDH23, harmonin and MYOVIIA) show overlapping expression in the inner most cell layer of the IRS directly connecting to the hair shaft. The function of these three proteins in hair- and whisker follicle are not known likewise are no phenotypic alterations in these organs described for *waltzer* or *shaker* mice defective in the genes encoding CDH23 or MYOVIIA respectively.

5.4. Introduction of Specific Muatations in the *Cdh23* Gene of the Mouse.

Our findings clearly demonstrate that CDH23 is part of the tip- and kinocilia linkage system of the auditory and vestibular hair bundle. Further, CDH23 and harmonin form a protein-protein complex via PDZ domain interactions. The structure of this complex depends on sequences encoded by the alternatively spliced exon 68 of CDH23 that is expressed in hair cell stereocilia but not in any other tissue analyzed thus far. The exclusiveness of exon 68 expression in the hair cell stereocilia points to a selective function in this particular tissue. Since the tip link is believed to be involved in transduction channel gating it is possible that exon 68 is important for auditory perception in the inner ear.

5.4a. The Targeting Constructs

To test this hypothesis we generated a targeting construct designed to specifically ablate exon 68 of the *Cdh23* gene from the mouse genome. In addition we generated a control targeting construct with the purpose to delete the complete cytosolic domain of the *Cdh23* gene, while leaving the extracellular and transmembrane portion intact. This deletion will abolish any CDH23 - harmonin interaction and any recruitment of other putative proteins to the CDH23 cytosolic domain.

A BAC clone containing the 3′end of the mouse *Cdh23* gene was used as starting material. 14000 bases (14 kb) of the *Cdh23* 3′region were subcloned and the respective genomic sequences for exon 68 or sequences encoding the complete cytosolic domain exchanged for a *neo-TK*-cassette encoding appropriate resistance markers for subsequent embryonic stem cell (ES-cell) selection (Fig. 5.7). The *neo-TK*-cassette employed for the targeting constructs was flanked by so-called LoxP-sites, allowing CRE-mediated ablation of the *neo-TK*-cassette after targeting to the *CDH23* genetic locus. The removal of the cassette is necessary to ensure proper expression of the truncated CDH23 protein products.

The sequences that were exchanged in case of the targeting construct for exon 68 deletion (CDH23-E68 Skip) encompasses the entire exon 68 coding sequence and the neighbouring intronic splice acceptor and splice donor sites. For the targeting construct deleting the complete cytosolic domain (CDH23-Δcyto), a stop codon was introduced downstream of the membrane-stop-transfer sequence in exon 64 and exons 65-69, encoding the cytosolic domain of CDH23, exchanged for the *neo-TK*-cassette.

ES-cells were electroporated with the constructs and ES-cell clones subjected to G418 selection. For each construct 100 clones were expanded and screened by Long Range PCR with primer pairs So5/Neo or So5/TK for homologous recombination of the CDH23-E68 Skip construct or the CDH23-Δcyto construct respectively (Fig. 5.8 panel A and B; primer positions are indicated in Figure 5.7). We obtained many positive clones for the CDH23-E68 Skip construct but only a few for the CDH23-Δcyto construct. Recombination was confirmed by Southern blot analysis (data not shown).

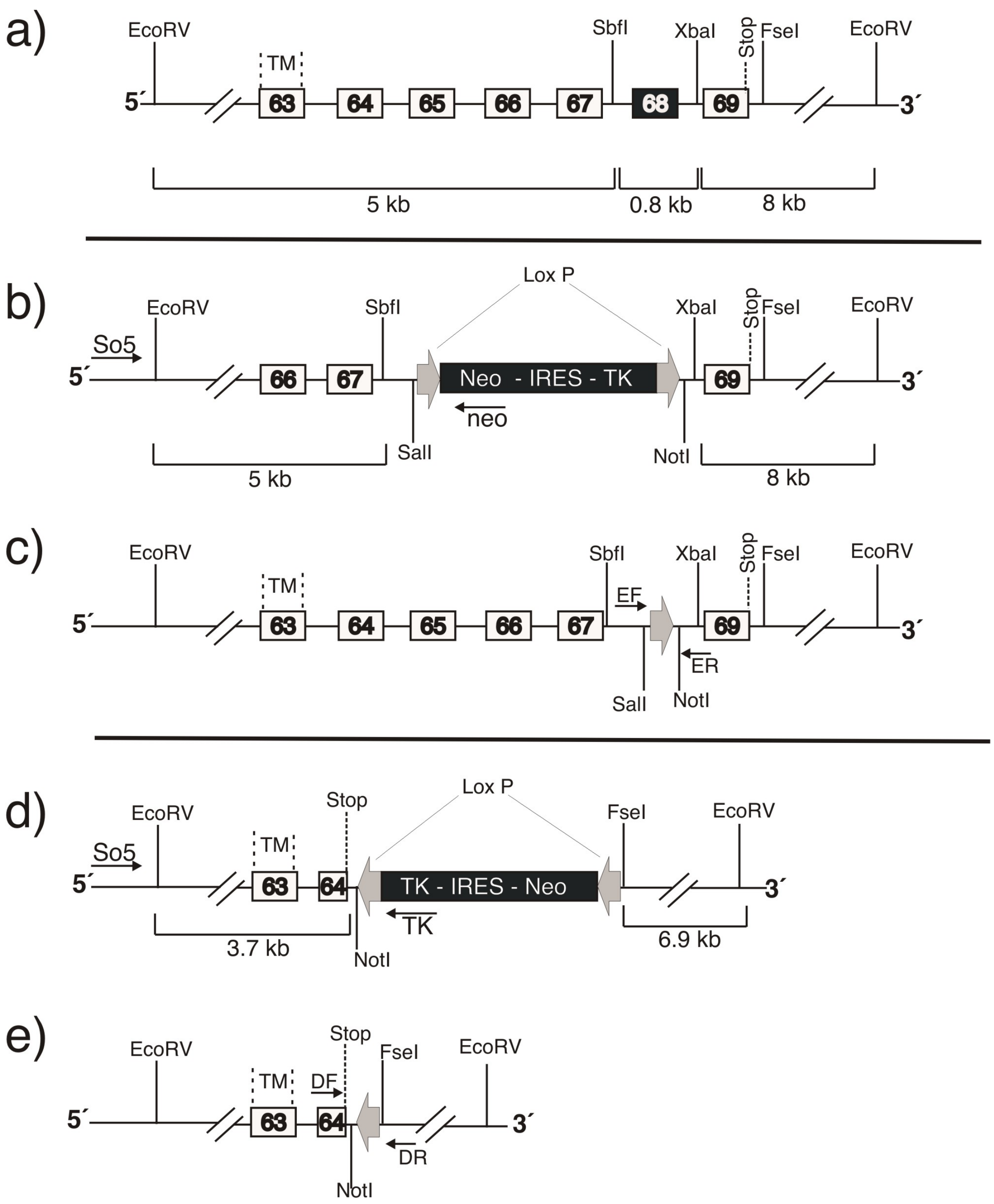
a)
EcoRV
SbfI
XbaI
Stop
FseI
EcoRV
TM
5′
63
64
65
66
67
68
69
3′
5 kb
0.8 kb
8 kb
b)
Lox P
EcoRV
SbfI
XbaI
Stop
FseI
EcoRV
So5
5′
66
67
Neo - IRES - TK
69
3′
neo
SalI
NotI
5 kb
8 kb
c)
EcoRV
SbfI
XbaI
Stop
FseI
EcoRV
TM
EF
5′
63
64
65
66
67
69
3′
ER
SalI
NotI
d)
Lox P
EcoRV
Stop
FseI
EcoRV
TM
So5
5′
63
64
TK - IRES - Neo
3′
TK
3.7 kb
NotI
6.9 kb
e)
Stop
EcoRV
FseI
EcoRV
TM
DF
5′
63
64
3′
DR
NotI

Figure 5.7. CDH23 Targeting Constructs.
Panel a) depicts the genomic organization of the last 7 exons (exons 63-69) of the mouse wild-type *Cdh23* locus in the 5′⇒ 3′direction. Labelled are relative positions of unique restrictions sites, exon 63 encoding the transmembrane domain (TM), and exon 69, which contains the stop codon. Panel b) shows targeting of the CDH23-Ex68 Skip construct before CRE-mediated recombination and in panel c) after CRE-mediated recombination. Panel d) depicts targeting of the CDH23-Δcyto construct before CRE-mediated recombination and panel e) after CRE-mediated recombination. The lower part of panel a), b) and d) shows the relative distances of genomic DNA fragments in 1000 base pairs (kb). Relative positions of the primer So5, neo, TK, EF, ER, DF and DR, used for screening of targeted ES-cell clones, are depicted in panels b) - e).

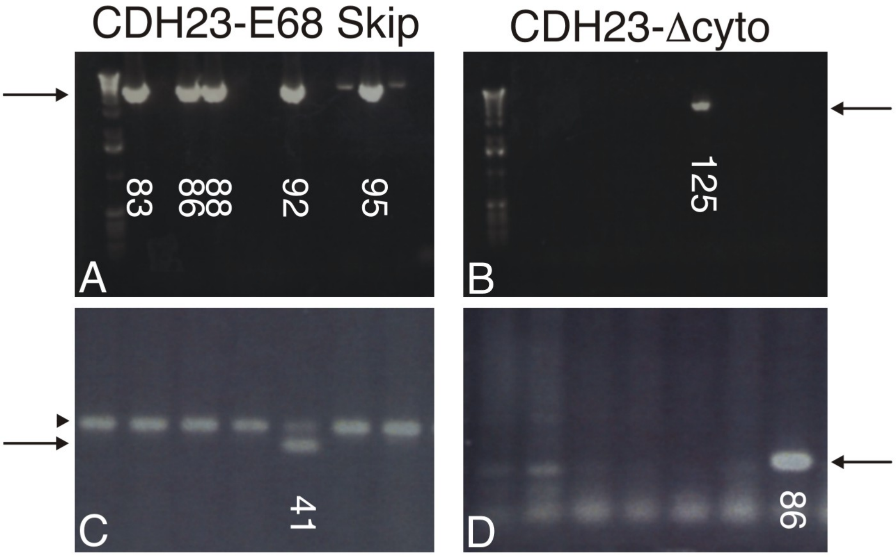

Figure 5.8. PCR-Screen for CDH23-E68 Skip and CDH23-Δcyto gene targeting in ES-cells.
Depicted are photographs of representative DNA gels showing PCR products amplified from genomic ES-cell DNA after electroporation with the indicated targeting constructs. Panel A and B are before CRE-mediated recombination and panel C and D show a PCR analysis of ES-cell DNA after CRE-mediated recombination of positive clones from A and B. Arrows point at the expected PCR product size, the arrowhead in C indicates the wild-type band. The identification numbers of positive ES-cell clones are indicated.

Next, an expression plasmid for CRE recombinase was introduced into positive ES-cell clones obtained from the previous ES-cell electroporation of the targeting constructs. The ES-cells were negatively selected against Thymidinkinase (TK) and their genomic DNA subsequently PCR-screened with primers EF/ER (in case of the CDH23-E68 Skip construct) or DF/DR (in case of the CDH23-Δcyto construct) for ablation of the *neo-TK*-cassette (Fig. 5.8 panel C and D; primer positions are indicated in Fig. 5.7).

We obtained several positive ES-cell clones that had lost the *neo-TK*-cassette from the *CDH23* genomic locus. Currently attempts are underway to obtain transgenic mice from those ES-cells.

5.4b. Anticipated Outcome of the Genomic Truncations of *Cdh23*

The strong expression of CDH23 along the entire length of the stereocilia during hair bundle maturation, points to a function of the protein in this developmental process next to its role as tip link in mature stereocilia. It is likely that CDH23 is necessary to keep hair bundle integrity during the elongation phase of the stereocilia, since the hair bundles are splayed in the *walzer* mice defective for *Cdh23.* By deleting specifically exon 68 of *Cdh23* we hope to circumvent the phenotype of splayed stereocilia, because the adhesive property of the cadherin should be retained.

If the hypothesis is right that exon 68 is necessary for a functional transduction apparatus, the CDH23-Ex68 Skip mice will be deaf, while an intact hair bundle is maintained. A complication could be that exon 68 contains sequences for proper localization of CDH23 to the stereocilia bundle in which case ablation of exon 68 would lead to mislocalization of the truncated CDH23. Mislocalization is even more likely for the Δ cyto form of CDH23 since it can not be recruited to its final destination by any putative cytosolic binding partner, such as the PDZ-domain protein harmonin. It is known for other PDZ-domain proteins to fulfill such a recruiting function (Harris and Lim, 2001).

Although CRE/Lox technology has been employed to keep genetic perturbation at a minimum, it is conceivable that the truncated proteins are only poorly expressed due to the deletion of sequences that are important for the stability of the protein.

Final Discussion

6. Final Discussion

„A fine filament between the tips of adjacent stereocilia“ was discovered by Pickles and colleagues two decades ago, immediately leading to the suggestion that these „tip links“ are the actual mechanical linkages to the auditory transduction channel (Pickles et al., 1984). In 1991 first direct evidence appeared supporting the hypothesis that the tip link is indeed involved in mechanical transduction (Assad et al., 1991). Since then a decent body of literature has accumulated strengthening the original idea and leading to the commonly accepted „tip-link“ model in which a rapid series of events during sound stimulation, the deflection of the stereocilia bundle - stretching of tip links - opening of transduction channels. Gating of the transduction channel leads to ion influx into hair cells, and therefore transformation of a mechanical stimulus into an electrochemical signal. (Corey, 2003; Müller and Evans, 2001; Sukharev and Corey, 2004). Nevertheless, neither the tip link nor the transduction channel have been identified at the molecular level.

We show here several lines of evidence that CDH23 is a core component of the tip- and kinociliar link. First of all an antibody raised against CDH23 labels tip- and kinociliar links. Biochemical properties known for the tip link and the related kinociliar link are identical to those of CDH23. We demonstrate that CDH23 is a Ca^{2+}-dependent homophilic adhesion receptor, a finding that may explain how tip links connect adjacent stereocilia, much like classical cadherins bring together neighboring cells. Additionally, in a heterologous expression system we find that the cytodomain of CDH23 co-immunoprecipitates with MYO1C, a protein known to play a role in auditory transduction positioned at the tips of stereocilia.

Mutations in the *CDH23* gene cause deafness and deaf-blindness in man and mice, the latter disease is known as Usher Syndrome. In a separate set of experiments we show for the first time that two genes involved in Usher syndrome, *CDH23* (giving rise to Usher 1D) (Bolz et al., 2001; Di Palma et al., 2001b) and *Harmonin* (giving rise to Usher 1C) (Bitner-Glindzicz et al., 2000), form a protein complex by means of PDZ-domain interactions and are therefore in a single molecular pathway involved in stereocilia function. We further demonstrate that an alternatively spliced exon of CDH23, exon 68, is exclusively expressed in the hair cell bundle and regulates complex formation with harmonin. Whether harmonin is part of the CDH23 tip link complex or only part of a transient complex during stereocilia maturation as suggested, is currently not known.

6.1. The Tip Link of Hair Cell Stereocilia

6.1a. Extracellular Matrix and the Tip Link

The tip link has been suggested to be comprised of extracellular matrix molecules such as elastin or titin. Two reasons lead to this suggestion: First, the susceptibility of the tip link to the protease elastase (Osborne and Comis, 1990), which digests elastin, and second, because of elastic properties assumed to reside in the tip link molecule (see the chapter 6.2. below). It is unlikely though, that elastin comprises part of the tip link because subsequent immunocytochemical studies did not detect any elastin near the tips of stereocilia (Katori et al., 1996). Further, the protease elastase is expected to digest many other proteins, one of them being CDH23, as we have shown in this study. Recent studies also argue that the tip link is not as elastic as suggested before, but instead rather stiff (Kachar et al., 2000)

Unpublished data gathered by ultrastructural analysis and subsequent molecular modelling suggested that an extracellular matrix receptor of the integrin family may reside in the insertion plaques of the tip link, implying that integrin substrates such as fibronectin are part of the tip link structure (Manfred Auer, unpublished observation). An integrin-fibronectin interaction would most likely not withstand the forces generated in the event of stereocilia deflection, making these molecules unlikely candidates for being tip link components.

Recently a study utilizing a monoclonal antibody, derived from a hybridoma screen intended to discover hair bundle proteins, defined an epitope that is common for tip links and kinociliary links (Goodyear and Richardson, 2003). The authors of the study refer to this molecule as tip link antigen, since its nature is unknown. While some experiments suggested that the monoclonal antibody used in the study reacts with the tip link, some biochemical properties indicate that it rather detects an epitope closely associated with the tip link. The putative molecular weight of this molecule is between 200 - 250 kilo Dalton (kD), as determined by SDS-gel electrophoresis, and therefore considerably smaller than CDH23, which has apparent molecular weight of around 400 kD (our observation and(Reiners et al., 2003). Also, the tip link antigen is to some degree resistant to Ca^{2+} chelation as determined by the investigators, unlike the the tip link itself, which breaks apart within seconds after Ca^{2+} removal (Assad et al., 1991).

The stereocilia exhibit a surface coat or so-called glycocalyx. The glycocalix resembles a shell-like rigid structure separately surrounding each stereocilium and kinocilium. This carbohydrate layer consists of glycoconjugates such as glycolipids, proteoglycans, mucopolysaccharides and glycoproteins (Takumida and Bagger-Sjoback, 1991; Takumida et al., 1988a). The glycocalix does not only mantle the stereocilia but appears to be continuous with the tip- and side linker molecules connecting adjacent stereocilia. It has therefore been suggested that the tip– and side links are related to the glycocalix (Takumida et al., 1990; Takumida et al., 1988b). A Freeze-Fracture electron microscopic analysis revealed however that the tip link appears to consist of two components; a carbohydrate-rich coat, the glycocalix, and a central filamentous core (Valk et al., 2002). This filamentous core appeared to consist of three helical strands (Tsuprun and Santi, 2000). The glycocalix may use the filamentous core of the tip link as a matrix to condense on top of it and subsequently engulf the filament. Thus it is reasonable to assume that the glycocalix may support the tip link during mechanical stimulation, while it is not the only component of it.

Several ultrastructural studies have indicated that the tip link is a cross-membrane structure connected to the underlying actin cytoskeleton, additionally suggesting that the linkers are not solely comprised of extracellular matrix molecules (Hackney and Furness, 1995).

6.1b. Cadherins – Interstereocilia Linker Molecules?

Classical cadherins are involved in tight junction formation, bringing together plasma membranes of opposing cells. They contain 5 EC-domains in their extracellular part, of which the outermost one engages in Ca^{2+}-dependent homophilic binding with the partner molecule projecting from the neighboring cell membrane (Angst et al., 2001). To link together two stereocilia at their tips, a large gap has to be bridged. Recently it has been suggested that gaps between cells can be spanned by novel cadherins with large numbers of repetitve extracellular EC-domains. Mouse FAT1 (mFAT1), a novel cadherin with 34 EC-domains and high sequence similarity to CDH23, is expressed in the slit junctions, the intercellular junctions between podocytes in the glomerular filtration membrane of the kidney (Inoue et al., 2001). Slit junctions are modified adhesion junctions, with a wide intercellular gap allowing renal filtration (Tryggvason and Pettersson, 2003). The analysis of the *mFAT1* knock out mouse provide evidence that this unusual large cadherin molecule bridges the slit junctions and generates the necessary intercellular adhesion between podocytes. In the absence of mFAT1 the ordered array of slit junctions disappears and the podocytes become closely apposed to one another, suggesting that mFAT1 is not only an adhesion molecule capable of bridging large intercellular gaps, but also has a role in spacing (Ciani et al., 2003).

CDH23 contains 27 EC domains and is therefore very suitable to bridge interstereocilia gaps. We and others detected CDH23 protein along the entire stereocilia membrane during hair bundle development in the immature mouse inner ear (Boeda et al., 2002; Siemens et al., 2002). Strong alleles of *waltzer* mice, believed to harbor loss-of-function mutations in the *CDH23* gene, display disorganized, splayed stereocilia bundle and the mice are deaf and have balance deficits (Di Palma et al., 2001b). These results together suggest that CDH23 is important for the integrity of the stereocilia bundle during hair bundle maturation and may link together adjacent stereocilia on their entire length during stereocilia elongation and positioning. We show here that CDH23 appears to be part of the kinociliar linker system as well, further strengthening the notion of the molecules developmental role in hair bundle stabilization.

After hair bundle morphogenesis is completed, CDH23 expression levels decreases drastically in inner ear hair cells, fueling speculations that CDH23 is absent from mature hair bundles and therefore has only a developmental function in hair cells (Boeda et al., 2002). However, several other pieces of evidence support the hypothesis that CDH23 has a second prominent function in mature hair bundles. First of all, different mutations in the *Cdh23* gene have been identified in zebrafish, some of which do not cause hair bundle disorganization while at the same time still interfering with mechanosensation of the hair bundle (Nicolson et al., 1998). Further, „milder“ mutations within the *Cdh23* gene in mice have been identified, which do not lead to immediate hearing loss, but instead increase susceptibility to age-related and noise-induced hearing loss (Davis et al., 2003; Davis et al., 2001; Holme and Steel, 2004; Noben-Trauth et al., 2003). These studies emphasize a function of CDH23 in auditory transduction other than a purely developmental role during hair bundle morphogenesis. We have presented here multiple lines of evidence that in addition to its developmental role, CDH23 is also part of the tip link in mature stereocilia bundle.

The tip link bridges a gap of around 150 to 300 nm between the tip of the shorter stereocilium and the side insertion plaque of the next taller one (Furness and Hackney, 1985; Kachar et al., 2000; Pickles et al., 1984). We performed calculations on the grounds of size estimations of a single EC domain of C-cadherin. The high resolution crystal structure of this molecule revealed that a distance of 4 nm can be spanned by one EC domain (Boggon et al., 2002). Assuming that the extracellular domain of CDH23 is folded in a similar way, two CDH23 molecules from opposing stereocilia would be capable of bridging a gap of 150-300 nm. Additionally, inter-EC domain protein sequences of CDH23 may also contribute to spanning of a large gap.

In this respect it is important to note, that neither for mFAT1 nor for CDH23 is it known which and how many EC domains engage in the homophilic interaction. This information needs to be taken into acount, when estimating the distance to be spanned by two cadherin molecules from opposing sites. It is possible that more than just one EC-domain engages in interactions as has been shown for C-cadherin (Chappuis-Flament et al., 2001; Sivasankar et al., 1999; Zhu et al., 2003). The strong forces generated by stereocilia deflection make it more than likely that multiple EC-domains of CDH23 engage in interactions in order to prevent disintegration of the tip link.

An interesting possibility is that multiple EC-domains of CDH23 engage in interactions within the tip link and that these EC-domains could slide past each other and bind in different register during hair bundle deflection conveying some elasticity to the CDH23 filaments. A rigorous analysis of the adhesion properties of all EC-domains within CDH23 protein will be necessary to define the adhesion mechanism inherent in the tip link. Additionally, the glycocalix coat, engulfing the tip link core, needs to be taken into account, since it may shape physical properties of the tip link complex more dramatically than anticipated from the data available today.

The tip link is an asymmetric structure by nature of its insertion points at the stereocilia membrane, one being at the tip of the shorter stereocilium and one being in the shaft of the taller stereocilium. Further, asymmetry has been observed on the ultrustructural level. At the upper end, the tip link consistently splits apart about 10-50 nm from the taller stereocilium so that two branches attach to the shaft of the taller stereocilium. At the tip of the shorter stereocilium the tip link appeared to branch into two or three strands before entering the tip´s plasma membrane (Kachar et al., 2000). While the function of the bifurcation or branching could very well be to distribute the force during deflection on a larger membrane area, this asymmetry raises the possibility that the tip link consists of two different molecules arising from the two different stereocilia. This may imply that CDH23 resides on one stereocilium and engages in heterophilic interactions with another molecule on the adjacent stereocilium to make up the tip link. This is conceivable, however, it is unlikely for several reasons. First of all we show here that CDH23 is a homophilic interaction molecule, a property that has been shown for other protocadherin family members (Goldberg et al., 2000; Obata et al., 1995) This by itself does not rule out the possibility that next to homophilic interaction CDH23 can also engage in heterophilic interactions as seen for B-cadherin and LCAM, which can form a heteromeric complex (Murphy-Erdosh et al., 1995). But more important, on the ultrastructural level we see labelling for CDH23 on both sides of the tip link end points, on the tip of the shorter stereocilium and on the shaft anchor point of the next taller stereocilium. This suggests strongly that the tip link is comprised of CDH23 molecules coming from plasma membranes of both of the adjacent stereocilia, and that the two molecules engage in homophilic interactions. It is possible that the postulated homophilic CDH23 dimer (trans interaction) clusters with more CDH23 molecules on the same membrane surface (cis interaction) into a larger adhesive complex, which may withstand stronger forces than the single dimer. Cis interaction occurs with classical cadherins and the CDH23 labelling pattern that we detected at the stereocilium tip, giving rise to multiple gold particles in the ultrstructural analysis, may be indicative for multiple CDH23 molecules at this location. Alternatively, multiple gold particles may reflect the fact the we used a polyclonal antiserum, which may label different epitopes within the the cytodomain of CDH23. CDH23 may also be associated extracellulary with other molecules such as the tip link antigen (Goodyear and Richardson, 2003)

One additional observation argues against a heterophilic adhesion mechanism of CDH23 in the tip link complex. On the ultrastructural level the center part of the tip link appears to be a homogenous helical strand consisting of two identical coiled filaments. A heterophilic interaction mechanism on the other hand would be expected to have a rather heterogenous appearance due to two filaments being of different molecular origin. With respect to the bifurcation and asymmetry of the tip link it is important to note that CDH23 seems to occur in different forms. We found mRNA isoforms of CDH23 lacking exons 45 to 47, most likely due to alternative splicing. This would lead to a putative protein missing the EC-domains 19 to 21 of the extracellular part of CDH23. Further, our biochemical analysis of CDH23 protein has revealed that two forms exist in the inner ear and the retina differing in their N-glycosylation pattern. Future studies need to determine if alternative splicing or post translational modification may regulate certain properties such as branching or orientation of the tip link.

A different scenario may be envisioned for the role of CDH23 in the kinociliar link. Although no detailed 3D reconstruction data is available as in the case of the tip link, it appears that the kinociliar links run perpendicular to the plasma membrane of stereocilia and kinocilium and not in an angle. This would result in a shorter distance to be bridged by the kinociliar link as compared to the tip link. While we were able to detect CDH23 strongly expressed in the largest stereocilia connecting to the kinocilium, it is not clear if the protein is present in the kinociliary membrane. Certainly more ultrastructural analysis of the kinocilium needs to be undertaken to clarify the presence or absence of CDH23 in the kinocilium. It is an intriguing possibility though, that different properties of the kinociliar link and stereociliar tip link, such as length, strength, elasticity and orientation, could be regulated by switching between a homophilic and heterophilic interaction modus.

One other novel cadherin-like molecule, Protocadherin 15 (PCDH15), has a causative link to Usher Syndrome (Alagramam et al., 2001a) and may be part of a separate linker system within the stereocilia bundle. PCDH15 expression has been reported in stereocilia but the exact sub-stereocilia localization is still a matter of investigation (Ahmed et al., 2003b). Likewise, putative adhesive properties are still unknown. PCDH15 contains only 11 EC-domains and would therefore be suitable to be part of the side/shaft links or ankle links. Unlike tip links which connect adjacent stereocilia in an angle, side link bridges are shorter since they run perpendicular to the plasma membrane and connect stereocilia in regions where they are closer opposed to each other. An interesting possibility is that PCDH15 engages in heterophilic interactions with CDH23 at kinociliar connection sites, a speculation that currently lacks any supporting experimental evidence.

In conclusion, there is compelling evidence that CDH23 engages in homophilic interactions to generate the core component of the tip link, connecting adjacent stereocilia. The impact of individual CDH23 EC-domains, alternative splicing or posttranslational modification in the regulation of tip link structure need to be determined. Other tip link components such as the glycocalix and the tip link antigen have to be defined, and their importance for mechanosensation needs to be uncovered.

6.2. Tip Link – Gate Keeper?

Evidence for the tip link playing a key role in the events of auditory transduction, by means of ion channel gating, is several fold. First of all the hair cells of all vertebrates examined so far possess tip links that are aligned along the axis of mechanical sensitivity (Hackney and Furness, 1995). This puts these linkers in a suitable position to exert a channel-opening function. Disruption of the tip link chemically or enzymatically abolishes mechanosensitivity, while regeneration of the link several hours later also recovers mechanical transduction (Assad et al., 1991; Duncan et al., 1998; Meyer et al., 1998; Zhao et al., 1996). We have shown here that CDH23 fits these biochemical criteria.

The tip link hypothesis requires, however, a functional and anatomic distinction between the different linker molecules along the stereocilia shaft, allowing specific and selective interaction of the tip link with the transduction apparatus. In support, it has been shown by Goodyear and Richardson that the ankle link and side/shaft link are of different molecular composition since different antibodies label ankle- and side link respectively but not the tip link (Goodyear and Richardson, 1999; Goodyear et al., 2003). We have shown here on the other hand that antibodies raised and affinity purified against CDH23 peptides selectively label tip links but not side and ankle links. Additionally, removal of the ankle link by subtilisin treatment does not affect transduction, while disruption of the tip link by elastase treatment abolishes channel gating (Meyer et al., 1998; Zhao et al., 1996).

These immunohistochemical and biochemical studies provide the basis for the molecular differences of the stereocilia linker molecules.

6.2a. Position of the Transduction Channel

Measurements of the current flow upon hair bundle stimulation show that it is greatest toward the tips rather than at the bases of the stereocilia (Hudspeth, 1982). The transduction channel is believed to be Ca^{2+} ion permeable (Lumpkin et al., 1997). Results obtained employing Ca^{2+} imaging techniques suggested that Ca^{2+} commences to enter first through the tips of the stereocilia as they are deflected (Denk et al., 1995; Lumpkin and Hudspeth, 1995).

Focal application of aminoglycoside antibiotics, which have been shown to block transduction currents and can cause deafness when applied systemically to human patients or mice, appear to be most effective nearest the tips of the stereocilia (Jaramillo and Hudspeth, 1991). While these studies clearly place the transduction channel in the tip region of the stereocila, spatial resolution of these techniques is too low to draw a conclusion about its potential tip link association. One protein of the auditory transduction cascade, MYO1C, has been found by ultrastructural analysis to be concentrated at the tips (Cyr et al., 2002; Metcalf, 1998; Steyger et al., 1998). Our analysis suggests that CDH23 is directly or indirectly connected to MYO1C via its cytoplasmic tail implying a link of CDH23 with the motor protein for slow adaptation of auditory transduction.

These immunocytochemical and ultrstructural observations provide such a good fit to Corey and Hudspeth´s model that it is widely assumed that the tip link is in the immediate spatial and functional vicinity of the transduction apparatus.

Nevertheless other models have been put forward, which assume a different position of the transduction apparatus distant to the tip link insertion sites.

One hypothesis places a putative transduction channel at a junction-like structure slightly below the tip link, where the stereocilia come into closest contact with their neighbors (Hackney and Furness, 1995; Neugebauer and Thurm, 1986). The basis for this model comes from observations that the transduction channel is sensitive to amiloride blockage (Jorgensen and Ohmori, 1988; Rusch et al., 1994). The subsequent immunological detection of an amiloride sensitive sodium channel by two different antibodies at these stereocilia contact sites, fueled this hypothesis

(Hackney and Furness, 1995; Hackney et al., 1992). One attraction of this model compared with the tip link hypothesis is that the gating of transduction channels located in the membrane could be analogous to that of stretch-activated channels found in the membranes of several other types of cells (Kudoh et al., 2003), without invoking the apparently unique arrangement required by the tip link hypothesis. Indeed there is evidence that the cell walls of outer hair cells contain stretch activated elements, which likely play a role in the signal amplification process (Ding et al., 1991). In this context it is interesting to note that the cloning of an amiloride sensitive ion channel revealed sequence similarity to degenerins, ion channel subunits that are involved in mechanosensation in the nematode *Caenorhabditis elegans* (Lingueglia et al., 1993).

One inherent problem here is that the transduction channel is unlikely to be a selective sodium channel due to the special ionic composition of the endocochlear fluid. A non-selective cationic conductance is more suitable for this role. Additionally, the junction-like structure between stereocilia, although observed in reptilian and mammalian stereocilia, is of questionable nature and not frequently observed in different preparations used for ultrustructural analysis. It is not clear if all stereocilia contain this junction, a prerequisite for this hypothesis to allow effective signal transmission to the hair cell body.

The only results that differ completely in terms of where to find the transduction channel come from studies performed on isolated chick hair cells. Ohmori was able to show on these cell preparations that manganese ions, which are believed to pass through the transduction channel, entered the hair cell at the base of the stereocilia upon deflection of the hair bundle (Ohmori, 1988). This technique also has limited spatial and temporal resolution, however, and therefore these results have been questioned.

Nevertheless, it should be noted that placing the transduction channel at the base of the stereocilia makes sense from an engineering point of view, because angular rotation of the hair bundle would lead to the greatest forces being produced at the „ankle" of the stereocilium. A mechanism such as this would be reminiscent of some insect mechanoreceptors where a long molecular lever exerts its transductory function at the point of highest force transmission (Keil, 1997). On the other hand, with respect to the lever-rule, the point of highest sensitivity during stereocilia deflection is at the stereocilia tips. Since the force requirements for transduction channel gating are unknown, it is highly speculative to argue for a particular channel localization based on grounds of energetic considerations.

A general problem with any ion channel that may arise as a candidate for the transduction conductance is the problem of how to discriminate between the primary transduction channel and secondary ion channels. Estimates suggest that there are only one or two active transduction channel proteins at each stereocilia tip, a number that is too small to allow a current to be large enough to reach the hair cell body on its own (Holton and Hudspeth, 1986; Kros et al., 1992). The electric signal would dissipate and not lead to a receptor/action potential at the basolateral side of the hair cell. Therefore it is more than likely that secondary ion channels amplify the initial signal and carry down the depolarization wave along the stereocilia shaft and further to the synapse. Certainly the transduction channel needs to be mechanosensitive according to the most likely theory. But even though a channel gene may be discovered eventually which is expressed in hair cell stereocilia and implicated in deafness, *in vitro* reconstitution of the whole mechanosensitive apparatus may be necessary to gain final proof for its unique role of being the transduction channel of the vertebrate auditory system.

Thus despite the undoubted elegance of the tip link hypothesis, immunocytochemical and ultrastructural observations suggest that there are other possible locations for the transduction channel than at the end of the tip links and other potential mechanisms for channel opening that could be consistent with the physiological data. In absence of several entities in the equation, the tip link should not be regarded as the only model for channel gating in the auditory system proposed by Corey and Hudspeth.

6.2b. The Gating Spring Model

How can channel gating by the tip link be envisioned to occur? According to the gating spring hypothesis proposed by Corey and Hudspeth deflection of the hair bundle would put tension on the tip link, which in turn is directly connected to the transduction channel positioned at either end of the tip link in the plasma membrane. The force transmitted by the tip link onto the connected ion channel subunit would open the channel pore and initiate an ion influx into the hair cell (Corey, 2003; Sukharev and Corey, 2004). A flexible or elastic element would be necessary to convey the tension force onto the channel. It was originally suggested that the tip link itself is an elastic molecule, much like a spring. More recent ultrastrucural analysis revealed that the tip link appears to consist of a pair of protofilaments arranged helically, which are significantly more rigid and stiffer than the gating spring. Since the membrane at the tip of a stereocilium often is tented away from the underlying cytoskeleton by tension of the tip link, the elastic element might be located underneath the membrane (Fig. 6.1), rather than within the tip link fiber (Kachar et al., 2000; Tsuprun and Santi, 2000).

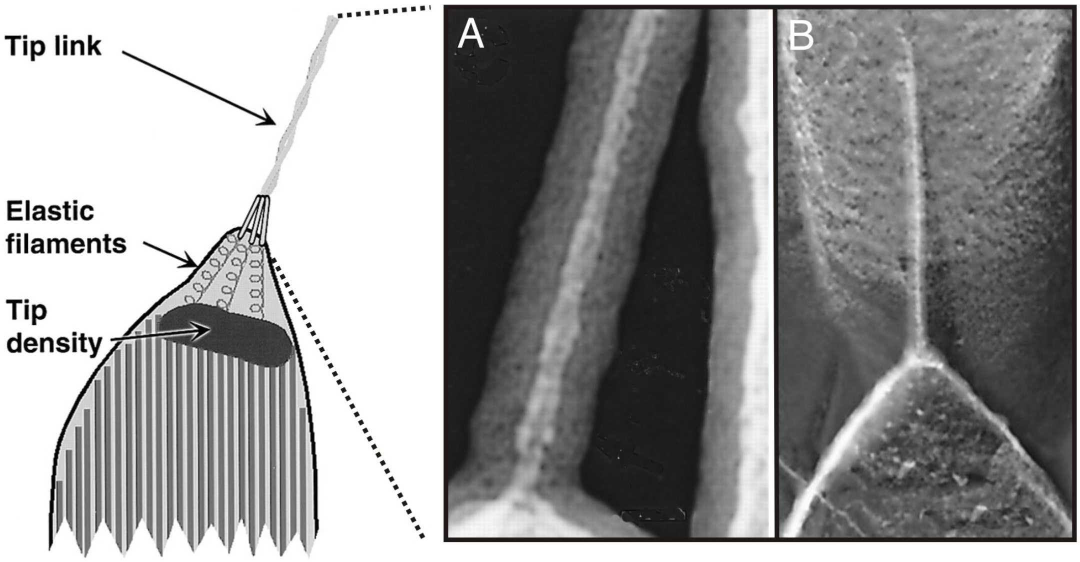

Figure 6.1. : Tip Link and Elastic Element
The schematic drawing on the left depicts the relative position of the tip link with respect to the putative elastic filaments and tip density in a stereocilium. Underlying are the actin filaments. On the right, panel A and B, electron micrographs show the tip link. The double helical structure of the tip link complex can be seen in panal A. Note tenting of the membrane at the stereocilia tip in panel B. (Modified from *Proc Natl Acad Sci USA;* 2000; 97; 13336-13341).

A direct extracellular interaction of the tip link with the putative transduction channel, as suggested by Corey and Hudspeth, is unlikely for several reasons. The forces generated during stereocilia deflection are strong enough to cause membrane deformations at the site of tip link insertion (Fig. 6.1.). A direct extracellular connection of the tip link to the transduction channel, is hardly conceivable. The strong forces conveyed upon a fragile ion channel subunit, gating the channel pore, are likely to rupture this protein complex. Additionally, there is currently no example to be found in the literature of a cadherin molecule interacting via one of its EC-domains with an ion channel subunit. That makes it unlikely that CDH23, as tip link component, interacts with its extracellular domain with an ion channel. Further, the distance to be bridged by a CDH23 molecule projecting from one stereocilium and interacting with a putative channel on the membrane of the adjacent stereocilium would be too large, if classical EC-domain folding is assumed for CDH23. As we estimated, the gap of 150 -300 nm can more likely be bridged by cadherin molecules from opposing stereocilia, that connect to each other approximately in the middle of the gap. We see labelling of CDH23 on both sides of the gap between adjacent stereocilia, making it even more likely that CDH23 engages in homophilic interaction rather than in heterophilic interaction with an ion channel.

6.2c. CDH23 Complexes via the Intracellular Domain

Alternatively, CDH23 may interact with the transduction channel via its intracellular domain. The only structural motifs we were able to find in the cytosolic tail of CDH23 were two PDZ binding domains. We and others have shown that CDH23 interacts with the PDZ-domain protein harmonin, which is expressed in hair cell stereocilia (Boeda et al., 2002; Siemens et al., 2002). Two of the three PDZ domains of harmonin interact with two complementary binding surfaces within the cytodomain of CDH23. Interestingly, only stereocilia contain a splice variant of CDH23 containing sequences encoded by exon 68 that disrupts the PDZ I binding site and therefore leaves PDZ I of harmonin free to engage into interaction with different proteins, while PDZ II is bound to the C-terminus of CDH23. PDZ domains are known interacters of channel proteins in various systems (Fanning and Anderson, 1999; Kornau et al., 1995; Sheng, 2001; Sheng and Pak, 2000; Sheng and Sala, 2001), implying the possibility that harmonin may be the adapter molecule between CDH23 and the putative transduction channel. In such a scenario, the tension force would be transmitted via CDH23 into the inside of the cell and relayed with the help of harmonin onto the channel protein, regulating channel opening. Although there is the possibility that PDZ I of harmonin interacts with the putative channel protein, we have evidence that this PDZ-domain is able to interact with the C-terminal PDZ binding motif within harmonin itself, thereby potentially facilitating the formation of larger complexes containing multiple harmonin molecules. This poses an interesting possibility to anchor the CDH23 complex at the membrane, which has to withstand strong forces in order not to be extracted from the membrane. Since only 10-20 pico Newton (pN) are required to extract a transmembrane protein from a bilayer, unanchored transmembrane tip links can not survive forces generated during large bundle deflections (Bell, 1978; Evans et al., 1991). While the model is tempting, it is at present unclear if harmonin has a role in stereocilia development only and vanishes from mature stereocilia as suggested or if it persists, a prerequisite for this model.

The protein whirlin also contains three PDZ-domains and was identified as the closest homolog of harmonin. It was shown that mutations in the gene encoding for whirlin causes deafness in patients suffering from a non-syndromic form of hearing loss (Mburu et al., 2003). Therefore, even if harmonin only plays a role in stereocilia development and disappears later on, whirlin may take over its role as a binding partner of CDH23, connecting it to a putative transduction channel. Neither the expression pattern of whirlin nor its binding properties towards CDH23 have been reported, both issues are currently under investigation in our laboratory.

In this respect it is worth noting that sensory signal transduction pathways in general are believed to be organized into multimolecular signaling complexes by scaffolding proteins. The best-studied example is the *Drosophila* photoreceptor, where several of the key phototransduction components, including the ion channel TRP, are clustered by the multi PDZ-domain protein INAD into the so-called signalplex (Montell, 1998; Montell, 1999). In vertebrate rod photoreceptors GARP proteins may fulfill a similar function (Korschen et al., 1999). There are obvious advantages for clustering the signaling components into larger complexes by scaffolding proteins. First of all, the close proximity of the components allows efficient and high speed signal transmission, a characteristic of auditory transduction. Such an assembly may also facilitate an “all or nothing” response to a minimal stimulus such as one photon for photoreceptors or subtle vibration in case of stereocilia. Additionally, preassembly of the complex during or right after protein biosynthesis could reduce the problem of the cell to target all components individually to the desired location (Huber, 2001). With respect to the later aspect it is interesting to note, that the authors of a recent study suggested that MYO1C, which we found to interact with CDH23, could transport the whole transduction apparatus including the tip link to the tips of stereocilia (Geleoc and Holt, 2003). Whether harmonin, whirlin or the vertebrate INAD ortholog, which likewise is expressed in inner ear hair cells (Walsh et al., 2002), cluster CDH23 and the putative transduction channel into „transducisomes“ awaits future analysis.

Recently it has been claimed that MYOVIIA, the protein product of the Usher gene USHIB, binds to PDZ1 of harmonin, giving rise to a ternary complex of three Usher gene products, CDH23, harmonin and MYOVIIA in stereocilia (Boeda et al., 2002). It appeared that one splice variant of harmonin was mislocalized in mouse mutants defective for the gene encoding MYOVIIA, supporting the evidence that harmonin and MYOVIIA form a complex and translocate together along actin filaments into stereocilia via the motor activity of MYOVIIA. However, since in stereocilia of the same *MyoVIIa* mouse mutants CDH23 was at the same time correctly positioned, this questioned the formation of the proposed ternary complex. Additionally, in a recent study, *waltzer* and *shaker* mice were crossed to give *Cdh23* and *MyoVIIa* double mutant mice, and no genetic interaction has been observed (Holme and Steel, 2002). While both genes are important for hair bundle function, this result argues that they may not be in a common molecular pathway. MYOVIIA and also harmonin (also referred to as AIE-75 or PDZ-73 protein) are much more widely distributed in other tissues compared to CDH23, pointing to additional roles of these two proteins besides a function in stereocilia (Kobayashi et al., 1999; Scanlan et al., 1999; Wolfrum et al., 1998).

6.2d. Lessons from Bacterial Mechanotransduction Channels

A further alternative hypothesis for auditory transduction channel gating arises from studies performed on bacterial mechanosensitive channels, the only model systems so far in which biophysical techniques have given insight into the molecular mechanism of channel gating, far advanced compared to what is known about eukaryotic channel gating (Blount, 2003; Koprowski and Kubalski, 2001). The bacterial channels MscL (for MechanoSensitive Channel of Large conductance) and MscS (for MechanoSensitive Channel of Smaller conductance) sense membrane tension as conveyed upon the bacterial wall by changes of the osmolarity in the environment. MscL shares an evolutionary origin with the eukaryotic transient receptor potential channels (TRP) and polycystin channels involved in several sensory systems including mechanosensation (Clapham, 2003). The Msc family of channels therefore serves as simplified model systems for mechanically gated eukaryotic channels. MscL and MscS are the only mechanosensitive channels that have been crystallized in open – and closed states of the channel pore, allowing structure/function analysis of the gating mechanism (Bass et al., 2002; Perozo et al., 2002). These studies revealed that the plasma membrane itself is of crucial importance for channel gating. Membrane thinning and increase in membrane curvature as a result of membrane stretch opens the channel pore. A multitude of additional studies deploying experiments on the influence of lipid composition or reagents inducing asymmetric membrane curvature have supported these findings (Martinac et al., 1990; Patel et al., 1998). An increase in the membrane curvature leads to a dramatic tilt of the membrane spanning alpha helices aligning the ion channel pore of MscL and MscS with a concomitant widening of the pore diameter to allow ion-flux into the cell. Although these studies clearly emphasize the important role of biophysical properties of membranes in channel gating, it is not yet known whether direct and specific protein-lipid interactions are crucial for the gating mechanism. This appears however likely in light of recent findings that lipid molecules such as phosphatidylinositol-4,5-bisphosphate (PIP_2) directly interact with TRP channel subunits to influence channel currents in mammalian sensory systems (Prescott and Julius, 2003).

Membrane curvature at the tip of vertebrate hair cell stereocilia, where the auditory transduction channel is assumed to reside, is very strong and more than likely the plasma membrane at this location has a special lipid composition, but a detailed analysis of the stereocilia membrane composition has not been carried out. It is conceivable that the membrane curvature and stretching during deflection of the stereocilia bundle triggers the auditory transduction channel to open its pore. In this model the transduction channel would only need to be peripherally linked to the tip link in such a way that the channel protein stays in the vicinity of the tip link insertion where the membrane experiences the maximal stretch deformation during stimulation. In this scenario the change in membrane curvature would render the transduction channel to open rather than direct pulling of the tip link on a channel subunit. Nevertheless, the tip link is absolutely essential in this model, because it conveys the stretch deformation force onto the membrane, as seen by the tented membrane in electromicroscopical analysis of the tip link vicinity (Kachar et al., 2000).

This model is compatible with the hypothesis that harmonin (or whirlin) connect the tip link to the transduction channel, but in this case rather holding the channel in place than actively being involved in its gating. Since strong tenting of the membrane has only been observed at the „tip-site“ of the tip link and not on the counter insertion site in the shaft of the next taller stereocilium, it is possible that effective channel gating takes place only at the tip insertion site of the tip link. But it may also be possible that membrane deformation on the shaft side has escaped detection for technical reasons.

In the absence of further experimental evidence, this model remains a purely speculative variation of the „gating spring“ model proposed by Corey and Hudspeth more than a decade ago, which implicated a direct interaction of tip link and transduction channel. Until the cloning of the putative transduction channel and investigation of its properties any model for auditory perception will be highly speculative.

If it turns out that indeed the plasma membrane is the active component in the gating mechanism, a further complication will arise as seen with the analysis of bacterial mechanosensitive gating mechanisms at present. Unlike proteins, membrane compartments or lipid components are much more difficult to access or manipulate in order to design experiments to understand their contribution to ion channel gating. It is, for example, not possible to genetically study lipid molecules. Further, the two phases, the lipid and the water phase, add to the complexity. New tools need to be developed to be able to design experiments, which take into account membrane properties in channel conductance.

6.2e. CDH23 and MYO1C

Several hearing and balance disorders are correlated with mutations in the genes encoding the unconventional myosins IIIa, VI, VIIa, IX and XV (Müller and Evans, 2001; Steel and Kros, 2001). As described in chapter one, individual actin-based motor proteins appear to fulfill specialized functions within hair cells, accordingly the subcellular distribution of the various myosin proteins differs. At present there are no mutations in the gene encoding MYO1C known that cause hearing or balance disorders. In fact, there is no disease in man or mice correlated with a genetic perturbation of *MYO1C*. Since MYO1C is broadly expressed in many tissues and implicated in Glucose metabolism (Bose et al., 2002; Ruppert et al., 1993), it is possible that a mutation in this gene would be fatal. Nevertheless, MYO1C protein has been localized to the tip link insertion plaques of stereocilia in several vertebrate species, making it a prime candidate for being involved in the mechanical transduction process in the inner ear (Metcalf, 1998; Steyger et al., 1998). Additionally, MYO1C has been linked to adaptation of the transduction channel (Holt et al., 2002).

We have shown in this study that MYO1C is in a complex with the cytoplasmic tail of CDH23. While the interaction domain in MYO1C responsible for binding to CDH23 is at present unknown and may be mediated by an adapter protein, Gillespie and Coworker defined calmodulin-binding domains within MYO1C as necessary for anchoring the protein to stereocilia tips (Cyr et al., 2002). It is therefore possible that this is the domain important for complex formation with CDH23, which may render this interaction Ca^{2+}-sensitive, since Ca^{2+}-calmodulin, also present at stereocilia tips, would be able to compete for this binding site (Gillespie and Cyr, 2002). Likewise the protein sequence within the cytodomain of CDH23 necessary for complex formation is not known. It appears though that it is different from the PDZ binding motif of CDH23 at the very C-terminus occupied by harmonin, since a truncation of this motif still permits CDH23-MYO1C interactions, either directly or by means of an intermediary protein.

MYO1C has been implicated in slow adaptation of the auditory transducer current. In contrast to fast adaptation, which is believed to involve Ca^{2+} ions directly decreasing the open probability of the transduction channel, slow adaptation takes place over tens of milliseconds. The MYO1C motor is hypothesized to link transduction channels directly or indirectly to the actin core of the stereocilium, climbing along the stereocilium to adjust the resting tension on the transduction channels. In response to the increased tension applied by an excitatory stimulus, the motor slips, tension decreases, and channels close (Corey, 2003). Despite extensive screening, no channel protein has been found to interact with MYO1C. It is also speculative whether tension directly applied onto the putative transduction channel protein is changing its opening probability, since tension of the plasma membrane itself may be a crucial determinant of channel gating as discussed above. Firm evidence that MYO1C is involved in the adaptation process comes from an elegant study utilizing transgenic mice with a subtle mutation in *MYO1C*, rendering the altered protein susceptible to chemical inhibition (Holt et al., 2002). In the mutant mice the transducer currents, induced by mechanical hair bundle deflection, decreased much more slowly than in wild-type controls suggesting altered adaptation properties upon MYO1C inhibition. Strikingly, the transducer current amplitudes decreased drastically for subsequent stimulations in the mutant mice, but not in wild-type controls. This points to an additional function of MYO1C not only in adaptation but also in gating or in biasing the open probability of the transducer channel. Further support for a more prominent function of MYO1C in transducer channel regulation comes from the observation that inhibition of calmodulin, a regulator of MYO1C at stereocilia tips, not only affects adaptation but also reduces transduction currents by 50% (Walker and Hudspeth, 1996).

Several studies have demonstrated that the basic C-terminal tail domain of MYO1C engages in electrostatic interactions with acidic phospholipids. This interaction is clearly important for membrane localization of MYO1C as described for different cell types expressing this motor protein (Ruppert et al., 1995; Tang et al., 2002; Tang and Ostap, 2001). In stereocilia the attachment to the plasma membrane, combined with the interaction to CDH23s cytodomain may give enough strength to hook up the complex to the actin cytoskeleton, even in moments of strong mechanical stress during sound stimulation.

The complex of MYO1C and CDH23 poses an interesting hypothetical addition to the current view of MYO1C´s function in slow adaptation of the auditory transducer current (Fig. 6.2). Upon hair bundle deflection and stretching of the membrane via CDH23, transduction channels open. Since MYO1C is connected to CDH23 and the plasma membrane, this motor protein is perfectly suited to reset the membrane to its original position by moving along actin filaments, thereby getting the transduction apparatus in the start position for another opening cycle. Blocking of MYO1C would prohibit restoration of the membrane complex and a subsequent stimulus would have a diminished effect on membrane deformation, resulting in decreased channel opening probability. This model suggests that MYO1C is part of the gating spring, possibly in conjunction with elastic fibers, since the sole inhibition of MYO1C does not result in complete loss of transduction currents. Alternatively, MYO1C may not have been totally blocked in the studies mentioned above (Holt et al., 2002), therefore it would be interesting to analyze whether transducer currents are reduced to zero in mice that carry a null allele for the *Myo1c* gene, albeit such experiments may be hampered by lethality of such a knock-out mouse as discussed above.

One complication of this model arises from the question whether MYO1C moves along actin fibers fast enough to restore membrane deformation during consecutive cycles of stimulation. Average stereocilia displacements resulting in small membrane deformation in the picometer to nanometer range appear to be manageable by MYO1C in the required time frame. *In vitro* myosins have an average velocity of 0.3 µm/s which is assumed to be even enhanced *in vivo* (Williams, 2002). Therefore, small membrane distortions could be restored in a time frame of microseconds, similar to the speed of transduction channel gating. Large membrane deformations can result in membrane hysteresis (PG. Gillespie, personal communication) -the phenomenon of incomplete membrane restoration- in agreement with the hypothesis that MYO1C is not capable to pull the membrane efficiently under these circumstances.

Figure 6.2. Model for Transduction Channel Gating (next page)
The schematic representation displays two stereocilia with transduction channels being in the „open“ state (upper panel) and in the „closed“ state (lower panel). Deflection of the hair bundle and tension conveyed by CDH23 results in membrane deformation and transduction channel opening. The membrane architecture is restored by MYO1C traveling along actin filaments thereby pulling CDH23 and the membrane back to the original state, priming the membrane complex for the next cycle of stimulation. Since myosin motors are moving towards the growing end of actin fibers, MYO1C can only travel the stereocilia upward. Additional putative elastic filaments, assisting in membrane restoration as part of the gating spring, are omitted in the diagram for clarity reasons. Interactions of the transduction channel with harmonin are purely speculative.

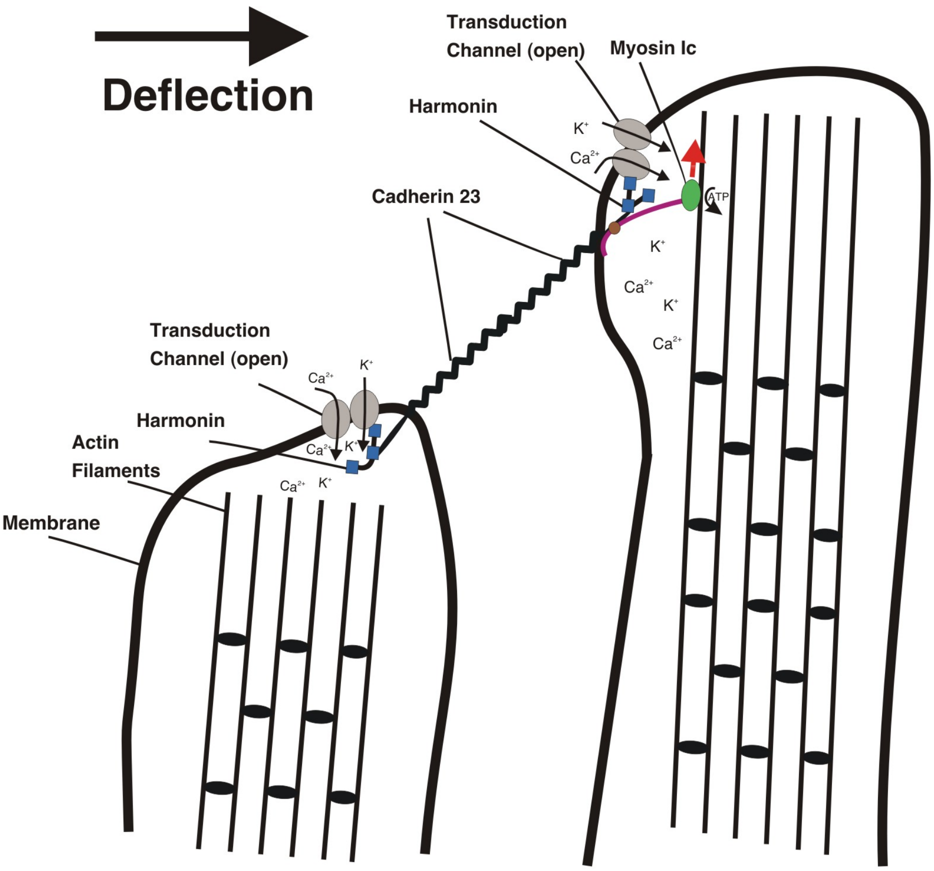
Deflection
Transduction Channel (open)
Myosin Ic
Harmonin
K+
Ca2+
ATP
Cadherin 23
K+
Ca2+
K+
Ca2+
Transduction Channel (open)
Ca2+
K+
Harmonin
Actin Filaments
Ca2+
K+
Ca2+
K+
Membrane

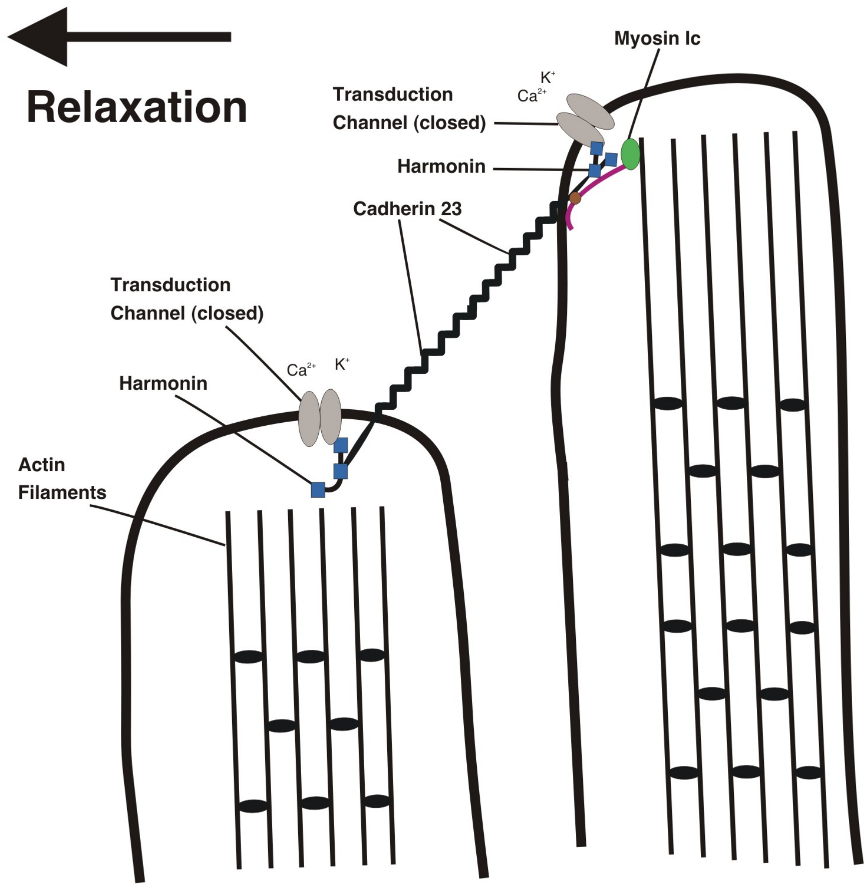
Relaxation
Myosin Ic
K+
Ca2+
Transduction Channel (closed)
Harmonin
Cadherin 23
Transduction Channel (closed)
Ca2+
K+
Harmonin
Actin Filaments

One general problem with this model is that MYO1C molecules –like all myosins- are believed to exclusively move towards the growing end (plus end) of actin filaments and therefore would accumulate at the stereocilia tips. It is difficult to conceive how this motor protein can apply tension onto any protein or lipid component at the tip if it cannot move in the opposite direction. Possibly MYO1C only applies tension onto CDH23 effectively at the side insertion plaque, where an upward movement is possible (Fig. 6.2). In this case there may be an asymmetry in complex architecture of the tip link with respect to tip- and side insertion. Alternatively, the tip may harbor undiscovered actin filaments of different polarity, in which case movement of the motor protein in a different direction could be envisioned. The model will have to be tested by rigorous experiments to proof its value.

6.3. CDH23 in Photoreceptors of the Vertebrate Retina

Mutations within the *CDH23* gene lead to Usher Syndrome in human patients, a disease which not only affects the senses of hearing and balance, but also vision. Visual abnormalities usually manifest in late childhood or adolescence. Pigmentary retinopathy is the clinical finding that provides a definitive diagnosis of Usher Syndrome and distinguishes it from non-syndromic sensorineural hearing impairment. Night blindness is often the first symptom of retinal degeneration, but retinitis pigmentosa may lead to total blindness eventually (Ahmed et al., 2003a; Keats and Corey, 1999; Petit, 2001).

Our experimental data and that from others provide evidence that the Usher Syndrome protein CDH23 is expressed in the photoreceptor cell layer as seen by histochemistry (Reiners et al., 2003). Furthermore, at the ultrastructural level we found CDH23 localized to the connecting cilium and to adjacent structures of rod-type photoreceptors in wild-type mice.

Vertebrate photoreceptor cells are highly polarized sensory cells with distinct functional compartments: a photosensitive outer segment, a cell body and a synaptic terminal, the latter two commonly referred to as inner segment. A thin cellular bridge, the so-called connecting cilium, serves to join the photoreceptor outer segment with the inner segment, which contains the protein synthesis machinery (Fig. 6.3). The photosensitive outer segment membranes are continually turned over. New disks are formed at the base of the outer segment whereas the distal tips are shed and subsequently phagocytozed by the cells of the retinal pigment epithelium. This turnover requires *de novo* synthesis of outer segment proteins in the proximal subcompartment of the metabolically active inner segment, followed by delivery of these proteins by intracellular transport through the connecting cilium to the base of the outer segment (Williams, 2002). Furthermore, protein components of the connecting cilium participate in the outer segment disk morphogenesis (Williams, 1991; Williams et al., 1992).

6.3a. Hair Cell Kinocilium and Photoreceptor Connecting Cilium: A Common Theme?

The microtubule-based axonem of the photoreceptor connecting cilium contains 9 peripheral microtubule doublets, no central microtubule pair (9x2+0 structure) and lacks accessory dynein arms commonly found in motile cilia (Rohlich, 1975). The kinocilium of the inner ear hair cells is likewise non-motile and the majority of the kinocilia have the same 9x2+0 microtubule architecture (Sobkowicz et al., 1995). Interestingly, the connecting cilium in photoreceptors contains an actin cytoskeleton distal to the microtubular axonem at the lateral membrane (Arikawa and Williams, 1991; Chaitin et al., 1984; Williams, 1991). MYOVIIA, the product of another Usher I gene, is believed to translocate along the actin cytoskeleton to move opsin through the photoreceptor connecting cilium (Liu et al., 1999; Liu et al., 1997). Kinesin II may assist in this function as it moves along the microtubules (Williams, 2002). Whether the hair cell kinocilium contains an actin cytoskeleton next to its microtubule-based axonem, similar to the photoreceptor connecting cilium, is at present unclear, but it appears that the actin motor MYO1C also localizes to the kinocilium as well as to stereocilia, suggesting that actin may be present in the kinocilium (Steyger et al., 1998). The discovery of „masked“ actin in the kinocilium would further strengthen the hypothesis that hair cell kinocilium and the photoreceptor connecting cilium are related structures.

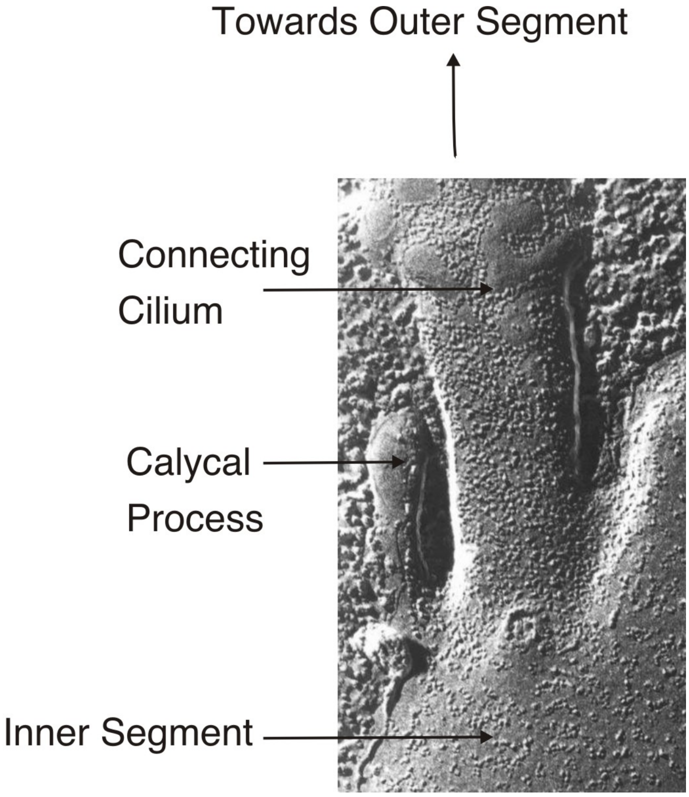

Figure 6.3.
A Freeze Fracture Electron Micrograph Displaying the Photoreceptor Connecting Cilium and an Adjacent Calycal Process. (Taken from: http://www.mardre.com/homepage/mic/tem/samples/bio/ros/risros6.html).

6.3b. Calycal Processes: The Stereocilia of the Photoreceptor?

Intriguingly, adjacent to the connecting cilium, also arising from the inner segment, are actin-rich microvillus-like projections, the so-called calycal processes. Evolutionary outer segments and calycal processes may have evolved from a common ancestral structure, the rhabdomere. In invertebrates the phototransduction apparatus or signalplex resides in tightly packed genuine actin-rich microvilli, the rabdomeres (Montell, 1999). During evolution the rhabdomere may have split up to give rise to two structures, the outer segment with lamellar stacks of membranous discs for phototransduction and the actin-rich calycal process for structural support.

These calycal processes have striking similarity with hair cell stereocilia not only because of their actin filaments, which have their plus ends pointing distally towards the tips (Burnside, 1978), similar to stereocilia, but also due to additional properties. Fimbrin, which is a major actin bundling protein in stereocilia appears to have a similar function in the calycal processes (Hofer and Drenckhahn, 1993). Whether espin, the other important bundling protein in stereocilia, is likewise prominent in the corresponding photoreceptor structure is unknown.

The ankle link antigen and the tip link antigen described by Goodyear and Richardson, which appear to be restrictively expressed in the inner ear and the retina as thus far analyzed, have a highly reminiscent ultrastructural localization in these two structures of the hair cell and the photoreceptor cell. While the ankle link antigen is found at the base of stereocilia and the base of calycal processes, the tip link antigen is distributed along the longest stereocilia facing the kinocilium and along the ciliary calyx (Goodyear and Richardson, 1999; Goodyear and Richardson, 2003).

Finally, the protein product MYOIIIA, the mammalian ortholog of *Drosophila NINAC*, which is essential for phototransduction in the fly eye (Li et al., 1998; Porter and Montell, 1993; Porter et al., 1993), exclusively localizes to the calycal processes of the photoreceptor cell and is expressed in hair cells of the inner ear (Dose et al., 2003). Interestingly, mutations have been found in the *MYOIIIA* gene that cause progressive non-syndromic hearing loss (DFNB30) (Walsh et al., 2002). The mutations in *MYOIIIA* that have been analyzed so far, do not cause loss of vision. That is surprising, given that MYOIIIA is highly expressed in the photoreceptor calycal processes and mutations of the *Drosophila* ortholog *NINAC* lead to retinal degeneration. However in human retina there may be functional redundancy of class IIII myosins as a close relative of MYOIIIA, MYOIIIb, is expressed in retina as well (Dose et al., 2003). Also it is possible that a yet unidentified *MYOIIIA* mutation may lead to loss of both hearing and vision, in analogy to other genes giving rise to Usher Syndrome and non syndromic forms of deafness. The function of MYOIIIA is neither known in the photoreceptor cells nor in the hair cells, it is possible though that the protein is present in hair cell stereocilia, since it has been shown that it translocates along actin bundles and localizes to filapodia tips when heterologously expressed (Les Erickson et al., 2003).

CDH23 appears to be localized to the membrane at the interface between the connecting cilium and the calycal process. Intriguingly, there is a gap between the microtubule-based connecting cilium and the actin-rich calycal process (Fig. 6.3), much like between the kinocilium and the stereocilia of hair cells, which are likewise apposing membrane systems protruding from the same cell. There is the possibility that these two membrane structures are also cross linked by CDH23 similar to kinocilium and stereocilia in hair cells. The gap between the connecting cilium and the calycal process has comparable dimensions with respect to the stereocilia system of approximately 200 nm, at least in some areas since the distance between these two structures appears not to be uniform. On the ultrastructural level, cross linker molecules can be observed, bridging the gap between the connecting cilium and the calycal process (Fetter and Corless, 1987). Whether these cross linker molecules consist of two helical filaments like the tip link in hair cell stereocilia, has not been analyzed.

While the function of the connecting cilium is to provide the outer segment with molecules for the phototransduction machinery and is involved in pinching of membrane in the course of disk morphogenesis at the outer segments base as discussed above, the function of the calycal process in the photoreceptor cell is not understood. It is possible that the calycal processes give structural support to the connecting cilium. There is some evidence that the calycal processes, by virtue of their position, define the disc perimeter of newly formed discs at the base of the outer segment and are therefore involved in disc morphogenesis similar to the connecting cilium. Treatment of photoreceptors with cytochalasin D, which disrupts actin filaments and triggers the collapse of calycal processes, affect disc morphogenesis (Hale et al., 1996; Williams et al., 1988). However, since the connecting cilium also contains peripheral actin filaments, this effect can not strictly be attributed to the disruption of calycal processes.

An alternative model for calycal process function comes from the observation that photoreceptors of some animal species change their shape. This retinomotor movement of photoreceptors occurs in response to light in order to position photosensory outer segments optimally to the incoming light stimulus (Burnside, 2001). In this respect it has been shown that calycal process are dynamic structures in the teleost fish (*Lepomis cyanellus*) and appear to be important in regulation of rod photoreceptor elongation, since shortening of the calycal process is correlated with elongation of the rod photoreceptor in light-dark cycles (Pagh-Roehl et al., 1992). An intriguing hypothesis is that CDH23 is part of a mechanoreceptive complex in the connecting cilium and/or calycal process that measures (and thereby regulates) photoreceptor elongation. This function would be analogous to the hypothesized function of CDH23 in hair cells of the inner ear. However, retinomotor movement appears to be important in lower vertebrates only, animals which lack a pupilary response. The pupil regulates the amount of light reaching the retina in higher vertebrates. It remains to be studied if retinomotor movement is completely abolished in higher vertebrates or occurs there as well.

In this respect it is interesting to note that rod-type photoreceptors of mice and other rodents only have rudimentary calycal processes as opposed to humans (David Williams personal communication), which may explain the „mild“ retinal phenotype observed in *waltzer* mice with a defect in CDH23 compared to human USHER1D patients as discussed below. Possibly, calycal processes do not play an essential role in rodent phototransduction compared to humans. Within the human eye, calycal processes of rod-type photoreceptors are more prominent than that of cone-type photoreceptors (Rana and Taraszka, 1991).

Since the membranous discs pinch off the connecting cilium at the base of the outer segment to be incorporated into the lamellar disc stacks, it is not so surprising that we found some of the CDH23 labelling also in these membrane stacks harboring the phototransduction machinery; but we did not detect CDH23 staining in outer segments of all the retinal samples analyzed and a recent study with a different antibody to CDH23 reported absence of this protein from the outer segments, and instead localization to the inner segment. However, the resolution of their immunofluorescent staining would also allow the conclusion that CDH23 resides in the vicinity of the connecting cilium in analogy to what we have observed (Reiners et al., 2003). Whether CDH23 has a function in photo-active discs of the outer segment, a structure, which can likewise be pictured as two apposing membranes with a gap in between, needs further analysis. It would be interesting to know if CDH23 deficiency may lead to altered compaction of disc stacks in human patients.

In light of our findings it is worth mentioning that localized adhesion activity is crucially important for outer segment integrity, since another member of the cadherin family, prCAD, is exclusively localized to the base of outer segments and its ablation leads to fragmentation of outer segments and subsequent photoreceptor loss (Rattner et al., 2001)

Mutations of *CDH23,* giving rise to Usher Syndrome, may also cause abnormalities of the connecting cilium and/or the calycal processes. Although tissue samples of the retina can only be collected postmortem from human patients, some cases of abnormal connecting cilia of photoreceptors in Usher Syndrome patients have been described. It is not possible to recapitulate if these patients suffered from USH1D caused by mutations in *CDH23,* or from a different form of USH1 (Barrong et al., 1992; Hunter et al., 1986). Since USH1B, caused by mutations in the gene encoding MYOVIIA, which also localizes to the connecting cilium as described above, is responsible for 75% of all USH1 cases (Petit, 2001), it is more likely that mutations of *MYOVIIA* lead to the abnormal connecting cilium in photoreceptors of the unclassified Usher Syndrome cases.

6.4. Usher Syndrome Type I

6.4a. Animal Models of Usher Syndrome: Differences in Mice and Man

Although mouse models for Usher Syndrome, such as *waltzer, shaker* or *ames waltzer* mice being defective in the genes for *CDH23, MYOVIIA* and *PCDH15* respectively, show congenital hearing loss similar to human patients, they fail to recapitulate retinal degeneration. Small electroretinographic anomalies can be detected in strong alleles of *waltzer* and *shaker* mice (Libby et al., 2003; Libby and Steel, 2001) but not in any of the *ames waltzer* alleles (Ball et al., 2003), while non of the mouse models display retinal degeneration associated with Usher Syndrome caused in humans by mutations in any of the three genes.

Several reasons are possible for this discrepancy. First of all, manifestation of retinal degeneration even in the most severe forms of Usher Syndrome occurs not before the first decade in the life of human patients (Keats and Corey, 1999). Mice have a much shorter life span, therefore a phenotype may escape detection simply because mice have not aged enough in order for the retinal degeneration to manifest.

Another possibility arises from the observation that mice, compared to humans, have rather poor vision and see mainly black and white. They do not rely on visual cues as much as humans do, because they live in the dark and make use of other sensory systems to gather information about their environment. This difference in visual perception reflected by a difference in architecture, density and distribution of rod and cone photoreceptors in the mouse retina compared to the primate one (Rodieck, 1988), may account for the fact that mice are less susceptible to a retinal degeneration phenotype. One example for a distinction of the cyto-architecture between the human and mouse retina is the size difference of calycal processes as discussed above.

In this respect it is interesting to note that mutations in all of the above mentioned genes may also cause non-syndromic forms of hearing loss not affecting the visual system while so far that is not true the other way around (Petit, 2001). No mutations within these three genes are known to cause non syndromic forms of retinal degeneration. Since numerous different mutations have been mapped affecting different parts of these genes, this observation allows two conclusions. First of all, there is no evidence that domains within the affected proteins are only critical for the function of the photoreceptor cell but not critical for hair cell function. Second, it seems that only severe mutations, either leading to the deletion of large parts of the respective protein or to its total loss of function, affect the retina, while „milder“ mutations compromise auditory function only. Therefore, these genes appear to be more critical for inner ear function than for the retina. The reason for this is unclear: one hypothesis is that CDH23, MYOVIIA and PCDH15 may serve a dual role in hair cells, first in development and maturation of the hair cell with its stereocilia bundle and then later in the mature hair cell as a component of the transduction apparatus. In the retina the protein products of the mutated genes may not play a decisive role in development but only in the mature photoreceptor. This may also explain why in USHI patients the onset of the retinal disorder manifests much later in life than congenital hearing loss: Because of developmental defects within the hair cell the auditory apparatus never reaches functionality, while the retinal photoreceptors at first develop normally. We detected strong CDH23 expression along the membrane of the entire stereocilia bundle in young mice during hair bundle formation while in mature stereocilia CDH23 localization was confined to their tips. In the retina, on the other hand, we only observed weak CDH23 expression with no apparent peak at any developmental time point. Some mutations in *CDH23*, which are believed to affect its function only moderately, increase susceptibility to age related hearing loss and noise-induced hearing loss, while hearing is not affected at first (Davis et al., 2003; Davis et al., 2001; Holme and Steel, 2004). One interpretation of this finding is that these mutations do not perturb the developmental function of the gene, while its stability as tip link in mature hair cells is compromised.

Further, the analysis of different alleles of *shaker* mice, defective in the Usher Syndrome gene *MyoVIIA*, showed that the gene product is required for normal hair cell development, as well as for the function of mature hair cells (Self et al., 1998). These findings argue for a double role of the Usher genes at two different developmental time points in mouse hair cells, while there is lack of evidence for the same phenomenon in the mouse retina.

Certainly there may be other reasons for the profound importance of Usher genes in the auditory tissue compared to a lesser demand in retinal tissue that can not be generalized to the whole group of Usher Syndrome genes. For example it has been suggested that MYOVIIA is of importance in the photoreceptor cells as well as in the retinal pigment epithelium (RPE) within the human retina while in the mouse MYOVIIA appears to be strongly expressed and functionally important in the RPE (Liu et al., 1998) but not in the photoreceptor cells (el-Amraoui et al., 1996). This may explain a „mild“ retinal phenotype in the respective mutant mice (*shaker* mice) compared to the retinal degeneration in human patients.

The reasons for differences and similarities in gene requirements of the retina and the inner ear will certainly be diverse. Nevertheless, the comparison of hair cell and photoreceptor cell in development, function and disease may help to understand both the auditory system and phototransduction and may even point to a common theme in the evolution of sensory systems.

6.4b. Usher Syndrome – A general ciliary deficit?

Mutations in *CDH23* affect hair cell function and most likely also directly impair photoreceptors, both of which are ciliated cells involved in sensory perception as discussed above. Another sensory system, involving ciliated neurons, is the olfactory system. We have investigated the expression of CDH23 protein in the olfactory epithelium of adult mice and detected CDH23 protein at the apical surface of the olfactory epithelium. Likewise, we detected harmonin and MYOVIIA, both of which together can form a membrane-bound complex with CDH23, in the sensory cilia and microvilli of the olfactory epithelium.

Interestingly, this sensory tissue again is comprised of a microtubule-based ciliated structure, the olfactory receptor dendrite, and neighboring actin-rich microvilli arising from Sustentacular cells supporting the sensory dendrite The dendritic cilia harbor the olfaction apparatus of the olfactory receptor cells, a bipolar sensory neuron population that constantly has to be replenished (Reed, 2004). This cyto-architecture again is reminiscent of hair cell kinocilium and stereocilia, with the important difference, that the mechanosensory apparatus in hair cells resides in the actin-rich stereocilia and not in dendritic, microtubules-based protrusions.

Although we did not carry out ultrastructural analysis of CDH23 expression in the olfactory epithelium, it can be envisioned that in analogy to hair cells in the inner ear and to photoreceptor cells in the retina, the olfactory cilia are likewise connected to actin-based microvilli and/or to each other by CDH23.

A correlation between Usher Syndrome and olfactory deficits is at present controversial. Some studies, carried out with mixed groups of Usher type 1 and Usher type 2 patients, find olfactory deficits in the affected patients (Arden and Fox, 1979; Zrada et al., 1996), but other studies do not show a correlation between Usher Syndrome and compromised smell perception (Seeliger et al., 1999). As for the mouse models for Usher Syndrome, no studies implicating olfactory abnormalities have been published.

A few cases of Usher Syndrome have been correlated with respiratory deficiencies and decreased sperm motility, both phenomena involving abnormal axonemal structures (Hunter et al., 1986). Therefore it has been suggested that some genes defective in USHI are of general importance for ciliary structures and causally linked with Ciliary Aplasia (Tosi et al., 2003). The Usher Syndrome gene encoding MYOVIIA, is a common component of cilia and microvilli in all the tissues analyzed so far (Sahly et al., 1997; Wolfrum et al., 1998). The expression of MYOVIIA in actin-based microvillar structures is not surprising and the protein is often found there in conjunction with Myosins I, III, and VI which are likewise expressed in hair cell stereocilia. By contrast, the presence of MYOVIIA in motile and non-motile cilia is somewhat puzzling given that cilia are primarily the domain of microtubules rather than actin filaments. It remains to be shown whether all the cilia found to harbor MYOVIIA also contain actin filaments like the connecting cilium of photoreceptors.

Harmonin, the protein product of the Usher gene giving rise to USHIC, has been shown to localize to microvillar structures, the brush border of the intestine (Kobayashi et al., 1999; Scanlan et al., 1999). So far there have been no reports about harmonin´s presence in cilia, in fact it seems to be absent from the connecting cilium in photoreceptors but instead concentrated at the ribbon synapse (David Williams, personal communication) (Reiners et al., 2003).

It is at present unclear, whether Usher Sydrome type I genes have a general function in ciliated structures. The expression profile of some Usher gene products such as MYOVIIA together with very few case reports of human Usher patients suggest that there could be a general role for Usher genes in axonemal structures. Future work, in particular the analysis of mouse models, will have to clarify this issue.

6.4c. CDH23, MYOVIIA and Harmonin in Hair Follicle

Additionally, we have also found CDH23, harmonin and MYOVIIA expression in mouse tissues not necessarily associated with microvillar and ciliary function, such as the inner root sheath cells of the whisker follicle and hair follicle of the mouse.

Although these cells may not harbor ciliated or actin-rich protrusions these structures are nevertheless sensors of mechanical stimuli like the hair cells. We detected strong expression of CDH23 in the cuticle of the inner root sheath, cells directly apposed to the hair shaft at the base of the follicle. This position is perfectly situated for detecting movement of the whisker or hair. Although the cuticle hairs are not innervated by sensory nerve endings, they are electrically coupled via an intricate network of gap junctions to outer root sheath cells, which receive innervation and therefore could pass on the mechanical perception onto sensory neurons (Rice et al., 1997).

Hair follicles have not been reported to be affected in Usher Syndrome patients and likewise *waltzer* mice defective in *CDH23* do not display an obvious phenotype in whisker follicle and hair follicle. What role CDH23 and the other Usher gene products play in these tissues is unclear.

In all the sensory tissues analyzed in our study the Usher Syndrome gene products CDH23, harmonin and MYOVIIA, appeared to be expressed in an overlapping fashion. In all cases CDH23 was more restrictively expressed, while harmonin and MYOVIIA showed a broader overlapping expression pattern. Whether these three Usher Syndrome gene products, and maybe others such as SANS and PCDH15, are in a common molecular pathway in hair cells and other tissues needs to be defined.

The puzzle of Usher Syndrome and genes implicated in the disease is far from being resolved. Most of the players of the game have been identified and their expression and localization patterns are well underway to be worked out. It is time that the molecular mechanisms and functions of these genes in the respective tissues will be addressed in detail.

Future Pospects

7. Future Prospects

Our data strongly suggests that the Usher Syndrome gene product CDH23 is part of the tip link in mature hair cells of the vertebrate inner ear. We have further shown that CDH23 and the multi PDZ-domain protein harmonin can form a protein complex. The architecture of this complex appears to be regulated by sequences encoded by exon 68 within the cytosolic domain of CDH23. It is likely that CDH23 serves a dual role in hair cells, since the protein is strongly expressed along the entire stereocilia bundle during hair bundle morphogenesis and later its localization is restricted to stereocilia tips

7.1. Function of Exon 68 Encoded Sequences within the CDH23-Cytodomain

To test the importance of exon 68, transgenic mice are currently generated that harbor a genetically modified *CDH23* gene, lacking exon 68, which renders the rest of the protein product intact and functional. In this way it may be possible to differentiate between the developmental hair cell phenotype of splayed stereocilia bundle observed in *waltzer* mice lacking functional CDH23 and the proposed channel gating function. Ablation of exon 68 would not interfere with a potential role of CDH23 in the Reissner´s Membrane, since this splice variant is not expressed there. In the current mouse model for USH1D/CDH23, the *waltzer* mouse, it can not be excluded that the severe phenotype observed may be in part due to abnormalities in the Reissner´s Membrane.

It is possible that amino acid residues encoded by exon 68 are needed for the developmental function of CDH23 as well, such as proper targeting to the stereocilia or other more general properties of the protein. In that case it would not be possible to dissect differences between the developmental role of CDH23 and its function in mature hair cells by this approach. A conditional/inducible knock-out of the *Cdh23* gene may then alternatively allow dissection of its developmental function versus a role in mechano transduction.

7.2. Function of Harmonin and MYOVIIA

The role of harmonin and MYOVIIA in development and/or auditory transduction is not understood. Unlike for CDH23, the presence or absence of harmonin in mature stereocilia has not been demonstrated. It is possible, that sparse amounts of harmonin protein is present at stereocilia tips forming a complex with CDH23. Therefore it is worthwhile to carry out rigorous ultrastructural analysis of harmonin expression and localization in mature hair cells with high affinity antibodies directed against the protein. This would be a first step towards the clarification whether harmonin has a pure developmental role in hair bundle morphogenesis or is involved in mechanosensation as well. If it would turn out that harmonin is absent from mature stereocilia, there is the possibility that its closest homolog whirlin, also implicated in deafness, may take over. Therefore, besides whirlin-CDH23 interaction studies, the spatio-temporal expression and localization pattern of whirlin is of significant interest as well.

7.3. Transport to Stereocilia

Another question is how proteins like CDH23 and harmonin are specifically enriched and transported along the stereocilia to the tips. For harmonin there is evidence that a translocation process along the stereocilia actin bundles involving the actin-motor MYOVIIA is taking place, but for CDH23 this seems not to be the case (Boeda et al., 2002). A recent study suggested that MYO1C may be involved in transporting the pre-assembled transduction apparatus, including the tip link, along the actin bundles to the stereocilia tips (Geleoc and Holt, 2003). We found that CDH23 interacts with MYO1C in a cellular environment. Defining the interaction domains within both proteins will be important. Once the critical protein sequence within CDH23 is known, it would be interesting to test whether this peptide sequence is sufficient to localize a tagged version of it to stereocilia tips in transfected hair cell organ cultures. Defining protein sequences necessary and sufficient for stereocilia transport may help to elucidate the transport mechanism. Complementary, it would be interesting to test, if chemical blockage of genetically engineered *Myo1c* in transgenic mice (Holt et al., 2002) leads to an altered CDH23 localization during hair cell maturation.

7.4. A Role for MYO1C in Transduction Channel Gating?

Chemical inhibition of genetically engineered *Myo1c* in transgenic mice has been shown to affect auditory adaptation responses (Holt et al., 2002). Additionally, these mice appear to lose the ability to open transduction channels over time. The transduction currents are not completely lost but decreased by 50%, which may be due to incomplete chemical inhibition, since wild-type *Myo1C* is still expressed in the transgenic mice. Therefore it would interesting to know, if mice with an ablation of the *Myo1c* gene display the same phenotype as the ones susceptible to chemical inhibition or may lose transduction currents completely, arguing for a more prominent role of MYO1C in auditory transduction than a sole function as adaptation motor. The possible lethality of this gene ablation may need to be overcome by conditional knock-out strategies.

7.5. Adhesion Properties of CDH23

We have shown that CDH23 can act as a homophilic adhesion receptor in an *in vitro* cell culture assay. It may be possible to employ tagged versions of purified protein fragments from CDH23 extracellular domain on cultured hair cells, to test if these can bind to stereocilia tips as well, strengthening the case, that indeed homophilic interaction takes place in the physiological environment of the hair bundle. Another biochemical question concerns the individual extracellular cadherin repeats (EC-domains) of CDH23. It is not known which and how many EC-domains of the protein are involved in the homophilic interaction. To resolve that issue it will be necessary to carry out interaction studies with individual EC-domains expressed in L929 fibroblasts, as we have done in this study with full length CDH23. As suggested earlier, it may be possible that multiple EC-domains engage in interactions and may be even in different registers, in order to convey the necessary strength to the tip link to withstand forces generated during stereocilia deflection. A good starting point for these interaction studies will be to analyze the first (N-terminal) EC-domain of the 27 possible in CDH23, since in classical cadherins the N-terminal EC-domain is critical for mediating homophilic interaction.

Atomic-Force Microscopy may provide a basis for measuring the interaction strength between certain EC-domains of CDH23 in the L929 fibroblast model system, a quantitative value that can be related to the forces generated during stereocilia deflection.

An important matter, shown to play a key role for adhesion strength of classical Cadherins, is the influence of the cytodomain. In the case of CDH23, no catenins can bind to its cytosolic portion, which hook up classical cadherins to the actin cytoskeleton. But we have shown that harmonin and MYO1C do interact with the cytosolic tail of CDH23, both of which have actin binding potential, and therefore may be important to guarantee resistance to prevent extraction of the protein from the membrane during strong pulling forces. Cytosolic deletions of CDH23 should be analyzed upon their adhesion potential; likewise co-expression with Harmonin and/or MYO1C may alter adhesion strength. Further, different splice variants of CDH23 may be utilized in this assay to address the influence of splicing on adhesion properties. Additionally, heterophilic binding properties with PCDH15, another Usher Syndrome gene product expressed in hair bundles, can be tested as well in this assay system. A general complication with this cell culture model system may be that the glycocalix, which wraps the tip links *in vivo* and may provide structural rigidity, is missing in the model system.

7.6. Reconstitution of the Mechanosensitive Apparatus *in vitro*

Ultimately, one goal can be to reconstitute the whole transduction system *in vitro*, once all the components have been identified. So far one of the key components, the putative transduction channel, has remained elusive in vertebrate inner ears. In zebrafish (*Danio rerio*) however, a member of the TRP family of ion channels, NompC, has been shown to be critical for mechanosensation in hair cells of zebrafish´s inner ear and lateral-line organ (Sidi et al., 2003). Extensive searches of genome databases and cDNA libraries have until now failed to identify a vertebrate copy of the *NompC* gene. Since all the Usher type I genes, CDH23, MYOVIIA, Harmonin and others have functionally conserved orthologs expressed in zebrafish hair cells, the overall transduction apparatus is, however, assumed to be identical between zebrafish and vertebrates (Nicolson et al., 1998). Therefore, it would be interesting to reconstitute NompC, CDH23, harmonin and MYO1C in a cell culture system and to analyze, if pulling on CDH23´s extracellular domain by atomic force microscopy can lead to gating of the introduced NompC channel. For this purpose either electrophysiological measurements or calcium imaging techniques can be applied.

7.7. Identification and Characterization of the Putative Transduction Channel

Biochemical approaches such as co-immunoprecipitation experiments or so-called pull-down experiments may be employed to obtain a handle on the putative transduction channel. Since we identified CDH23 as a component of the tip link, believed to reside in a complex with the putative transduction channel, immunoprecipitation of this protein (with antibodies we raised) from hair cells or hair cell-cell lines may pull down the ion channel or other components of the transduction machinery. Their identification can be aided by subsequent mass spectroscopic analysis.

The possibility remains that the transduction channel is linked to CDH23 via the PDZ-domain protein Harmonin. A yeast two-hybrid analysis with PDZ I and PDZ III of Harmonin as bait may reveal interaction candidates, among them potentially ion channels. A prerequisite for this type of screen is a high quality cDNA library from inner ear hair cells. RNA, the template for cDNA, is difficult to obtain in large enough amounts from a couple of thousand hair cells per ear. But with new RNA isolation and amplification technologies available, it should now be possible to generate a cDNA library of appropriate quality.

Despite the fact that the transduction channel has not been identified yet, there are ways to characterize its properties nevertheless. To gain insight into its gating properties, techniques and tools established to characterize mechanosensitive channels of bacteria can be employed. Osmosensitivity is regarded as a feature of several mechanosensitive channels (Zhou et al., 2003). Therefore it may be possible to test if the putative auditory transduction channel responds to changes in osmolarity by Ca^{2+} imaging of stereocilia tips in hair cell organ cultures, or measuring FM1-43 uptake, an organic dye known to pass through the transduction channel. Both techniques have been successfully employed for visualizing hair cell stimulation before (Denk et al., 1995; Lumpkin and Hudspeth, 1995; Meyers et al., 2003).

Similarly, bacterial mechanoreceptors have been shown to open their ionic pore by incubation with amphipaths, which intercalate into the plasma membrane asymmetrically and thereby either crenating the membrane inward, or causing a cup-shaped conformation, depending on the reagent used (Martinac et al., 1990; Patel et al., 1998). Incubation of hair cell cultures with amphipaths may give insight into the mechanosensitivity of the transducer channel assessed again by calcium imaging techniques.

In this respect it may be of interest to test the effect of other pharmacological substances on transduction channel gating. The paradigm of Corey and Hudspeth´s gating spring model discussed before, requires an association of the transduction channel or a closely associated component of the transduction apparatus to be linked to the actin cytoskelton, in order for gating to occur. To address the importance of the actin cytoskeleton in mechanosensation, reagents either disrupting or stabilizing actin filaments, can be tested in this assay on their influence on channel gating. While these biochemical approaches will by no means render the molecular identification of the transduction channel unnecessary, they may help to characterize its properties and thereby dismiss old or suggest new candidate ion channels.

7.8. Function of Usher Proteins in Cells other than Hair Cells

We have found CDH23 expressed in other cells in the inner ear besides hair cells. Epithelial cells within the Reissner´s membrane express the large protein as well. The function of CDH23 in the Reissner´s Membrane is totally obscure. This two cell layer-thick barrier is important to separate the endolymphatic duct from the perilymphatic compartment. This seal has to be very tight, as a steep electrochemical gradient is laying across this two cell layer structure. This gradient gives rise to a measurable electrochemical potential known as the endocochlear potential. It is possible that CDH23 is part of the tight seal. As a first step towards the understanding of CDH23´s function in the Reissner´s Membrane it would be interesting to measure the endocochlear potential of *waltzer* mice, defective in CDH23, and to see if there is a leakiness of the seal, which may explain part of the auditory phenotype seen in those mice.

Additionally, we have detected CDH23 together with its putative interactor proteins harmonin and MYOVIIA in other sensory tissues outside the inner ear. All three proteins appeared to reside at the apical surface of the olfactory epithelium. Although harmonin and MYOVIIA appeared to be broader expressed compared to CDH23, it is possible that all three proteins colocalize in dendritic cilia, which –like stereocilia- harbor a sensory machinery. Our immuno histochemical analysis did not reveal the fine olfactory cilia with high enough resolution to prove colocalization of all three proteins, likewise no marker for olfactory receptor dendrites was employed to exactly know which structures contain the products of the three Usher Syndrome genes. Therefore ultrastructural analysis of the olfactory epithelium should clarify their localization in this tissue. It is also not clear if these three proteins are equally distributed in both the main olfactory epithelium and the neighboring vomeronasal organ responsive to pheromones. It should be addressed if *waltzer* and *shaker* mice, defective in *CDH23* and *MYOVIIA* respectively show absence (or mislocalization) of the two proteins in the olfactory epithelium and if that can be related to structural abnormalities of the dendritic cilia of microvilli and finally to perturbed olfaction.

A similar analysis can be envisioned for the whisker/hair follicle, a structure likewise expressing the three proteins in mice. Whether any of the three proteins play a role in whisker mechanosensation may be addressed by behavioral tests of the mutant mice. Alternatively, it may be possible that the cycling of the hair/whisker follicle or follicle transition between different morphological stages (anagen, catagen and/or telogen) is altered in mutant mice, a mild defect that may not be particularly obvious but potentially detectable by measuring the time of follicle cycling.

References

8. References

Adam, J., Myat, A., Le Roux, I., Eddison, M., Henrique, D., Ish-Horowicz, D., and Lewis, J. (1998). Cell fate choices and the expression of Notch, Delta and Serrate homologues in the chick inner ear: parallels with Drosophila sense-organ development. Development *125*, 4645-4654.

Ahmed, Z., Riazuddin, S., and Wilcox, E. (2003a). The molecular genetics of Usher syndrome. Clin Genet *63*, 431-444.

Ahmed, Z. M., Riazuddin, S., Ahmad, J., Bernstein, S. L., Guo, Y., Sabar, M. F., Sieving, P., Griffith, A. J., Friedman, T. B., Belyantseva, I. A., and Wilcox, E. R. (2003b). PCDH15 is expressed in the neurosensory epithelium of the eye and ear and mutant alleles are responsible for both USH1F and DFNB23. Hum Mol Genet *12*, 3215-3223.

Ahmed, Z. M., Riazuddin, S., Bernstein, S. L., Ahmed, Z., Khan, S., Griffith, A. J., Morell, R. J., Friedman, T. B., and Wilcox, E. R. (2001). Mutations of the protocadherin gene PCDH15 cause Usher syndrome type 1F. Am J Hum Genet *69*, 25-34.

Akiyama, S. K., Yamada, S. S., Yamada, K. M., and LaFlamme, S. E. (1994). Transmembrane signal transduction by integrin cytoplasmic domains expressed in single-subunit chimeras. J Biol Chem *269*, 15961-15964.

Alagramam, K. N., Murcia, C. L., Kwon, H. Y., Pawlowski, K. S., Wright, C. G., and Woychik, R. P. (2001a). The mouse Ames waltzer hearing-loss mutant is caused by mutation of Pcdh15, a novel protocadherin gene. Nat Genet *27*, 99-102.

Alagramam, K. N., Yuan, H., Kuehn, M. H., Murcia, C. L., Wayne, S., Srisailpathy, C. R., Lowry, R. B., Knaus, R., Van Laer, L., Bernier, F. P., et al. (2001b). Mutations in the novel protocadherin PCDH15 cause Usher syndrome type 1F. Hum Mol Genet *10*, 1709-1718.

Alagramam, K. N., Zahorsky-Reeves, J., Wright, C. G., Pawlowski, K. S., Erway, L. C., Stubbs, L., and Woychik, R. P. (2000). Neuroepithelial defects of the inner ear in a new allele of the mouse mutation Ames waltzer. Hear Res *148*, 181-191.

Angst, B. D., Marcozzi, C., and Magee, A. I. (2001). The cadherin superfamily: diversity in form and function. J Cell Sci *114*, 629-641.

Arden, G. B., and Fox, B. (1979). Increased incidence of abnormal nasal cilia in patients with retinitis pigmentosa. Nature *279*, 534-536.

Arikawa, K., and Williams, D. S. (1991). Alpha-actinin and actin in the outer retina: a double immunoelectron microscopic study. Cell Motil Cytoskeleton *18*, 15-25.

Arndt, K., and Redies, C. (1998). Development of cadherin-defined parasagittal subdivisions in the embryonic chicken cerebellum. J Comp Neurol *401*, 367-381.

Assad, J. A., Shepherd, G. M., and Corey, D. P. (1991). Tip-link integrity and mechanical transduction in vertebrate hair cells. Neuron *7*, 985-994.

Astuto, L. M., Bork, J. M., Weston, M. D., Askew, J. W., Fields, R. R., Orten, D. J., Ohliger, S. J., Riazuddin, S., Morell, R. J., Khan, S., et al. (2002). CDH23 mutation and phenotype heterogeneity: a profile of 107 diverse families with Usher syndrome and nonsyndromic deafness. Am J Hum Genet *71*, 262-275.

Ball, S. L., Bardenstein, D., and Alagramam, K. N. (2003). Assessment of retinal structure and function in Ames waltzer mice. Invest Ophthalmol Vis Sci *44*, 3986-3992.

Barrong, S. D., Chaitin, M. H., Fliesler, S. J., Possin, D. E., Jacobson, S. G., and Milam, A. H. (1992). Ultrastructure of connecting cilia in different forms of retinitis pigmentosa. Arch Ophthalmol *110*, 706-710.

Bartles, J. R., Zheng, L., Li, A., Wierda, A., and Chen, B. (1998). Small espin: a third actin-bundling protein and potential forked protein ortholog in brush border microvilli. J Cell Biol *143*, 107-119.

Bass, R. B., Strop, P., Barclay, M., and Rees, D. C. (2002). Crystal structure of Escherichia coli MscS, a voltage-modulated and mechanosensitive channel. Science *298*, 1582-1587.

Bell, G. I. (1978). Models for the specific adhesion of cells to cells. Science *200*, 618-627.

Belyantseva, I. A., Boger, E. T., and Friedman, T. B. (2003). Myosin XVa localizes to the tips of inner ear sensory cell stereocilia and is essential for staircase formation of the hair bundle. Proc Natl Acad Sci U S A *100*, 13958-13963.

Ben-Yosef, T., Ness, S. L., Madeo, A. C., Bar-Lev, A., Wolfman, J. H., Ahmed, Z. M., Desnick, R. J., Willner, J. P., Avraham, K. B., Ostrer, H., et al. (2003). A mutation of PCDH15 among Ashkenazi Jews with the type 1 Usher syndrome. N Engl J Med *348*, 1664-1670.

Bermingham, N. A., Hassan, B. A., Price, S. D., Vollrath, M. A., Ben-Arie, N., Eatock, R. A., Bellen, H. J., Lysakowski, A., and Zoghbi, H. Y. (1999). Math1: an essential gene for the generation of inner ear hair cells. Science *284*, 1837-1841.

Bitner-Glindzicz, M., Lindley, K. J., Rutland, P., Blaydon, D., Smith, V. V., Milla, P. J., Hussain, K., Furth-Lavi, J., Cosgrove, K. E., Shepherd, R. M., et al. (2000). A recessive contiguous gene deletion causing infantile hyperinsulinism, enteropathy and deafness identifies the Usher type 1C gene. Nat Genet *26*, 56-60.

Bixby, J. L., and Jhabvala, P. (1993). Tyrosine phosphorylation in early embryonic growth cones. J Neurosci *13*, 3421-3432.

Blount, P. (2003). Molecular mechanisms of mechanosensation: big lessons from small cells. Neuron *37*, 731-734.

Boeda, B., El-Amraoui, A., Bahloul, A., Goodyear, R., Daviet, L., Blanchard, S., Perfettini, I., Fath, K. R., Shorte, S., Reiners, J., et al. (2002). Myosin VIIa, harmonin and cadherin 23, three Usher I gene products that cooperate to shape the sensory hair cell bundle. Embo J *21*, 6689-6699.

Boggon, T. J., Murray, J., Chappuis-Flament, S., Wong, E., Gumbiner, B. M., and Shapiro, L. (2002). C-cadherin ectodomain structure and implications for cell adhesion mechanisms. Science *296*, 1308-1313.

Bolz, H., von Brederlow, B., Ramirez, A., Bryda, E. C., Kutsche, K., Nothwang, H. G., Seeliger, M., del, C. S. C. M., Vila, M. C., Molina, O. P., et al. (2001). Mutation of CDH23, encoding a new member of the cadherin gene family, causes Usher syndrome type 1D. Nat Genet *27*, 108-112.

Bork, J. M., Peters, L. M., Riazuddin, S., Bernstein, S. L., Ahmed, Z. M., Ness, S. L., Polomeno, R., Ramesh, A., Schloss, M., Srisailpathy, C. R., et al. (2001). Usher syndrome 1D and nonsyndromic autosomal recessive deafness DFNB12 are caused by allelic mutations of the novel cadherin-like gene CDH23. Am J Hum Genet *68*, 26-37.

Bose, A., Guilherme, A., Robida, S. I., Nicoloro, S. M., Zhou, Q. L., Jiang, Z. Y., Pomerleau, D. P., and Czech, M. P. (2002). Glucose transporter recycling in response to insulin is facilitated by myosin Myo1c. Nature *420*, 821-824.

Bosher, S. K., and Warren, R. L. (1978). Very low calcium content of cochlear endolymph, an extracellular fluid. Nature *273*, 377-378.

Boughman, J. A., Vernon, M., and Shaver, K. A. (1983). Usher syndrome: definition and estimate of prevalence from two high-risk populations. J Chronic Dis *36*, 595-603.

Brakebusch, C., and Fassler, R. (2003). The integrin-actin connection, an eternal love affair. Embo J *22*, 2324-2333.

Bray, S. (1998). Notch signalling in Drosophila: three ways to use a pathway. Semin Cell Dev Biol *9*, 591-597.

Brigande, J. V., Kiernan, A. E., Gao, X., Iten, L. E., and Fekete, D. M. (2000). Molecular genetics of pattern formation in the inner ear: do compartment boundaries play a role? Proc Natl Acad Sci U S A *97*, 11700-11706.

Brownell, W. E., Bader, C. R., Bertrand, D., and de Ribaupierre, Y. (1985). Evoked mechanical responses of isolated cochlear outer hair cells. Science *227*, 194-196.

Bryant, J., Goodyear, R. J., and Richardson, G. P. (2002). Sensory organ development in the inner ear: molecular and cellular mechanisms. Br Med Bull *63*, 39-57.

Buratovich, M. A., and Bryant, P. J. (1997). Enhancement of overgrowth by gene interactions in lethal(2)giant discs imaginal discs from Drosophila melanogaster. Genetics *147*, 657-670.

Burnside, B. (1978). Thin (actin) and thick (myosinlike) filaments in cone contraction in the teleost retina. J Cell Biol *78*, 227-246.

Burnside, B. (2001). Light and circadian regulation of retinomotor movement. Prog Brain Res *131*, 477-485.

Cantos, R., Cole, L. K., Acampora, D., Simeone, A., and Wu, D. K. (2000). Patterning of the mammalian cochlea. Proc Natl Acad Sci U S A *97*, 11707-11713.

Chaitin, M. H., Schneider, B. G., Hall, M. O., and Papermaster, D. S. (1984). Actin in the photoreceptor connecting cilium: immunocytochemical localization to the site of outer segment disk formation. J Cell Biol *99*, 239-247.

Chappuis-Flament, S., Wong, E., Hicks, L. D., Kay, C. M., and Gumbiner, B. M. (2001). Multiple cadherin extracellular repeats mediate homophilic binding and adhesion. J Cell Biol *154*, 231-243.

Chen, B., Li, A., Wang, D., Wang, M., Zheng, L., and Bartles, J. R. (1999). Espin contains an additional actin-binding site in its N terminus and is a major actin-bundling protein of the Sertoli cell-spermatid ectoplasmic specialization junctional plaque. Mol Biol Cell *10*, 4327-4339.

Chen, C., and Okayama, H. (1987). High-efficiency transformation of mammalian cells by plasmid DNA. Mol Cell Biol *7*, 2745-2752.

Ciani, L., Patel, A., Allen, N. D., and ffrench-Constant, C. (2003). Mice lacking the giant protocadherin mFAT1 exhibit renal slit junction abnormalities and a partially penetrant cyclopia and anophthalmia phenotype. Mol Cell Biol *23*, 3575-3582.

Clapham, D. (2003). TRP channels as cellular sensors. Nature *426*, 517-524.

Clark, H. F., Brentrup, D., Schneitz, K., Bieber, A., Goodman, C., and Noll, M. (1995). Dachsous encodes a member of the cadherin superfamily that controls imaginal disc morphogenesis in Drosophila. Genes Dev *9*, 1530-1542.

Corey, D. (2003). Sensory transduction in the ear. J Cell Sci *116*, 1-3.

Corey, D. P., and Hudspeth, A. J. (1983a). Kinetics of the receptor current in bullfrog saccular hair cells. J Neurosci *3*, 962-976.

Corey, D. P., and Hudspeth, A. J. (1983b). Kinetics of the receptor current in bullfrog saccular hair cells. J Neurosci *3*, 962-976.

Corwin, J. T., and Warchol, M. E. (1991). Auditory hair cells: structure, function, development, and regeneration. Annu Rev Neurosci *14*, 301-333.

Cosgrove, D., Samuelson, G., Meehan, D. T., Miller, C., McGee, J., Walsh, E. J., and Siegel, M. (1998). Ultrastructural, physiological, and molecular defects in the inner ear of a gene-knockout mouse model for autosomal Alport syndrome. Hear Res *121*, 84-98.

Cuppen, E., Gerrits, H., Pepers, B., Wieringa, B., and Hendriks, W. (1998). PDZ motifs in PTP-BL and RIL bind to internal protein segments in the LIM domain protein RIL. Mol Biol Cell *9*, 671-683.

Curtin, J. A., Quint, E., Tsipouri, V., Arkell, R. M., Cattanach, B., Copp, A. J., Henderson, D. J., Spurr, N., Stanier, P., Fisher, E. M., et al. (2003). Mutation of Celsr1 disrupts planar polarity of inner ear hair cells and causes severe neural tube defects in the mouse. Curr Biol *13*, 1129-1133.

Cyr, J. L., Dumont, R. A., and Gillespie, P. G. (2002). Myosin-1c interacts with hair-cell receptors through its calmodulin-binding IQ domains. J Neurosci *22*, 2487-2495.

D'Arcangelo, G., Homayouni, R., Keshvara, L., Rice, D. S., Sheldon, M., and Curran, T. (1999). Reelin is a ligand for lipoprotein receptors. Neuron *24*, 471-479.

Dabdoub, A., Donohue, M. J., Brennan, A., Wolf, V., Montcouquiol, M., Sassoon, D. A., Hseih, J. C., Rubin, J. S., Salinas, P. C., and Kelley, M. W. (2003). Wnt signaling mediates reorientation of outer hair cell stereociliary bundles in the mammalian cochlea. Development *130*, 2375-2384.

Dallos, P. (1996). Overview: Cochlear Neurobiology (New York, Springer).

Davenport, S., and Omenn, G. (1977). The Heterogeneity of Usher Syndrome. Paper presented at: Int. Conf. Birth Defects (Montreal).

Davis, R. R., Kozel, P., and Erway, L. C. (2003). Genetic influences in individual susceptibility to noise: a review. Noise Health *5*, 19-28.

Davis, R. R., Newlander, J. K., Ling, X., Cortopassi, G. A., Krieg, E. F., and Erway, L. C. (2001). Genetic basis for susceptibility to noise-induced hearing loss in mice. Hear Res *155*, 82-90.

Denk, W., Holt, J. R., Shepherd, G. M., and Corey, D. P. (1995). Calcium imaging of single stereocilia in hair cells: localization of transduction channels at both ends of tip links. Neuron *15*, 1311-1321.

Denman-Johnson, K., and Forge, A. (1999). Establishment of hair bundle polarity and orientation in the developing vestibular system of the mouse. J Neurocytol *28*, 821-835.

Dhouailly, D., Xu, C., Manabe, M., Schermer, A., and Sun, T. T. (1989). Expression of hair-related keratins in a soft epithelium: subpopulations of human and mouse dorsal tongue keratinocytes express keratin markers for hair-, skin- and esophageal-types of differentiation. Exp Cell Res *181*, 141-158.

Di Palma, F., Holme, R. H., Bryda, E. C., Belyantseva, I. A., Pellegrino, R., Kachar, B., Steel, K. P., and Noben-Trauth, K. (2001a). Mutations in Cdh23, encoding a new type of cadherin, cause stereocilia disorganization in waltzer, the mouse model for Usher syndrome type 1D. Nat Genet *27*, 103-107.

Di Palma, F., Holme, R. H., Bryda, E. C., Belyantseva, I. A., Pellegrino, R., Kachar, B., Steel, K. P., and Noben-Trauth, K. (2001b). Mutations in Cdh23, encoding a new type of cadherin, cause stereocilia disorganization in waltzer, the mouse model for Usher syndrome type 1D. Nat Genet *27*, 103-107.

Di Palma, F., Pellegrino, R., and Noben-Trauth, K. (2001c). Genomic structure, alternative splice forms and normal and mutant alleles of cadherin 23 (Cdh23). Gene *281*, 31-41.

Ding, J. P., Salvi, R. J., and Sachs, F. (1991). Stretch-activated ion channels in guinea pig outer hair cells. Hear Res *56*, 19-28.

Dose, A. C., Hillman, D. W., Wong, C., Sohlberg, L., Lin-Jones, J., and Burnside, B. (2003). Myo3A, one of two class III myosin genes expressed in vertebrate retina, is localized to the calycal processes of rod and cone photoreceptors and is expressed in the sacculus. Mol Biol Cell *14*, 1058-1073.

Drenckhahn, D., Engel, K., Hofer, D., Merte, C., Tilney, L., and Tilney, M. (1991). Three different actin filament assemblies occur in every hair cell: each contains a specific actin crosslinking protein. J Cell Biol *112*, 641-651.

Duncan, R. K., Dyce, O. H., and Saunders, J. C. (1998). Low calcium abolishes tip links and alters relative stereocilia motion in chick cochlear hair cells. Hear Res *124*, 69-77.

Eaton, S. (1997). Planar polarization of Drosophila and vertebrate epithelia. Curr Opin Cell Biol *9*, 860-866.

Eddison, M., Le Roux, I., and Lewis, J. (2000). Notch signaling in the development of the inner ear: lessons from Drosophila. Proc Natl Acad Sci U S A *97*, 11692-11699.

el-Amraoui, A., Sahly, I., Picaud, S., Sahel, J., Abitbol, M., and Petit, C. (1996). Human Usher 1B/mouse shaker-1: the retinal phenotype discrepancy explained by the presence/absence of myosin VIIA in the photoreceptor cells. Hum Mol Genet *5*, 1171-1178.

Erkman, L., McEvilly, R. J., Luo, L., Ryan, A. K., Hooshmand, F., O'Connell, S. M., Keithley, E. M., Rapaport, D. H., Ryan, A. F., and Rosenfeld, M. G. (1996). Role of transcription factors Brn-3.1 and Brn-3.2 in auditory and visual system development. Nature *381*, 603-606.

Ernest, S., Rauch, G. J., Haffter, P., Geisler, R., Petit, C., and Nicolson, T. (2000). Mariner is defective in myosin VIIA: a zebrafish model for human hereditary deafness. Hum Mol Genet *9*, 2189-2196.

Evans, E., Berk, D., and Leung, A. (1991). Detachment of agglutinin-bonded red blood cells. I. Forces to rupture molecular-point attachments. Biophys J *59*, 838-848.

Fanning, A. S., and Anderson, J. M. (1999). Protein modules as organizers of membrane structure. Curr Opin Cell Biol *11*, 432-439.

Fekete, D. M., Muthukumar, S., and Karagogeos, D. (1998). Hair cells and supporting cells share a common progenitor in the avian inner ear. J Neurosci *18*, 7811-7821.

Fekete, D. M., and Wu, D. K. (2002). Revisiting cell fate specification in the inner ear. Curr Opin Neurobiol *12*, 35-42.

Fetter, R. D., and Corless, J. M. (1987). Morphological components associated with frog cone outer segment disc margins. Invest Ophthalmol Vis Sci *28*, 646-657.

Flock, A., Flock, B., and Murray, E. (1977). Studies on the sensory hairs of receptor cells in the inner ear. Acta Otolaryngol *83*, 85-91.

Frank, M., and Kemler, R. (2002). Protocadherins. Curr Opin Cell Biol *14*, 557-562.

Friedman, T. B., Sellers, J. R., and Avraham, K. B. (1999). Unconventional myosins and the genetics of hearing loss. Am J Med Genet *89*, 147-157.

Fritzsch, B., Tessarollo, L., Coppola, E., and Reichardt, L. F. (2004). Neurotrophins in the ear: their roles in sensory neuron survival and fiber guidance. Prog Brain Res *146*, 265-278.

Furness, D. N., and Hackney, C. M. (1985). Cross-links between stereocilia in the guinea pig cochlea. Hear Res *18*, 177-188.

Furness, D. N., Karkanevatos, A., West, B., and Hackney, C. M. (2002). An immunogold investigation of the distribution of calmodulin in the apex of cochlear hair cells. Hear Res *173*, 10-20.

Garcia, J. A., Yee, A. G., Gillespie, P. G., and Corey, D. P. (1998). Localization of myosin-Ibeta near both ends of tip links in frog saccular hair cells. J Neurosci *18*, 8637-8647.

Geleoc, G. S., and Holt, J. R. (2003). Developmental acquisition of sensory transduction in hair cells of the mouse inner ear. Nat Neurosci *6*, 1019-1020.

Giancotti, F. G., and Ruoslahti, E. (1999). Integrin signaling. Science *285*, 1028-1032.

Gibson, F., Walsh, J., Mburu, P., Varela, A., Brown, K. A., Antonio, M., Beisel, K. W., Steel, K. P., and Brown, S. D. (1995). A type VII myosin encoded by the mouse deafness gene shaker-1. Nature *374*, 62-64.

Gietz, R. D., and Woods, R. A. (2002). Screening for protein-protein interactions in the yeast two-hybrid system. Methods Mol Biol *185*, 471-486.

Gillespie, P. G., and Corey, D. P. (1997). Myosin and adaptation by hair cells. Neuron *19*, 955-958.

Gillespie, P. G., and Cyr, J. L. (2002). Calmodulin binding to recombinant myosin-1c and myosin-1c IQ peptides. BMC Biochem *3*, 31.

Gillespie, P. G., and Walker, R. G. (2001). Molecular basis of mechanosensory transduction. Nature *413*, 194-202.

Goldberg, M., Peshkovsky, C., Shifteh, A., and Al-Awqati, Q. (2000). mu-Protocadherin, a novel developmentally regulated protocadherin with mucin-like domains. J Biol Chem *275*, 24622-24629.

Goodyear, R., and Richardson, G. (1999). The ankle-link antigen: an epitope sensitive to calcium chelation associated with the hair-cell surface and the calycal processes of photoreceptors. J Neurosci *19*, 3761-3772.

Goodyear, R. J., Kwan, T., Oh, S. H., Raphael, Y., and Richardson, G. P. (2001). The cell adhesion molecule BEN defines a prosensory patch in the developing avian otocyst. J Comp Neurol *434*, 275-288.

Goodyear, R. J., Legan, P. K., Wright, M. B., Marcotti, W., Oganesian, A., Coats, S. A., Booth, C. J., Kros, C. J., Seifert, R. A., Bowen-Pope, D. F., and Richardson, G. P. (2003). A receptor-like inositol lipid phosphatase is required for the maturation of developing cochlear hair bundles. J Neurosci *23*, 9208-9219.

Goodyear, R. J., and Richardson, G. P. (2003). A novel antigen sensitive to calcium chelation that is associated with the tip links and kinocilial links of sensory hair bundles. J Neurosci *23*, 4878-4887.

Gorlin, R. (1995). Hereditary Hearing Loss and Its Syndromes (New York/Oxford, Oxford Univ. Press).

Grant, S. G., O'Dell, T. J., Karl, K. A., Stein, P. L., Soriano, P., and Kandel, E. R. (1992). Impaired long-term potentiation, spatial learning, and hippocampal development in fyn mutant mice. Science *258*, 1903-1910.

Grondahl, J. (1987). Estimation of prognosis and prevalence of retinitis pigmentosa and Usher syndrome in Norway. Clin Genet *31*, 255-264.

Grosse, R., Copeland, J. W., Newsome, T. P., Way, M., and Treisman, R. (2003). A role for VASP in RhoA-Diaphanous signalling to actin dynamics and SRF activity. Embo J *22*, 3050-3061.

Guy, P. M., Kenny, D. A., and Gill, G. N. (1999). The PDZ domain of the LIM protein enigma binds to beta-tropomyosin. Mol Biol Cell *10*, 1973-1984.

Hackney, C. M., and Furness, D. N. (1995). Mechanotransduction in vertebrate hair cells: structure and function of the stereociliary bundle. Am J Physiol *268*, C1-13.

Hackney, C. M., Furness, D. N., Benos, D. J., Woodley, J. F., and Barratt, J. (1992). Putative immunolocalization of the mechanoelectrical transduction channels in mammalian cochlear hair cells. Proc R Soc Lond B Biol Sci *248*, 215-221.

Hale, I. L., Fisher, S. K., and Matsumoto, B. (1996). The actin network in the ciliary stalk of photoreceptors functions in the generation of new outer segment discs. J Comp Neurol *376*, 128-142.

Hallgren, B. (1959). Retinitis pigmentosa combined with congenital deafness; with vestibulo-cerebellar ataxia and mental abnormality in a proportion of cases: A clinical and genetico-statistical study. Acta Psychiatr Scand *34(Suppl 138)*, 1-101.

Harlow, E., and Lane, D. (1999). Using antibodies: a laboratory manual (Cold Spring Harbor, NY, Cold Spring Harbor Laboratory Press).

Harris, B. Z., Hillier, B. J., and Lim, W. A. (2001). Energetic determinants of internal motif recognition by PDZ domains. Biochemistry *40*, 5921-5930.

Harris, B. Z., and Lim, W. A. (2001). Mechanism and role of PDZ domains in signaling complex assembly. J Cell Sci *114*, 3219-3231.

Hasson, T., Gillespie, P. G., Garcia, J. A., MacDonald, R. B., Zhao, Y., Yee, A. G., Mooseker, M. S., and Corey, D. P. (1997). Unconventional myosins in inner-ear sensory epithelia. J Cell Biol *137*, 1287-1307.

Hemler, M. (1999). Integrins (Oxford, Sambrook and Tooze at Oxford University Press).

Hillier, B. J., Christopherson, K. S., Prehoda, K. E., Bredt, D. S., and Lim, W. A. (1999). Unexpected modes of PDZ domain scaffolding revealed by structure of nNOS-syntrophin complex. Science *284*, 812-815.

Hirokawa, N., and Tilney, L. G. (1982). Interactions between actin filaments and between actin filaments and membranes in quick-frozen and deeply etched hair cells of the chick ear. J Cell Biol *95*, 249-261.

Hofer, D., and Drenckhahn, D. (1993). Molecular heterogeneity of the actin filament cytoskeleton associated with microvilli of photoreceptors, Muller's glial cells and pigment epithelial cells of the retina. Histochemistry *99*, 29-35.

Hollyday, M., McMahon, J. A., and McMahon, A. P. (1995). Wnt expression patterns in chick embryo nervous system. Mech Dev *52*, 9-25.

Holme, R. H., and Steel, K. P. (2002). Stereocilia defects in waltzer (Cdh23), shaker1 (Myo7a) and double waltzer/shaker1 mutant mice. Hear Res *169*, 13-23.

Holme, R. H., and Steel, K. P. (2004). Progressive Hearing Loss and Increased Susceptibility to Noise-Induced Hearing Loss in Mice Carrying a Cdh23 but not a Myo7a Mutation. J Assoc Res Otolaryngol *5*, 66-79.

Holt, J. R., and Corey, D. P. (2000). Two mechanisms for transducer adaptation in vertebrate hair cells. Proc Natl Acad Sci U S A *97*, 11730-11735.

Holt, J. R., Gillespie, S. K., Provance, D. W., Shah, K., Shokat, K. M., Corey, D. P., Mercer, J. A., and Gillespie, P. G. (2002). A chemical-genetic strategy implicates myosin-1c in adaptation by hair cells. Cell *108*, 371-381.

Holton, T., and Hudspeth, A. J. (1986). The transduction channel of hair cells from the bull-frog characterized by noise analysis. J Physiol *375*, 195-227.

Hone, S. W., and Smith, R. J. (2001). Genetics of hearing impairment. Semin Neonatol *6*, 531-541.

Hope, C. I., Bundey, S., Proops, D., and Fielder, A. R. (1997). Usher syndrome in the city of Birmingham--prevalence and clinical classification. Br J Ophthalmol *81*, 46-53.

Huber, A. (2001). Scaffolding proteins organize multimolecular protein complexes for sensory signal transduction. Eur J Neurosci *14*, 769-776.

Hudspeth, A. J. (1982). Extracellular current flow and the site of transduction by vertebrate hair cells. J Neurosci *2*, 1-10.

Hudspeth, A. J. (1992). Hair-bundle mechanics and a model for mechanoelectrical transduction by hair cells. Soc Gen Physiol Ser *47*, 357-370.

Hudspeth, A. J. (1997). How hearing happens. Neuron *19*, 947-950.

Hudspeth, A. J., and Gillespie, P. G. (1994). Pulling springs to tune transduction: adaptation by hair cells. Neuron *12*, 1-9.

Hudspeth, A. J., and Jacobs, R. (1979). Stereocilia mediate transduction in vertebrate hair cells (auditory system/cilium/vestibular system). Proc Natl Acad Sci U S A *76*, 1506-1509.

Hunter, D. G., Fishman, G. A., Mehta, R. S., and Kretzer, F. L. (1986). Abnormal sperm and photoreceptor axonemes in Usher's syndrome. Arch Ophthalmol *104*, 385-389.

Hyafil, F., Babinet, C., and Jacob, F. (1981). Cell-cell interactions in early embryogenesis: a molecular approach to the role of calcium. Cell *26*, 447-454.

Inoue, T., Yaoita, E., Kurihara, H., Shimizu, F., Sakai, T., Kobayashi, T., Ohshiro, K., Kawachi, H., Okada, H., Suzuki, H., et al. (2001). FAT is a component of glomerular slit diaphragms. Kidney Int *59*, 1003-1012.

Jaramillo, F., and Hudspeth, A. J. (1991). Localization of the hair cell's transduction channels at the hair bundle's top by iontophoretic application of a channel blocker. Neuron *7*, 409-420.

Jarman, A. P., Grau, Y., Jan, L. Y., and Jan, Y. N. (1993). atonal is a proneural gene that directs chordotonal organ formation in the Drosophila peripheral nervous system. Cell *73*, 1307-1321.

Jasoni, C., Hendrickson, A., and Roelink, H. (1999). Analysis of chicken Wnt-13 expression demonstrates coincidence with cell division in the developing eye and is consistent with a role in induction. Dev Dyn *215*, 215-224.

Jorgensen, F., and Ohmori, H. (1988). Amiloride blocks the mechano-electrical transduction channel of hair cells of the chick. J Physiol *403*, 577-588.

Kachar, B., Parakkal, M., Kurc, M., Zhao, Y., and Gillespie, P. G. (2000). High-resolution structure of hair-cell tip links. Proc Natl Acad Sci U S A *97*, 13336-13341.

Kashtan, C. E. (2000). Alport syndrome: abnormalities of type IV collagen genes and proteins. Ren Fail *22*, 737-749.

Katori, Y., Hackney, C. M., and Furness, D. N. (1996). Immunoreactivity of sensory hair bundles of the guinea-pig cochlea to antibodies against elastin and keratan sulphate. Cell Tissue Res *284*, 473-479.

Keats, B. J., and Corey, D. P. (1999). The usher syndromes. Am J Med Genet *89*, 158-166.

Keil, T. A. (1997). Functional morphology of insect mechanoreceptors. Microsc Res Tech *39*, 506-531.

Keithley, E. M., Erkman, L., Bennett, T., Lou, L., and Ryan, A. F. (1999). Effects of a hair cell transcription factor, Brn-3.1, gene deletion on homozygous and heterozygous mouse cochleas in adulthood and aging. Hear Res *134*, 71-76.

Kikkawa, Y., Shitara, H., Wakana, S., Kohara, Y., Takada, T., Okamoto, M., Taya, C., Kamiya, K., Yoshikawa, Y., Tokano, H., et al. (2003). Mutations in a new scaffold protein Sans cause deafness in Jackson shaker mice. Hum Mol Genet *12*, 453-461.

Kim, E., Niethammer, M., Rothschild, A., Jan, Y. N., and Sheng, M. (1995). Clustering of Shaker-type K+ channels by interaction with a family of membrane-associated guanylate kinases. Nature *378*, 85-88.

Kobayashi, I., Imamura, K., Kubota, M., Ishikawa, S., Yamada, M., Tonoki, H., Okano, M., Storch, W. B., Moriuchi, T., Sakiyama, Y., and Kobayashi, K. (1999). Identification of an autoimmune enteropathy-related 75-kilodalton antigen. Gastroenterology *117*, 823-830.

Kohmura, N., Senzaki, K., Hamada, S., Kai, N., Yasuda, R., Watanabe, M., Ishii, H., Yasuda, M., Mishina, M., and Yagi, T. (1998). Diversity revealed by a novel family of cadherins expressed in neurons at a synaptic complex. Neuron *20*, 1137-1151.

Koprowski, P., and Kubalski, A. (2001). Bacterial ion channels and their eukaryotic homologues. Bioessays *23*, 1148-1158.

Kornau, H. C., Schenker, L. T., Kennedy, M. B., and Seeburg, P. H. (1995). Domain interaction between NMDA receptor subunits and the postsynaptic density protein PSD-95. Science *269*, 1737-1740.

Korschen, H. G., Beyermann, M., Muller, F., Heck, M., Vantler, M., Koch, K. W., Kellner, R., Wolfrum, U., Bode, C., Hofmann, K. P., and Kaupp, U. B. (1999). Interaction of glutamic-acid-rich proteins with the cGMP signalling pathway in rod photoreceptors. Nature *400*, 761-766.

Kros, C. J., Marcotti, W., van Netten, S. M., Self, T. J., Libby, R. T., Brown, S. D., Richardson, G. P., and Steel, K. P. (2002). Reduced climbing and increased slipping adaptation in cochlear hair cells of mice with Myo7a mutations. Nat Neurosci *5*, 41-47.

Kros, C. J., Rusch, A., and Richardson, G. P. (1992). Mechano-electrical transducer currents in hair cells of the cultured neonatal mouse cochlea. Proc R Soc Lond B Biol Sci *249*, 185-193.

Kudoh, S., Akazawa, H., Takano, H., Zou, Y., Toko, H., Nagai, T., and Komuro, I. (2003). Stretch-modulation of second messengers: effects on cardiomyocyte ion transport. Prog Biophys Mol Biol *82*, 57-66.

Kussel-Andermann, P., El-Amraoui, A., Safieddine, S., Nouaille, S., Perfettini, I., Lecuit, M., Cossart, P., Wolfrum, U., and Petit, C. (2000). Vezatin, a novel transmembrane protein, bridges myosin VIIA to the cadherin-catenins complex. Embo J *19*, 6020-6029.

Lanford, P. J., Lan, Y., Jiang, R., Lindsell, C., Weinmaster, G., Gridley, T., and Kelley, M. W. (1999). Notch signalling pathway mediates hair cell development in mammalian cochlea. Nat Genet *21*, 289-292.

Lang, H., and Fekete, D. M. (2001). Lineage analysis in the chicken inner ear shows differences in clonal dispersion for epithelial, neuronal, and mesenchymal cells. Dev Biol *234*, 120-137.

Legan, P. K., Lukashkina, V. A., Goodyear, R. J., Kossi, M., Russell, I. J., and Richardson, G. P. (2000). A targeted deletion in alpha-tectorin reveals that the tectorial membrane is required for the gain and timing of cochlear feedback. Neuron *28*, 273-285.

Les Erickson, F., Corsa, A. C., Dose, A. C., and Burnside, B. (2003). Localization of a class III myosin to filopodia tips in transfected HeLa cells requires an actin-binding site in its tail domain. Mol Biol Cell *14*, 4173-4180.

Lewis, J., and Davies, A. (2002). Planar cell polarity in the inner ear: how do hair cells acquire their oriented structure? J Neurobiol *53*, 190-201.

Li, H. S., Porter, J. A., and Montell, C. (1998). Requirement for the NINAC kinase/myosin for stable termination of the visual cascade. J Neurosci *18*, 9601-9606.

Libby, R. T., Kitamoto, J., Holme, R. H., Williams, D. S., and Steel, K. P. (2003). Cdh23 mutations in the mouse are associated with retinal dysfunction but not retinal degeneration. Exp Eye Res *77*, 731-739.

Libby, R. T., and Steel, K. P. (2001). Electroretinographic anomalies in mice with mutations in Myo7a, the gene involved in human Usher syndrome type 1B. Invest Ophthalmol Vis Sci *42*, 770-778.

Liberman, M. C., Gao, J., He, D. Z., Wu, X., Jia, S., and Zuo, J. (2002). Prestin is required for electromotility of the outer hair cell and for the cochlear amplifier. Nature *419*, 300-304.

Lingueglia, E., Voilley, N., Waldmann, R., Lazdunski, M., and Barbry, P. (1993). Expression cloning of an epithelial amiloride-sensitive Na+ channel. A new channel type with homologies to Caenorhabditis elegans degenerins. FEBS Lett *318*, 95-99.

Littlewood Evans, A., and Muller, U. (2000). Stereocilia defects in the sensory hair cells of the inner ear in mice deficient in integrin alpha8beta1. Nat Genet *24*, 424-428.

Liu, X., Ondek, B., and Williams, D. S. (1998). Mutant myosin VIIa causes defective melanosome distribution in the RPE of shaker-1 mice. Nat Genet *19*, 117-118.

Liu, X., Udovichenko, I. P., Brown, S. D., Steel, K. P., and Williams, D. S. (1999). Myosin VIIa participates in opsin transport through the photoreceptor cilium. J Neurosci *19*, 6267-6274.

Liu, X., Vansant, G., Udovichenko, I. P., Wolfrum, U., and Williams, D. S. (1997). Myosin VIIa, the product of the Usher 1B syndrome gene, is concentrated in the connecting cilia of photoreceptor cells. Cell Motil Cytoskeleton *37*, 240-252.

Liu, X. Z., Ouyang, X. M., Xia, X. J., Zheng, J., Pandya, A., Li, F., Du, L. L., Welch, K. O., Petit, C., Smith, R. J., et al. (2003). Prestin, a cochlear motor protein, is defective in non-syndromic hearing loss. Hum Mol Genet *12*, 1155-1162.

Lumpkin, E. A., and Hudspeth, A. J. (1995). Detection of Ca2+ entry through mechanosensitive channels localizes the site of mechanoelectrical transduction in hair cells. Proc Natl Acad Sci U S A *92*, 10297-10301.

Lumpkin, E. A., Marquis, R. E., and Hudspeth, A. J. (1997). The selectivity of the hair cell's mechanoelectrical-transduction channel promotes Ca2+ flux at low Ca2+ concentrations. Proc Natl Acad Sci U S A *94*, 10997-11002.

Lynch, E. D., Lee, M. K., Morrow, J. E., Welcsh, P. L., Leon, P. E., and King, M. C. (1997). Nonsyndromic deafness DFNA1 associated with mutation of a human homolog of the Drosophila gene diaphanous. Science *278*, 1315-1318.

Lynch, M. H., O'Guin, W. M., Hardy, C., Mak, L., and Sun, T. T. (1986). Acidic and basic hair/nail ("hard") keratins: their colocalization in upper cortical and cuticle cells of the human hair follicle and their relationship to "soft" keratins. J Cell Biol *103*, 2593-2606.

Mahoney, P. A., Weber, U., Onofrechuk, P., Biessmann, H., Bryant, P. J., and Goodman, C. S. (1991). The fat tumor suppressor gene in Drosophila encodes a novel member of the cadherin gene superfamily. Cell *67*, 853-868.

Marfatia, S. M., Morais-Cabral, J. H., Kim, A. C., Byron, O., and Chishti, A. H. (1997). The PDZ domain of human erythrocyte p55 mediates its binding to the cytoplasmic carboxyl terminus of glycophorin C. Analysis of the binding interface by in vitro mutagenesis. J Biol Chem *272*, 24191-24197.

Martinac, B., Adler, J., and Kung, C. (1990). Mechanosensitive ion channels of E. coli activated by amphipaths. Nature *348*, 261-263.

Mburu, P., Mustapha, M., Varela, A., Weil, D., El-Amraoui, A., Holme, R. H., Rump, A., Hardisty, R. E., Blanchard, S., Coimbra, R. S., et al. (2003). Defects in whirlin, a PDZ domain molecule involved in stereocilia elongation, cause deafness in the whirler mouse and families with DFNB31. Nat Genet *34*, 421-428.

Mermall, V., Post, P. L., and Mooseker, M. S. (1998). Unconventional myosins in cell movement, membrane traffic, and signal transduction. Science *279*, 527-533.

Metcalf, A. B. (1998). Immunolocalization of myosin Ibeta in the hair cell's hair bundle. Cell Motil Cytoskeleton *39*, 159-165.

Meyer, J., Furness, D. N., Zenner, H. P., Hackney, C. M., and Gummer, A. W. (1998). Evidence for opening of hair-cell transducer channels after tip-link loss. J Neurosci *18*, 6748-6756.

Meyers, J. R., MacDonald, R. B., Duggan, A., Lenzi, D., Standaert, D. G., Corwin, J. T., and Corey, D. P. (2003). Lighting up the senses: FM1-43 loading of sensory cells through nonselective ion channels. J Neurosci *23*, 4054-4065.

Moloney, D. J., Panin, V. M., Johnston, S. H., Chen, J., Shao, L., Wilson, R., Wang, Y., Stanley, P., Irvine, K. D., Haltiwanger, R. S., and Vogt, T. F. (2000). Fringe is a glycosyltransferase that modifies Notch. Nature *406*, 369-375.

Montcouquiol, M., Rachel, R. A., Lanford, P. J., Copeland, N. G., Jenkins, N. A., and Kelley, M. W. (2003). Identification of Vangl2 and Scrb1 as planar polarity genes in mammals. Nature *423*, 173-177.

Montell, C. (1998). TRP trapped in fly signaling web. Curr Opin Neurobiol *8*, 389-397.

Montell, C. (1999). Visual transduction in Drosophila. Annu Rev Cell Dev Biol *15*, 231-268.

Morrison, A., Hodgetts, C., Gossler, A., Hrabe de Angelis, M., and Lewis, J. (1999). Expression of Delta1 and Serrate1 (Jagged1) in the mouse inner ear. Mech Dev *84*, 169-172.

Muller, U., Bossy, B., Venstrom, K., and Reichardt, L. F. (1995). Integrin alpha 8 beta 1 promotes attachment, cell spreading, and neurite outgrowth on fibronectin. Mol Biol Cell *6*, 433-448.

Müller, U., and Evans, A. L. (2001). Mechanisms that regulate mechanosensory hair cell differentiation. Trends in Cell Biology *11*, 334-342.

Murphy-Erdosh, C., Yoshida, C. K., Paradies, N., and Reichardt, L. F. (1995). The cadherin-binding specificities of B-cadherin and LCAM. J Cell Biol *129*, 1379-1390.

Nagafuchi, A. (2001). Molecular architecture of adherens junctions. Curr Opin Cell Biol *13*, 600-603.

Nagafuchi, A., and Takeichi, M. (1988). Cell binding function of E-cadherin is regulated by the cytoplasmic domain. Embo J *7*, 3679-3684.

Nakano, K., Takaishi, K., Kodama, A., Mammoto, A., Shiozaki, H., Monden, M., and Takai, Y. (1999). Distinct actions and cooperative roles of ROCK and mDia in Rho small G protein-induced reorganization of the actin cytoskeleton in Madin-Darby canine kidney cells. Mol Biol Cell *10*, 2481-2491.

Neugebauer, D. C., and Thurm, U. (1986). Surface charges influence the distances between vestibular stereovilli. Naturwissenschaften *73*, 508-509.

Nicolson, T., Rusch, A., Friedrich, R. W., Granato, M., Ruppersberg, J. P., and Nusslein-Volhard, C. (1998). Genetic analysis of vertebrate sensory hair cell mechanosensation: the zebrafish circler mutants. Neuron *20*, 271-283.

Noben-Trauth, K., Zheng, Q. Y., and Johnson, K. R. (2003). Association of cadherin 23 with polygenic inheritance and genetic modification of sensorineural hearing loss. Nat Genet *35*, 21-23.

Nose, A., Nagafuchi, A., and Takeichi, M. (1987). Isolation of placental cadherin cDNA: identification of a novel gene family of cell-cell adhesion molecules. Embo J *6*, 3655-3661.

Nuutila, A. (1970). Dystrophia retinae pigmentosa--dysacusis syndrome (DRD): a study of the Usher- or Hallgren syndrome. J Genet Hum *18*, 57-88.

O'Guin, W. M., Sun, T. T., and Manabe, M. (1992). Interaction of trichohyalin with intermediate filaments: three immunologically defined stages of trichohyalin maturation. J Invest Dermatol *98*, 24-32.

Obata, S., Sago, H., Mori, N., Rochelle, J. M., Seldin, M. F., Davidson, M., St John, T., Taketani, S., and Suzuki, S. T. (1995). Protocadherin Pcdh2 shows properties similar to, but distinct from, those of classical cadherins. J Cell Sci *108 (Pt 12)*, 3765-3773.

Ohmori, H. (1988). Mechanical stimulation and Fura-2 fluorescence in the hair bundle of dissociated hair cells of the chick. J Physiol *399*, 115-137.

Osborne, M. P., and Comis, S. D. (1990). Action of elastase, collagenase and other enzymes upon linkages between stereocilia in the guinea-pig cochlea. Acta Otolaryngol *110*, 37-45.

Pagh-Roehl, K., Wang, E., and Burnside, B. (1992). Shortening of the calycal process actin cytoskeleton is correlated with myoid elongation in teleost rods. Exp Eye Res *55*, 735-746.

Palazzo, A. F., Eng, C. H., Schlaepfer, D. D., Marcantonio, E. E., and Gundersen, G. G. (2004). Localized stabilization of microtubules by integrin- and FAK-facilitated Rho signaling. Science *303*, 836-839.

Patel, A. J., Honore, E., Maingret, F., Lesage, F., Fink, M., Duprat, F., and Lazdunski, M. (1998). A mammalian two pore domain mechano-gated S-like K+ channel. Embo J *17*, 4283-4290.

Perozo, E., Cortes, D. M., Sompornpisut, P., Kloda, A., and Martinac, B. (2002). Open channel structure of MscL and the gating mechanism of mechanosensitive channels. Nature *418*, 942-948.

Petit, C. (2001). Usher syndrome: from genetics to pathogenesis. Annu Rev Genomics Hum Genet *2*, 271-297.

Peyrieras, N., Hyafil, F., Louvard, D., Ploegh, H. L., and Jacob, F. (1983). Uvomorulin: a nonintegral membrane protein of early mouse embryo. Proc Natl Acad Sci U S A *80*, 6274-6277.

Pickles, J. O., Comis, S. D., and Osborne, M. P. (1984). Cross-links between stereocilia in the guinea pig organ of Corti, and their possible relation to sensory transduction. Hear Res *15*, 103-112.

Pickles, J. O., von Perger, M., Rouse, G. W., and Brix, J. (1991). The development of links between stereocilia in hair cells of the chick basilar papilla. Hear Res *54*, 153-163.

Pirvola, U., and Ylikoski, J. (2003). Neurotrophic factors during inner ear development. Curr Top Dev Biol *57*, 207-223.

Porter, J. A., and Montell, C. (1993). Distinct roles of the Drosophila ninaC kinase and myosin domains revealed by systematic mutagenesis. J Cell Biol *122*, 601-612.

Porter, J. A., Yu, M., Doberstein, S. K., Pollard, T. D., and Montell, C. (1993). Dependence of calmodulin localization in the retina on the NINAC unconventional myosin. Science *262*, 1038-1042.

Pourquie, O., Corbel, C., Le Caer, J. P., Rossier, J., and Le Douarin, N. M. (1992). BEN, a surface glycoprotein of the immunoglobulin superfamily, is expressed in a variety of developing systems. Proc Natl Acad Sci U S A *89*, 5261-5265.

Prescott, E. D., and Julius, D. (2003). A modular PIP2 binding site as a determinant of capsaicin receptor sensitivity. Science *300*, 1284-1288.

Rana, M. W., and Taraszka, S. R. (1991). Monkey photoreceptor calycal processes and interphotoreceptor matrix as observed by scanning electron microscopy. Am J Anat *192*, 472-477.

Raphael, Y., Kobayashi, K. N., Dootz, G. A., Beyer, L. A., Dolan, D. F., and Burmeister, M. (2001). Severe vestibular and auditory impairment in three alleles of Ames waltzer (av) mice. Hear Res *151*, 237-249.

Rattner, A., Smallwood, P. M., Williams, J., Cooke, C., Savchenko, A., Lyubarsky, A., Pugh, E. N., and Nathans, J. (2001). A photoreceptor-specific cadherin is essential for the structural integrity of the outer segment and for photoreceptor survival. Neuron *32*, 775-786.

Reed, R. R. (2004). After the holy grail: establishing a molecular basis for Mammalian olfaction. Cell *116*, 329-336.

Reiners, J., Reidel, B., El-Amraoui, A., Boeda, B., Huber, I., Petit, C., and Wolfrum, U. (2003). Differential distribution of harmonin isoforms and their possible role in Usher-1 protein complexes in mammalian photoreceptor cells. Invest Ophthalmol Vis Sci *44*, 5006-5015.

Rice, F. L., Fundin, B. T., Arvidsson, J., Aldskogius, H., and Johansson, O. (1997). Comprehensive immunofluorescence and lectin binding analysis of vibrissal follicle sinus complex innervation in the mystacial pad of the rat. J Comp Neurol *385*, 149-184.

Richardson, G. P., Bartolami, S., and Russell, I. J. (1990). Identification of a 275-kD protein associated with the apical surfaces of sensory hair cells in the avian inner ear. J Cell Biol *110*, 1055-1066.

Riley, B. B., Chiang, M., Farmer, L., and Heck, R. (1999). The deltaA gene of zebrafish mediates lateral inhibition of hair cells in the inner ear and is regulated by pax2.1. Development *126*, 5669-5678.

Rodieck, R. (1988). The Primate Retina, Comparative Primate Biology. In Neurosciences (San Francisco), pp. 203-278.

Rohlich, P. (1975). The sensory cilium of retinal rods is analogous to the transitional zone of motile cilia. Cell Tissue Res *161*, 421-430.

Rosenberg, T., Haim, M., Hauch, A. M., and Parving, A. (1997). The prevalence of Usher syndrome and other retinal dystrophy-hearing impairment associations. Clin Genet *51*, 314-321.

Rubel, E. W., and Fritzsch, B. (2002). Auditory system development: primary auditory neurons and their targets. Annu Rev Neurosci *25*, 51-101.

Ruppert, C., Godel, J., Muller, R. T., Kroschewski, R., Reinhard, J., and Bahler, M. (1995). Localization of the rat myosin I molecules myr 1 and myr 2 and in vivo targeting of their tail domains. J Cell Sci *108 (Pt 12)*, 3775-3786.

Ruppert, C., Kroschewski, R., and Bahler, M. (1993). Identification, characterization and cloning of myr 1, a mammalian myosin-I. J Cell Biol *120*, 1393-1403.

Rusch, A., Kros, C. J., and Richardson, G. P. (1994). Block by amiloride and its derivatives of mechano-electrical transduction in outer hair cells of mouse cochlear cultures. J Physiol *474*, 75-86.

Sahly, I., El-Amraoui, A., Abitbol, M., Petit, C., and Dufier, J. L. (1997). Expression of myosin VIIA during mouse embryogenesis. Anat Embryol (Berl) *196*, 159-170.

Sambrook, J., and Russell, D. W. (2001). Molecular cloning: a laboratory manual (Cold Spring Harbor, NY, Cold Spring Harbor Laboratory Press).

Sano, K., Tanihara, H., Heimark, R. L., Obata, S., Davidson, M., St John, T., Taketani, S., and Suzuki, S. (1993). Protocadherins: a large family of cadherin-related molecules in central nervous system. Embo J *12*, 2249-2256.

Scanlan, M. J., Williamson, B., Jungbluth, A., Stockert, E., Arden, K. C., Viars, C. S., Gure, A. O., Gordan, J. D., Chen, Y. T., and Old, L. J. (1999). Isoforms of the human PDZ-73 protein exhibit differential tissue expression. Biochim Biophys Acta *1445*, 39-52.

Seeliger, M., Pfister, M., Gendo, K., Paasch, S., Apfelstedt-Sylla, E., Plinkert, P., Zenner, H. P., and Zrenner, E. (1999). Comparative study of visual, auditory, and olfactory function in Usher syndrome. Graefes Arch Clin Exp Ophthalmol *237*, 301-307.

Self, T., Mahony, M., Fleming, J., Walsh, J., Brown, S. D., and Steel, K. P. (1998). Shaker-1 mutations reveal roles for myosin VIIA in both development and function of cochlear hair cells. Development *125*, 557-566.

Self, T., Sobe, T., Copeland, N. G., Jenkins, N. A., Avraham, K. B., and Steel, K. P. (1999). Role of myosin VI in the differentiation of cochlear hair cells. Dev Biol *214*, 331-341.

Senzaki, K., Ogawa, M., and Yagi, T. (1999). Proteins of the CNR family are multiple receptors for Reelin. Cell *99*, 635-647.

Shapiro, L., and Colman, D. R. (1999). The diversity of cadherins and implications for a synaptic adhesive code in the CNS. Neuron *23*, 427-430.

Sheng, M. (2001). Molecular organization of the postsynaptic specialization. Proc Natl Acad Sci U S A *98*, 7058-7061.

Sheng, M., and Pak, D. T. (2000). Ligand-gated ion channel interactions with cytoskeletal and signaling proteins. Annu Rev Physiol *62*, 755-778.

Sheng, M., and Sala, C. (2001). PDZ domains and the organization of supramolecular complexes. Annu Rev Neurosci *24*, 1-29.

Shepherd, G. M., and Corey, D. P. (1992). Sensational science. Sensory Transduction: 45th Annual Symposium of the Society of General Physiologists, Marine Biological Laboratory, Woods Hole, MA, USA, September 5-8, 1991. New Biol *4*, 48-52.

Shima, Y., Copeland, N. G., Gilbert, D. J., Jenkins, N. A., Chisaka, O., Takeichi, M., and Uemura, T. (2002). Differential expression of the seven-pass transmembrane cadherin genes Celsr1-3 and distribution of the Celsr2 protein during mouse development. Dev Dyn *223*, 321-332.

Shotwell, S. L., Jacobs, R., and Hudspeth, A. J. (1981). Directional sensitivity of individual vertebrate hair cells to controlled deflection of their hair bundles. Ann N Y Acad Sci *374*, 1-10.

Sidi, S., Friedrich, R. W., and Nicolson, T. (2003). NompC TRP channel required for vertebrate sensory hair cell mechanotransduction. Science *301*, 96-99.

Siemens, J., Kazmierczak, P., Reynolds, A., Sticker, M., Littlewood-Evans, A., and Muller, U. (2002). The Usher syndrome proteins cadherin 23 and harmonin form a complex by means of PDZ-domain interactions. Proc Natl Acad Sci U S A *99*, 14946-14951.

Siemens, J., Littlewood Evans, A., Senften, M., and Muller, U. (2001). Genes, deafness, and balance disorders. Gene Funct and Dis *2*, 76-82.

Simmler, M. C., Cohen-Salmon, M., El-Amraoui, A., Guillaud, L., Benichou, J. C., Petit, C., and Panthier, J. J. (2000b). Targeted disruption of otog results in deafness and severe imbalance. Nat Genet *24*, 139-143.

Simmler, M. C., Zwaenepoel, I., Verpy, E., Guillaud, L., Elbaz, C., Petit, C., and Panthier, J. J. (2000a). Twister mutant mice are defective for otogelin, a component specific to inner ear acellular membranes. Mamm Genome *11*, 960-966.

Sivasankar, S., Brieher, W., Lavrik, N., Gumbiner, B., and Leckband, D. (1999). Direct molecular force measurements of multiple adhesive interactions between cadherin ectodomains. Proc Natl Acad Sci U S A *96*, 11820-11824.

Slepecky, N., and Chamberlain, S. C. (1985). Immunoelectron microscopic and immunofluorescent localization of cytoskeletal and muscle-like contractile proteins in inner ear sensory hair cells. Hear Res *20*, 245-260.

Slepecky, N. B. (1996). Structure of the mammalian cochlea (New York, Springer).

Slepecky, N. B., and Ulfendahl, M. (1992). Actin-binding and microtubule-associated proteins in the organ of Corti. Hear Res *57*, 201-215.

Sobkowicz, H. M., Slapnick, S. M., and August, B. K. (1995). The kinocilium of auditory hair cells and evidence for its morphogenetic role during the regeneration of stereocilia and cuticular plates. J Neurocytol *24*, 633-653.

Songyang, Z., Fanning, A. S., Fu, C., Xu, J., Marfatia, S. M., Chishti, A. H., Crompton, A., Chan, A. C., Anderson, J. M., and Cantley, L. C. (1997). Recognition of unique carboxyl-terminal motifs by distinct PDZ domains. Science *275*, 73-77.

Stark, M. R., Biggs, J. J., Schoenwolf, G. C., and Rao, M. S. (2000). Characterization of avian frizzled genes in cranial placode development. Mech Dev *93*, 195-200.

Steel, K. P., and Kros, C. J. (2001). A genetic approach to understanding auditory function. Nat Genet *27*, 143-149.

Steyger, P. S., Gillespie, P. G., and Baird, R. A. (1998). Myosin Ibeta is located at tip link anchors in vestibular hair bundles. J Neurosci *18*, 4603-4615.

Sukharev, S., and Corey, D. P. (2004). Mechanosensitive channels: multiplicity of families and gating paradigms. Sci STKE *2004*, re4.

Takeichi, M. (1990). Cadherins: a molecular family important in selective cell-cell adhesion. Annu Rev Biochem *59*, 237-252.

Takumida, M., and Bagger-Sjoback, D. (1991). Carbohydrates of the vestibular end organs. An ultrastructural study using gold-labeled lectins. ORL J Otorhinolaryngol Relat Spec *53*, 86-90.

Takumida, M., Harada, Y., Wersall, J., and Bagger-Sjoback, D. (1988a). The glycocalyx of inner ear sensory and supporting cells. Acta Otolaryngol Suppl *458*, 84-89.

Takumida, M., Suzuki, M., Harada, Y., and Bagger-Sjoback, D. (1990). Glycocalyx and ciliary interconnections of the human vestibular end organs: an investigation by scanning electron microscopy. ORL J Otorhinolaryngol Relat Spec *52*, 137-142.

Takumida, M., Wersall, J., and Bagger-Sjoback, D. (1988b). Stereociliary glycocalyx and interconnections in the guinea pig vestibular organs. Acta Otolaryngol *106*, 130-139.

Tamayo, M. L., Bernal, J. E., Tamayo, G. E., Frias, J. L., Alvira, G., Vergara, O., Rodriguez, V., Uribe, J. I., and Silva, J. C. (1991). Usher syndrome: results of a screening program in Colombia. Clin Genet *40*, 304-311.

Tang, N., Lin, T., and Ostap, E. M. (2002). Dynamics of myo1c (myosin-ibeta) lipid binding and dissociation. J Biol Chem *277*, 42763-42768.

Tang, N., and Ostap, E. M. (2001). Motor domain-dependent localization of myo1b (myr-1). Curr Biol *11*, 1131-1135.

Tilney, L. G., and DeRosier, D. J. (1986). Actin filaments, stereocilia, and hair cells of the bird cochlea. IV. How the actin filaments become organized in developing stereocilia and in the cuticular plate. Dev Biol *116*, 119-129.

Tilney, L. G., Egelman, E. H., DeRosier, D. J., and Saunder, J. C. (1983). Actin filaments, stereocilia, and hair cells of the bird cochlea. II. Packing of actin filaments in the stereocilia and in the cuticular plate and what happens to the organization when the stereocilia are bent. J Cell Biol *96*, 822-834.

Tilney, L. G., and Saunders, J. C. (1983). Actin filaments, stereocilia, and hair cells of the bird cochlea. I. Length, number, width, and distribution of stereocilia of each hair cell are related to the position of the hair cell on the cochlea. J Cell Biol *96*, 807-821.

Tilney, L. G., Tilney, M. S., and Cotanche, D. A. (1988). Actin filaments, stereocilia, and hair cells of the bird cochlea. V. How the staircase pattern of stereociliary lengths is generated. J Cell Biol *106*, 355-365.

Tilney, L. G., Tilney, M. S., and DeRosier, D. J. (1992). Actin filaments, stereocilia, and hair cells: how cells count and measure. Annu Rev Cell Biol *8*, 257-274.

Tilney, L. G., Tilney, M. S., Saunders, J. S., and DeRosier, D. J. (1986). Actin filaments, stereocilia, and hair cells of the bird cochlea. III. The development and differentiation of hair cells and stereocilia. Dev Biol *116*, 100-118.

Torres, M., and Giraldez, F. (1998). The development of the vertebrate inner ear. Mech Dev *71*, 5-21.

Tosi, G. M., de Santi, M. M., Pradal, U., Braggion, C., and Luzi, P. (2003). Clinicopathologic reports, case reports, and small case series: usher syndrome type 1 associated with primary ciliary aplasia. Arch Ophthalmol *121*, 407-408.

Tryggvason, K., and Pettersson, E. (2003). Causes and consequences of proteinuria: the kidney filtration barrier and progressive renal failure. J Intern Med *254*, 216-224.

Tsuprun, V., and Santi, P. (1998). Structure of outer hair cell stereocilia links in the chinchilla. J Neurocytol *27*, 517-528.

Tsuprun, V., and Santi, P. (2000). Helical structure of hair cell stereocilia tip links in the chinchilla cochlea. J Assoc Res Otolaryngol *1*, 224-231.

Vaccaro, P., and Dente, L. (2002). PDZ domains: troubles in classification. FEBS Lett *512*, 345-349.

Valk, W. L., Oei, M. L., Segenhout, J. M., Dijk, F., Stokroos, I., and Albers, F. W. (2002). The glycocalyx and stereociliary interconnections of the vestibular sensory epithelia of the guinea pig. A freeze-fracture, low-voltage cryo-SEM, SEM and TEM study. ORL J Otorhinolaryngol Relat Spec *64*, 242-246.

Verpy, E., Leibovici, M., Zwaenepoel, I., Liu, X. Z., Gal, A., Salem, N., Mansour, A., Blanchard, S., Kobayashi, I., Keats, B. J., et al. (2000). A defect in harmonin, a PDZ domain-containing protein expressed in the inner ear sensory hair cells, underlies Usher syndrome type 1C. Nat Genet *26*, 51-55.

Walker, R. G., and Hudspeth, A. J. (1996). Calmodulin controls adaptation of mechanoelectrical transduction by hair cells of the bullfrog's sacculus. Proc Natl Acad Sci U S A *93*, 2203-2207.

Walker, R. G., Hudspeth, A. J., and Gillespie, P. G. (1993). Calmodulin and calmodulin-binding proteins in hair bundles. Proc Natl Acad Sci U S A *90*, 2807-2811.

Wallar, B. J., and Alberts, A. S. (2003). The formins: active scaffolds that remodel the cytoskeleton. Trends Cell Biol *13*, 435-446.

Walsh, T., Walsh, V., Vreugde, S., Hertzano, R., Shahin, H., Haika, S., Lee, M. K., Kanaan, M., King, M. C., and Avraham, K. B. (2002). From flies' eyes to our ears: mutations in a human class III myosin cause progressive nonsyndromic hearing loss DFNB30. Proc Natl Acad Sci U S A *99*, 7518-7523.

Wang, X., Weiner, J. A., Levi, S., Craig, A. M., Bradley, A., and Sanes, J. R. (2002). Gamma protocadherins are required for survival of spinal interneurons. Neuron *36*, 843-854.

Wangemann, P. (2002). K(+) cycling and its regulation in the cochlea and the vestibular labyrinth. Audiol Neurootol *7*, 199-205.

Wasserman, S. (1998). FH proteins as cytoskeletal organizers. Trends Cell Biol *8*, 111-115.

Weil, D., Blanchard, S., Kaplan, J., Guilford, P., Gibson, F., Walsh, J., Mburu, P., Varela, A., Levilliers, J., Weston, M. D., and et al. (1995). Defective myosin VIIA gene responsible for Usher syndrome type 1B. Nature *374*, 60-61.

Weil, D., El-Amraoui, A., Masmoudi, S., Mustapha, M., Kikkawa, Y., Laine, S., Delmaghani, S., Adato, A., Nadifi, S., Zina, Z. B., et al. (2003). Usher syndrome type I G (USH1G) is caused by mutations in the gene encoding SANS, a protein that associates with the USH1C protein, harmonin. Hum Mol Genet *12*, 463-471.

Williams, D. S. (1991). Actin filaments and photoreceptor membrane turnover. Bioessays *13*, 171-178.

Williams, D. S. (2002). Transport to the photoreceptor outer segment by myosin VIIa and kinesin II. Vision Res *42*, 455-462.

Williams, D. S., Hallett, M. A., and Arikawa, K. (1992). Association of myosin with the connecting cilium of rod photoreceptors. J Cell Sci *103 (Pt 1)*, 183-190.

Williams, D. S., Linberg, K. A., Vaughan, D. K., Fariss, R. N., and Fisher, S. K. (1988). Disruption of microfilament organization and deregulation of disk membrane morphogenesis by cytochalasin D in rod and cone photoreceptors. J Comp Neurol *272*, 161-176.

Wilson, S. M., Householder, D. B., Coppola, V., Tessarollo, L., Fritzsch, B., Lee, E. C., Goss, D., Carlson, G. A., Copeland, N. G., and Jenkins, N. A. (2001). Mutations in Cdh23 cause nonsyndromic hearing loss in waltzer mice. Genomics *74*, 228-233.

Wolfrum, U., Liu, X., Schmitt, A., Udovichenko, I. P., and Williams, D. S. (1998). Myosin VIIa as a common component of cilia and microvilli. Cell Motil Cytoskeleton *40*, 261-271.

Wu, D. K., and Oh, S. H. (1996). Sensory organ generation in the chick inner ear. J Neurosci *16*, 6454-6462.

Wu, Q., and Maniatis, T. (1999). A striking organization of a large family of human neural cadherin-like cell adhesion genes. Cell *97*, 779-790.

Xiang, M., Gao, W. Q., Hasson, T., and Shin, J. J. (1998). Requirement for Brn-3c in maturation and survival, but not in fate determination of inner ear hair cells. Development *125*, 3935-3946.

Yagi, T. (1999). Molecular mechanisms of Fyn-tyrosine kinase for regulating mammalian behaviors and ethanol sensitivity. Biochem Pharmacol *57*, 845-850.

Yagi, T., and Takeichi, M. (2000a). Cadherin superfamily genes: functions, genomic organization, and neurologic diversity. Genes Dev *14*, 1169-1180.

Yagi, T., and Takeichi, M. (2000b). Cadherin superfamily genes: functions, genomic organization, and neurologic diversity. Genes Dev *14*, 1169-1180.

Zhang, N., Martin, G. V., Kelley, M. W., and Gridley, T. (2000). A mutation in the Lunatic fringe gene suppresses the effects of a Jagged2 mutation on inner hair cell development in the cochlea. Curr Biol *10*, 659-662.

Zhao, Y., Yamoah, E. N., and Gillespie, P. G. (1996). Regeneration of broken tip links and restoration of mechanical transduction in hair cells. Proc Natl Acad Sci U S A *93*, 15469-15474.

Zheng, J., Shen, W., He, D. Z., Long, K. B., Madison, L. D., and Dallos, P. (2000a). Prestin is the motor protein of cochlear outer hair cells. Nature *405*, 149-155.

Zheng, J. L., and Gao, W. Q. (2000). Overexpression of Math1 induces robust production of extra hair cells in postnatal rat inner ears. Nat Neurosci *3*, 580-586.

Zheng, J. L., Shou, J., Guillemot, F., Kageyama, R., and Gao, W. Q. (2000b). Hes1 is a negative regulator of inner ear hair cell differentiation. Development *127*, 4551-4560.

Zheng, L., Sekerkova, G., Vranich, K., Tilney, L. G., Mugnaini, E., Bartles, J. R., Avraham, K. B., Hasson, T., Steel, K. P., Kingsley, D. M., et al. (2000c). The deaf jerker mouse has a mutation in the gene encoding the espin actin-bundling proteins of hair cell stereocilia and lacks espins. Cell *102*, 377-385. required for structural integrity of inner ear hair cells.

Zhou, X. L., Batiza, A. F., Loukin, S. H., Palmer, C. P., Kung, C., and Saimi, Y. (2003). The transient receptor potential channel on the yeast vacuole is mechanosensitive. Proc Natl Acad Sci U S A *100*, 7105-7110.

Zhu, B., Chappuis-Flament, S., Wong, E., Jensen, I. E., Gumbiner, B. M., and Leckband, D. (2003). Functional analysis of the structural basis of homophilic cadherin adhesion. Biophys J *84*, 4033-4042.

Zine, A., Aubert, A., Qiu, J., Therianos, S., Guillemot, F., Kageyama, R., and de Ribaupierre, F. (2001). Hes1 and Hes5 activities are required for the normal development of the hair cells in the mammalian inner ear. J Neurosci *21*, 4712-4720.

Zine, A., Hafidi, A., and Romand, R. (1995). Fimbrin expression in the developing rat cochlea. Hear Res *87*, 165-169.

Zine, A., Van De Water, T. R., and de Ribaupierre, F. (2000). Notch signaling regulates the pattern of auditory hair cell differentiation in mammals. Development *127*, 3373-3383.

Zrada, S. E., Braat, K., Doty, R. L., and Laties, A. M. (1996). Olfactory loss in Usher syndrome: another sensory deficit? Am J Med Genet *64*, 602-603.

Acknowledgements

I would like to thank...

...Uli Müller for providing me with the possibility to work in a very stimulating environment on this exciting project, for his support and guidance and the freedom to follow own ideas. I very much enjoyed being in his lab.

...Katrin Schrenk for her friendship and her support not only in Basel but also in the distance during my (not entirely easy) time in San Diego.

...Amanda Littlewood-Evans for her invaluable help with the project and revisions of this manuscript, for her time and patience teaching me the histology of the mouse inner ear.

...Conchi Lillo, Rachel A. Dumont, David S. Williams and Peter G. Gillespie for an invaluable exchange of ideas and expertise and for a nice team effort; that is what science is also about.

...Piotr Kazmierczak for stimulating discussions regarding various aspects of the project, mechanosensation and life (-science) in general.

...Sandra Blaess, Marco Leu, Diana Graus-Porta, Anna Reynolds (no hard feelings anymore), Mathias Senften, Randor Radakovits and Martin Schwander for technical advise, a friendly atmosphere and a good time in the lab and beyond.

...My thesis committee members Denis Monard and Esther Stoeckli for their support of the project.

...Andrew Matus for the opportunity to finish up some work in his lab.

...All members of the lab in particular also Angela Glenn for her help with administrative matters and recreational affairs (the Mexico Trip was really fun).

...Anne-Catherine Feutz and Melanie Sticker for help with whisker-follicle preparation and general histological techniques.

Finally, I would like to thank my parents and my brother for their support, open mindedness and patience during all those years.

Curriculum Vitae

Curriculum Vitae

Personal details

- Surname: Siemens
- First names: Jan Erik
- Title: Diplom Biochemist
- Nationality: German
- Date/Place of birth: 01-27-1973; Place: Schleswig, Germany;
- Work address: ICND-222, The Scripps Research Institute, 10550 North
  Torrey Pines Rd., La Jolla, CA 92037-1000, USA
  Tel.:+858-784-7306, Fax: +858-784-7299

Pre-universitary activities

1980-1984	Primary school in Hamburg, Germany
1984-1993	Highschool (Hermann-Tast-Gymnasium) in Husum, Germany
1990-1991	Highschool (Union Local) in Bethesda, Ohio, USA (participation in a student exchange program to USA)
Aug. 1993-Oct. 1994	Civil substitute for military service ("Zivildienst") in a mobile healthcare Institution ("Diakoniestation") in Husum, Germany

Scientific education

1993	University entrance qualification (Abitur): Graduation from Highschool (Hermann-Tast Gymnasium) in Husum, Germany (Grade: 1,9)
1994-1996	Biochemistry (basic studies) Ruhruniversitaet Bochum, Germany
1996-1998	Biochemistry (main studies) J. W. Goethe-Universität, Frankfurt am Main, Germany
Feb. 1999-Apr. 2000	Diploma Thesis at the Eberhard-Karls-Universität, Tübingen, Germany at the Institute for Diabetis headed by Prof. Dr. U. Haering; Diploma Thesis Advisor: Dr. R. Lammers; Title: „Proteolytical Processing of Protein Tyrosine Phosphatase PTP alpha". Degree: Diplom Biochemist (Grade: 1.0)
Since July 2000-April 2004	Ph.D project in Dr. U. Muellers lab at the Friedrich-Miescher Institute (FMI) in Basel, Switzerland. Title: „Characterization of the Usher Syndrome Gene CDH23: Implications for Mechanosensation in the Vertebrate Inner Ear". The Ph.D Project is funded by a Scholarship from Boehringer Ingelheim Fonds. Thesis Committee: Prof. Dr. Esther Stoeckli, Prof. Dr. Denis Monard, and Prof. Dr. Ulrich Mueller. Thesis Defense at the Philosophisch-Naturwissenschaftlichen Fakultaet, University Basel. Grade: Summa cum Laude
January 2003	Relocalization of the Mueller lab to the Scripps Research Institute in San Diego, USA

Additional Practical work during University vacation

March 1995	Practical as a summer student at the Institute of Genetics, Forschungszentrum Karlsruhe, Germany. Advisor: Dr. M. Goettlicher (Director: Prof. Dr. P. Herrlich)
February 1997	Practical course at the University of Saarland, Germany. Institute of Physiology. Title: "Basic work with Xenopus" Advisor: Prof. Dr. H.-P. Richter.
Aug./Sep. 1997	Practical as a summer student at the Institute of Genetics, Forschungszentrum Karlsruhe, Germany. Advisor: Dr. A. Kato (Director: Prof. Dr. P. Herrlich).
Summer 1998	Practical as a summer student in the Company Merck, Darmstadt, Germany in the Department for Preclinical Pharma Research II.

Conferences

1) Molecular Biology of Hearing and Deafness, Bethesda Maryland, October 4-7, 2001
2) Mechanotransduction and Gravity Signaling in Biological Systems, Connecticut College, Connecticut, July 20-25, 2003

Publications

2. Genes, Deafness, and Balance Disorders
   Jan Siemens, Amanda Littlewood-Evans, Mathias Senften, and Ulrich Mueller
   2001, *Gene Funct. Dis.,* 2, 76-82

3. The Sound of Silence - Diseases that cause Deafness and Disequilibrium
   Jan Siemens, Amanda Littlewood-Evans, and Ulrich Mueller
   2001, *B.I.F. Futura,* 16, 222-228

4. The Usher Syndrome Proteins Cadherin 23 and Harmonin form a Complex by means of PDZ Domain Interactions
   Jan Siemens, Piotr Kazmierczak, Anna Reynolds, Melanie Sticker, Amanda Littlewood-Evans, and Ulrich Mueller
   2002, *PNAS*, 99, 14946-14951

4) Cadherin 23 is a Component of the Tip Link in Hair Cell Stereocilia
   Jan Siemens, Concepcion Lillo, Rachel A. Dumont, David Williams, Peter Gillespie, and Ulrich Müller
   (2004, *Nature,* 428, 950-955)

5) Mutations in Cadherin 23 Affect Tipp Links in Zebrafish Sensory Hair Cells
   Christian Soellner, Gerd-Joerg Rauch, Jan Siemens, Robert Geisler, Stephan C. Schuster, the Tuebingen 2000 Screen Consortium, Ulrich Mueller and Teresa Nicolson
   (2004, *Nature,* 428, 955-959)